

**University of Alberta**

**Pyrolysis of Lipids for the Production of Renewable Fuels and Chemicals**

by

**Kelly Dawn Maher**



A thesis submitted to the Faculty of Graduate Studies and Research  
in partial fulfillment of the requirements for the degree of

**Master of Science**

in

**Bioresource and Food Engineering**

**Agricultural, Food & Nutritional Science**

**Edmonton, Alberta**

**Fall 2007**



Library and  
Archives Canada

Bibliothèque et  
Archives Canada

Published Heritage  
Branch

Direction du  
Patrimoine de l'édition

395 Wellington Street  
Ottawa ON K1A 0N4  
Canada

395, rue Wellington  
Ottawa ON K1A 0N4  
Canada

*Your file* *Votre référence*  
*ISBN: 978-0-494-33301-3*  
*Our file* *Notre référence*  
*ISBN: 978-0-494-33301-3*

#### NOTICE:

The author has granted a non-exclusive license allowing Library and Archives Canada to reproduce, publish, archive, preserve, conserve, communicate to the public by telecommunication or on the Internet, loan, distribute and sell theses worldwide, for commercial or non-commercial purposes, in microform, paper, electronic and/or any other formats.

The author retains copyright ownership and moral rights in this thesis. Neither the thesis nor substantial extracts from it may be printed or otherwise reproduced without the author's permission.

#### AVIS:

L'auteur a accordé une licence non exclusive permettant à la Bibliothèque et Archives Canada de reproduire, publier, archiver, sauvegarder, conserver, transmettre au public par télécommunication ou par l'Internet, prêter, distribuer et vendre des thèses partout dans le monde, à des fins commerciales ou autres, sur support microforme, papier, électronique et/ou autres formats.

L'auteur conserve la propriété du droit d'auteur et des droits moraux qui protègent cette thèse. Ni la thèse ni des extraits substantiels de celle-ci ne doivent être imprimés ou autrement reproduits sans son autorisation.

---

In compliance with the Canadian Privacy Act some supporting forms may have been removed from this thesis.

Conformément à la loi canadienne sur la protection de la vie privée, quelques formulaires secondaires ont été enlevés de cette thèse.

While these forms may be included in the document page count, their removal does not represent any loss of content from the thesis.

Bien que ces formulaires aient inclus dans la pagination, il n'y aura aucun contenu manquant.

  
**Canada**

*For Scott, Mom, Dad, Brendan, Tahn, Cheetah, Tigger, & Rocket*

## **ABSTRACT**

The primary objective of this work was to study the pyrolytic conversion of lipids to produce deoxygenated, liquid hydrocarbon products for use as renewable chemicals or fuels. The focus of this fundamental work included identification of primary lipid pyrolysis products at different reaction conditions. Stearic acid was used as a model compound and reacted at different conditions in 15 ml batch reactors. Results show the formation of a distinct n-alkane/alkene series formed by decarboxylation of stearic acid and subsequent thermal cracking. Reaction temperatures from 410-430 °C and times ranging from 1-8 hours appear to be the optimal conditions for obtaining a liquid product of n-alkanes/alkenes with minimal gas, solid and aromatic formation. Neat oils and fats were first hydrolyzed to convert triglycerides into free fatty acids and then pyrolyzed. Results show the presence of the n-alkane/alkene series as well as numerous branched hydrocarbon products.

## **ACKNOWLEDGEMENTS**

I would like to express the utmost gratitude to Dr. David Bressler, for being a supervisor, mentor and friend during my M.Sc. program. Thank-you for challenging me, guiding me and for giving me the opportunity to work in a great lab. Thank-you for your patience and support and for helping me on both my career and life paths.

I would also like to thank my supervisor committee, Dr. Feral Temelli and Dr. Gray, for there extensive knowledge, support and encouragement. I would also like to thank Dr. Gray for the use of his lab throughout my program.

Thank-you to all those who provided technical support during my project. I would like to say a special thank-you to Kelvin Lein for helping me with all of my GC analysis and for being patient and always willing to help

I would like to thank all my lab mates who provided continuous support and encouragement and made working in the lab fun.

Last but not least, I would like to thank my family, Scott and all the pets for supporting me in every way imaginable.

# TABLE OF CONTENTS

<b>CHAPTER 1: INTRODUCTION.....</b>	<b>1</b>
1.1 PROJECT BACKGROUND .....	1
1.2 SIGNIFICANCE .....	4
1.3 OBJECTIVES .....	5
1.4 HYPOTHESIS.....	6
<b>CHAPTER 2: LITERATURE REVIEW .....</b>	<b>7</b>
2.1 THE EMERGING BIOINDUSTRY.....	7
2.1.1 BIOMASS CONVERSION TECHNOLOGIES .....	10
2.1.2 PYROLYTIC OILS FROM BIOMASS (BIO-OIL) .....	12
2.1.2.2 Bio-oil applications .....	14
2.1.3 VEGETABLE OIL (TRIGLYCERIDE-BASED) FUELS.....	15
2.1.4 BIODIESEL .....	17
2.1.4.1 Biodiesel applications .....	18
2.1.4.2 Biodiesel properties .....	18
2.2 PYROLYSIS (THERMAL CRACKING) OF TRIGLYCERIDES FOR FUELS AND CHEMICALS .....	20
2.2.1 PYROLYSIS OF TRIGLYCERIDES .....	21
2.2.2 PYROLYSIS OF FATTY ACID SOAPS .....	26
2.2.3 REACTION MECHANISMS.....	27
2.3 CATALYTIC CRACKING OF TRIGLYCERIDES FOR FUELS AND CHEMICALS.....	33
2.3.1 ACTIVATED ALUMINA.....	34
2.3.2 MOLECULAR SIEVE.....	35
2.3.3 TRANSITION METAL CATALYSTS .....	40
2.3.4 SODIUM CARBONATE .....	42
2.3.5 REACTION MECHANISMS.....	44
2.3.5.1 Activated alumina catalysts .....	44
2.3.5.2 Molecular sieve catalysts .....	45
2.4 PROPERTIES OF PYROLYZED TRIGLYCERIDES .....	46
2.4.1 DIESEL .....	47

2.4.2 GASOLINE.....	50
<b>2.5 DECARBOXYLATION OF FATTY ACIDS AND SUBSEQUENT THERMAL CRACKING</b> .....	<b>51</b>
2.5.1 CRACKING OF LINEAR HYDROCARBON CHAINS .....	52
2.6 HYDROLYSIS OF OILS AND FATS.....	55
2.7 CONCLUSIONS .....	57
<b>CHAPTER 3: EXPERIMENTAL PROCEDURES .....</b>	<b>59</b>
3.1 MATERIALS AND CHEMICALS .....	59
3.1.1 REACTOR FEED .....	59
3.2. MICROREACTORS AND SAND BATH.....	62
3.2.1.1. Batch microreactors .....	63
3.2.1.1.1 Replacing the reactors .....	63
3.2.1.2 Microreactor purge system .....	65
3.2.1.3 Sand bath system .....	66
3.2.1.4 Modified Reactors for Measurement of Internal Reaction Conditions.....	68
3.3 EXPERIMENTAL PROCEDURE .....	70
3.3.1 PYROLYSIS REACTIONS .....	70
3.3.1.1 Extraction of reaction products.....	72
3.3.1.2 Gas chromatography (GC) .....	72
3.3.1.2.1 Liquid extracts .....	72
3.3.1.2.2 Gaseous samples.....	73
3.3.1.3 Gas Chromatography - Mass Spectrometry (GC-MS).....	75
3.3.1.4 Extent of Reaction.....	75
3.3.1.4.1 Derivatization with diazomethane .....	76
3.3.1.4.2 GC analysis of lipid materials .....	77
3.3.1.5 Percentage of liquid and gas fractions .....	77
3.3.2 HYDROLYSIS REACTIONS .....	78
3.3.2.1 Fatty acid composition of the feed.....	79
3.3.2.1.1. Derivatization with boron trifluoride.....	79
3.3.2.2 Analysis of hydrolysates using TLC-FID.....	80
3.3.2.3 Analysis of hydrolysates using GC-FID.....	80
3.3.2.2.1 Derivatization with sodium methoxide and methanolic HCL .....	81

<b>CHAPTER 4: RESULTS .....</b>	<b>83</b>
<b>4.1 PYROLYSIS OF MODEL COMPOUNDS .....</b>	<b>83</b>
<b>4.1.1 PRELIMINARY PYROLYSIS STUDIES USING STEARIC ACID .....</b>	<b>83</b>
4.1.1.1 Pentane insolubles extracted using toluene .....	84
<b>4.1.2 PRODUCT IDENTIFICATION .....</b>	<b>90</b>
4.1.2.1 GC/MS analysis.....	90
4.1.2.2 Product verification using external standards on GC-FID .....	92
<b>4.1.3 STEARIC ACID PYROLYSIS AT VARIOUS TIMES AND TEMPERATURES .....</b>	<b>95</b>
<b>4.1.4 QUANTITATION OF IN STEARIC ACID PYROLYSIS PRODUCTS .....</b>	<b>100</b>
4.1.4.1 Appearance of reactions products .....	101
The appearance of the reaction products varied greatly with time and temperature. At the.....	101
4.1.4.2 Product distributions .....	104
4.1.4.3 Estimation of C <sub>8</sub> -C <sub>20</sub> n-alkanes and alkenes .....	112
4.1.4.4 Cracking behavior of C <sub>8</sub> -C <sub>20</sub> hydrocarbons .....	116
4.1.4.4.1 Molar Yields of C <sub>8</sub> -C <sub>17</sub> n-Alkanes .....	117
4.1.4.4.2 Molar Yields of C <sub>18</sub> + n-alkanes .....	121
4.1.4.4.3 2-Nonadecanone .....	122
4.1.4.4.4 n-Alkane:Alkene Ratio .....	122
4.1.4.4.5 Molar ratios of C <sub>17</sub> .....	127
<b>4.1.5 ANALYSIS OF LIGHT ENDS (GAS FRACTION).....</b>	<b>129</b>
4.1.5.1 Composition .....	129
4.1.5.2 Percent gas formed .....	131
<b>4.1.6 ESTIMATE OF LIQUID YIELD .....</b>	<b>132</b>
<b>4.1.7 EXTENT OF REACTION.....</b>	<b>134</b>
<b>4.1.8 MINIMUM CRACKING TEMPERATURE.....</b>	<b>135</b>
<b>4.1.9 PYROLYSIS OF OLEIC ACID.....</b>	<b>137</b>
<b>4.1.10 PYROLYSIS AT HIGH PRESSURE .....</b>	<b>140</b>
<b>4.1.11 PYROLYSIS WITH ALUMINA CATALYST .....</b>	<b>141</b>
<b>4.1.13 AROMATIC CONTENT .....</b>	<b>142</b>
4.1.13.1 Nuclear Magnetic Resonance (NMR).....	142
4.1.13.2 GC/MS analysis.....	146
<b>4.1.14 DETAILED CHARACTERIZATION OF PRODUCTS .....</b>	<b>146</b>
<b>4.2 HYDROLYSIS AND PYROLYSIS OF NEAT OILS AND FATS .....</b>	<b>149</b>
<b>4.2.1 HYDROLYSATE ANALYSIS .....</b>	<b>149</b>
4.2.1.1 TLC-FID analysis .....	149
4.2.1.1 GC-FID analysis .....	153



4.2.2 PYROLYSIS REACTIONS .....	154
4.3.2.1 Analysis of product on GC-FID.....	154
4.2.2.2 GC/MS analysis after derivatization with diazomethane.....	162
<b>CHAPTER 5: DISCUSSION .....</b>	<b>167</b>
5.2 MODEL COMPOUND WORK.....	167
5.2.1 MAJOR REACTION PRODUCTS.....	167
5.2.1.1 n-Alkanes and alkene series.....	168
5.2.1.2 Carboxylic acid series.....	169
5.2.1.3 Other products.....	170
5.2.2 INITIAL DECARBOXYLATION.....	171
5.2.3 CRACKING BEHAVIOR AND PRODUCT DISTRIBUTIONS AT DIFFERENT REACTION TIMES AND TEMPERATURES.....	171
5.2.4 EFFECT OF OTHER VARIABLES ON REACTION PRODUCTS.....	174
5.2.4.1 Initial feed weight.....	174
5.2.6 OLEIC ACID PYROLYSIS PRODUCTS.....	176
5.2.7 PRODUCT YIELDS.....	177
5.2.7.1 Mass Balance.....	178
5.2.8 SELECTION OF OPTIMAL CONDITIONS.....	179
5.2.8.1 Supercritical Nitrogen.....	182
5.3 HYDROLYSIS AND PYROLYSIS OF NEAT OILS AND FATS.....	183
<b>CHAPTER 6: CONCLUSIONS AND RECOMMENDATIONS .....</b>	<b>188</b>
<b>CHAPTER 7: REFERENCES.....</b>	<b>193</b>
<b>APPENDIX A: ADDITIONAL TABLES AND FIGURES.....</b>	<b>202</b>
<b>APPENDIX B: SAMPLE CALCULATIONS.....</b>	<b>213</b>
<b>APPENDIX C: EXPERIMENTAL VALIDATION AND ADDITIONAL PROCEDURAL DEVELOPMENT.....</b>	<b>219</b>

## LIST OF TABLES

<b>Table 2.1</b> ASTM D 975 Requirements for Diesel Fuel (ASTM D 975-04c, 2006).....	48
<b>Table 3.1</b> Chemicals used in this work .....	60
<b>Table 3.2</b> Fatty acid composition of feed fats and oil determined by GC-FID.....	61
<b>Table 3.3</b> Percentage of saturated and unsaturated fatty acid in feed fats and oil determined by GC-FID .....	61
<b>Table 3.4</b> Sand bath specifications.....	66
<b>Table 3.5</b> Groups methylated by different derivatization compounds.....	82
<b>Table 4.1</b> Experimental conditions for preliminary pyrolysis reactions (each X indicates one reaction run) .....	84
<b>Table 4.2</b> Experimental conditions for reaction runs that had an initial pentane and subsequent toluene extraction (each X represents a single reaction run). .....	87
<b>Table 4.3</b> Experimental conditions for stearic acid pyrolysis at various times and temperatures (each X represents a single reaction run). .....	99
<b>Table 4.4</b> Experimental conditions for the pyrolysis of stearic acid (each X represents a single reaction run). .....	101
<b>Table 4.5</b> Appearance of reaction products after pentane extraction at various times and temperatures.....	103
<b>Table A.1</b> n-Alkane/alkene molar ratio as a function of temperature and time for complete set of conditions .....	204
<b>Table B.1</b> Reaction data for duplicate 1 hr reactions at 410 °C.....	215
<b>Table B.2</b> Peak integrations for duplicate 1 hr reactions at 410 °C.....	215
<b>Table B.3</b> Sample calculation of mass yield for C <sub>8</sub> -C <sub>20</sub> alkanes and alkenes based on initial feed (Eqn. B.3) .....	216
<b>Table B.4</b> Sample calculation of molar yield for C <sub>8</sub> -C <sub>20</sub> alkanes and alkenes based on initial feed (Eqn. B.4) .....	216
<b>Table B.5</b> Calculation of n-alkane/alkene molar ratio (Eqn. B.5) .....	217

## LIST OF FIGURES

<b>Figure 1.1</b> Triglyceride molecule (Tristearin) .....	3
<b>Figure 1.2</b> Proposed thermal cracking sequence for a stearic acid molecule .....	3
<b>Figure 1.3</b> Flow diagram showing the proposed process flow. Key process information includes 1. Feed Composition; 2. Energy requirements for hydrolysis; 3. Composition of the fat layer (pyrolysis feed); 4. Energy requirements for pyrolysis; 5. Composition of gas product; and 6. Composition of the product. ....	4
<b>Figure 2.1</b> Decomposition of Triglycerides (Chang and Wan, 1947) .....	29
<b>Figure 2.2</b> Reaction Mechanism for the Pyrolysis of Saturated Triglycerides (Alencar et al., 1983) .....	30
<b>Figure 2.3</b> Reaction Mechanism for the Pyrolysis of Triglycerides (Schwab et al., 1988) .....	30
<b>Figure 2.4</b> Reaction Mechanism for the Pyrolysis of Saturated and Unsaturated Triglycerides (Idem et al., 1996) .....	32
<b>Figure 2.5</b> Proposed Mechanism for the Catalytic Cracking of Canola Oil (Katikaneni et al., 1996) .....	46
<b>Figure 3.1</b> Picture of (a) sand bath and purge system and (b) microreactor .....	62
<b>Figure 3.2</b> Schematic of closed microreactor .....	64
<b>Figure 3.3</b> Schematic of the microreactor purge system .....	65
<b>Figure 3.4</b> Picture of the sand bath system .....	67
<b>Figure 3.5</b> Schematic of Techne SBS-4 sand bath.....	68
<b>Figure 3.6</b> Picture of the modified reactor for measuring internal reactor temperature ...	69
<b>Figure 3.7</b> Picture of the modified reactor for measuring internal reactor pressure .....	69
<b>Figure 3.8</b> GC-FID column temperature profile for liquid analysis of pyrolysis products in pentane.....	73
<b>Figure 3.9</b> GC-TCD column temperature profile for gas analysis of pyrolysis products.	74
<b>Figure 3.10</b> GC column temperature profile for lipid analysis (30 m column) .....	78

<b>Figure 3.11</b> GC –FID column temperature profile for lipid analysis (100 m column).....	81
<b>Figure 4.1</b> GC-FID chromatogram showing the pentane soluble pyrolysis products of stearic acid after 30 min reactions at temperatures between 350 °C and 500 °C. Reactions were conducted in N <sub>2</sub> atmosphere and were initially at atmospheric pressure.	85
<b>Figure 4.2</b> GC-FID chromatogram showing the pentane soluble pyrolysis products of stearic acid after 5 min reactions at temperatures between 400 °C and 550 °C. Reactions were conducted in N <sub>2</sub> atmosphere and were initially at atmospheric pressure.....	86
<b>Figure 4.3</b> GC- FID chromatograms showing pyrolysis products from a 5 min, 400 °C reaction in (A) pentane (first extraction) and (B) toluene (second extraction). Reaction was conducted in N <sub>2</sub> atmosphere and was initially at atmospheric pressure.....	88
<b>Figure 4.4</b> GC- FID chromatograms showing pyrolysis products from a 5 min, 500 °C reaction in (A) pentane (first extraction) and (B) toluene (second extraction). Reaction was conducted in N <sub>2</sub> atmosphere and was initially at atmospheric pressure.....	89
<b>Figure 4.5</b> Identification of the typical ladder series formed during pyrolysis of stearic acid. Reaction was conducted in N <sub>2</sub> atmosphere and was initially at atmospheric pressure. ....	91
<b>Figure 4.6</b> GC-FID chromatogram showing the external standards run for verification of pyrolysis products. The standards were (1) a C <sub>8</sub> -C <sub>20</sub> n-alkane mixture purchased from Fluka (Table 3.1) and (2) a carboxylic acid standard prepared in-house using carboxylic acids. ....	93
<b>Figure 4.7</b> Typical pentane soluble pyrolysis products of stearic acid after 5 min at 500 °C verified by running external standards. Reaction was conducted in N <sub>2</sub> atmosphere and was initially at atmospheric pressure. ....	94
<b>Figure 4.8</b> GC-FID chromatograms showing stearic acid pyrolysis products for 1 h reactions at temperatures ranging from 390-440 °C. Reactions were conducted in N <sub>2</sub> atmosphere and were initially at atmospheric pressure. ....	96
<b>Figure 4.9</b> GC-FID chromatograms showing stearic acid pyrolysis products for 1 h reactions with temperatures ranging from 450-500 °C. Reactions were conducted in N <sub>2</sub> atmosphere and were initially at atmospheric pressure. ....	97
<b>Figure 4.10</b> GC-FID chromatograms showing stearic acid pyrolysis products for 6 h reactions with temperatures ranging from 380-420 °C. Reactions were conducted in N <sub>2</sub> atmosphere and were initially at atmospheric pressure. ....	98
<b>Figure 4.11</b> GC-FID chromatograms showing pentane soluble stearic acid pyrolysis products from batch reactions at T = 350 °C and t = 4 and 8 hrs. Reactions were conducted in N <sub>2</sub> atmosphere and were initially at atmospheric pressure. ....	105

<b>Figure 4.12</b> GC-FID chromatograms showing pentane soluble stearic acid pyrolysis products from batch reactions at T = 370 °C and t = 1-8 hrs. Reactions were conducted in N <sub>2</sub> atmosphere and were initially at atmospheric pressure.....	106
<b>Figure 4.13</b> GC-FID chromatograms showing pentane soluble stearic acid pyrolysis products from batch reactions at T = 390 °C and t = 0.5-8 hrs. Reactions were conducted in N <sub>2</sub> atmosphere and were initially at atmospheric pressure.....	107
<b>Figure 4.14</b> GC-FID chromatograms showing pentane soluble stearic acid pyrolysis products from batch reactions at T = 410 °C and t = 0.5-8 hrs. Reactions were conducted in N <sub>2</sub> atmosphere and were initially at atmospheric pressure.....	108
<b>Figure 4.15</b> GC-FID chromatograms showing pentane soluble stearic acid pyrolysis products from batch reactions at T = 430 °C and t = 0.5-8 hrs. Reactions were conducted in N <sub>2</sub> atmosphere and were initially at atmospheric pressure.....	109
<b>Figure 4.16</b> GC-FID chromatograms showing pentane soluble stearic acid pyrolysis products from batch reactions at T = 450 °C and t = 0.5-8 hrs. Reactions were conducted in N <sub>2</sub> atmosphere and were initially at atmospheric pressure.....	110
<b>Figure 4.17</b> GC-FID chromatograms showing pentane soluble stearic acid pyrolysis products from batch reactions at T = 500 °C and t = 0.5-4 hrs. Reactions were conducted in N <sub>2</sub> atmosphere and were initially at atmospheric pressure.....	111
<b>Figure 4.18</b> Percentage (wt) of C <sub>8</sub> -C <sub>20</sub> n-alkanes formed based on initial feed weight as a function of temperature and time.....	114
<b>Figure 4.19</b> Percentage (wt) of C <sub>8</sub> -C <sub>20</sub> alkenes formed based on initial feed weight as a function of temperature and time.....	115
<b>Figure 4.20</b> Molar yields of C <sub>8</sub> -C <sub>20</sub> n-alkanes as a function of temperature for 0.5 hr reactions.....	118
<b>Figure 4.21</b> Molar yields of C <sub>8</sub> -C <sub>20</sub> n-alkanes as a function of temperature for 1 hr reactions.....	118
<b>Figure 4.22</b> Molar yields of C <sub>8</sub> -C <sub>20</sub> n-alkanes as a function of temperature for 4 hr reactions.....	119
<b>Figure 4.23</b> Molar yields of C <sub>8</sub> -C <sub>20</sub> n-alkanes as a function of temperature for 8 hr reactions.....	119
<b>Figure 4.24</b> Molar ratio of n-alkanes to alkenes as a function of carbon number and reaction time at T=390°C.....	123

<b>Figure 4.25</b> Molar ratio of n-alkanes to alkenes as a function of carbon number and reaction time at T=410°C.....	123
<b>Figure 4.26</b> Molar ratio of n-alkanes to alkenes as a function of carbon number and reaction time at T=430°C.....	124
<b>Figure 4.27</b> Molar ratio of n-alkanes to alkenes as a function of carbon number and reaction time at T=450°C.....	124
<b>Figure 4.28</b> Molar ratio of n-alkanes to alkenes for C <sub>17</sub> as a function of temperature and time .....	128
<b>Figure 4.29</b> Typical gas composition from stearic acid pyrolysis from a 1 hr reaction at 410 °C as analyzed on GC-TCD.....	129
<b>Figure 4.30</b> Methane (CH <sub>4</sub> ), carbon dioxide (CO <sub>2</sub> ), and air standards as analyzed on GC-TCD .....	130
<b>Figure 4.31</b> Percent of gas products formed during 1 hr stearic acid pyrolysis reactions as a function of temperature. Initial pressure was atmospheric and the reactions were conducted in N <sub>2</sub> .....	132
<b>Figure 4.32</b> Percent liquid products formed during stearic acid pyrolysis as a function of temperature and time. Initial pressure was atmospheric and the reactions were conducted in N <sub>2</sub> .....	133
<b>Figure 4.33</b> Percentage of initial stearic acid feed that was converted during 1 hr pyrolysis reactions as a function of temperature. Initial pressure was atmospheric and the reactions were conducted in N <sub>2</sub> .....	135
<b>Figure 4.34</b> Chromatogram (GC-FID) showing stearic acid pyrolysis products after a 4 hr reaction at 255°C. Initial pressure was atmospheric and the reactions were conducted in N <sub>2</sub> .....	136
<b>Figure 4.35</b> Chromatogram (GC-TCD) showing gaseous reaction products after a 4 hr reaction at 255°C. Initial pressure was atmospheric and the reactions were conducted in N <sub>2</sub> .....	137
<b>Figure 4.36</b> Chromatogram (GC-FID) showing oleic acid pyrolysis products after a 1 hr reaction at 410°C. Initial pressure was atmospheric and the reactions were conducted in N <sub>2</sub> .....	139
<b>Figure 4.37</b> Main products of oleic acid pyrolysis after 1 hr at 410 °C.....	139

<b>Figure 4.38</b> GC-TCD chromatogram showing the gas products from oleic acid pyrolysis after 1 hr at 410 °C. Initial pressure was atmospheric and the reactions were conducted in N <sub>2</sub> .	140
<b>Figure 4.39</b> GC-FID chromatograms showing the pentane soluble pyrolysis products of stearic acid after 1 hr reactions at 400 °C with an initial reactor pressure at atmospheric and 6.89 MPa. Reactions were conducted in N <sub>2</sub> atmosphere.	143
<b>Figure 4.40</b> GC-FID chromatograms showing the pentane soluble pyrolysis products of stearic acid after 1 hr reactions at 410 °C with an initial reactor pressure at atmospheric and 6.89 MPa. Reactions were conducted in N <sub>2</sub> atmosphere.	144
<b>Figure 4.41</b> GC-FID chromatograms showing the pentane soluble pyrolysis products of stearic acid after 1 hr reactions at 410 °C with	145
<b>Figure 4.42</b> GC-FID chromatograms showing aromatic compounds formed at 430 °C, 450 °C, and 500 °C after 1 hr reactions. Initial pressure was atmospheric and the reactions were conducted in N <sub>2</sub> .	148
<b>Figure 4.43</b> Reaction products formed after a 1 hr reaction at 390 °C. Initial pressure was atmospheric and the reactions were conducted in N <sub>2</sub> .	149
<b>Figure 4.44</b> TLC-FID chromatogram showing canola oil hydrolysates	150
<b>Figure 4.45</b> TLC-FID chromatogram showing the bleached fancy tallow hydrolysates	150
<b>Figure 4.46</b> TLC-FID chromatogram showing the oleic acid standard mixture	151
<b>Figure 4.47</b> TLC-FID chromatogram showing the oleic acid standard mixture spiked with bleached fancy tallow hydrolysates (2:1 by volume standard:sample).	151
<b>Figure 4.48</b> GC-FID chromatogram showing the fatty acid profile of bleached fancy tallow hydrolysates after derivatization with diazomethane	155
<b>Figure 4.49</b> GC-FID chromatogram showing the fatty acid profile of bleached fancy tallow hydrolysates after derivatization with methanolic HCL	155
<b>Figure 4.50</b> GC-FID chromatogram showing poultry tallow pyrolysis products from a 4 hr reaction at 410 °C. Reactions were conducted in N <sub>2</sub> atmosphere and were initially at atmospheric pressure.	157
<b>Figure 4.51</b> GC-FID chromatogram showing canola oil pyrolysis products from a 1 hr reaction at 410 °C. Reaction was conducted in N <sub>2</sub> atmosphere and was initially at atmospheric pressure.	158
<b>Figure 4.52</b> GC-FID chromatogram showing yellow grease tallow pyrolysis products from a 1 hr reaction at 410 °C. Reactions were conducted in N <sub>2</sub> atmosphere and were	

initially at atmospheric pressure. ....	159
<b>Figure 4.53</b> GC-FIDatogram showing bleached fancy tallow pyrolysis products from a 1 hr reaction at 410 °C compared to stearic acid pyrolysis products at the same conditions. Reactions were conducted in N <sub>2</sub> atmosphere and were initially at atmospheric pressure. ....	160
<b>Figure 4.54</b> GC-FID chromatogram showing bleached fancy tallow pyrolysis products from a 1 hr reaction at 390 °C. Reaction was conducted in N <sub>2</sub> atmosphere and was initially at atmospheric pressure. ....	161
<b>Figure 4.55</b> GC/MS chromatogram showing derivatized and underivatized samples of bleached fancy tallow pyrolysis products after 1h reaction at 410 °C. Reactions were conducted in N <sub>2</sub> atmosphere and were initially at atmospheric pressure. ....	163
<b>Figure 4.56</b> GC/MS chromatogram showing derivatized bleached fancy tallow pyrolysis products after 1 h reaction at 410 °C. Reactions were conducted in N <sub>2</sub> atmosphere and were initially at atmospheric pressure. ....	165
<b>Figure 4.57</b> Close-up of GC/MS chromatogram showing derivatized bleached fancy tallow pyrolysis products after 1 h reaction at 410 °C. Reactions were conducted in N <sub>2</sub> atmosphere and were initially at atmospheric pressure. ....	166
<b>Figure A.1</b> GC-FID chromatogram showing stearic acid with no thermal treatment ....	202
<b>Figure A.2</b> GC-FID Chromatogram showing the retention time of the primary internal standard used in this work, nonadecanoic acid methyl ester .....	203
<b>Figure A.3</b> Mass yield of C <sub>8</sub> -C <sub>20</sub> n-alkanes and alkenes based on converted feed.....	205
<b>Figure A.4</b> GC-FID chromatograms showing the gas products from stearic acid pyrolysis at 390 °C after 1 hr.....	206
<b>Figure A.5</b> GC-FID chromatogram showing the gas products from stearic acid pyrolysis at 500 °C after 30 min.....	206
<b>Figure A.6</b> n-Alkane/alkene molar ratios for 1 hr reactions conducted at 410 °C as a function of initial pressure .....	207
<b>Figure A.7</b> Alkane yeild for 1 hr reactions conducted at 410 °C as a function of initial pressure .....	207
<b>Figure A.8</b> C13 NMR scan of stearic acid pyrolysis products at 390 °C after 1 hr.....	208
<b>Figure A.9</b> C-13 NMR Scan of stearic acid pyrolysis products at 410 °C after 1 hr.....	209



<b>Figure A.10</b> GC-FID chromatogram showing the standard fatty acid curve. GC conditions were the same as sample conditions outlined in section 3.3.2.3.....	210
<b>Figure A.11</b> GC-FID chromatogram showing bleached fancy tallow hydrolysates from a 1 hr reaction at 410 °C dissolved in pentane. Reactions were conducted in N <sub>2</sub> atmosphere and were initially at atmospheric pressure.....	211
<b>Figure A.12</b> GC-FID chromatogram showing poultry tallow pyrolysis products from a 4 hr reaction at 410 °C after a water extraction step. Reaction was conducted in N <sub>2</sub> atmosphere and was initially at atmospheric pressure.....	212
<b>Figure C.1</b> Internal reactor temperature during stearic acid pyrolysis as a function of time for controller set-point temperatures of 370 °C, 410 °C, and 450 °C. Reactions were conducted in N <sub>2</sub> atmosphere and were initially at atmospheric pressure. ....	220
<b>Figure C.2</b> GC-FID chromatogram showing the difference in product distributions before (A) and after drying and re-suspension (B) of stearic acid pyrolysis products for 1 hr reactions conducted at 450 °C . Reactions were conducted in N <sub>2</sub> atmosphere and were initially at atmospheric pressure. ....	223

## NOMENCLATURE

$A_i$	GC peak area of compound i
$A_s$	GC peak area of internal standard
$C_s$	concentration of internal standard solution (mg/ml)
$M$	molecular weight (g/mol)
$m_{\text{feed}}$	mass of feed (g)
$m_i$	mass of compound i (g)
$n_{\text{feed}}$	moles of feed (mol)
$n_i$	moles of compound i (mol)
$P_c$	critical pressure
$P_o$	initial reactor pressure (MPa)
$S_E$	standard error
$t$	time (minutes, hours)
$T$	temperature ( $^{\circ}\text{C}$ )
$T_c$	critical temperature
$T_{\text{reactor}}$	internal reactor temperature ( $^{\circ}\text{C}$ )
$V_{\text{ext}}$	volume of extraction solvent (ml)
$\sigma$	standard deviation

# CHAPTER 1: INTRODUCTION

## 1.1 PROJECT BACKGROUND

The popularity of alternative energy and interest in development of renewable fuels and chemicals is rapidly increasing. On the demand side, interest has been shown from chemical suppliers for renewable chemicals such as solvents. A potential feedstock for production of renewable chemicals is beef tallow, a by-product from rendering operations. The recent BSE (bovine spongiform encephalopathy) or mad cow crisis in Alberta has resulted in regulations that have caused a drop in tallow value and demand. Therefore, it is of interest to the cattle industry to explore alternative uses for tallow. One option is thermo-chemical conversion into renewable and biodegradable chemicals or fuel. The successful conversion of tallow into bio-based, value-added, petroleum replacements such as platform chemicals, industrial solvents, or bitumen diluents could be economically rewarding for the industry. Furthermore, the production of bio-based products as opposed to fossil derived products is an attractive option for applications that value renewability and sustainability. This research deals with thermo-chemical biomass conversion, a branch of renewable energy research that is extremely exciting and rapidly gaining industrial importance.

Tallow is composed of primarily of triglyceride molecules. Triglycerides are good sources of energy making them a good option for conversion into chemicals and fuels. Structurally, triglycerides consist of a glycerol backbone with three fatty acid chains attached through ester bonds (Figure 1.1). These fatty acids can be liberated through

various hydrolysis procedures such as acid, base, high temperature and pressure, or catalytic, resulting in free fatty acids (FFA) and glycerol. The structure of FFA's is such that if the carboxyl group at the end of the chain can be removed (decarboxylation), a deoxygenated hydrocarbon chain is produced. This hydrocarbon chain could be processed further to yield shorter chain hydrocarbons that could potentially be used as petroleum replacements (Figure 1.2). Triglyceride pyrolysis has been studied before, however the process described in this thesis is unique because it focuses on pyrolysis of free fatty acids rather than the whole triglyceride molecule. Pyrolysis of the whole triglyceride has been shown to result in oxygenated products (Ali and Hanna, 1994; Ma and Hanna, 1999) and it is likely the process is more difficult to control as it involves a more functionally complex starting molecule. Hydrolysis and pyrolysis are the key processing steps and are studied in this thesis. A simplified flow diagram of the proposed process is shown in Figure 1.3. The intent of this work was to understand fundamental chemistry at key points in the process for optimization of reaction conditions and to assess the feasibility of scale-up. Depending on the purity of the feed, some pre-treatment steps might also be required and further process development would likely involve optimizing the process and looking at downstream product separation techniques. Pyrolysis or thermal cracking is a good option for conversion because it is relatively inexpensive and requires lower temperatures than gasification processes. Pyrolysis is especially appealing in Alberta where the oil and gas industry, which employs similar technology, is well established. Although the idea for this project originated with utilization of beef tallow from the rendering industry, potential applications span beyond

this industry. The feedstock for this novel process could potentially be any type of lipid feed.

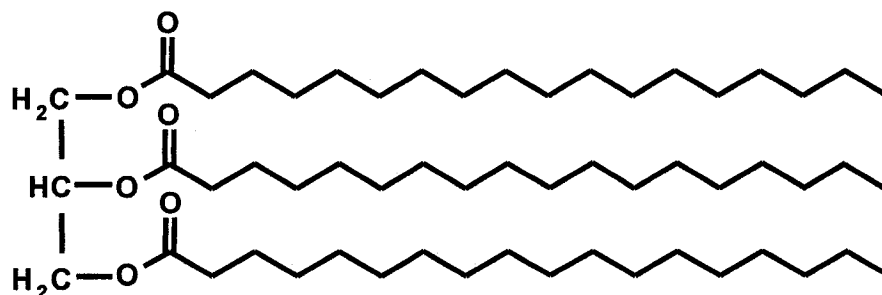


**Figure 2.1** Triglyceride molecule (Tristearin)

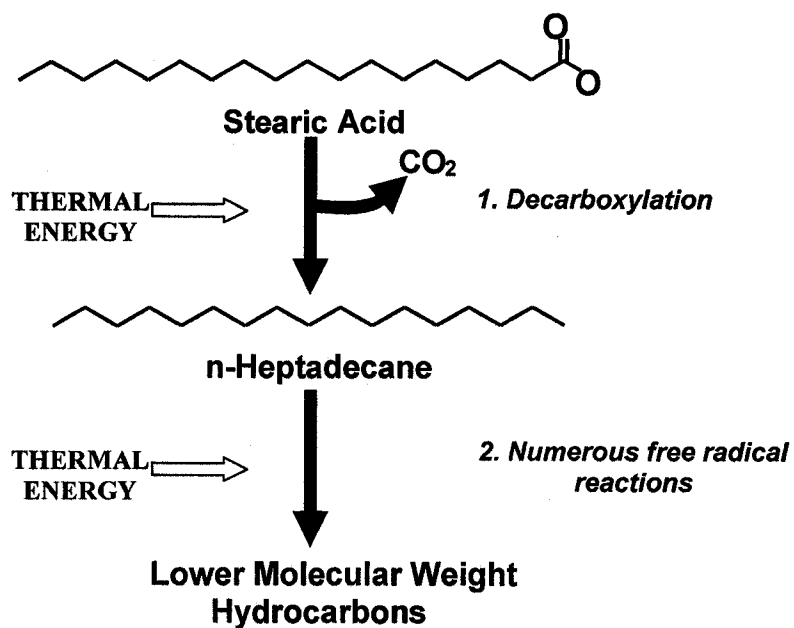


**Figure 2.2** Proposed thermal cracking sequence for a stearic acid molecule

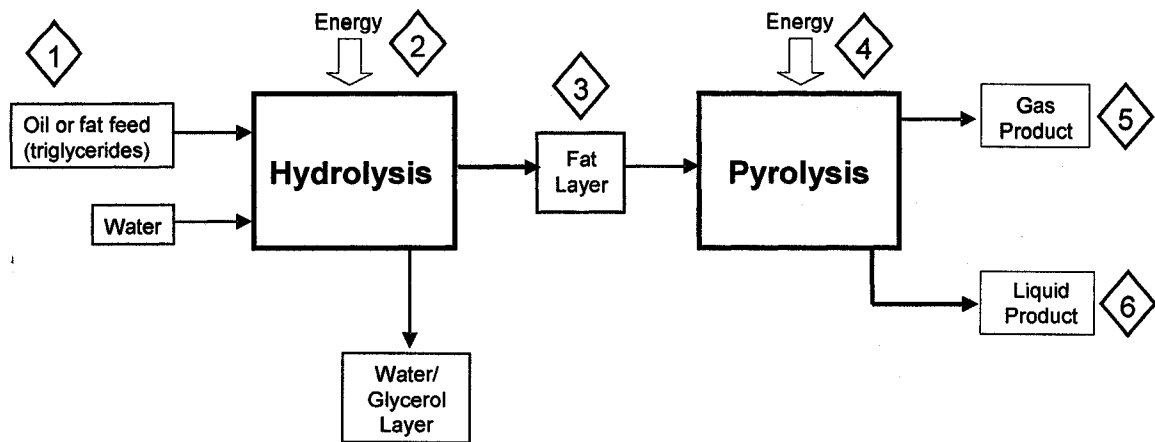


**Figure 2.3** Flow diagram showing the proposed process flow. Key process information includes 1. Feed Composition; 2. Energy requirements for hydrolysis; 3. Composition of the fat layer (pyrolysis feed); 4. Energy requirements for pyrolysis; 5. Composition of gas product; and 6. Composition of the product.

## 1.2 SIGNIFICANCE

The results of this project are significant on several levels:

### 1. Future sustainability

This research involves study in the area of renewable fuels and chemicals, which is an extremely important topic in today's society. This is a global concern. Development of viable renewable energy sources to help supplant fossil resources is of critical importance to future sustainability. Depleting reserves, environmental concerns, and political and social factors have all played key roles in the increasing interest in renewable energy research.

## **2. Development of value-added products and utilization of undervalued by-products**

This research involves studying the conversion of beef tallow, a currently undervalued by-product of Alberta's rendering industry. As a result, conversion into a value-added product has the potential to be economically rewarding for this industry.

## **3. Supplementing Alberta's oil and gas industry**

The technology chosen for conversion is pyrolysis, a high temperature reaction. Alberta already has well developed oil and gas processing infrastructure, which employs similar reaction technology but utilizes different feedstock. Incorporation of different feeds could result in potential benefits for this industry such as product diversification and potential market expansion.

### **1.3 OBJECTIVES**

This research involves studying the pyrolysis reaction of fatty acids from animal fats and vegetable oils such as canola oil and beef tallow and stearic acid, a model compound found in beef tallow. The main objectives of this study are as follows:

- To determine the pyrolysis products of stearic acid at temperatures between 300°C and 500°C,
- To determine if decarboxylation is the first step in thermal cracking of fatty acids,

- To study the effects of various reaction conditions, primarily temperature and time, on pyrolysis products in order to optimize the reaction to select for desired products, and
- To determine the pyrolysis products of fatty acids from hydrolyzed beef tallow and canola oil.

#### **1.4 HYPOTHESIS**

1. Thermal cracking of fatty acids at certain conditions will result in liquid n-alkanes and alkenes.
2. The lowest temperature reaction in thermal cracking of fatty acids is decarboxylation.
3. Reaction conditions including temperature, time, and pressure will affect the types of reaction products.



## **CHAPTER 2: LITERATURE REVIEW**

Utilization of lipids for the production of renewable, liquid bio-products by thermo-chemical techniques is an exciting branch of renewable energy research. An especially exciting area within this field is pyrolysis of triglyceride-based materials such as vegetable oils and animal fats for the production of renewable fuels and chemicals. This chapter is divided into five main sections. The first section, 2.1, includes an overview of the renewable energy and bioindustry and introduces two important renewable fuels, biodiesel and bio-oil. Literature dealing with thermo-chemical conversion of triglycerides is divided into (1) direct thermal cracking (pyrolysis) and (2) combination of thermal and catalytic cracking and is discussed in sections 2.2 and 2.3, respectively. A discussion on the properties of pyrolyzed oil is presented in section 2.4. The final section, 2.5, focuses on literature that is directly related to this thesis work including thermo-chemical decarboxylation of fatty acids and includes a discussion on possible cracking mechanisms.

### **2.1 THE EMERGING BIOINDUSTRY\***

The majority of the world's energy is supplied by petroleum derived fuels (Royal Dutch/Shell Group, 1983; Brown, 2003) and petroleum-based distillates are used in a

---

\* A version of this section has been previously published in Maher, K.D. and Bressler D.C. 2007. Pyrolysis of Triglycerides for the Production of Renewable Fuels and Chemicals. *Bioresource Technology* 98, 2351-2368.

wide range of industrial applications. Petrochemicals serve as raw materials for the chemical industry in the production of solvents, lubricants, paints, and lacquers. The spectacular growth in consumption of crude petroleum during the middle and late twentieth century can be attributed to the ease with which petroleum can be discovered, produced, transported, processed, and utilized (Royal Dutch/Shell Group, 1983). The oil crisis in the 1970s, depleting reserves, national scarcity issues, price uncertainty, and growing environmental concern over the combustion of fossil fuels highlight major issues associated with the extensive use of petroleum in our society. As a result, there has been renewed interest in the discovery of non-petroleum or “green” fuels and chemicals.

Alternative and renewable energy includes a wide range of technologies including wind power, solar power, hydrogen production, fuel cells, and biomass. A significant portion of renewable energy research is devoted to harnessing energy from biomass. Biomass is the only renewable energy source that yields solid, gaseous and liquid fuels (Bridgwater and Peacocke, 2000) and has been described as the renewable energy source with the highest potential to contribute to the energy needs of modern society (Bridgwater, 2003). One technique used to convert biomass into valuable liquid derivatives also known as bio-oil is pyrolysis. Pyrolysis is a severe form of thermal cracking with subsequent rearrangement of fragments (Royal Dutch/Shell Group, 1983). The resulting bio-oil can then be used as fuel or for the production of chemicals and other “bio-based” products.

It is well known that triglyceride-based vegetable oils or animal fats have the potential to be a suitable source of fuel or hydrocarbons under the right processing conditions.

Pyrolysis of triglyceride materials is not as well established as other lignocellulosic biomass sources and it has been shown that these two types of bio-oils are entirely different in nature (Katikaneni et al., 1995c). The notion of vegetable oil-based fuels is not new. Research in this area is highly focused on the production of biodiesel through a transesterification reaction rather than on pyrolysis. It is the intent of this review to examine the production of fuels and chemicals through pyrolysis of triglyceride-based materials both with and without catalysts. The advantages and disadvantages of these processes and products in comparison to its main market competitors, bio-oils from other biomass sources and biodiesel will also be highlighted.

The disadvantages associated with using petroleum for fuels and chemicals have led to a surge in renewable energy research over the past several decades. Biomass, a naturally abundant resource, is gaining increasing recognition for its potential as a viable renewable energy source. In its broadest definition, the term biomass encompasses all natural matter of vegetables and animals (Karaosmanoglu et al., 1999) and can include a variety of natural and derived materials. It has also been described as all non-fossil-based living and dead organisms and organic materials that have intrinsic chemical energy content (Klass, 2004). Today, there is a large range of bio-products available for both consumers and industry, which have been manufactured at least in part from biomass. Examples include solvents, pharmaceuticals, resins, polymers, ethanol from corn, and inks, paints, and cosmetics from vegetable oils (Paster et al., 2003). Many of these products are only partly manufactured from biomass and still contain large amounts of petroleum derived products. It is believed that with continual improvement in biomass

conversion technologies and as more and more bio-products enter the market, a new “bio-industry” complete with “bio-refineries” will emerge and eventually all products currently produced from fossil sources will be replaced with bio-products produced entirely from biomass. An extensive report on this concept as well as the status of the bio-industry has been compiled for the U.S. Department of Energy (Paster et al., 2003).

### **2.1.1 BIOMASS CONVERSION TECHNOLOGIES**

Industrial bio-products can be categorized into four major areas including (1) Sugar and starch-based bio-products (2) Lipid-based bio-products (3) Gum-based and wood chemical-based (forest derivatives) bio-products; and (4) Cellulose derivatives, fibers and plastics (Paster et al., 2003). Energy can be harnessed from these biomass sources by physical, chemical, thermal, and biological methods. One of the most well known biological processes is fermentation of corn to produce ethanol. If the biomass feedstock is starch or sugar by-products then biochemical conversion techniques are almost always used. It has recently been shown that liquid fuels in the form of longer chain alkanes can be produced from biomass carbohydrates using aqueous phase processing with acid catalysts (Huber et al., 2005). For other types of biomass feed, thermo-chemical conversion methods are preferred. Thermo-chemical conversion techniques represent one of the most common and convenient methods of harnessing energy from biomass. Common examples include direct combustion, gasification, liquefaction, and carbonization. These processes are described elsewhere (Bridgwater and Peacocke, 2000; Bridgwater, 2003; Brown, 2003; Paster et al. 2003). Of these thermo-chemical

conversion techniques, gasification has attracted the greatest interest. There are still drawbacks of gasification including expensive set-up, costly storage and transport of the product, and a build-up of tar in the gasification unit (Bridgwater, 2003). The products of gasification, called biosyngas, can include CO, CO<sub>2</sub>, H<sub>2</sub>, CH<sub>4</sub>, and N<sub>2</sub>. These can be used in turbines and boilers or as feed gas for the production of liquid alkanes by Fischer-Tropsch synthesis (Boerrigter et al., 2002). The integrated biomass gasification/Fischer-Tropsch synthesis (BG-FT) approach appears promising as individually both technologies are well established; however, problems exist with the combination of these technologies. One of the main problems with this approach is effective cleaning of the biosyngas prior to Fischer-Tropsch synthesis (Boerrigter et al., 2002).

Liquefaction processes result in a liquid product, which can be easily stored and transported and require lower process temperatures. Due to these advantages, it is increasingly evident that liquid products offer more potential for the production of bio-based products than gas products and this is reflected in the rapid development of these processes and the large amount of research in this area. Examples of liquefaction processes include high temperature pyrolysis, high pressure liquefaction and 'ultra' or 'flash' pyrolysis. The other notable research area to mention is the production of biodiesel through the transesterification of vegetable oils and animal fats. This is an example of a chemical process that results in a mixture of alkyl esters that can be used as a diesel fuel substitute. The production of biodiesel as well as the pyrolysis of lignocellulosic biomass to produce bio-oil represent two major areas of renewable energy

research and will be discussed further in subsequent sections. Ethanol production via fermentation is a biological method and is beyond the scope of this thesis.

### **2.1.2 PYROLYTIC OILS FROM BIOMASS (BIO-OIL)**

Pyrolysis is an alternative to gasification and is becoming an increasingly popular option for converting biomass to solid, liquid, and gaseous fuels. The advantages of pyrolysis include the fact that it is simple and inexpensive to construct (Onay and Kockar, 2004). The literature on pyrolysis of biomass to produce pyrolytic oils is vast and is summarized in several review articles (Bridgwater and Peacocke, 2000; Bridgwater, 2003; Yaman, 2003) and book (Brown, 2003)

The application of heat to biomass will yield pyrolytic products with gaseous, liquid, and solid fractions, the proportions of which are heavily dependent on the pyrolysis conditions. The liquid or oil fraction is commonly called pyrolytic oil or bio-oil. Slow pyrolysis, which employs lower process temperatures and longer reaction times, favors charcoal production (Karaosmanoglu et al., 1999; Bridgwater, 2003; Yaman, 2003). Currently, most research is focused on maximizing the yield of liquid product as opposed to char. The liquid pyrolytic product can be easily stored and transported, readily upgraded and refined to produce high quality fuels, and may contain chemicals in economically recoverable amounts (Karaosmanoglu et al., 1999). It can be maximized by using short residence times (generally less than a few seconds) and high heating rates (Yaman, 2003; Onay and Kockar, 2004) that characterize the fast pyrolysis method.

Temperatures are approximately 500 °C (Bridgwater, 2003). A comprehensive compilation of fast pyrolysis technologies is presented by Bridgwater and Peacocke (2000).

#### **2.1.2.1 Bio-oil properties**

Fast pyrolysis yields up to 80 wt % liquid on dry feed (Bridgwater and Peacocke, 2000). Gaseous products consisting of aerosols, true vapors, non-condensable gases, and solid char make up the balance. The crude pyrolysis liquid or bio-oil, is dark brown in color, approximates to biomass in elemental composition and is a complex mixture of oxygenated hydrocarbons and an appreciable amount of water (Bridgwater, 2003). One of the main drawbacks of the bio-oil is that the composition of the pyrolytic oils is very similar to that of the original biomass and is very different from petroleum derived fuels and chemicals. The term biomass encompasses such a large range of feeds that the characteristics of the bio-oil can vary greatly depending on the starting material. The primary disadvantages of using the bio-oil as a diesel fuel most notably include the low HHV (Higher heating value), which is approximately 40 % less than that of fuel oil, its high viscosity, and substantial solids content (Bridgwater, 2003). As well, bio-oil typically contains up to 25 wt % water that cannot be readily separated (Bridgwater, 2003). This causes miscibility problems with conventional fuel oils and as a result, blends cannot be achieved. Pyrolysis oils have also been described as acidic, corrosive, polar, thermally unstable, and highly oxygenated (Kantikaneni et al., 1995c).

### **2.1.2.2 Bio-oil applications**

Bio-oil can be used as a liquid fuel or for the production of chemicals. An overview of applications of pyrolytic oils from biomass is presented in a recent review article (Czernik and Bridgwater, 2004). Fast pyrolysis has achieved commercial success for the production of chemicals and continual advancements are being made for upgrading the oils into useable transportation fuels. Pyrolysis oils can be subjected to upgrading and deoxygenation techniques such as hydrotreating and catalytic vapor cracking over zeolites to produce high grade transportation fuels (Chantal et al., 1984; Evans and Milne, 1988; Horne and Williams, 1994). The products are typically comparable to high grade gasolines and contain increased amounts of aromatics and decreased amounts of oxygen. Potential renewable chemicals from bio-oil include phenolics and cyclic ketones for resins and solvents, levoglucosan and levoglucosenon for polymers, and aromatic hydrocarbons for fuel and solvents (Elliot, 2004).

Research in the area of biomass pyrolysis is relatively advanced and there has been significant process development. Many fast pyrolysis processes are operating on a pilot or commercial scale (Bridgwater, 2003; Bridgwater and Peacocke, 2000; Elliot, 2004). Although bio-oil production from pyrolysis of biomass has been proven on a commercial scale and is a very promising option for production of renewable chemicals and fuels, there are still barriers to widespread use and commercialization. These barriers are both economic and technological and are described in several articles (Bridgwater, 2004; Czernik and; Elliot, 2004; Klass, 2004).



### **2.1.3 VEGETABLE OIL (TRIGLYCERIDE-BASED) FUELS**

Alternative feeds for the production of fuels from biomass are triglyceride-based agricultural fats and oils. Fats and oils are primarily water insoluble, hydrophobic substances in the plant and animal kingdom that are made up of one mole of glycerol and three moles of fatty acids and are commonly referred to as triglycerides (Sonntag, 1979). Vegetable oils are comprised almost completely of triglycerides and small amounts of mono- and diglycerides. These materials can be pyrolyzed to produce hydrocarbon rich liquid fuels and may have the potential to supplement a fraction of petroleum-based distillates and petrochemicals (Graboski and McCormick, 1998). Advantages of using vegetable oils include their liquid nature, which is convenient for transport and processing, and their high heat content, which is close to 90 % of diesel fuel (Karaosmanoglu, 1999). As well, vegetable oil fuels are pH neutral, contain no water, and are relatively stable (Katikaneni et al., 1995c).

The feasibility of using triglycerides as a source of energy was realized nearly a century ago when Rudolph Diesel demonstrated that vegetable oils could be used to run engines (Shay, 1993). In the past, widespread use and commercialization of vegetable oil fuels has been hindered by economics and poor properties (Knothe et al., 1997). Historically, petroleum derived fuels have been cheaper to produce. The high cost of virgin vegetable oils, which have high value in the edible oil market, is a main contributor to the overall economics of vegetable oil fuels. Recently crude oil prices have been \$70-80 US/barrel making vegetable oil fuels, namely biodiesel, more economically feasible. If oil prices

continue to rise biodiesel may become economically competitive with diesel.

Furthermore, if lower value oils such as waste oil or agricultural residues could be used as feedstock for biodiesel production, economics could be improved further. A recent review on using waste cooking oil as a source for biodiesel has recently been published (Kulkarni and Dalai, 2006). Besides economic feasibility, direct use of vegetable oils as diesel fuel has not been successful due to poor properties such as low volatility, reactivity of the unsaturated molecules, and high viscosity, which can lead to coking on engine injectors, carbon deposits, and plugged orifices during prolonged engine performance evaluations (Ali and Hanna, 1994; Karaosmanoglu, 1999; Tat and Van Gerpen, 2000; Demirbas, 2003a). Vegetable oils are suitable for diesel fuel because of their molecular structure and high energy content. Long-chain, saturated, unbranched hydrocarbons are especially suitable for diesel fuels (Knothe et al., 1997). Generally, the heat content of raw fats and oils is approximately 80-90 % of No. 2 diesel fuel (Ali and Hanna, 1994; Knothe et al., 1997; Ma and Hanna, 1999). Vegetable oils represent a promising alternative fuel source if these disadvantages can be overcome; however, the properties of unprocessed vegetable oils must be significantly improved before they can be used as fuel or petrochemical feedstock. Typically, four methods are used to improve the properties of vegetable oils and fats. These methods include (1) dilution with diesel fuel or solvents, (2) microemulsification, (3) transesterification, and (4) pyrolysis (Ali and Hanna, 1994; Knothe et al., 1997; Ma and Hanna, 1999). The two most popular techniques are transesterification and pyrolysis; however, the focus has been on the production of biodiesel via transesterification.

#### **2.1.4 BIODIESEL**

Vegetable oils and animal fats can be transesterified to produce what is commonly referred to as biodiesel. In past literature, the term biodiesel has been used to describe a variety of different products including neat vegetable oils, blends of conventional diesel fuel with vegetable oils, tallow and their esters or the alkyl esters of vegetable oils and animal fats (Knothe et al., 1997). It is now formally defined as a “fuel comprised of mono-alkyl esters of long chain fatty acids derived from vegetable oils or animal fats, designated B100” (ASTM D6751-03a, 2005). These alkyl esters are produced by transesterification reactions. During transesterification one mole of triglyceride molecules reacts with three moles of alcohol to produce a mixture of alkyl esters (biodiesel) and glycerol. Transesterification reactions have been investigated under different reaction conditions and with a variety of catalysts including acids, bases, lipases and non-ionic bases. For commercial production strong base catalysts such as sodium or potassium hydroxide are typically used; however, alkoxide catalysts have recently gained attention because they offer some advantages over base catalysts (Knothe et al., 2005). Several reviews have been written on these subjects (Ali and Hanna, 1994; Schuchardt et al., 1998; Ma and Hanna, 1999; Kann et al., 2002; Knothe et al., 1997, 2005; Pinto et al., 2005). As with bio-oil there is extensive biodiesel literature available. Some excellent review articles are cited in the following sections and for further information readers should refer to “The Biodiesel Handbook” (Knothe et al., 2005) and “Biodiesel: Growing a New Energy Economy” (Pahl , 2005).

#### **2.1.4.1 Biodiesel applications**

Biodiesel is primarily used as a diesel fuel substitute or in a diesel fuel blend but it can also be used as a feedstock in the chemical industry. It is utilized in farm equipment and military vehicles and is available commercially across the United States (National Biodiesel Board, 2005). Biodiesel also has the potential to be used for other chemical applications. They can have application as non-ionic surfactants or as emulsifying, thickening, and plastifying agents (Schuchardt et al., 1998). The glycerol by-product can be sold and used in applications such as cosmetics, pharmaceuticals, food, lacquers, resins, plastics, and explosives (Schuchardt et al., 1998). However, if biodiesel production steadily increases as expected then glycerol will continue to drop in value due to excess supply. Another issue with glycerol from biodiesel is that it contains methanol that can't be fully separated from the biodiesel product (Knothe et al. 2005).

#### **2.1.4.2 Biodiesel properties**

There are a variety of different properties, which are used to assess the quality of biodiesel. Some of these properties are the same as the properties used to assess diesel fuel quality such as combustion characteristics and cleanliness, while others pertain specifically to biodiesel such as the glycerine content, glyceride content, iodine value, and acid value. Descriptions of these properties and their importance in biodiesel quality are described elsewhere (Knothe et al., 1997, 2005; ASTM D6751-03a, 2005). In the U.S., biodiesel standards are outlined in ASTM D6751. In Europe, biodiesel standards

(for use as an automotive fuel) are outlined in EN 14214 and apply to all countries that are members of the European Committee for Standardization (CEN). For a comprehensive list of various worldwide standards as well as descriptions of some of the important properties refer to the Appendix B of The Biodiesel Handbook (Knothe et al., 2005). There have been numerous studies conducted assessing the properties of biodiesel using different feeds and reaction parameters and comparing them to conventional diesel fuel. A comprehensive review conducted by Graboski and McCormick (1998) lists typical properties of various biodiesels. Further information on the properties of biodiesel can be found in extensive reviews published by Knothe et al. (1997), Ma and Hanna (1999), Srivastava and Prasad (2000), Kann et al. (2002), and Demirbas (2003b).

Typically, biodiesel easily meets the cetane requirement for petroleum diesels, an indicator of diesel combustion and quality, and can be used in a regular diesel engine with little or no modification to the existing engine. As well, many harmful emissions, which are a major concern of fossil fuel combustion, are reduced. Biodiesel also exhibits superior lubricity to conventional diesel (Knothe and Steidley, 2005). Lubricity has recently been added to the ASTM diesel fuel standards (ASTM D975) and is becoming more of an issue because the new low sulfur diesels, required for regulatory reasons, exhibit low lubricity resulting in failure of fuel injectors and pumps (Knothe and Steidley, 2005). Another significant advantage of biodiesel is its net positive energy balance. Life-cycle analysis of biodiesel has shown that approximately 3.2 units of energy are generated for every unit of fossil energy used to produce the fuel (Sheehan et al. 1998).

Although biodiesel shows great promise as a renewable, alternative fuel it is important to note that there are still disadvantages associated with its production and use. Biodiesel exhibits poor cold flow properties, which can be problematic for engine performance and increased NO<sub>x</sub> emissions. Biodiesel contains oxygen, which may not be desirable for certain applications. The presence of oxygen lowers the heat content as shown by the heating values of biodiesel, which are 9-13 % lower than those of conventional diesel fuels on a mass basis (Demirbas, 2003a) and can also cause stability problems. It is well known that vegetable oil derivatives are prone to deterioration through hydrolytic and oxidative reactions. A comprehensive review on oxidative stability of biodiesel is presented in Chapter 6 of The Biodiesel Handbook (Knothe et al., 2005). Bio-oil and biodiesel represent very promising alternative fuels; however, there still are some drawbacks associated with each of the products, which may not be desirable depending on the application. As such, there is still opportunity for development of other renewable fuels and chemicals.

## **2.2 PYROLYSIS (THERMAL CRACKING) OF TRIGLYCERIDES FOR FUELS AND CHEMICALS\***

Pyrolysis or thermal cracking of triglyceride materials represents an alternative method of producing renewable bio-based products suitable for use in fuel and chemical

---

\* A version of this section has been previously published in Maher, K.D. and Bressler D.C. 2007. Pyrolysis of Triglycerides for the Production of Renewable Fuels and Chemicals. *Bioresource Technology* 98, 2351-2368.

applications. This option is especially promising in areas where the hydroprocessing industry is well established because the technology is very similar to that of conventional petroleum refining. There are significant advantages of this type of technology over transesterification including lower processing costs, compatibility with infrastructure, engines, and fuel standards, and feed stock flexibility (Stumborg et al.,1996). More importantly, the final products are similar to diesel fuel in composition. The literature on pyrolysis of triglycerides was reviewed and the research was divided into catalytic and non-catalytic processes. Thermal cracking of both the whole triglyceride molecule and components of the triglyceride molecule including fatty acids and fatty acid salts are discussed below. Catalytic cracking is discussed in section 2.3.

### **2.2.1 PYROLYSIS OF TRIGLYCERIDES**

There are several studies that have investigated the thermal cracking of triglycerides. These studies fall into two categories. One focuses on pyrolysis of model triglycerides for food science research (Crossley et al., 1962; Nawar, 1969; Kitamura, 1971; Nichols and Holman, 1972; Higman et al., 1973) while the other is devoted to cracking vegetable oils and fats for fuel applications (Egloff and Morrell, 1932; Egloff and Nelson, 1933; Chang and Wan, 1947; Alencar et al., 1983; Neihaus et al., 1986; Schwab et al., 1988; Idem et al., 1996; Dandik and Aksoy, 1998a; Fortes and Baugh, 1999, 2004; Lima et al., 2004; Adenbanjo et al., 2005;).

Model triglycerides including trilaurin (Kitamura, 1971), tripalmitin (Kitamura, 1971; Higman et al., 1973) and tristearin (Higman et al., 1973) have been subjected to pyrolytic conditions to determine reaction products and elucidate thermal decomposition pathways. These studies were mainly conducted for food science research; however, reaction products were reported. Typical reaction products included hydrocarbons, carboxylic acids, ketones, esters, and acrolein. Studies involving non-catalytic pyrolysis of vegetable oils for fuel span over the past century. Examples of early work include the cracking of cottonseed oil (Egloff and Morrell, 1932) and Alaskan fur seal oil (Egloff and Nelson, 1933). These studies were conducted at elevated temperatures (445 °C-485 °C) and under pressure 0.93-1.3 MPa (135-200 psi) and produced between 57-60 % gasoline range hydrocarbons. In 1947, motor fuels were produced from Tung oil on a large scale in response to potential fuel shortages during the war (Chang and Wan, 1947). The system was modeled after petroleum cracking processes from America and a commercial crude oil yield of 70 % (v/v) of the original tung oil was reported. Twenty-five percent (volume basis) of this crude oil was reported to be gasoline. Thermal cracking was loosely categorized as (1) destructive distillation and subsequent cracking of the vapors; (2) direct thermal cracking with or without a catalyst; and (3) cracking of soaps. Political and economic factors during the last three decades have resulted in a renewed interest in pyrolysis of vegetable oils for fuel production. Advances in instrumental and analytical techniques have allowed better characterization of reaction products and understanding of reaction mechanisms associated with the thermal decomposition of triglycerides.



Cracking studies have typically been carried out in batch reactors at temperatures ranging from 300-500 °C and atmospheric pressures. The organic phase of the resulting bio-oil is typically collected and analyzed. Feeds have included a range of plant and vegetable oils including tung oil (Chang and Wan, 1947), sunflower oil (Schwab et al., 1988), safflower oil (Schwab et al., 1988), canola oil (Idem et al., 1996), soybean oil (Lima et al., 2004), palm oil (Lima et al., 2004), macauba fruit oil (Fortes and Baugh, 1999, 2004), used cooking oil (Dandik and Aksoy, 1998a), castor oil (Lima et al., 2004), and various tropical vegetable oils (Alencar et al., 1983). In 1983, Alencar et al. studied the pyrolysis products of piqui, babbassu and palm oils. The cracking reactions were carried out at 300-500 °C and atmospheric pressure. The results show that the chief products were alkanes and 1-alkenes (Alencar et al., 1983). Schwab et al. (1988) simultaneously cracked and distilled soybean and high oleic safflower oil through destructive distillation. Seventy-seven percent of the soybean oil and 79 % of the high oleic safflower oil were collected as distillates and the primary products included alkanes, alkenes, aromatics, and carboxylic acids with carbon numbers ranging from 4 to greater than 20. The percentage of aromatics ranged from 1.9-2.3 % and carboxylic acids from 9.6-16.1 %. The fuel properties of the pyrolysates were tested and it was found that pyrolysis resulted in products with lower viscosity and higher cetane values than the parent oil indicating that this process improved the properties of the oils. Lima et al. (2004) studied the pyrolysis of soybean, palm tree, and castor oils from 350-400 °C. The pyrolysis products were distilled into four fractions and the heavy fraction (distillation temperature >200°C) was analyzed. It was found that the pyrolysis products of the palm oil, which contains a higher percentage of saturated fatty acids, contained the largest heavy fraction. The

primary products formed included hydrocarbons and oxygenated organic compounds such as alkanes, alkenes, alkadienes, and carboxylic acids. No aromatics were detected, which is contrary to previous results (Schwab et al., 1988).

The aforementioned studies were conducted in batch reactors for research purposes. Batch processes can be impractical in larger scale operations as they require clean-up and charging of the feed after each run and often experience low throughput and frequent interruptions (Idem et al., 1996). Idem et al. (1996) studied thermal cracking of canola oil in a flow type reactor over a fixed bed of inert materials. Pyrolysis was carried out at temperatures between 300-500 °C and atmospheric pressure with gas hourly space velocities ranging from 3.3-640 h<sup>-1</sup>. The effect of steam was also investigated. Results showed that conversions ranged between 54-100 % and were heavily dependent on operating variables. The products essentially consisted of C<sub>4</sub> and C<sub>5</sub> hydrocarbons, aromatic and C<sub>6</sub> aliphatic hydrocarbons, and C<sub>2</sub>-C<sub>4</sub> olefins as well as a diesel like fuel and hydrogen. Earlier work by this research group showed very low oil conversions (14 %) and little gas production even though the conditions and reactor were similar. Twenty-six percent of the liquid products consisted of C<sub>6</sub>-C<sub>12</sub> non-aromatic hydrocarbons. No aromatic compounds were detected in the liquid fraction.

Many of the feeds that have been tested have high value in other markets such as the edible oil market making these processes uneconomical. Pyrolysis of waste oils may help alleviate this problem. The conversion of used cooking oil to fuel and chemical feedstock through use of a fractionating pyrolysis reactor has been investigated (Dandik

and Aksoy, 1998a). Used cooking oil was fed to a special fractionating pyrolysis reactor at temperatures of 400 °C and 420 °C for approximately 180 min. The pyrolysis oil was found to contain a variety of hydrocarbons in the C<sub>5</sub>-C<sub>17</sub> range including paraffins, olefins and their isomers, aromatics, cycloparaffins, and cycloolefins. It was found that it was possible to produce high concentrations of liquid hydrocarbons in the gasoline boiling range in high conversions, without the aid of a catalyst.

Most studies involving the pyrolysis of vegetable oils are generally conducted at temperature ranges between 300-500 °C with longer residence times. They do not necessarily represent true “fast or flash pyrolysis”, which is generally characterized by temperatures around 500 °C and reaction times in the order of seconds. Fortes and Baugh (1999, 2004) studied the pyrolysis of macauba fruit oil under conditions more representative of fast pyrolysis. In comparison to other studies on the pyrolysis of triglyceride-based oils, the temperatures were high (400-1000 °C) and the times were very short (10-30 seconds). The main products were found to be aldehydes, alkenes, and carboxylic acids and the secondary products consisted of alkanes, cycloalkanes, and unknowns.

Only recently have studies been published involving the pyrolysis of fat instead of vegetable oil feeds. Adebanjo et al. (2005) pyrolyzed lard in a continuous microreactor loaded with different sized quartz chips at atmospheric pressure and temperatures of 600 °C and 800 °C. The lard was heated until liquefied and fed at varying flow rates with

nitrogen gas. The results showed that up to 61 wt % yield of liquid product could be obtained and that a portion of this liquid fraction resembled diesel fuel.

### **2.2.2 PYROLYSIS OF FATTY ACID SOAPS**

Although the thermal cracking of triglycerides has been studied, the cracking behavior of fatty acids, a major component of the triglycerides, and fatty acid soaps have not been studied extensively. In one study (Alencar et al., 1983), oleic acid was pyrolyzed; however, only 11.27 % (v/v) of the pyrolysis products were accounted for in the form of cycloalkanes. In a different study (Jaw et al., 2001), the thermal decomposition behavior of stearic acid was analyzed using thermogravimetric and differential thermal analysis and kinetic parameters such as activation energy were determined.

There have been some studies conducted on the thermal cracking of fatty acid salts or soaps of various oils (Chang and Wan, 1947; Hsu et al. 1950; Fortes and Baugh, 1994; Demirbas, 2002). Soaps are created via saponification of a fat with an alkali and the products include glycerin and vegetable oil soap. In the early half of the twentieth century several studies were conducted on the thermal cracking of fatty acid soaps; however, complete chemical data was not given (Hsu et al., 1950). In 1947, large scale thermal cracking of tung oil calcium soap was reported (Chang and Wan, 1947). The tung oil was saponified with lime and the calcium soap was thermally cracked to yield a diesel like fuel and small amounts of gasoline and kerosene. In a similar study, it was found that cracking the calcium salts of tung oil and stearic acid resulted in materials

resembling petroleum products (Hsu et al., 1950). There were differences in the products of the two types of salts. The products from the cracked tung oil salt resulted in 41.5 % cracked distillate and 48 % coke, while the cracking of stearic acid salts resulted in a higher yield of distillate (76.0 %) and a much lower yield of coke (17.3 %). From this data, reaction mechanisms were proposed. More recently, Fortes and Baugh (1994) developed a method for analyzing calcium soap pyrolysates for hydrocarbon, ketone, and aldehyde fractions. They found that aside from the presence of some ketones, the organic phase of the pyrolysates had similar composition to diesel fuel.

These studies show that high conversions and reasonable yields of diesel like fuel can be obtained from direct thermal cracking of triglycerides. There are still undesirable, oxygenated compounds present in the products and thus researchers' focus has shifted to catalytic cracking to increase conversion and liquid yield and to improve product properties. For this thesis project the focus is on thermal or catalytic cracking of protonated fatty acids. Studies in this area are discussed in Section 2.5.

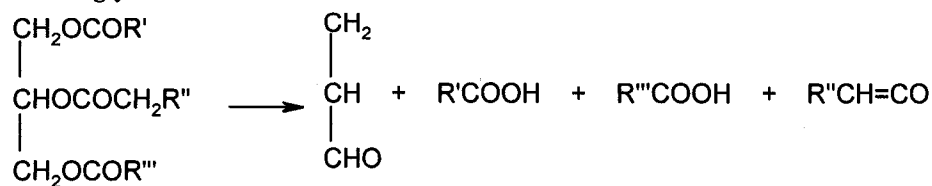
### **2.2.3 REACTION MECHANISMS**

There have been studies conducted on the decomposition of both saturated and unsaturated triglycerides during the applications of heat (Crossley et al., 1962; Nawar, 1969; Kitamura, 1971; Higman et al., 1973; Lipinski et al., 1985). It is well recognized that at 300 °C the gross pyrolysis of fats results in the formation of fatty acids and acrolein. At higher temperatures (400-500 °C) cracking occurs producing short chain

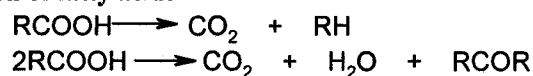
hydrocarbons (Crossley et al., 1962). The mechanisms involved in thermal cracking of saturated triglycerides have been studied (Chang and Wan, 1947; Alencar et al., 1983;). Chang and Wan (1947) proposed a reaction scheme (Figure 2.1) for the pyrolysis of saturated triglycerides, which includes 16 types of reactions. It is believed that the larger part of the acids, acrolein, ketenes formed in equation (1) are rapidly decomposed according to equations (2) and (3) and that equations (6) and (11) are chiefly responsible for the formation of hydrocarbons constituting liquid fuels, especially in the gasoline fraction. Based on the scheme proposed by Chang and Wan (1947) and on results by Greensfelder et al. (1949), Alencar et al. (1983) also proposed a scheme for the cracking of saturated triglycerides. The scheme is presented in Figure 2.2. The cracking of the triglyceride produces free radicals (A)  $\text{RCOO}\cdot$  and (B)  $\text{RCH}_2\text{O}\cdot$ . The odd n-alkanes and 1-alkenes are formed by decarboxylation of Radical (A) and then by subsequent disproportionation and ethylene elimination. The even series of alkanes and alkenes are produced by the loss of a ketene from radical (B) and followed again by disproportionation and ethylene elimination.

Because plant oils also contain unsaturated components, it is useful to study the impact of heat on unsaturated fatty acids. In 1988, Schwab et al. proposed a mechanism (Figure 2.3) to account for the formation of alkanes, alkenes, alkadienes, aromatics, and carboxylic acids from the pyrolysis of unsaturated triglycerides. Generally, the thermal decomposition of these structures proceeds through either a free radical or carbonium ion mechanism as previously proposed and generally follows the Rice free radical theory

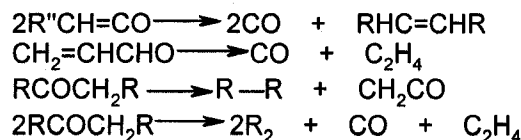
**(1) Decomposition of the glyceride**



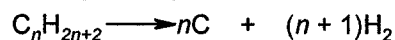
**(2) Decomposition of fatty acids**



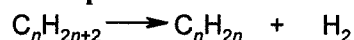
**(3) Decomposition of ketenes and acrolein**



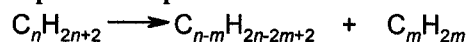
**(4) Decomposition into elements**



**(5) Dehydrogenation of paraffins**

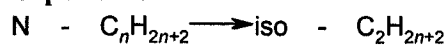


**(6) Splitting/Decomposition of paraffins**

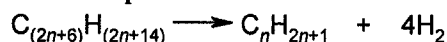


**(7) Alkylation of paraffins, the reverse of (6)**

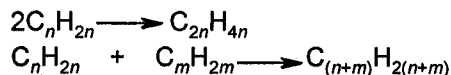
**(8) Isomerization of paraffins**



**(9) Aromatic cyclization of paraffins**



**(10) Polymerization of olefins**



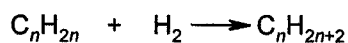
**(11) Depolymerization of olefins, reverse of (10)**

**(12) Decomposition of olefins to diolefins**

**(13) Decomposition of olefins to acetylenic hydrocarbons**

**(14) Aromatization or cyclization of olefins**

**(15) Hydrogenation of olefins**



**(16) Isomerization of olefins**

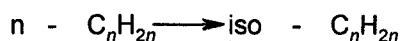


**Figure 2.1** Decomposition of Triglycerides (Chang and Wan, 1947)

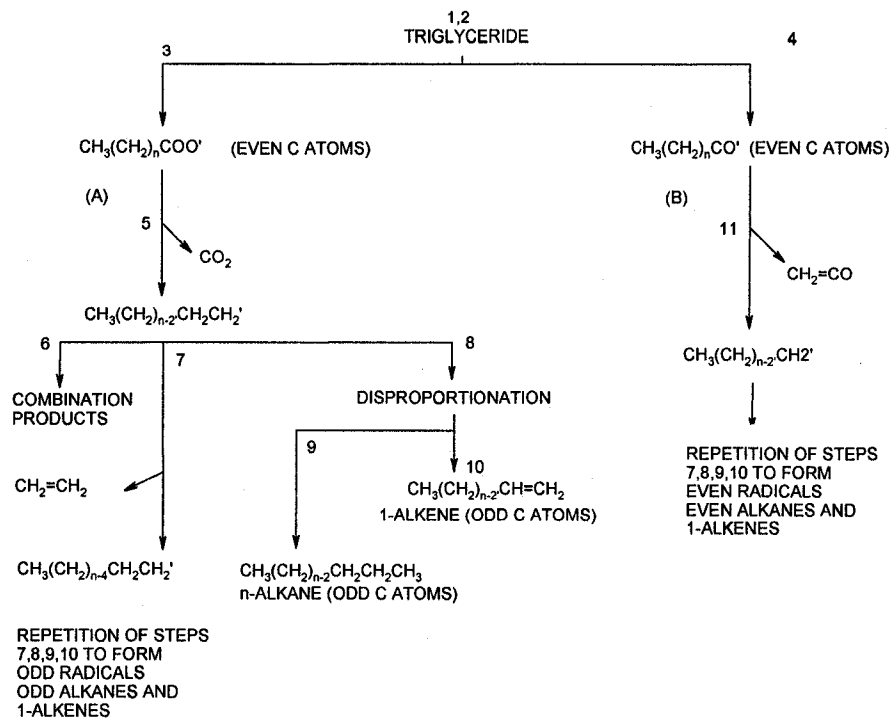


**Figure 2.2** Reaction Mechanism for the Pyrolysis of Saturated Triglycerides (Alencar et al., 1983)

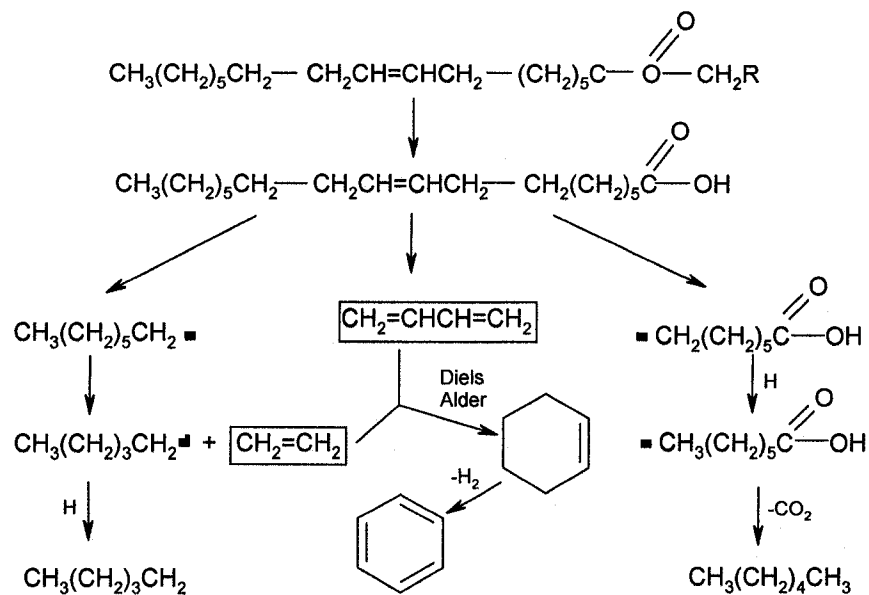


**Figure 2.3** Reaction Mechanism for the Pyrolysis of Triglycerides (Schwab et al., 1988)



modified by Kossiakoff (Alencar et al., 1983). The formation of alkanes and alkenes can be attributed to the generation of an  $\text{RCOO}\cdot$  radical through triglyceride cleavage followed by decarboxylation. Unsaturated sites enhance cleavage at the C-C double bond at a position  $\alpha,\beta$  to the unsaturation and this cleavage is a dominant reaction. The formation of aromatics is supported by Diels-Alder ethylene addition of a conjugated diene and carboxylic acids are most likely formed through cleavage of the glycerol moiety as suggested by Nawar (1969). This also results in the formation of acrolein, which was also detected in the pyrolysis of sunflower oil (Schwab et al., 1988).

In reality, vegetable and plant oils contain a complex mixture of unsaturated and saturated triglycerides. Idem et al. (1996) studied the thermal cracking of canola oil in the presence and absence of steam and postulated a reaction scheme to account for the thermal cracking of both the unsaturated and saturated components. This scheme is more complex but builds on mechanisms previously proposed (Alencar et al., 1983; Chang and Wan, 1947; Kitamura, 1971; Nawar, 1969; Nichols and Holman, 1972; Schwab et al., 1988). The reaction scheme is shown in Figure 2.4 and accounts for the formation of heavy oxygenated compounds including ketones, aldehydes, and esters, carbon monoxide and carbon dioxide,  $\text{C}_1\text{-C}_5$  straight and branched chain hydrocarbons, alcohols and dimethyl ether, diolefinic, cyclic and acetylenic hydrocarbon gases,  $\text{C}_6+$  aliphatic hydrocarbons, aromatics, heavy hydrocarbons, coke, and hydrogen during the cracking of canola oil in the absence of a catalyst. The degree of unsaturation of the triglyceride has a significant effect on the cracking behavior. For example, the radical intermediates that will eventually react to form  $\text{C}_1\text{-C}_5$  hydrocarbons can be produced via the decomposition

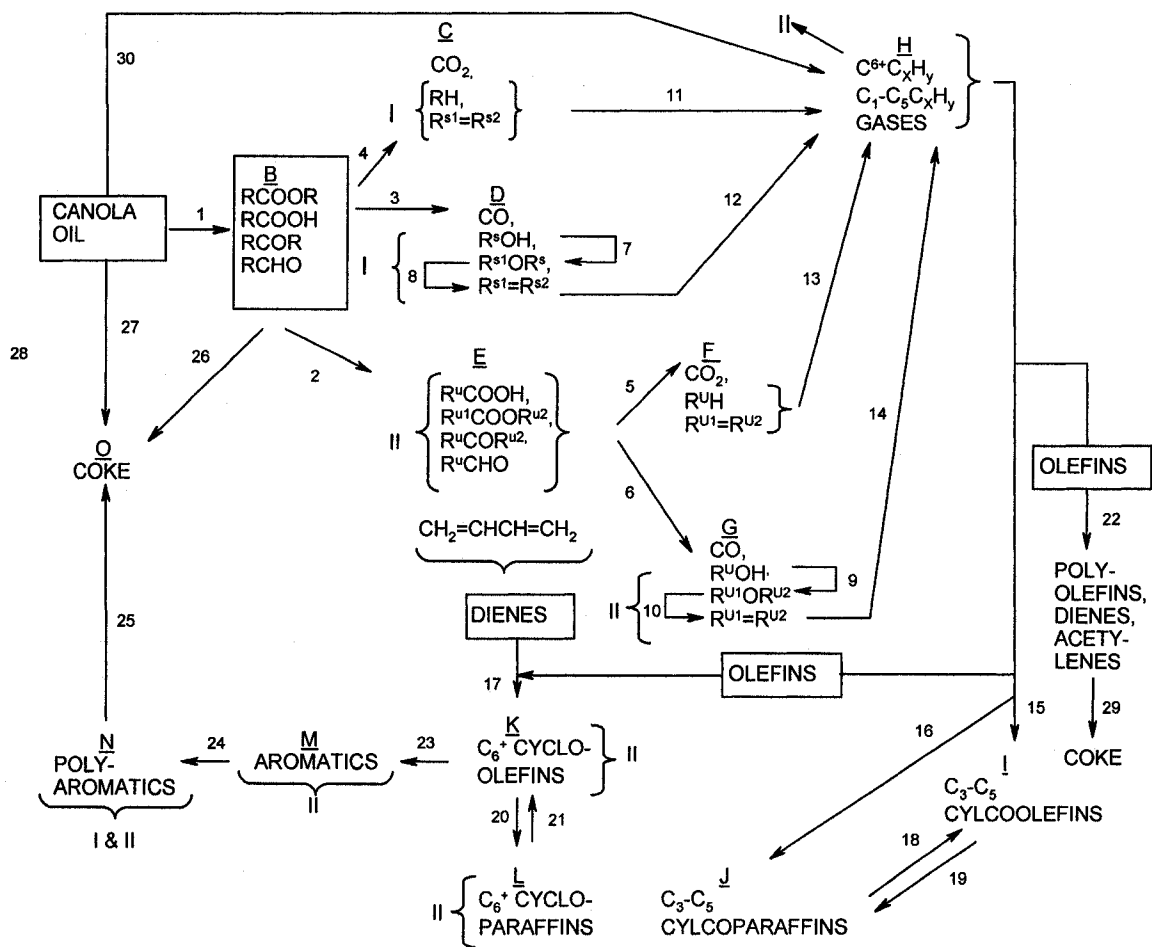


**Figure 2.4** Reaction Mechanism for the Pyrolysis of Saturated and Unsaturated Triglycerides (Idem et al., 1996)

of the heavily oxygenated compounds by different routes. Decarboxylation and decarbonylation can occur before or after the C-C bond cleavage. If the triglyceride is

unsaturated, the cleavage most likely occurs before the decarboxylation and decarbonylation. It has also been shown that C-C bond cleavage for unsaturated and saturated molecules results in different products (Idem et al., 1996).

These studies show the complexity of pyrolysis reactions and possible products. Cheng et al. (2004) recognized that historical studies have often neglected the possible control measures needed to form ideal products by selecting proper pyrolysis temperatures and conditions. In an attempt to better understand the pyrolysis of vegetable oils Cheng et al. (2004) studied the thermodynamics of vegetable oil process by computer simulation. The main findings were that cleavage of the C-O bond takes place at 288 °C and that scission of C=C takes place at 400 °C.

## **2.3 CATALYTIC CRACKING OF TRIGLYCERIDES FOR FUELS AND CHEMICALS\***

In most studies involving the conversion of triglycerides into hydrocarbons at high temperatures a catalyst is used and there is a rich body of literature in this area. A comprehensive list of early studies using a variety of different catalysts is outlined in US Patent 4,102,938 (Rao, 1978). Over the past several decades, a variety of conventional hydrotreating catalysts have been studied in the conversion of triglyceride materials to

---

\* A version of this section has been previously published in Maher, K.D. and Bressler D.C. 2007. Pyrolysis of Triglycerides for the Production of Renewable Fuels and Chemicals. *Bioresource Technology* 98, 2351-2368.

fuels. The two major groups of catalysts used include transition metal catalysts, which are common in the hydroprocessing industry, and molecular sieve type catalysts. The use of transition metal catalysts under high hydrogen partial pressures result in diesel like products while molecular sieve catalysts result in highly aromatic, gasoline type products. Pure insulator oxides, most notably activated alumina, and sodium carbonate represent two other groups of catalysts that have been used for these applications and will also be discussed.

### **2.3.1 ACTIVATED ALUMINA**

Pure insulator oxides including MgO, SiO<sub>2</sub> and Al<sub>2</sub>O<sub>3</sub> represent an important group of catalysts. In their pure state they are not notably acidic and their main activity is dehydration (Campbell, 1983). Alumina (Al<sub>2</sub>O<sub>3</sub>) can exist in several forms and depending on preparation method and treatment it can become activated (acidic) meaning it shows high catalytic activity. A common alumina catalyst is  $\gamma$ -alumina, which is prepared by heating and evaporating the water of a trihydrate initially formed by hydrolysis of sodium aluminate (Campbell, 1983). It has been shown that activated alumina is an effective catalyst for decarboxylation of fatty acids at atmospheric pressure and 450 °C (Vonghia et al., 1995) and has been used in a series of studies investigating the production of alkanes and alkenes from sewage sludge that contains triglycerides (Boocock et al., 1992a, 1992b). Triolein, canola oil, trilaurin, and coconut oil were pyrolysed over activated alumina at 450 °C under atmospheric pressure and the liquid product yields ranging from 65-79 % were found to be hydrocarbon mixtures containing

n-alkanes and n-alkenes. Elemental composition showed an absence of oxygen. Subsequent studies from the same group of researchers yielded similar results (Konar et al., 1994). Dos Anjos et al. (1983) showed that at temperatures of 300-350 °C crude and hydrogenated soya oil pyrolyzed over MgO and alumina resulted in only partial conversion to hydrocarbons. The products contained approximately 50 % carboxylic acids and 25-28 % hydrocarbons (Dos Anjos, 1983). Activated alumina is one of the catalysts used for cracking a range of vegetable oils in US Patent 5,233,109 (Chow, 1993). In this patent, it was found that the products consisted of gaseous and liquid hydrocarbons, water and coke, but that suitable fuel fractions could only be obtained with further fractional distillation. Some model work has been conducted using activated alumina catalysts to crack fatty acids. These studies are discussed in Section 2.5.

### **2.3.2 MOLECULAR SIEVE**

Molecular sieve catalysts are highly crystalline and porous and exhibit size selectivity. This means that only molecules of a certain size can pass through and therefore, aside from being highly reactive the pore size can be altered to obtain specific reaction products. There have been many studies which have used zeolite catalysts for conversion of triglyceride-based oils and fats to hydrocarbons (Weisz et al., 1979; Prasad et al., 1986a, 1986b; Dandik et al., 1998c; Twaiq et al., 1999, 2004; Katikaneni et al., 1995a, 1995b, 1995c, 1996; Sang et al., 2003, 2004). Zeolite catalysts are crystalline aluminosilicate materials based on a three dimensional network of  $AlO_4$  and  $SiO_4$  tetrahedrally linked through oxygen atoms (Campbell, 1983). Their crystalline structure and

tetrahedral shape offers significant advantages over amorphous silica-alumina catalysts. Localized regions of high electrostatic field associated with the presence of cations are highly reactive. This enhances catalytic activity and thus increases cracking. Pore size can be altered depending on what molecules are to be cracked and what reaction products are desired. When considering hydrocarbon cracking, an important zeolite catalyst is the ZSM-5. It is synthetic and its basic structure consists of layers of silica-alumina pentagon chains linked by oxygen atoms. In 1972, a new high-silica zeolite catalyst, HZSM-5, was discovered and has since been shown to have the ability to convert a remarkable range of materials to high-octane, aromatic, gasoline-like products (Milne et al., 1990). This catalyst has been used for the conversion of vegetable oils to gasoline boiling range compounds. It has been reported that the activity and selectivity of these catalysts depend on factors such as acidity, pore size and distribution, and pore shape (Twaiq et al., 1999). One of the first studies using the HZSM-5 catalyst to convert vegetable oils to hydrocarbons was conducted using corn and peanut oils (Weisz et al., 1979). The products were reported as percentages of fuel gas ( $C_1$  and  $C_2$  compounds), liquefied petroleum gas ( $C_3$  and  $C_4$  compounds), gasoline, and light distillate (jet fuel, kerosene, or light diesel and heating oils). A high degree of conversion to aromatics (benzene, toluene and xylene) was found in all cases. The product mixture was found to be comparable to high grade gasoline and with an octane number of 90-96 showing the potential of this type of catalyst to produce a high quality, renewable motor vehicle fuel.

One group of researchers has extensively studied the conversion of vegetable oils, primarily canola, over a variety of zeolite catalysts at a variety of reaction conditions

(Prasad et al., 1986a, 1986b; Katikaneni et al., 1995a, 1995b, 1995c, 1996;) and with the addition of steam (Prasad et al., 1986a; Katikaneni et al., 1995a). The catalysts used include HZSM-5 as well as a variety of hybrids. Reactions were carried out in fixed bed micro reactors at temperatures between 300-500 °C, atmospheric pressure and WHSV (weight hourly space velocities) between 1.8-3.6 h<sup>-1</sup>. Typical results showed high conversions (up to 100 wt %) of the canola oil with high concentrations of aromatics in the organic liquid product fraction. It was also shown that the HZSM-5 catalyst was the most effective type of zeolite catalyst for converting vegetable oil to gasoline range hydrocarbons (Katikaneni et al., 1995a, 1995b, 1995c).

The pyrolysis of used sunflower oil in a packed fractionation column of varying lengths has been studied using the HZSM-5 catalyst (Dandik et al., 1998). The temperature ranged between 400-420 °C and the amount of HZSM-5 catalyst used was varied. Nearly complete conversion (96.6 %) of the used oil and the maximum hydrocarbon yield (33 %) was obtained at the highest temperature, catalyst content, and lowest column length. The liquid hydrocarbon phases consisted of n-alkanes, alkenes, and only small amounts of aromatics. These results are not typical of similar reactions but were attributed to the fractionating batch reactor configuration used. A significant percentage of gasoline boiling range hydrocarbons (C<sub>5</sub>-C<sub>11</sub>) was also produced.

Significant work has been done in Malaysia to convert palm oil into liquid hydrocarbons (Twaiq et al. 1999, 2003a, 2003b, 2004; Yean-Sang et al., 2003, 2004) using mesoporous catalysts. In the first study by this research group (1999), palm oil was cracked in a fixed

bed microreactor at atmospheric pressure, temperatures ranging from 350-450 ° C and WHSV's between 1-4 h<sup>-1</sup>. The catalysts used were HZSM-5, zeolite B, USY (Ultra-stable Y), hybrids of the three and HZSM-5 impregnated with potassium. The main findings were that among the HZSM-5, Zeolite B and USY catalysts, the HZSM-5 had the highest conversion and gasoline yield, lowest coke formation, and had the highest selectivity for aromatics; however, it also had the highest yield of gaseous hydrocarbons. The potassium impregnated catalysts were shown to decrease the aromatic content of the gasoline product, likely due to a change in the acidity of the catalyst. The gasoline yield was shown to increase when the HZSM-5-USY hybrid catalyst was used.

The results of the aforementioned study provided that basis for several follow-up studies by this research group. Although HZSM-5 catalysts are promising, they still exhibit high gas formation, which will decrease the formation of the desired liquid fraction. Different types of catalysts have been studied in an attempt to minimize the gas fraction and maximize the liquid fraction. One option is mesoporous catalysts such as the MCM-41, which has shown to be selective for C5+ olefinic products (Twaiq et al., 2003a). The effect of pore size and surface area and percent of alumina in the catalyst on product distributions of cracked palm oil was studied (Twaiq et al., 2003a, 2003b). It was found that an increase in alumina increased catalyst acidity and activity to an optimum level; however, the activity was lower than the HZSM-5 catalyst. Overall, the mesoporous catalysts resulted in lower gas formation but were more selective for linear hydrocarbons in the diesel boiling range rather than gasoline range hydrocarbons (Twaiq et al., 2003a). It was also found that the surface area and pore size affected the selectivity for different



product types. Both the HZSM-5 and MCM-41 catalysts show desirable characteristics for converting palm oil to liquid hydrocarbons. The synthesis of these two catalysts to create a composite zeolite-mesoporous catalyst was also studied (Twaiq et al., 2004). The results of this study showed that the composite catalysts had good selectivity to the formation of aromatics. In a similar study the performance of HZSM-5, MCM-41, and the composite catalysts were compared (Yean-Sang et al., 2003). The composite catalyst resulted in the highest conversion (99 wt %) and highest gasoline yield. Design of experiment was also used to determine the effects of reaction variable and to optimize the reaction conditioned for the production of aromatic gasoline fractions (Yean-Sang et al., 2004). Reaction temperature, catalyst ratio, and WHSV were found to be important operating variables in terms of the final product distribution. The optimum yield of gasoline was found at a reaction temperature of 440 °C, fatty acid to catalyst ratio of 9.64 and WHSV of 3.66 h<sup>-1</sup>.

The use of zeolite catalysts has shown to be effective at converting triglyceride-based vegetable oils to liquid gasoline range hydrocarbons. These studies indicate that the nature of the catalyst significantly impacts the product distribution. It was recognized that although the HZSM-5 catalyst was shown to be highly effective, it still exhibited formation of gaseous products. In an attempt to minimize this fraction, mesoporous MCM-41 was used. A hybrid of these two catalysts was found to be most effective at maximizing the gasoline fraction.

### 2.3.3 TRANSITION METAL CATALYSTS

Transition metal catalysts have been used for the production of diesel-like hydrocarbons from triglycerides (Craig and Coxworth, 1987; Gusmao et al., 1989; Craig, 1991; da Rocha Filho et al., 1992, 1993; Craig and Soveran, 1993; Stumborg et al., 1996; Monnier et al., 1998;). These catalysts are traditionally used for hydroprocessing in the heavy oil industry at temperatures in the range of 350-450 °C and high pressures (1-25 MPa) in the presence of hydrogen. The formation of alkanes, alkylcycloalkanes, and alkylbenzenes during the catalytic hydrocracking of vegetable oils was investigated by da Rocha et al. (1992) using a NiMo/Al<sub>2</sub>O<sub>3</sub> catalyst in the presence of elemental sulfur (da Rocha Filho et al., 1993). The vegetable oils tested included maracuja, tucuma, buriti, babassu, and soybean oils and the primary reaction products consisted of alkanes with carbon numbers ranging from C<sub>11</sub>-C<sub>18</sub> (65.3-76.8 wt % of feed). Reactions were carried out in batch micro reactors at temperatures ranging from 350-450 °C and pressures between 7-14 MPa. In a similar study (da Rocha Filho et al., 1992) seringa and ucuuba oils were cracked using the same catalyst at 360 °C and 14 MPa (140 bars). Conversions of almost 100% were obtained and the primary products were found to be alkanes and cycloalkanes. The gas phase, aromatics, and acid values were not as significant. Vegetable oil cracking has also been studied in a batch reactor under high hydrogen partial pressure 1-20 MPa (10-200 bars) and at temperatures ranging from 350-400 °C. The corresponding products were essentially mixtures of n-alkanes.

Although vegetable oil fuel is considered an alternative source of energy, conventional refining technologies already in place in the petroleum industry may be used to convert the vegetable oils into hydrocarbons (Craig, 1991; Craig and Coxworth, 1987; Craig and Soveran, 1993; Stumborg et al., 1996). Craig and Coxworth (1987) used a conventional fluid catalytic cracking (FCC) bench scale unit and hydrocracking/hydrotreating techniques to convert canola oil into hydrocarbons. It was shown that the oil cracked readily and produced products with yields similar to conventional petroleum-based feedstocks in the FCC unit and that subsequent hydrotreating yielded fuels in the diesel boiling range (Craig and Coxworth, 1987). In a similar study funded by the Saskatchewan Research Council (SRC), Natural Resources Canada, and Agriculture and Agri-Food Canada, a conventional medium severity hydroprocess was used to convert canola oil into a super cetane product in the diesel boiling range (Stumborg et al., 1996). The process consisted of a combination of hydrocracking, hydrotreating, and hydrogenation. These processes are described in greater detail in Canadian patent 1,313,200 (Craig and Soveran, 1993) and US patent 4,992,605 (Craig, 1991).

The success of these studies has led to the commercialization of a “super cetane” product to be used as a diesel fuel additive. This technology was developed by CANMET Technology Center, a division of Natural Resources Canada. This technology utilizes conventional refining technology with different fatty feeds. The product is separated into three fractions: naphtha, middle distillates, and waxy residues. The middle distillate or super cetane has similar characteristics to diesel fuel and a cetane number of

approximately 100. It is composed primarily of straight chain hydrocarbons (Natural Resources Canada, 2005).

Tall oil is an alternative feed that can be used for the production of hydrocarbons using the aforementioned technologies. Tall oil has been subjected to similar hydrotreatments to produce diesel like fuel (Liu et al., 1998; Monnier et al., 1994; 1998). Tall oil differs in composition compared to other vegetable oils because it is composed of C<sub>18</sub> fatty acids as well as other compounds such as resin acids, diterpenic hydrocarbons, and diterpenic alcohols and aldehydes (Feng et al., 1993). The resulting product is a high quality cetane enhancer that can be used as a fuel additive.

#### **2.3.4 SODIUM CARBONATE**

Sodium carbonate catalyst has also been used in the pyrolysis of vegetable oils (Konwer et al., 1989; Zaher and Taman, 1993; Dandik and Aksoy, 1998b). Konwer et al. (1989) used solid sodium carbonate as a catalyst to produce liquid fuel from the pyrolysis of *Mesua ferrea L.* seed oil and the pure forms of its primary fatty acids including linolenic, linoleic, oleic, palmitic and stearic acids. Earlier studies by this research group showed that pyrolysis of *Mesua ferrea L.* oil in the presence of 1 % sodium carbonate and at 500 °C produced black pyrolytic oil similar to crude oil and that the fractions could be suitable for various applications including gasoline and diesel (Konwer et al., 1989). The unsaturated fatty acids produced significant concentrations of aromatics and lower concentrations of olefins, while the concentration of aromatics formed from the saturated

fatty acids was very low and the olefin yield was high (Konwer et al., 1989). Analysis of the saturated components of the pyrolysis oil, which comprised 20-25 wt % of both the saturated and unsaturated fatty acids, showed that the main products were n-alkanes. Sodium carbonate has also been used in pyrolysis of used sunflower oil in a reactor equipped with a fractionating packed column (Dandik and Aksoy, 1998b). Contrary to previous results (Konwer et al., 1989), this study showed very low concentrations of aromatics in the pyrolysis products. Conversions were lower than previous results (Konwer et al., 1989) and almost half of the feed formed coke-residual oil. The primary pyrolysis products consisted of liquid and gaseous hydrocarbons phases with lesser amounts of acids, water, H<sub>2</sub>, CO, and CO<sub>2</sub>. The liquid phase contained mostly C<sub>5</sub>-C<sub>11</sub> hydrocarbons (19.45-32.87 %) and the gaseous phase was mainly composed of C<sub>1</sub>-C<sub>3</sub> hydrocarbons (13.65-26.18 %). Cottonseed oil was pyrolyzed in the presence of 1 % sodium carbonate (Zaher and Taman, 1993). The thermally decomposed oil (approximately 70 wt % of the original oil) was collected and analyzed. Alkanes were the primary products accounting for nearly 70 % of the pyrolyzed oil. The products also contained 21.7 % aromatics.

Dandik and Aksoy (1999) compared the pyrolysis of used sunflower oil using sodium carbonate, silica-alumina, and HZSM-5 catalysts. At the conditions tested, the highest conversion (73.17 wt %) was obtained using the sodium carbonate as a catalyst. The sodium carbonate also resulted in the highest yield of liquid product primarily consisting of gasoline-range hydrocarbons.

A possible concern with sodium carbonate is that traces of sodium may be present in the product, impeding its use. In the literature reviewed, there were no reports of sodium present in the desired product, which was the organic oil. It is likely that the sodium carbonate first reacts with fatty acids to produce sodium salts, which are then further decomposed into hydrocarbons as shown by the results presented from Dandik and Aksoy (1998b) and Konwer et al. (1989).

### **2.3.5 REACTION MECHANISMS**

#### **2.3.5.1 Activated alumina catalysts**

The mechanism for the deoxygenation of triglycerides to aliphatic hydrocarbons over activated alumina has been investigated (Vonghia et al., 1995). Unlike other catalysts, most notably zeolites, where determination of conversion pathways can be complex, activated alumina is ideal for studying primary decomposition pathways because it deoxygenates the substrate solely to acyclic alkenes and some alkanes (Vonghia et al., 1995). It was concluded that triglyceride decomposition occurs initially via two mechanisms, either a  $\beta$ -elimination to produce carboxylic acids or a  $\gamma$ -hydrogen transfer mechanism to yield alkenes as observed elsewhere (Bahadur et al., 1995), both occurring through bonding of a carbonyl oxygen to a Lewis Acid site on the alumina catalyst. It is then postulated that the carboxylic acids form symmetrical ketones, which may undergo another  $\gamma$ -hydrogen transfer to produce monoalkenes and methyl ketones. The methyl ketones will eventually be converted to monoalkenes through an unknown mechanism followed by a dehydration or undergo the  $\gamma$ -hydrogen rearrangement. It is also believed

that the methyl ketone can isomerize into aldehydes, which are then oxidized to produce carboxylic acids. In order to better understand the cracking behavior and kinetics of catalytic conversion of triglycerides to hydrocarbons using an activated alumina catalyst, octanoic acid was used as a model compound in a series of cracking studies (Billaud et al., 2001, 2003). The results validated previous studies (Leung et al., 1995) and kinetic parameters were determined.

### **2.3.5.2 Molecular sieve catalysts**

It has been reported that when using catalysts, the primary reaction step in the decomposition of a triglyceride is still the thermal breakdown of the triglyceride into heavy oxygenated components such as ketones and aldehydes (Katikaneni et al., 1996) as was postulated and verified earlier (Chang and Wan, 1947; Alencar et al., 1983; Schwab et al., 1988; Idem et al., 1996). A reaction scheme for the catalytic cracking of canola oil over zeolite type catalysts has been proposed and is shown in Figure 2.5. After the thermal breakdown of the triglyceride molecule, the heavily oxygenated compounds are deoxygenated and then cracked into paraffins and olefins as a result of thermal and catalytic mechanisms (Figure 2.5 - equations 2 and 3). The subsequent conversions of the light olefins into C<sub>2</sub>-C<sub>10</sub> olefins, aromatics, and aliphatics (Figure 5 - equations 4 and 5) are due to catalytic mechanisms such as cyclization and aromatization of C<sub>2</sub>-C<sub>10</sub> olefins in the pores of zeolites (Katikaneni et al., 1996). Coke is then produced thermally or catalytically by the polymerization of large aromatics (Katikaneni et al., 1996).

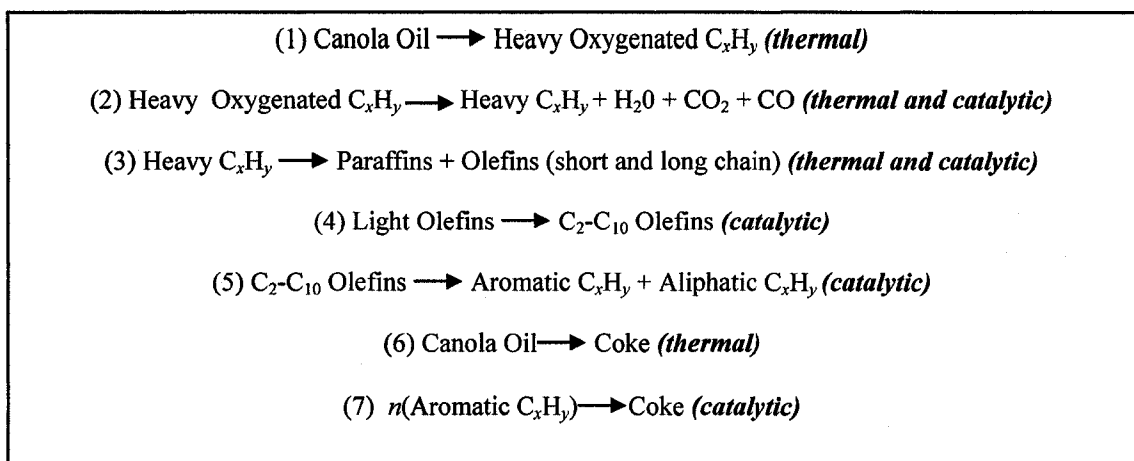


**Figure 2.5** Proposed Mechanism for the Catalytic Cracking of Canola Oil (Katikaneni et al., 1996)

## 2.4 PROPERTIES OF PYROLYZED TRIGLYCERIDES\*

Research on biodiesel and its properties is very comprehensive; however, research on the properties of bio-oils from the pyrolysis of triglyceride materials such as vegetable oils and animal fats is not as common. There have been numerous studies conducted on pyrolysis of vegetable oils; however, few go into detailed characterization of the properties. Furthermore, the range of products produced in these studies varies considerably depending on the reaction conditions and whether or not a catalyst was used. In some studies, the goal has been to produce gasoline range hydrocarbons and in others diesel range hydrocarbons. As well,

---

\* A version of this section has been previously published in Maher, K.D. and Bressler D.C. 2007. Pyrolysis of Triglycerides for the Production of Renewable Fuels and Chemicals. *Bioresource Technology* 98, 2351-2368.



some studies have separated the pyrolysis products by distillation and analyzed particular fractions.

#### **2.4.1 DIESEL**

Diesel fuel ranks second in usage, behind only gasoline, as fuel for internal combustion engines (Hochhauser, 2004). Diesel fuel quality is assessed by measuring various properties related to handling and storage, safety, ignition and combustion, and engine performance (Bahadur, 1994; Hochhauser, 2004; ASTM 975-04c, 2005;). These tests are outlined in ASTM D975. Table 2.1 outlines some of the major requirements for No. 2 diesel fuel from both ASTM and EN standards. No. 2 diesel is the grade most commonly used for smaller trucks and automobiles. The properties of the heavy fractions of pyrolysis oils from triglyceride materials both with and without catalysts have been investigated and compared to diesel fuel specifications (Neihaus et al., 1986; Schwab et al., 1988; Agra et al., 1992; Boocock et al., 1992; Stumborg et al., 1996). These pyrolytic oils were produced by direct thermal cracking (Neihaus et al., 1986; Schwab et al., 1988; Lima et al., 2004;), by hydroprocessing with transition metal type catalysts (Craig and Coxworth, 1987; Stumborg et al., 1996), catalytic pyrolysis with activated alumina (Boocock et al., 1992b), potassium hydroxide (Agra et al., 1992), sodium carbonate (Zaher and Taman, 1993), and calcium oxide (Megahed et al., 2004).

**Table 2.1** ASTM D 975 Requirements for Diesel Fuel (ASTM D 975-04c, 2006)

Property	ASTM Method	Grade No. 2-D S15
Flash Point, °C, min.	D 93	52
Water and Sediment, % vol, max.	D 2709	0.05
Distillation Temperature, °C, 90 % vol. recovered	D 86	
min.		282
max.		338
Kinematic viscosity, mm <sup>2</sup> /s at 40°C (104°F)	D 445	
min.		1.9
max.		4.1
Ramsbottom Carbon Residue on 10% distillation residue, % mass, max.	D 524	0.35
Ash, % mass, max.	D 482	0.01
Sulfur, % mass, max.	D 129	-
	D 2622	0.05
Copper Strip Corrosion Rating, max. 3 h at 50°C	D 130	No. 3
Cetane number, min.	D 613	40
One of the following properties must be met		
(1) Cetane Index, min	D 976-80	40
(2) Aromacity, % vol, max	D 1319	35
Lubricity, HFRR @ 60 °C, micron, max	D 6079	520

The cetane number was determined for the pyrolysis products of soybean oil (Lima et al., 2004 ; Neihaus et al., 1986; Schwab et al., 1988), palm oil (Lima et al., 2004), castor oil (Lima et al., 2004). The castor oil product was the only oil whose pyrolysis products exhibited a lower cetane value than the specified ASTM value of 40. The cetane number is related to ignition delay or the amount of time it takes for combustion to begin after fuel injection. Short ignition delays correspond to high cetane numbers, which indicate good combustion and high fuel quality.

The viscosity of the pyrolytic oil has also been studied (Neihaus et al., 1986; Schwab et al., 1988; Craig and Coxworth, 1987; Agra et al., 1992; Stumborg et al., 1996; Lima et al., 2004). Viscosity, a fuel's resistance to flow, is important in pump and fuel injector performance. If the viscosity of a fuel is too high the fuel will not atomize properly resulting in poor engine performance. Only two of the six studies that reported viscosity values (Neihaus et al., 1986; Schwab et al., 1988) found the viscosity to be higher than 4.0 mm/s<sup>2</sup> (4.0 cSt); however, in these cases the viscosity was measured at slightly lower temperature (37.8°C) than the standard test method of 40°C. The cold flow properties of the pyrolytic oils have also been measured (Neihaus et al., 1986; Schwab et al., 1988; Agra et al., 1992; Stumborg et al., 1996). As in the case of biodiesel, the cold flow properties of the pyrolysis oils are poor. The cold flow properties such as pour and cloud point measure the fuel's ability to flow at cold temperatures by assessing the temperature at which long chain waxes or paraffins start to form. These highly viscous compounds may prevent proper flow of the fuel or plug filters. This property is especially important

in climate with cold ambient temperatures. Typical cloud points range from 21-25 °C and pour points from 4.4 -28 °C. These values are significantly higher than the cloud and pour points reported for No. 2 diesel (Graboski and McCormick, 1998).

Other properties that have been measured including sulfur content (Neihaus et al., 1986; Schwab et al., 1988; Lima et al., 2004;), specific gravity (Agra et al., 1992; Boocock et al., 1992; Stumborg et al., 1996; Lima et al., 2004), ash content (Neihaus et al., 1986; Schwab et al., 1988; Agra et al., 1992; Stumborg et al., 1996), corrosion (Neihaus et al., 1986; Schwab et al., 1988; Agra et al., 1992; Stumborg et al., 1996), carbon residue (Schwab et al., 1988; Agra et al., 1992) and water and sediment (Schwab et al., 1988; Neihaus et al., 1986). The results show that these properties generally fall within the specified ranges for No.2 diesel fuel regardless of whether or not a catalyst was used. Although lubricity of fuel is becoming a more important parameter, as shown by its addition to the ASTM standards, none of these studies tested the lubricity of the pyrolyzed oil.

#### **2.4.2 GASOLINE**

Gasoline is the most widely used motor vehicle fuel (Hochhauser, 2004). As with diesel, the quality of gasoline is also assessed by ASTM testing methods. The fuel quality of gasoline is measured by similar parameters to that of diesel fuels. The ignition quality of gasoline is measured primarily by its octane number also known as antiknock index (ASTM D4814-04a, 2005). The octane number is calculated by taking the average of the

research octane number and the motor octane number, which measure antiknock level under mild and more severe conditions, respectively.

Although many studies on producing hydrocarbons by vegetable oil pyrolysis report products in the gasoline range little work has been done testing the properties of the gasoline and comparing them to ASTM standards. In one study, (Weisz et al., 1979) it was found that gasoline range hydrocarbons with octane numbers ranging from 90-96 could be obtained by catalytic conversion of the pyrolysis products of various vegetable oils.

## **2.5 DECARBOXYLATION OF FATTY ACIDS AND SUBSEQUENT THERMAL CRACKING**

The intent of the thesis work is to investigate the thermal cracking of protonated fatty acids. The literature in this area is scarce. There are some studies evaluating the deoxygenation of fatty acids using different catalysts; however, there are no detailed studies involving decarboxylation or deoxygenation of fatty acids solely by thermal means. The most recent study published (Maki-Arvela et al., 2007) investigated the liquid phase cracking of fatty acids and fatty acid methyl esters. The typical solvent used for the liquid phase was dodecene. A variety of Pd/C catalysts were used to decarboxylate fatty acids, namely stearic acid, in a semi-batch reactor at temperatures between 300-320 °C and pressures from 0.6-1.75 MPa (6-17.5 bar). In the case of the fatty acid cracking, the main product was n-heptadecane. A yield of 97 % n-heptadecane

was obtained at 300 °C, with a Pd/C catalyst under helium atmosphere at 0.6 MPa. The reaction time was approximately 90 min. This study was a follow-up to an earlier study where it was found that 60 % of n-heptadecane could be produced using the same system in a hydrogen/argon atmosphere (Kubickova et al., 2005). Because the main product from stearic acid ( $C_{18}H_{36}O_2$ ) is n-heptadecane ( $C_{17}H_{36}$ ), it is likely that the initial step is decarboxylation of the fatty acid. Analysis of gaseous samples from these reactions yielded  $CO_2$ , further confirming this fact. To gain a better understanding of thermal decarboxylation of carboxylic acids, it would be useful to know the activation energy, or the amount of energy required for decarboxylation to occur. In the literature reviewed throughout this work, this parameter could not be found.

### **2.5.1 CRACKING OF LINEAR HYDROCARBON CHAINS**

If the first step is decarboxylation and a hydrocarbon chain remains, then subsequent cracking may be similar to that of linear hydrocarbons. Thermal and catalytic cracking of straight chain hydrocarbons has been studied extensively, primarily due to its importance in the petroleum industry. Mechanisms for thermal decomposition of hydrocarbons proposed by Rice and Herzfeld (1934) and Kossiakoff and Rice (1943) involving numerous free radical pathways are widely accepted by many researchers. Hydrocarbon pyrolysis can be described by five elementary reactions including : (1) initiation, propagation via (2) hydrogen abstraction, (3)  $\beta$ -scission, or (4) isomerization, and (5) termination (Poutsma, 2000; Savage, 2000). These complex free radical reactions are influenced by variety of parameters including the reaction phase, temperature, time,

pressure, and initial concentration of the reactants. Reactions are initiated by cleavage of the C-H or C-C bond to form two radicals (Rice and Herzfeld, 1934). Propagation of the free radical reaction can then occur via  $\beta$ -scission or hydrogen abstraction. Isomerization was added later to the theory (Kossiakoff and Rice, 1943).  $\beta$ -scission involves a unimolecular reaction with a higher activation energy than hydrogen abstraction and favors the production of alkenes. On the other hand, hydrogen abstraction involves bimolecular reactions, requires lower activation energies, and favours n-alkane production (Potsma, 2000; Wanatabe et al. 2000). Product distributions depend on what propagation mechanism is favored, which in turn depends on the reaction conditions. In many cases, n-hexadecane has been used to study pyrolysis behavior and to design models to predict product distribution and reaction rates at different conditions for both liquid phase reactions (Blouri et al., 1984; Ford, 1986; Khorasheh and Gray, 1993) and gas phase reactions (Voge and Good, 1949; Fabuss et al., 1962, 1964; Wu et al., 1996). Key points regarding hydrocarbon pyrolysis, which may be relevant to this thesis are briefly discussed with a focus on product distribution rather than kinetic data. Although kinetics also provide important information about the reactions and are discussed at length in many of these papers, because kinetics were not studied in this thesis, they will not be addressed. It should be noted that this is a very simplistic overview of hydrocarbon pyrolysis. More detail is provided in the references mentioned in this section.

According to the theory of Kossiak of and Rice (1943), n-hexadecane pyrolysis results in a series of C<sub>2</sub>-C<sub>15</sub> olefins, methane, and ethane as primary products at low pressures and

temperatures greater than 600 °C. At lower pressures,  $\beta$ -scission is favored and alkyl radicals undergo multi-step cracking. Fabuss et al. (1962, 1964) described a one-step mechanism (F-S-S) to account for the decomposition of n-hexadecane during gas phase cracking at high pressures. In this case, hydrogen abstraction is preferred over  $\beta$ -scission resulting in a corresponding series of alkanes. It has been reported that this F-S-S mechanism occurs at pressures between 1-7 MPa and temperatures between 350-450 °C and results in nearly equi-molar distributions of n-alkenes and  $\alpha$ -olefins. High pressure liquid phase cracking has also been shown to favor hydrogen abstraction and the production of alkanes (Khorasheh and Gray, 1993). Wu et al. (1996) compared liquid and gas phase cracking and found that liquid phase cracking resulted in equi-molar mixtures of alkanes and alkenes while gas phase cracking favored alkene production. In addition to the prominent n-alkane and  $\alpha$ -olefins, Khorasheh and Gray (1993) reported minor isomerization products including branched alkanes and internal alkenes. In particular, a series of cis- and trans-2-olefins were identified. It has also been reported that low pressure liquid phase cracking (Ford, 1986; Khorasheh and Gray, 1993) and high pressure gas phase cracking (Fabuss et al., 1962, 1964) of n-hexadecane results in addition products (i.e. products greater than C<sub>16</sub>) but that the addition products are present in relatively minor concentrations as compared to the other reaction products. According to Fabuss et al. (1962, 1964), these addition compounds consisted of alkanes in the C<sub>18</sub>-C<sub>20</sub> range. Figure 2.6 shows the product distribution of liquid and gas phase cracking of n-hexadecane (Wu et al., 1996).



## 2.6 HYDROLYSIS OF OILS AND FATS

Crude beef tallow is composed predominantly of triglyceride molecules, which are composed of a glycerol backbone with three fatty acids. It is the free fatty acid that is the desired feed for the pyrolysis reactions, therefore prior to thermal processing, the fatty acids must be separated from the glycerol backbone. This can be accomplished by a hydrolysis reaction as shown in Figure 2.7. This reaction is reversible but can be shifted to the right by using high temperature, pressure, or a large excess of water. Various catalysts can also be used. Four typical hydrolysis methods include (1) acid hydrolysis,

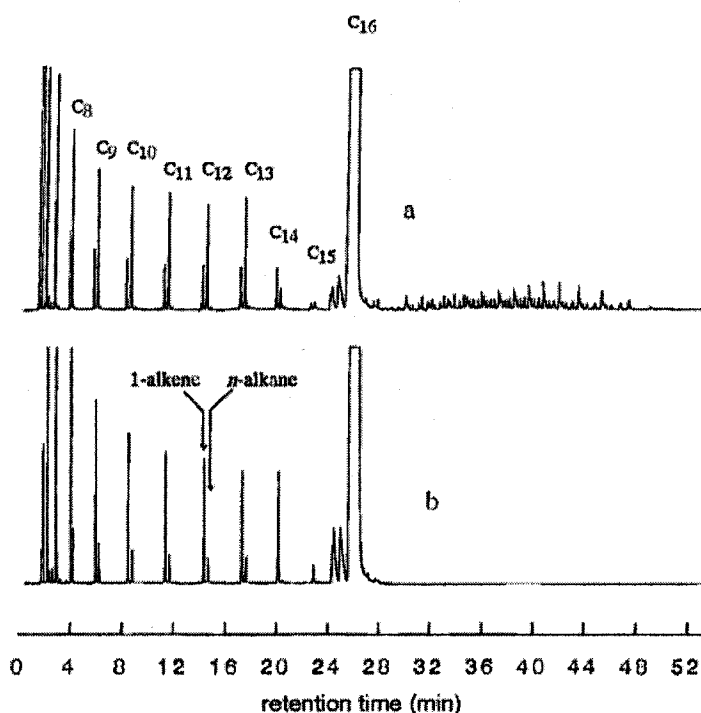


**Figure 2.6** Typical chromatograms of liquid products from thermal cracking of hexadecane: (a) liquid phase, 375 °C, 13 h; (b) gas phase, 375 °C, 12 h. (Wu et al. (1996))

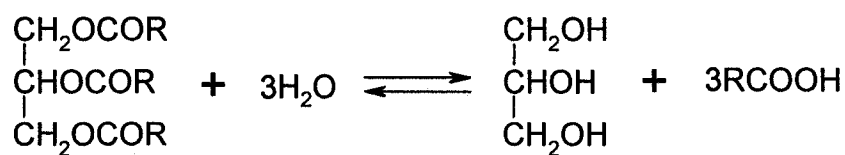


**Figure 2.7** Reaction showing triglyceride hydrolysis

(2) base hydrolysis, (3) hydrolysis under high pressures, and (4) enzymatic hydrolysis (Brockmann et al., 2005). Base or alkali hydrolysis, also known as saponification, results in the production of fatty acid soaps, not the protonated free fatty acid that is desired for the pyrolysis feed. There has been a lot of research focused on enzymatic hydrolysis using lipase catalysts; however, this can be costly, is still very much in the research stage, and has not yet been applied commercially (Brockman et al., 2005). Out of the two remaining options, high pressure hydrolysis appears to be the better option primarily because it does not involve the addition of any reagents such as the acid catalyst or surfactant, which are typically used in these processes. Furthermore, ambient pressure, acid catalyzed processes such as the Twitchell process, have long reaction times of up to 24 h for a single stage reaction (Lascaray, 1949; Hartman, 1953; Anozie and Dzobo, 2006). Because the surfactants used for these types of reactions are not typically water soluble, separation from the fatty acid mixture could prove difficult. The fatty acid feed used in the pyrolysis reaction should be as pure as possible. Acids may also cause corrosion issues at higher temperatures (Brockmann et al., 2005). Due to its simplicity

and relative cost effectiveness as compared to other hydrolysis methods, hydrolysis under pressure is the methods typically employed in industry. Typical conditions include pressures in the range of 2-6 MPa and temperatures between 150-260 °C (Sedelies et al., 1992). Figure 2.8 shows the typical course of a hydrolysis reaction of beef tallow at 235 °C and 3.5 MPa using 1 part oil and 2 parts water (Brockman et al., 2005).

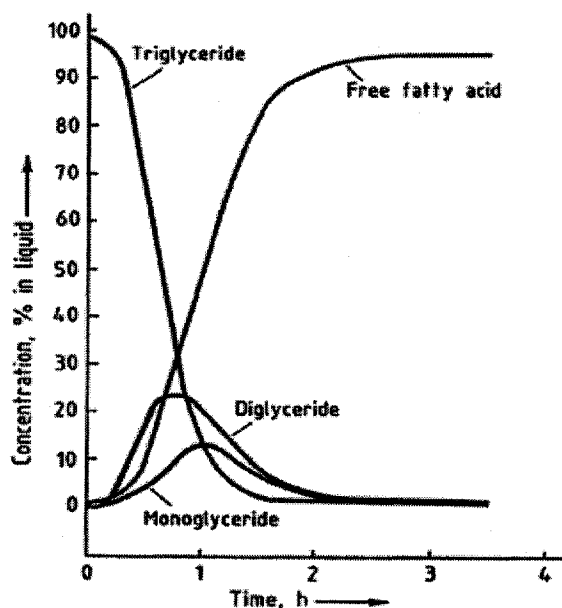


**Figure 2.8** Typical course of hydrolysis reaction (hydrolysis of beef tallow at 235°C and 3.5 MPa using 1 part oil and 2 parts water) [Brockmann et al., 2005]

## 2.7 CONCLUSIONS

Over the past several decades, there has been renewed interest in using fats and oils for energy and fuels, especially in the production of biodiesel through a transesterification reaction. Although biodiesel is recognized as a good diesel fuel alternative, it contains

oxygen. Oxygenated products have lower heat contents, are prone to undesirable oxidative reactions, and may be unsuitable for certain applications. Another recognized renewable fuel is bio-oil produced from the pyrolysis of lignocellulosic biomass. Like biodiesel, bio-oil also contains a high percentage of oxygenated compounds and also contains heterocycles and has been described as acidic, corrosive, polar, and thermally unstable.

An alternative option to the aforementioned biofuels is to pyrolyze or thermally crack triglyceride materials. To date, the majority of studies in this area show that this process also results in oxygenated products. Triglycerides consist of three fatty acid chains bound to a glycerol backbone, which can be liberated via various hydrolysis methods. There has been little work on pyrolysis of free fatty acids, which may result in a cleaner product. This would represent a unique and novel approach to triglyceride pyrolysis. Fatty acids consist of a hydrocarbon chain with an end carboxyl group. Decomposition of organic substrates occurs via complex free radical reactions. Mechanisms have been elucidated for decomposition of triglyceride molecules; however, mechanisms involving thermal decomposition of fatty acids after initial decarboxylation has not been reported. Understanding of these mechanisms and identifying the primary reaction products of free fatty acid decomposition is key in assessing the feasibility of this process as a means of producing deoxygenated hydrocarbons.

## **CHAPTER 3: EXPERIMENTAL PROCEDURES**

### **3.1 MATERIALS AND CHEMICALS**

The chemicals used in this work, excluding the reactor feedstocks (Section 3.2), are listed in Table 3.1.

#### **3.1.1 REACTOR FEED**

The feedstocks used in this thesis experiments included:

- (1) Stearic acid (95 %) purchased from Sigma Chemical Co. (St. Louis, MO)
- (2) Oleic acid purchased from Sigma Chemical Co. (St. Louis, MO)
- (3) Poultry tallow from Lomax Inc. (Montreal, Quebec)
- (4) Bleached fancy beef tallow (BF) from SaniMax (Montreal, Quebec)
- (5) Yellow grease beef tallow (YG) SaniMax (Montreal, Quebec)
- (6) Presidents Choice® brand canola oil (Food Grade) purchased locally (Superstore, Edmonton, AB)

The composition of the neat oil and fats were determined by derivatization with boron trifluoride (section 3.3.2.1.1) and GC-FID analysis (section 3.3.1.4.2). The results are presented in Tables 3.2 and 3.3.

**Table 3.1** Chemicals used in this work

<b>Name</b>	<b>Catalogue Number (Year)</b>	<b>Manufacturer</b>	<b>Supplier</b>
Pentane (HPLC Grade)	P399-4 (2005)	Fisher Chemicals	Fisher Scientific Fair Lawn, NJ
Toluene (HPLC Grade)	T290-4 (2005)	Fisher Chemicals	Fisher Scientific Fair Lawn, NJ
Nonadecanoic Methyl Ester (min 98%, GC)	N5377 (2005)	Sigma	Sigma-Aldrich Co. St. Louis, MO
Alkane Standard Solution C <sub>8</sub> -C <sub>20</sub>	04070 (2005)	Fluka	Sigma-Aldrich Co. St. Louis, MO
Carboxylic Acid Standard (GC) Solution	N/A	Sigma	Sigma-Aldrich Co. St. Louis, MO
Alumina, desiccant (Grade H-152)	A-2935 (2003)	Sigma	Sigma-Aldrich Co. St. Louis, MO
Nitrogen, Compressed P.P. 4.8	N/A	Praxair	Praxair Edmonton, AB
Chloroform (HPLC Grade)	C606-4 (2006)	Fisher Chemicals	Fisher Scientific Fair Lawn, NJ
Hexane (HPLC Grade)	H302-4 (2005)	Fisher Chemicals	Fisher Scientific Fair Lawn, NJ
Acetic Acid, glacial (ACS Reagent Grade)	A-0808 (2006)	Sigma	Sigma-Aldrich Co. St. Louis, MO
TLC Standard, 25% (w/w) of each of oleic acid, monoolein, diolein and triolein	-	Nu-Chek Prep Inc.	Nu-Chek Prep Inc. Elysian, MN
Ether, extra dry (<50 ppm water, stabilized)	AC32686 (2007)	Acros Organics	Fisher Scientific Fair Lawn, NJ
Diazald, 99 %	D28000 (2007)	Aldrich	Sigma-Aldrich Co. St. Louis, MO
Dithylene glycol monoethyl ether (laboratory grade)	D51-4 (2007)	Fisher Chemicals	Fisher Scientific Fair Lawn, NJ

**Table 3.2** Fatty acid composition of feed fats and oil determined by GC-FID

Feed Material	Fatty Acid (wt %)										
	C14:0	C16:0	C16:1 cis	C17:0	C18:0	C18:1 trans	C18:1 cis	C18:2	C20:0	C18:3	C22:0
Bleached Fancy Tallow	2.56	24.98	3.13	1.05	16.52	2.61	37.82	5.87	0.18	0.61	-
Yellow Grease Tallow	1.14	15.39	2.45	0.36	7.45	4.43	46.19	15.48	0.30	2.26	0.18
Canola Oil	0.07	5.10	0.29	0.06	2.21	-	63.63	17.33	0.62	6.91	0.30
Poultry Tallow	0.76	22.54	7.25	0.14	5.67	0.68	43.92	14.66	0.10	1.16	0.03

**Table 3.3** Percentage of saturated and unsaturated fatty acid in feed fats and oil determined by GC-FID

Feed Material	Saturates (%)	Monounsaturates (%)	Polyunsaturates (%)
Bleached Fancy Tallow	46.22	44.76	7.24
Yellow Grease Tallow	25.37	54.18	18.43
Canola Oil	8.62	65.55	24.57
Poultry Tallow	29.62	52.55	16.95

### 3.2. MICROREACTORS AND SAND BATH

Pyrolysis reactions were conducted in 15 mL batch microreactors (also referred to as the reactors) heated with a fluidized sand bath as shown in Figure 3.1. The experimental set-up consisted of three main components including (1) stainless steel microreactors; (2) microreactor purge system; and (3) fluidized sand bath system for heating.

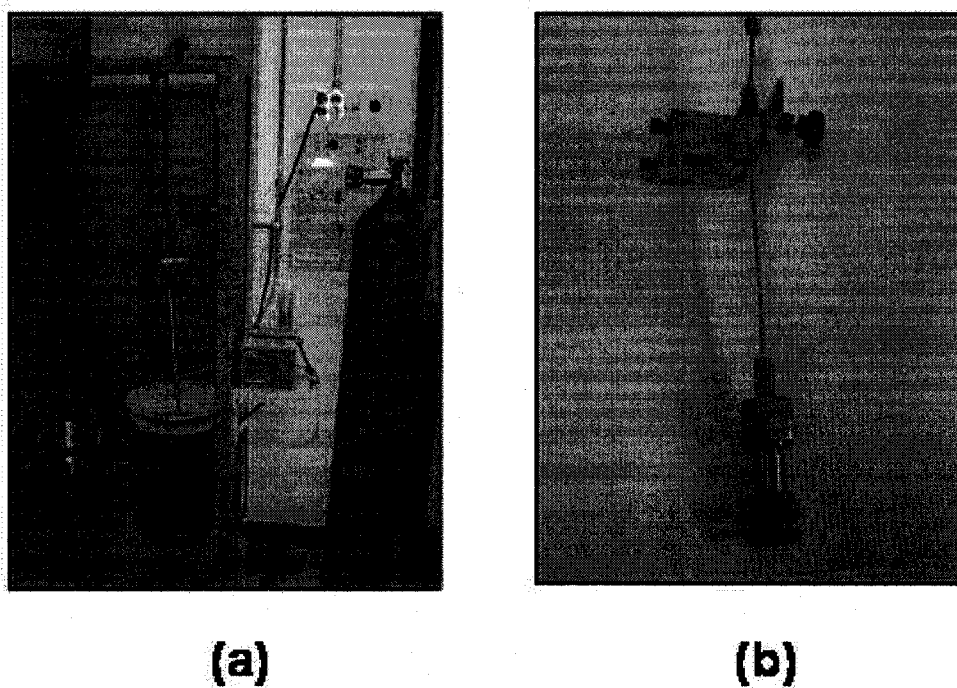


**Figure 3.1** Picture of (a) sand bath and purge system and (b) microreactor



### **3.2.1.1. Batch microreactors**

The 15 mL microreactors used in these experiments were constructed with stainless steel (S.S.) Swagelok® fittings and tubing. A schematic of the closed microreactor is shown in Figure 3.2. The microreactors consisted of a bottom cap, central tube, and a top cap with a 1/4" opening. Stainless steel tubing (1/8"), approximately 15 cm in length, was connected to this opening with a reducing union and a needle valve was situated near the end of this tube (approximately 13 cm above the reactor top) to open and close the reactor. A mount (not shown in schematic) was also attached to this tubing so that the microreactors could be attached to the sand bath system. Similar microreactors have been used in previous studies at the University of Alberta by researchers in the Chemical Engineering Department (Tanabe and Gray, 1997; Richardson and Gray, 1997; Bressler and Gray, 2003; Kanda, 2003). All reactors were built by the Chemical Engineering Department Machine Shop and were constructed using similar methods.

#### *3.2.1.1.1 Replacing the reactors*

The microreactors were used until they failed leak testing after loading or seized during the reaction and could not be opened, at which time they were replaced. Typically, microreactors lasted between 10-20 reactions.

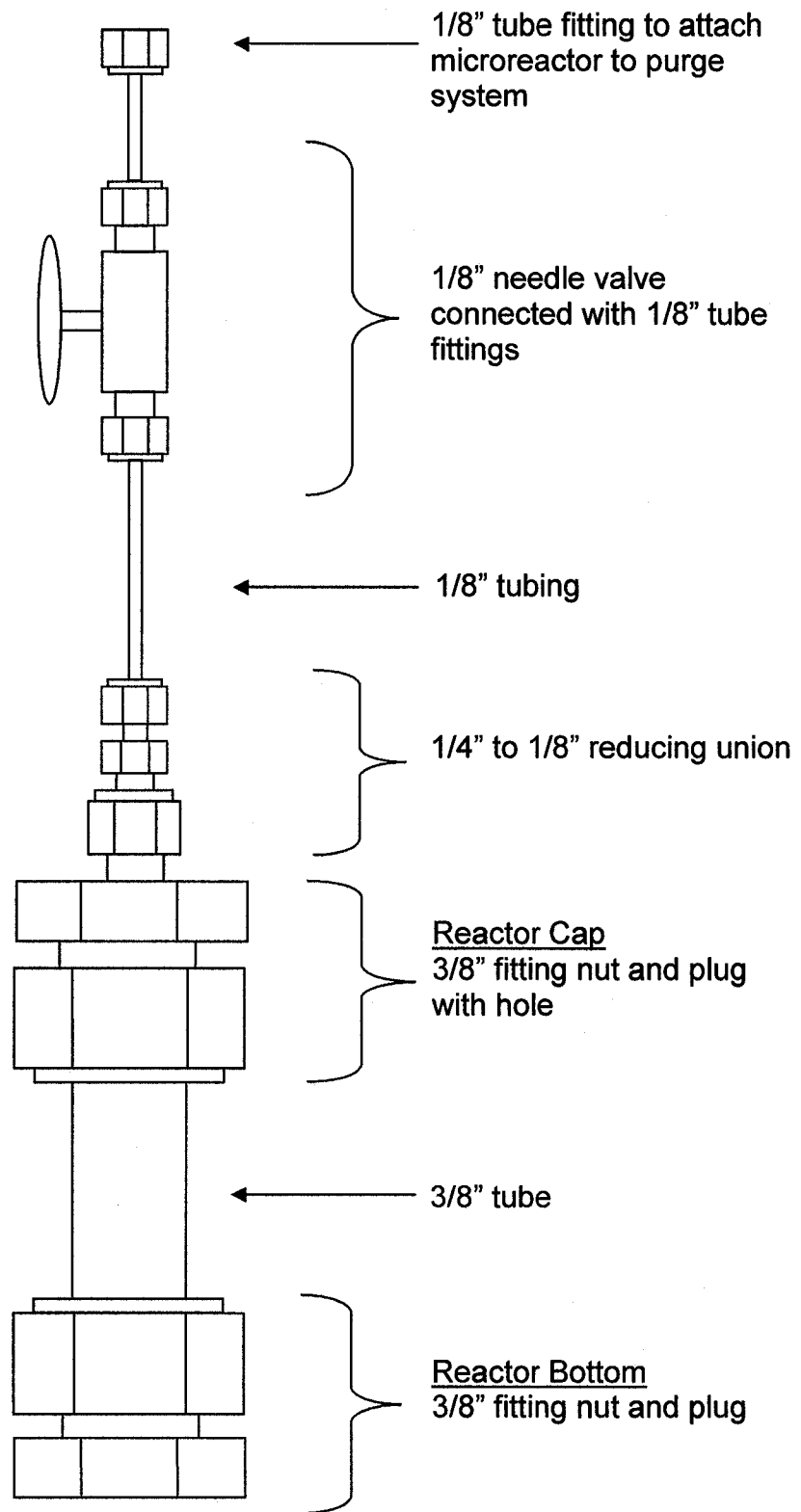


**Figure 3.2** Schematic of closed microreactor

### 3.2.1.2 Microreactor purge system

The microreactor design allows for connection to a high pressure gas source for pressurization or purging. A schematic of the microreactor purge system used in this work is shown in Figure 3.3 with all valves initially closed. Microreactors were connected to the purge system and the tank valves, V1, and the microreactor valves (not shown on schematic) were opened to allow nitrogen into the reactor. The pressure was set by reading P1 and adjusting the tank regulator. Once pressurized or purged, the tank and microreactor valves were closed and the pressure in the line was vented through V2. The reactor was then removed from the system.

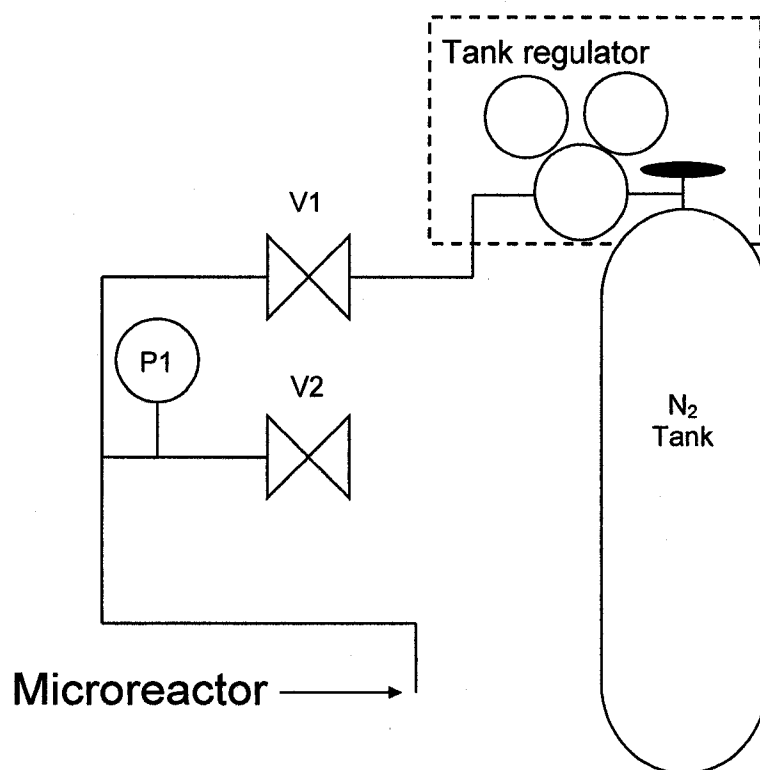


**Figure 3.3** Schematic of the microreactor purge system

### 3.2.1.3 Sand bath system

The microreactors were heated in a Techne Model SBS-4 fluidized sand bath (Burlington, NJ). The main components of the sand bath system are highlighted in Figure 3.4 and include the sand bath, motor and arm, air supply, and temperature controller. A schematic of the sand bath is shown in Figure 3.5 and its dimensions are presented in Table 3.3. The sand bath was filled to approximately 1-2” below the top with aluminum oxide sand [Techne, Burlington, NJ]. To fluidize the sand, compressed air was blown into the bath near the bottom and through a porous plate for more uniform air distribution. A Techne TC-8D temperature controller (Burlington, NJ) was used to maintain the bath at a constant temperature throughout the reaction. The temperature of the bath was measured by a K-type thermocouple located near the center of the bath. The heating elements were located at the bottom of the sand bath, above the porous plate. An off-center wheel connected to a motor and arm was used to agitate the microreactor for the duration of the reaction.

**Table 3.4** Sand bath specifications

<b>Techne SBS-4 Sand Bath Specifications</b>	
Overall Size (Diameter x Height), m	0.34 x 0.46
Working Volume (Diameter x Height), m	0.18 x 0.14
Temperature, °C	50-600
Temperature Stability @ 50°C with TC-8D	± 0.3 °C
Air Pressure, kPa	20.7
Air Flow m <sup>3</sup> /s	0.001
Weight of Media, kg	8.98

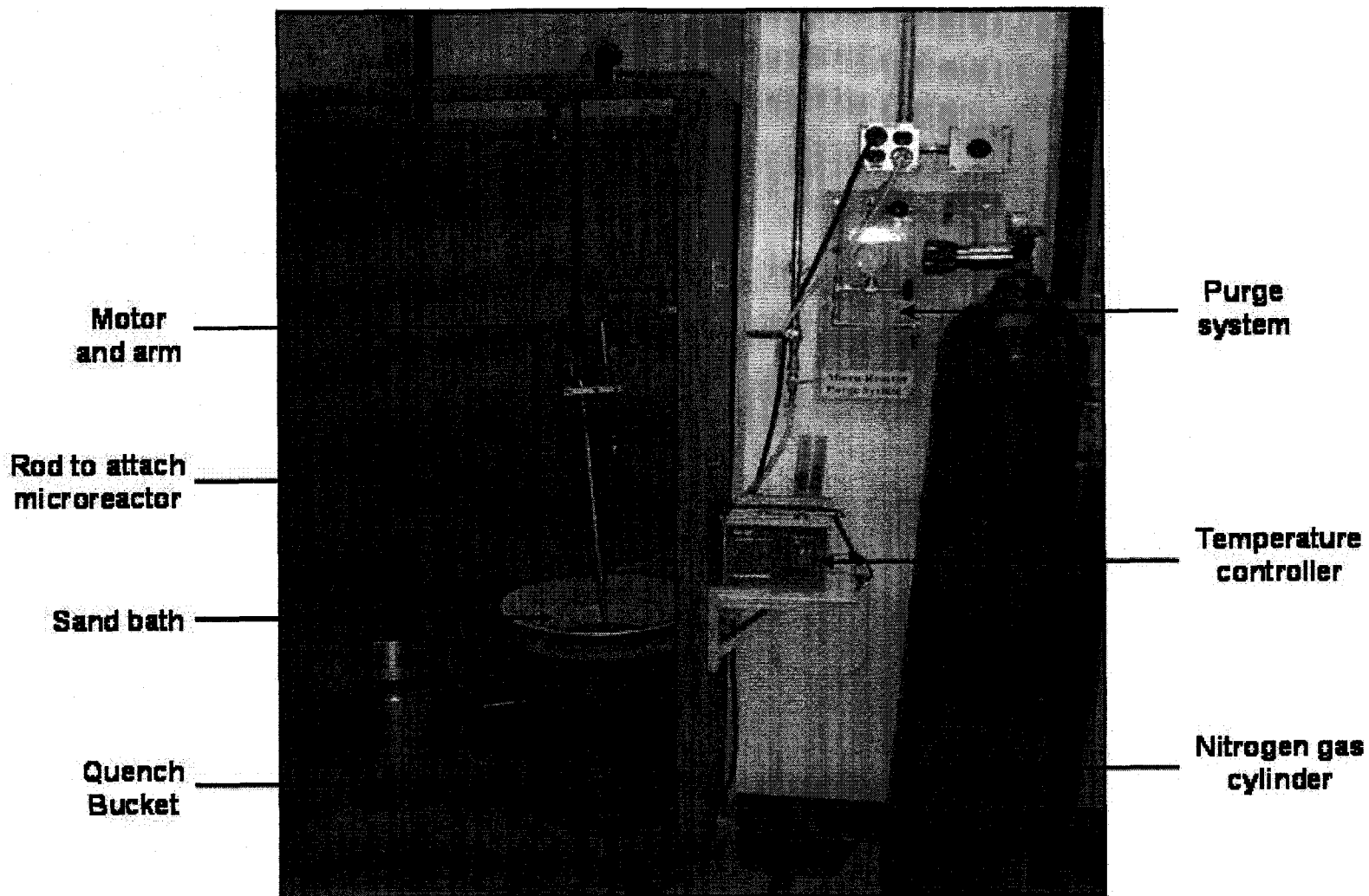
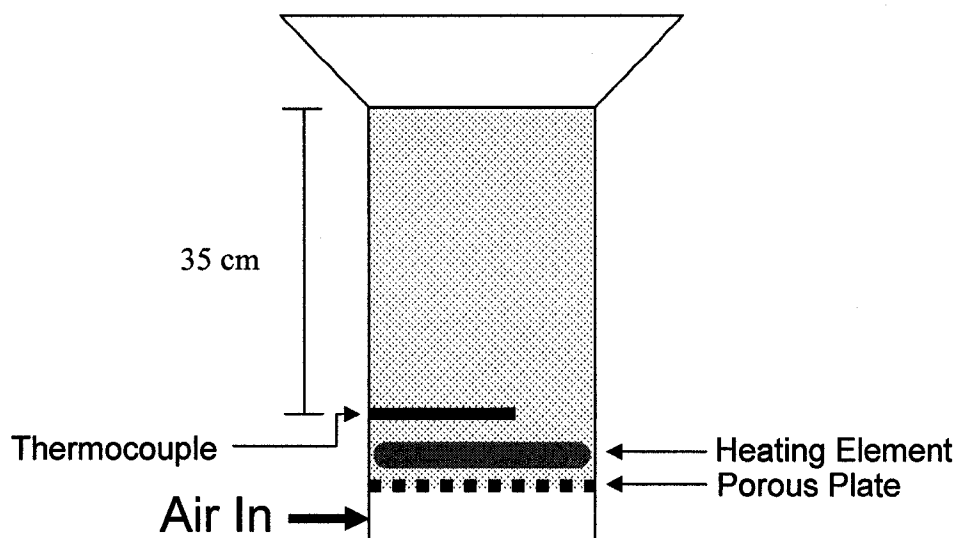


Figure 3.4 Picture of the sand bath system



**Figure 3.5** Schematic of Techne SBS-4 sand bath

### **3.2.1.4 Modified Reactors for Measurement of Internal Reaction Conditions**

The batch microreactors were modified to allow measurement of temperature and pressure inside the reactors during the reaction runs. A 1/16" K-type thermocouple (Aircom Industries, Edmonton, AB) was inserted through the top of one of the reactors such that the tip was situated approximately 1 mm above the reactor bottom. The thermocouple was connected to the reactor mount tubing using Swagelok® fittings as shown in Figure 3.6. The thermocouple was connected to a Digi-Sense Dual JTEK thermocouple thermometer (Cole-Parmer Instrument Company, Vernon Hills, IL) to measure the temperature. Figure 3.7 shows a second modified reactor allow pressure measurement. A Swagelok® pressure gauge (Swagelok, Edmonton, AB) was attached to the reactor mount tubing with Swagelok® fittings.

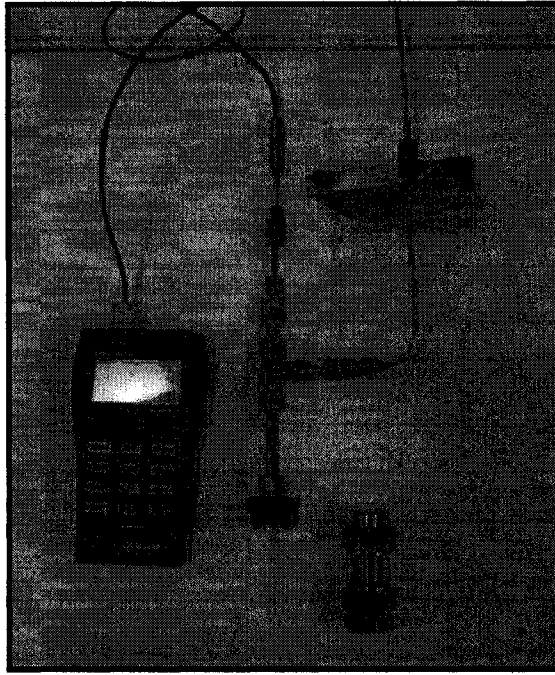


**Figure 3.6** Picture of the modified reactor for measuring internal reactor temperature

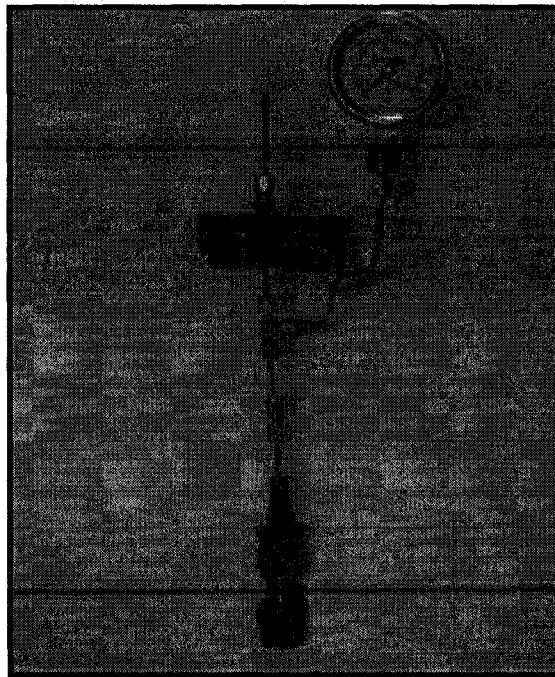


**Figure 3.7** Picture of the modified reactor for measuring internal reactor pressure

### **3.3 EXPERIMENTAL PROCEDURE**

#### **3.3.1 PYROLYSIS REACTIONS**

All pyrolysis reactions were conducted in the microreactors. Prior to loading the reactors, the fluidized sand bath was turned on and the temperature controller was set to the desired temperature for that particular reaction. The airflow into the reactor was adjusted so that the sand fluidized enough to form bubbles 1-2" in diameter or just even with the top of the sand bath. The sand bath was allowed to heat up until it reached the steady state temperature as determined by a stable temperature reading on the controller for at least 15 min. Heating times of the sandbath ranged between 1.5 and 2.5 h depending on the set temperature. As the sand bath heated, the air also heated and expanded causing the amount of fluidization and the bubble size to increase. To keep the bubble size constant, the airflow was adjusted manually throughout the heating process.

Between reactions the microreactors were scrubbed thoroughly with metal brushes, washed with soap and water, and rinsed with distilled water and wash acetone to ensure they were completely clean and free of residue from the previous reaction. After the microreactors were completely dry, feedstock was weighed into the reactor. Anti-seize lubricant was applied to the threading on the reactor cap and the reactor was closed and tightened. The microreactor was connected to the nitrogen purge system, all valves were opened, and the microreactors were tested for leaks using Swagelok Snoop®. If a leak was detected, the microreactor was removed from the purge system and re-tightened. If a seal could not be obtained after being re-tightened several times, the microreactor was



replaced. Once the microreactor was completely sealed and free of leaks, it was purged three times (filled and emptied) before closing the microreactor valve and disconnecting from the purge system.

Once the microreactor was prepared for the reaction, it was attached to the sand bath rod and lowered into the center of the sand bath. The position of the microreactors on the rod was kept constant so that the microreactors were always in approximately the same location in the bath and did not contact any part of the sand bath during the reaction. To begin the reaction, the microreactors were dropped into the bath ensuring complete immersion in the sand and the motor was switched on to begin agitating immediately after the reactor contacted the sand. Upon completion of the reaction, the microreactors were lifted from the sand bath and immediately quenched in a bucket of room temperature water to end the reaction. The reactors were vented in the fumehood to release any gaseous products formed during the reactions and opened for extraction unless the gas products were collected for analysis as described in section 3.3.1.2.2.

To measure the internal reactor temperature and pressure, reactors were loaded and purged as normal; however, the modified reactor mounts described in section 3.2.1.4 were used. The temperature was recorded by reading the digital thermometer every 30 s for the first 10 min of the reaction, at every min from 10-15 min and then again at 30, 45, and 60 min. The pressure was recorded throughout the run as well as after quenching to determine the amount of pressure generated from the formation of gaseous product.

### **3.3.1.1 Extraction of reaction products**

The reaction products were extracted from the microreactor using 10 mL of pentane spiked with internal standard unless otherwise specified. Nonadecanoic methyl ester was used as the internal standard and was prepared with pentane in concentrations of approximately 0.5 or 1 mg/mL. The pentane/internal standard mixture was measured into the microreactor using a positive displacement pipet and stirred so that any solid material in the microreactor was scraped off the microreactor sides and broken apart. After approximately 15 min, the liquid extract was transferred to a sample vial. All products were stored in dram vials with screw tops and Teflon® liners and stored at 4°C.

Nonadecanoic acid was chosen as an internal standard because it is similar in structure to the starting compound. When this standard was run on GC-FID it gave a sharp clean peak and did not overlap with any of the potential pyrolysis products.

### **3.3.1.2 Gas chromatography (GC)**

#### *3.3.1.2.1 Liquid extracts*

The pentane extracts were analyzed on a Varian 3400 Gas Chromatograph equipped with a Varian 8200 autosampler (Varian Inc., Palo Alto, CA) coupled with a flame ionization detector (FID) operated at 320 °C. Operating head pressure remained constant at 151 kPa (22.5 PSI). An RH1 column from Rose Scientific (Mississauga, Ontario, CA) was used

for all analyses with a 1  $\mu$ l cool on-column injection. The injector temperature was set at 50  $^{\circ}$ C. The column temperature profile used is shown in Figure 3.8 for a total run time of 29.9 min. Data analysis was conducted using Shimadzu Class VPTM 4 software (Shimadzu Scientific Instruments, Columbia, MD).

Two external standards were run for product verification. These were (1) a C<sub>8</sub>-C<sub>20</sub> alkane mixture (Fluka) and (2) a C<sub>3:0</sub>-C<sub>20:0</sub> carboxylic acid mixture prepared in-house using carboxylic acids purchased from Sigma. These internal standards were run throughout the GC analysis to account for potential shifting of the peaks.

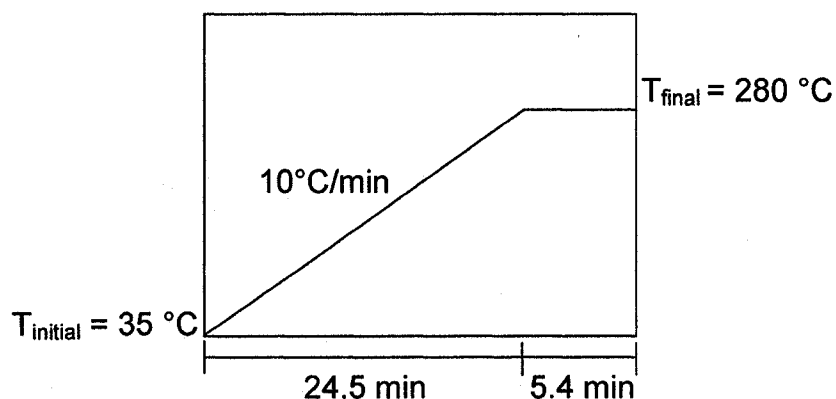


**Figure 3.8** GC-FID column temperature profile for liquid analysis of pyrolysis products in pentane

### 3.3.1.2.2 Gaseous samples

To collect gas samples from the microreactor for analysis, a 1/4" Swagelok® tube fitting with a septum was screwed into the fitting used to connect the microreactor to the purge

system. A glass syringe and needle was inserted through the septum and the reactor valve was opened. Four mL of gas was drawn from the reactor using the syringe and expelled into a 5 mL vacutainer. This was repeated for a total of 8 mL of gas product in each 5 mL vacutainer. Gas samples were analyzed on a Hewlett Packard Series II 5890 gas chromatograph coupled to a TCD (total conductivity detector) set at 80°C (Hewlett Packard Co., Palo Alto, CA). A glass syringe was used to manually inject 100 µL of the gas sample onto a 30 m Agilent HP-plotq column with an I.D. of 0.53 µm (Agilent Technologies Inc., Santa Clara, CA). The temperature program used is shown in Figure 3.9. The total run time was 10 min. Select gas samples were also run on GC-FID at the conditions outlined in section 3.3.1.2.1. Data analysis was conducted using Shimadzu Class VPTM 4 software (Shimadzu Scientific Instruments, Columbia, MD).

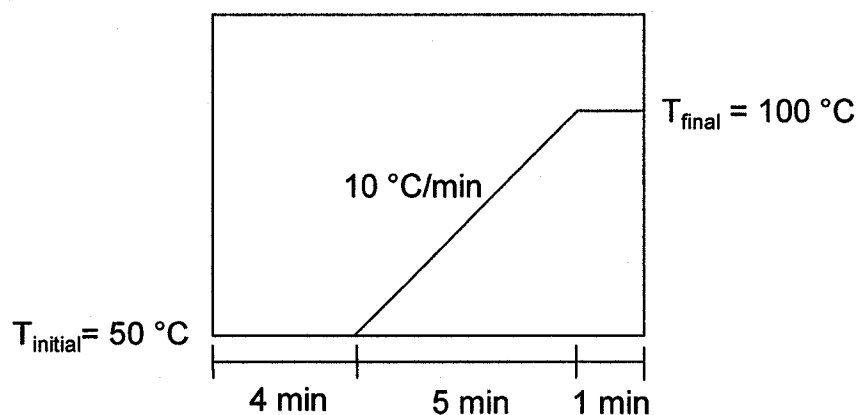


**Figure 3.9** GC-TCD column temperature profile for gas analysis of pyrolysis products

### **3.3.1.3 Gas Chromatography - Mass Spectrometry (GC-MS)**

Initial GC-MS analyses was conducted on select samples using a Waters (formerly Micromass, Milford, MA) Trio 2000 equipped with a HP5890 Series II GC in the University of Alberta's Chemistry Department. The remainder of the GC/MS analyses were conducted on a model 5975B EI/CI GC/MS with a 7683B series injector and autosampler from Agilent Technologies Inc. (Santa Clara, CA). The inlet heater was set at 300 °C, pressure at 46.5 kPa, and detector at 250 °C. The total flow was set at 104 mL/min with a split ratio of 100:1 and on-column injection. All GC/MS analyses were conducted using the column temperature profile outlined in Figure 3.8 with a standard DB1 column (Agilent Technologies Inc., Santa Clara, CA). Data were analyzed using Enhanced MSD ChemStation™ D.03.00.611 software (Agilent Technologies Inc, Santa Clara, CA).

### **3.3.1.4 Extent of Reaction**

To determine the extent of reaction it was necessary to dissolve all of the stearic acid feed remaining in the reactor. In previous experiments, pentane was used as the extraction solvent and may not have dissolved all of the unreacted feed. This is described in more detail in Chapter 4. Chloroform was used as an extraction solvent because of the relatively high solubility of stearic acid in this solvent compared to pentane. Reaction products were washed out of the microreactors with approximately 100 mL of chloroform into a round bottom flask until no product remained inside the reactor. The chloroform

was then removed by roto-evaporation. During the evaporation/drying process, it is likely that some of the volatile products were lost, but because stearic acid (non-volatile) was the focus of quantification it is not anticipated that this step will affect the results. Thirty mL of chloroform spiked with internal standard was pipetted into the flask with the remaining products and swirled until all the product had dissolved. Based on the solubility of stearic acid in chloroform, 30 mL was more than sufficient to dissolve the maximum possible stearic acid product (1 gram if no reaction occurred). Samples were taken and stored at 4 °C in dram vials with Teflon liners until analysis. Controls were conducted using the extraction procedure with no thermal treatment.

#### *3.3.1.4.1 Derivatization with diazomethane*

A 250 µL sample of the above sample was added to a one dram vial and completely dried under N<sub>2</sub> before excess amounts of diazomethane, prepared in-house, was added to the vial. The diazomethane (alcohol free) was prepared following procedures outlined in Aldrich technical information bulletin AL-180 using the Diazald® distillation kit with Clear Seal® joints purchased from Aldrich (St. Louis, MO). Diazald®/ether solution was added dropwise to a solution of 2-(2-ethoxyethoxy) ethanol and potassium hydroxide, also in ether in a reaction vessel. The diazomethane was collected in a condenser and stored at -20 °C in dram vials with Teflon® liners. The concentration of the final diazomethane/ether solution was approximately 3500 mg in 40 mL or 83 mmol diazomethane. After the reaction was complete (i.e. no more bubble formation), the

sample was dried again with N<sub>2</sub> and then resuspended with a known volume of chloroform before analysis on GC.

#### *3.3.1.4.2 GC analysis of lipid materials*

Analysis of the above samples were conducted using standardized fatty acid protocol developed by the GC lab in the Department of Agricultural, Food, and Nutritional Science at the University of Alberta. The samples were analyzed on a Varian 3400 Gas Chromatograph equipped with a Varian 8200 autosampler (Varian Inc., Palo Alto, CA) coupled with a flame ionization detector (FID) operated at 320 °C. Operating head pressure was 283 kPa (41 psi). The conditions used are outlined in Figure 3.10. Samples (1 µL) were injected onto a SGE BPX 70 (30 m x 0.25 mm I.D. x 0.25 µm thickness) column (SGE Analytical Science, Austin, TX). The initial injector temperature was set at 70 °C and immediately ramped to 230°C at 100 °C/min where it was held for 16 min. Total runtime was 18.9 min.

#### **3.3.1.5 Percentage of liquid and gas fractions**

To get a crude estimate of the liquid yield, the reactor was opened and the liquid product was extracted with a Pasteur pipet and weighed. To get a crude estimate of the mass of the gas product, the reactor was weighed before and after venting the gas. For these reactions, 5.000 g of stearic acid was used as feed instead of the typical 1.000g so that the difference could be ascertained to a higher degree of accuracy.

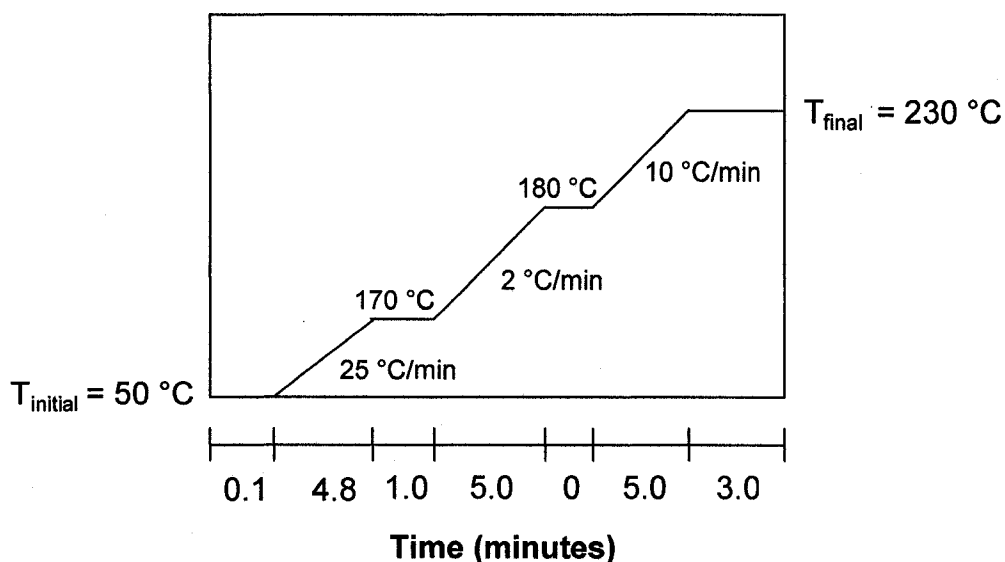


**Figure 3.10** GC column temperature profile for lipid analysis (30 m column)

### 3.3.2 HYDROLYSIS REACTIONS

Before the vegetable oils and animal fats were pyrolyzed, they were first hydrolyzed. Small-scale hydrolysis reactions were conducted in the same microreactors as the pyrolysis reactions. Approximately 3 g of the various tallows or oils and 6 g of distilled water were added to the microreactors for a 1:2 ratio (by weight) of oil/tallow to water. The reactors were sealed as described previously and pressurized with  $N_2$  to 3.48 MPa (500 PSI). The hydrolysis reaction was conducted at 250 °C for 4 h. When the reactors were opened, they were placed in a beaker of hot tap water (~ 60 °C) so that the products remained in liquid state and were transferred to a glass sample vial with a Pasteur pipet. The fat layer was allowed to separate from the glycerol/water layer and was pipeted into a separate glass vial. Samples were stored at 4 °C until pyrolysis or derivatization. It was assumed that if any water remained in the sample, the rate of hydrolysis would be negligible at this low temperature. This fat or oil layer will herein be referred to as the oil



or fat hydrolysates, so as not to confuse these products with the products formed after pyrolysis (i.e. the pyrolysates or pyrolytic oil).

### **3.3.2.1 Fatty acid composition of the feed**

The fatty acid composition of the yellow grease tallow, bleached fancy tallow, poultry tallow, and canola oil was determined by derivatizing samples with boron-trifluoride and analyzing them on GC-FID. The derivatization procedure is outlined below and the GC analysis was the standard fatty acid protocol as described in section 3.3.1.4.2.

#### *3.3.2.1.1. Derivatization with boron trifluoride*

For derivatization with boron trifluoride, approximately 30 mg of sample was weighed into a test tube and 5 mL of a 14 % boron trifluoride-methanol/methanol/hexane mixture (35:45:20 v:v:v) was added. The tubes were tightly sealed and heated in boiling water for 45 min. After the tubes had cooled, 4 mL of water and 4 mL of hexane were added and the tube was shaken for 1-2 min. The layers were allowed to separate and the hexane layer was extracted with a Pasteur pipet and stored in a dram vial with Teflon liner at 4 °C until analysis.

### **3.3.2.2 Analysis of hydrolysates using TLC-FID**

The composition of the hydrolysates was determined using thin layer chromatography coupled with an FID detector (TLC-FID) as described by Moquin et al. (2006). Samples were prepared for analysis by weighing approximately 0.03 g of the fatty hydrolysates into a screw cap vial and adding 5 mL of HPLC grade hexane. A specific volume of sample was spotted on silica gel Chromarods-SIII using a needle and syringe in 0.2  $\mu$ L increments. The rods were then placed in a developing tank containing a mixture of hexane/diethyl ether/acetic acid (80:20:1 v:v:v) for 20 min and dried at 120 °C for 10 min. Lipid analysis was conducted using an Iatroscan TH-10 (IARON-Laboratories Inc., Tokyo, Japan) with a hydrogen pressure of 113 kPa, air flow rate of 2000 mL/min, and a scan speed of 30 s/rod. A reference standard containing 25% (w/w) each of oleic acid, monoolein, diolein and triolein was obtained from Nu-Chek Prep Inc. (Elysian, MN).

### **3.3.2.3 Analysis of hydrolysates using GC-FID**

To determine the composition of unreacted or non-hydrolyzed feed, if any, GC-FID analysis was conducted on samples of bleached fancy tallow hydrolysates derivatized by four different methods, which methylate different lipid classes outlined in Table 3.5. Diazomethane derivatization was conducted using the procedure outline in section 3.3.1.4.1. The other three methods are discussed below. GC-FID analysis was conducted on the same instrument described in section 3.3.1.4.2. with a longer column for better separation. The column temperature profile used is shown in Figure 3.11. A 100 m x 25

mm x 0.25  $\mu\text{m}$  column from Supelco Inc. (Bellefonte, PA) was used for the analysis.

The initial injection temperature was set at 50  $^{\circ}\text{C}$  and held for 0.2 min before ramping up to 230  $^{\circ}\text{C}$  at a rate of 150  $^{\circ}\text{C}/\text{min}$  where it was held for 78 min. Injection volume was 0.5  $\mu\text{l}$  and the total run time was 80 min.

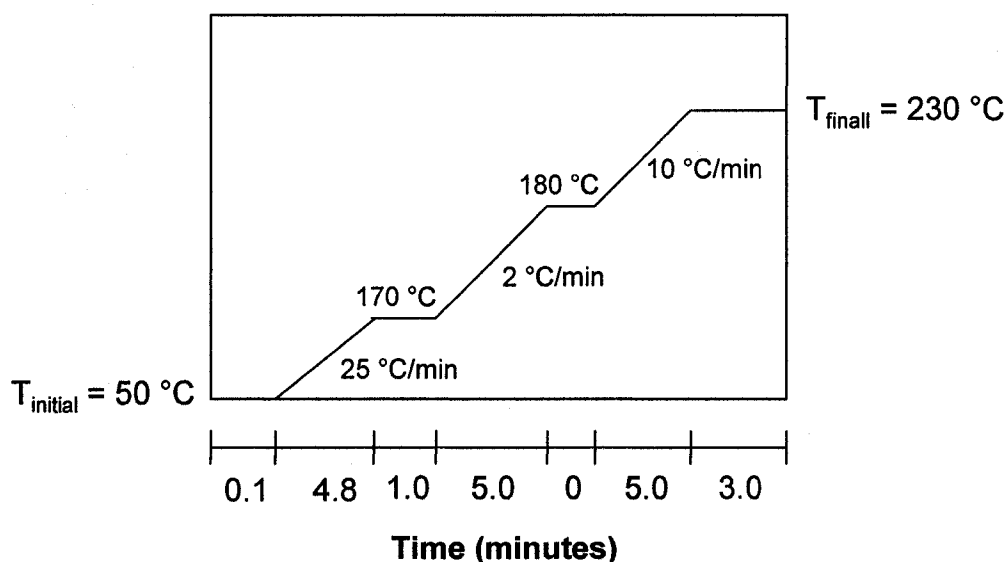


**Figure 3.11** GC –FID column temperature profile for lipid analysis (100 m column)

#### 3.3.2.2.1 Derivatization with sodium methoxide and methanolic HCl

The same procedure was used for derivatization with sodium methoxide and methanolic HCl. A 10-30 mg oil or fat sample was weighed into the bottom of a test tube with 50  $\mu\text{l}$  of benzene to solubilize the sample. The sample was allowed to sit for 20-30 min before 2 mL of either sodium methoxide or methanolic HCl was added to the test tube. The

**Table 3.5** Groups methylated by different derivatization compounds

<b>Derivatization Compound</b>	<b>Types of compounds methylated</b>
Boron Trifluoride	• TAG <sup>(1)</sup> , DAG <sup>(2)</sup> , MAG <sup>(3)</sup> , FFA <sup>(4)</sup>
Diazomethane	• FFA
Sodium methoxide	• TAG, DAG, MAG, FFA
Methanolic HCL	• TAG, DAG, MAG

(1) TAG=triglyceride

(2) DAG=diglyceride

(3) MAG=monoglyceride

(4) FFA=Free fatty acid

samples were then heated in a water bath (30 min for sodium methoxide, 50 min for methanolic HCl) at 50 °C. The samples were allowed to cool before 100 µl of water and 2 mL of hexane were added to the test tubes. The tubes were shaken and allowed to sit while the organic and aqueous layers developed. The hexane (organic) layer was extracted and stored in a vial with a Teflon® liner at 4 °C.

### 3.4 EXPERIMENTAL DESIGN

This work consisted of many experiments. For ease of understanding, the experimental designs for each experiment, in terms of the number of reactions conducted and at what conditions, are incorporated into Chapter 4.

## **CHAPTER 4: RESULTS**

### **4.1 PYROLYSIS OF MODEL COMPOUNDS**

#### **4.1.1 PRELIMINARY PYROLYSIS STUDIES USING STEARIC ACID**

The experimental conditions chosen for the preliminary pyrolysis reactions are shown in Table 4.1. The temperatures chosen were based on previous literature (Dandik and Askoy, 1998a; Idem et al., 1996; Schwab et al., 1998). Relatively short reaction times (5 and 30 min) were chosen as a starting point so that initial data could be obtained relatively quickly. Immediately after quenching, the reactor was opened and 10 ml of pentane was added to the products and swirled. The pentane soluble products were extracted with a Pasteur pipet into a flask. Two subsequent 10 ml extractions were also conducted for a total of 3 x 10 ml pooled extractions before an aliquot of approximately 3 ml was transferred to a sample vial with a Teflon® lined screw cap. Liquid extracts were analyzed on GC-FID. For this set of runs, no internal standards were added but unreacted stearic acid was dissolved in pentane and analyzed on GC-FID to determine its retention time under the same conditions. The results are shown in Figures 4.1 and 4.2. Duplicate chromatograms (not shown) appear virtually identical for all runs.

Figures 4.1 and 4.2 clearly show that product distribution changes substantially with temperature and time. A 30 min reaction at 350 °C (Figure 4.1) resulted in low conversion as indicated by the absence of peaks in comparison to the other runs and the relatively large stearic acid peak at approximately 22.5 min., which was identified by

**Table 4.1** Experimental conditions for preliminary pyrolysis reactions (each X indicates one reaction run)

Time (min)	Temperature (°C)				
	350	400	450	500	550
30	XX	XX	XX	XX	-
5	-	XX	XX	XX	XX

comparing retention times of the sample with the stearic acid solution that did not undergo thermal treatment (Figure A.1, Appendix A). At 400 °C, distinct series of peaks began to form and at 450 °C, these series continued to develop. At 500 °C, the series began to degenerate resulting in numerous peaks cluttered at low retention times. The same trend was evident for the 5 min reactions but at slightly higher temperatures. At 400 °C (Figure 4.2) the series were just beginning to develop and increased in intensity at both 450 °C and 500 °C. Although the series were still present at 500 °C, more peaks were starting to form at retention times of less than 5 min. At 550 °C, these series were completely degenerated and resulted in a similar looking distribution as the 30 min reaction at 500 °C.

#### **4.1.1.1 Pentane insolubles extracted using toluene**

After the pentane extraction, there was still some residual material in the reactor at the milder reaction conditions. It was possible that the residue was not soluble in pentane or

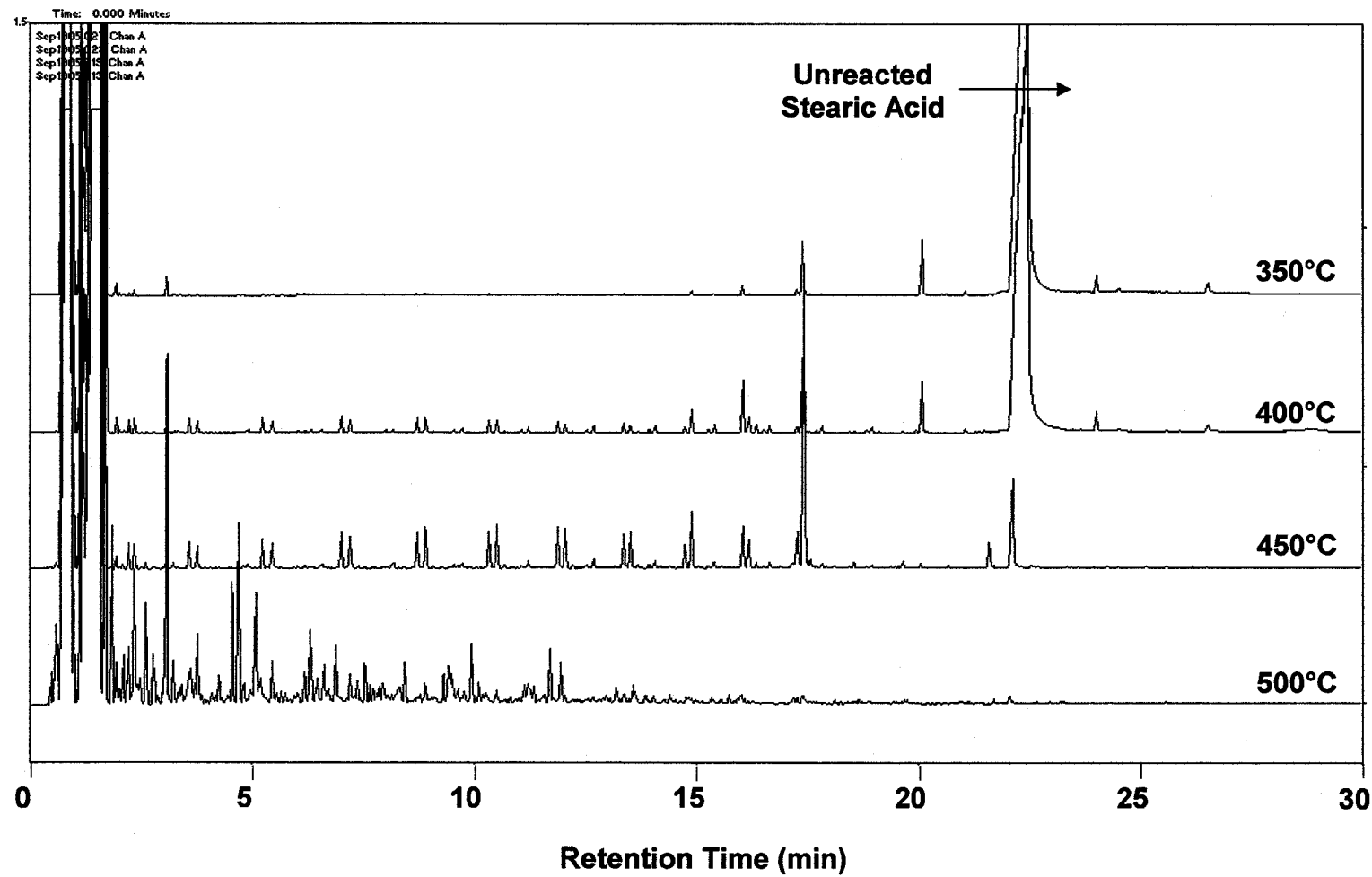


**Figure 4.1** GC-FID chromatogram showing the pentane soluble pyrolysis products of stearic acid after 30 min reactions at temperatures between 350 °C and 500 °C. Reactions were conducted in N<sub>2</sub> atmosphere and were initially at atmospheric pressure.

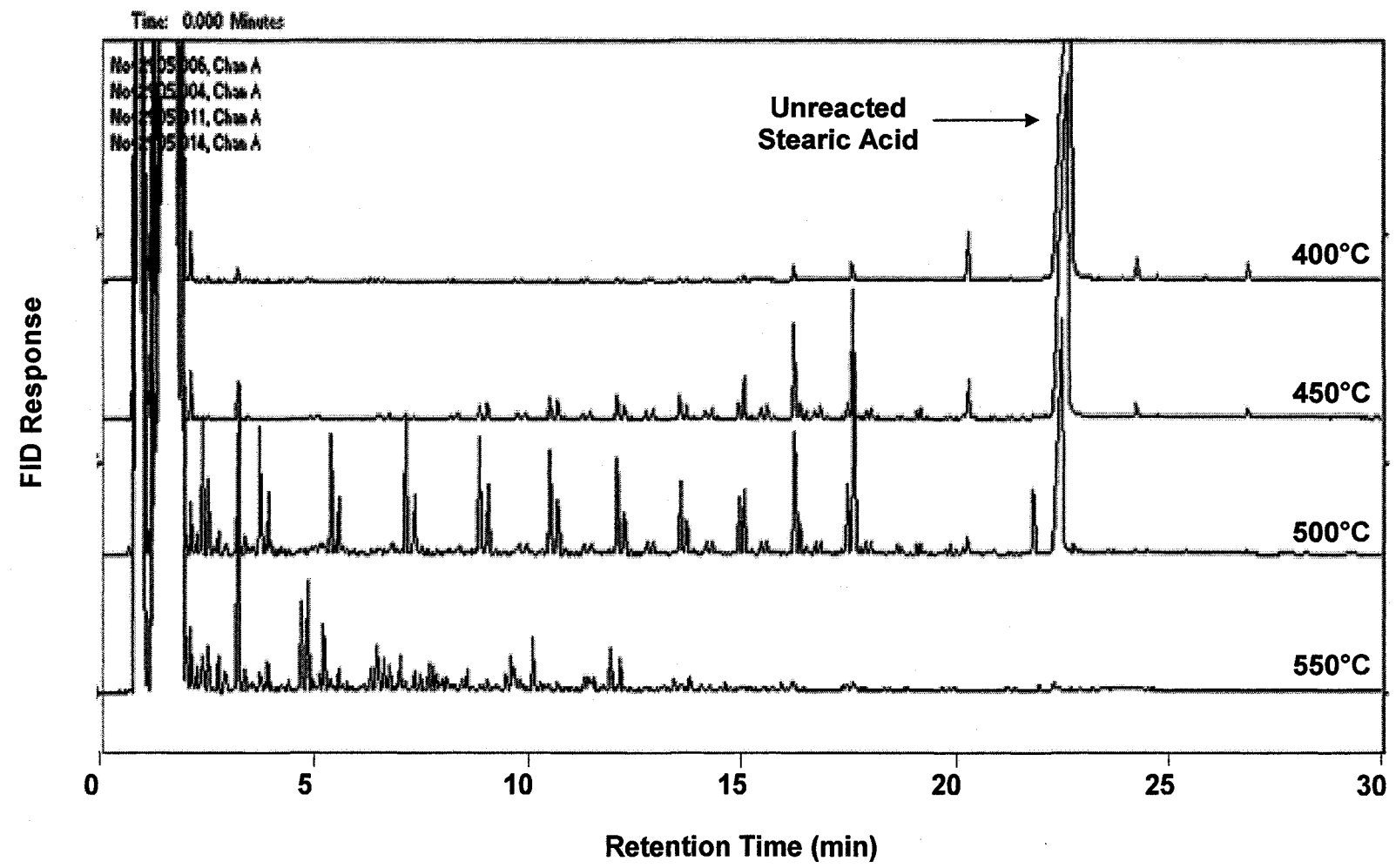


**Figure 4.2** GC-FID chromatogram showing the pentane soluble pyrolysis products of stearic acid after 5 min reactions at temperatures between 400 °C and 550 °C. Reactions were conducted in N<sub>2</sub> atmosphere and were initially at atmospheric pressure



That the solubility limit of the pentane was reached and unable to dissolve anything more. Stearic acid has low solubility in pentane so it was possible that the residue was unreacted feed. In order to determine what types of products were still in the microreactor after the pentane extraction, subsequent 3 x 10 mL toluene extractions were conducted for the 5 min runs and collected for analysis as shown in Table 4.2.

**Table 4.2** Experimental conditions for reaction runs that had an initial pentane and subsequent toluene extraction (each X represents a single reaction run).

Time (min)	Temperature (°C)			
	400	450	500	550
5	XX	XX	XX	XX

Select chromatograms are presented in Figures 4.3 and 4.4. Figure 4.3 shows that at 400 °C the toluene extract contains only the starting stearic acid compound not previously dissolved in the pentane. The small peaks on either side of the large stearic acid peak at retention times of approximately 20, 24, and 26 min are impurities in the feedstock material (determined by running controls with no thermal treatment) and the peaks at retention times less than 10 min are impurities in the toluene (determined by running toluene through the GC). The reactor appeared to be empty after the toluene extraction indicating that the toluene picked up all the material left in the reactor after the initial pentane extraction. The results are similar at 450 °C (chromatograms not shown). At 500 °C (Figure 4.4), more product is produced and there is less unreacted feed. At these

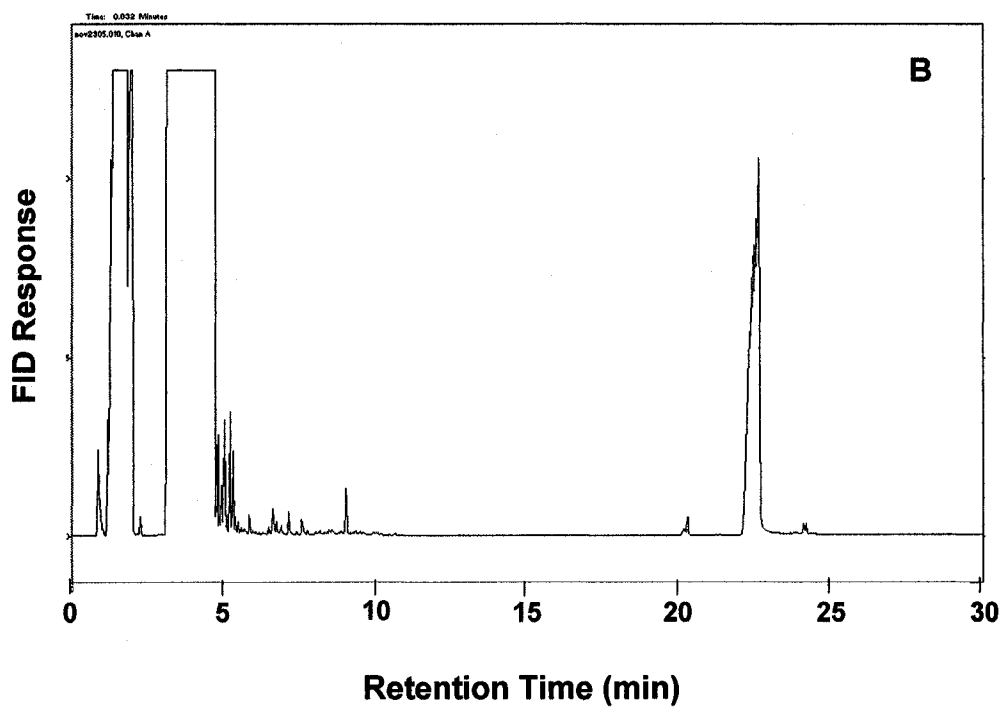
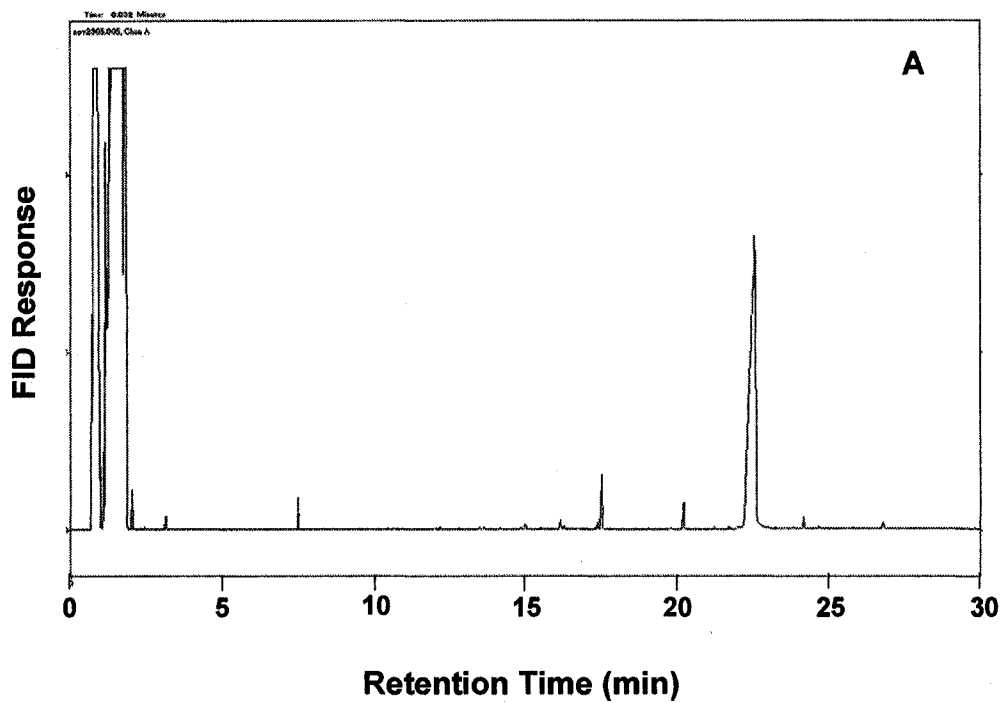


**Figure 4.3** GC- FID chromatograms showing pyrolysis products from a 5 min, 400 °C reaction in (A) pentane (first extraction) and (B) toluene (second extraction). Reaction was conducted in N<sub>2</sub> atmosphere and was initially at atmospheric pressure.

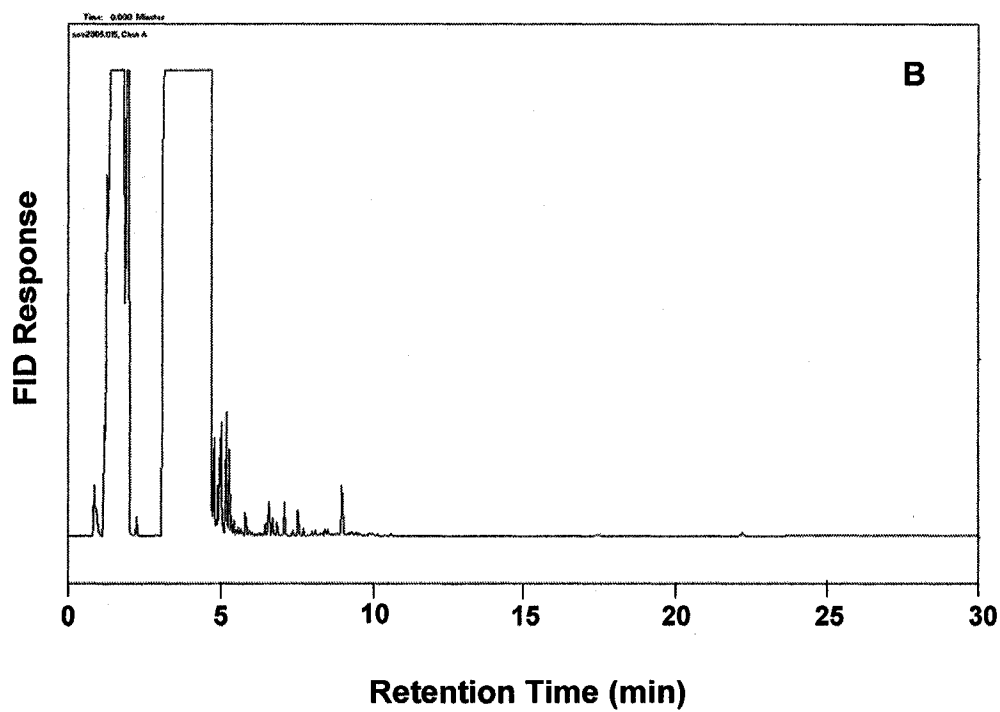
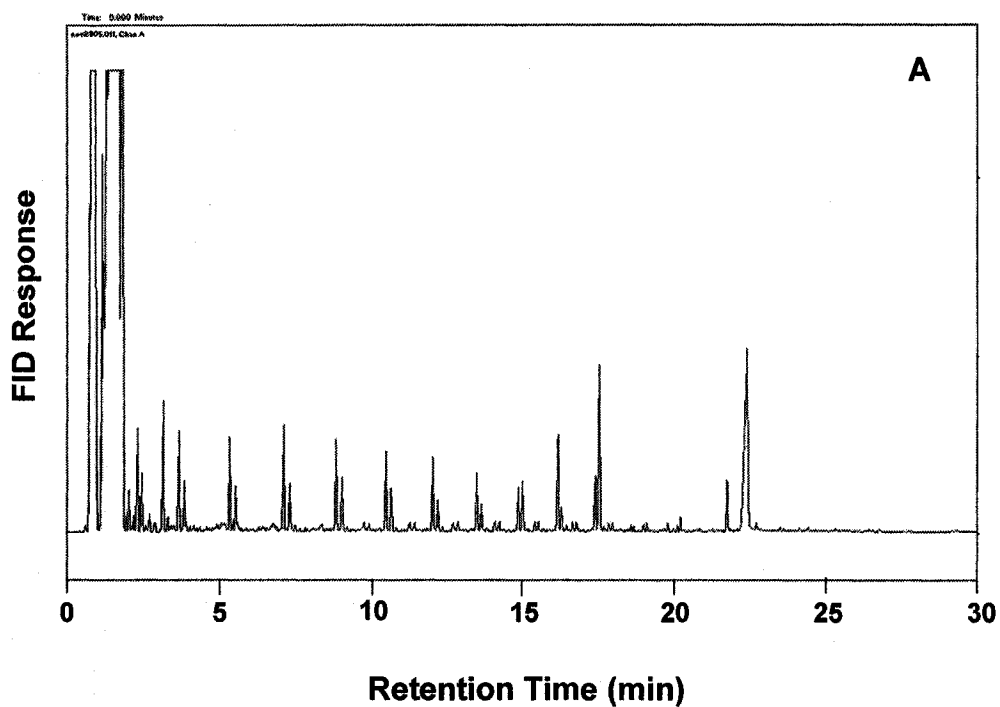


**Figure 4.4** GC- FID chromatograms showing pyrolysis products from a 5 min, 500 °C reaction in (A) pentane (first extraction) and (B) toluene (second extraction). Reaction was conducted in N<sub>2</sub> atmosphere and was initially at atmospheric pressure.

conditions, the pentane dissolved the majority of the reactor products including all of the unreacted feed as confirmed by the absence or trace quantities of any compounds in the toluene fraction. This experiment shows that for these experiments, the pentane is likely dissolving all of the reaction products, except some of the unreacted feed at the lower temperatures. Although no internal standards were used in these runs, the same volume of solvent was used for each extraction and the samples were analyzed on GC-FID without further dilution.

## **4.1.2 PRODUCT IDENTIFICATION**

### **4.1.2.1 GC/MS analysis**

To identify the peaks, two samples were taken to University of Alberta's Chemistry Department Mass Spectrometry Laboratory. They were (1) stearic acid breakdown products after a 5 min reaction at 500 °C (chromatogram shown in Figure 4.2) and (2) stearic acid breakdown products after a 5 min reaction at 550 °C (chromatogram shown in Figure 4.2). A search was conducted using the NIST (National Institute of Standards and Technology) mass spectra library and the best spectra matches were determined. The results show that after 5 min at 500 °C, five distinct series were formed including: an alkane series, two alkene series with peaks before (alkene series #1) and after (alkene series #2) the n-alkane peak on the chromatograms, a saturated carboxylic acid series, and an unsaturated carboxylic acid series with one double bond (Figure 4.5). The spectra indicate that the double bond in the first alkene series is likely in the one position and the double bond in the unsaturated carboxylic acids is at the end position opposite the

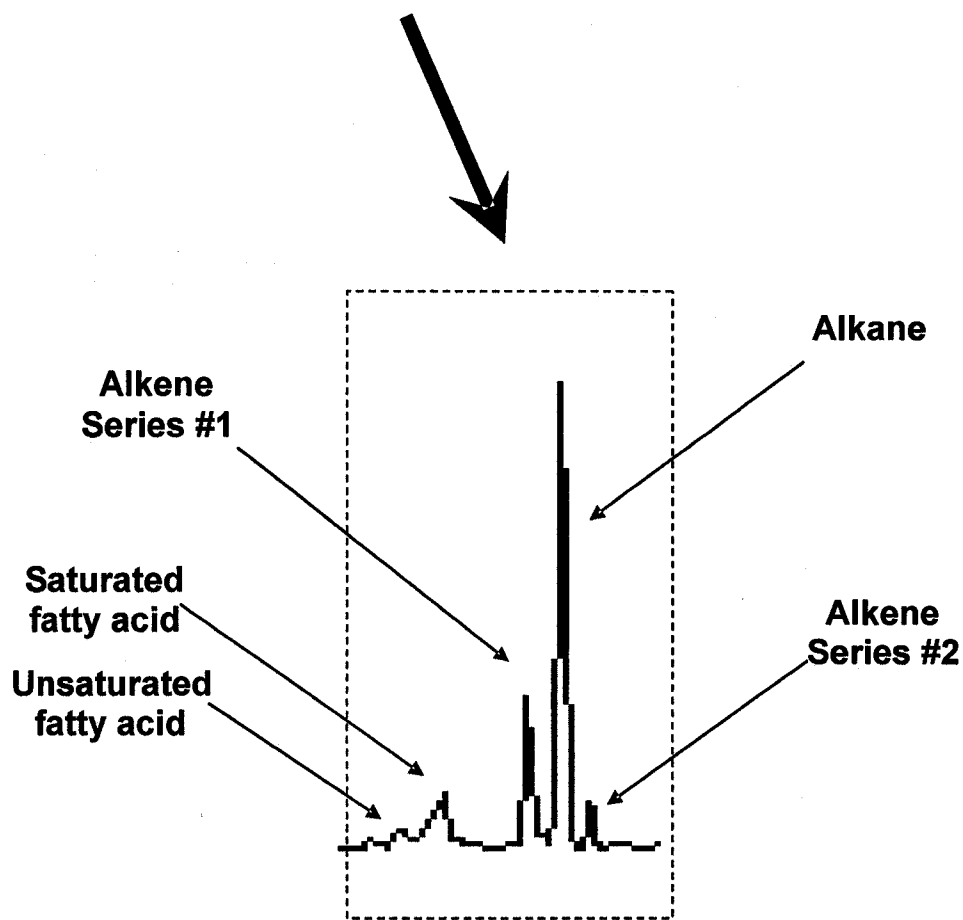
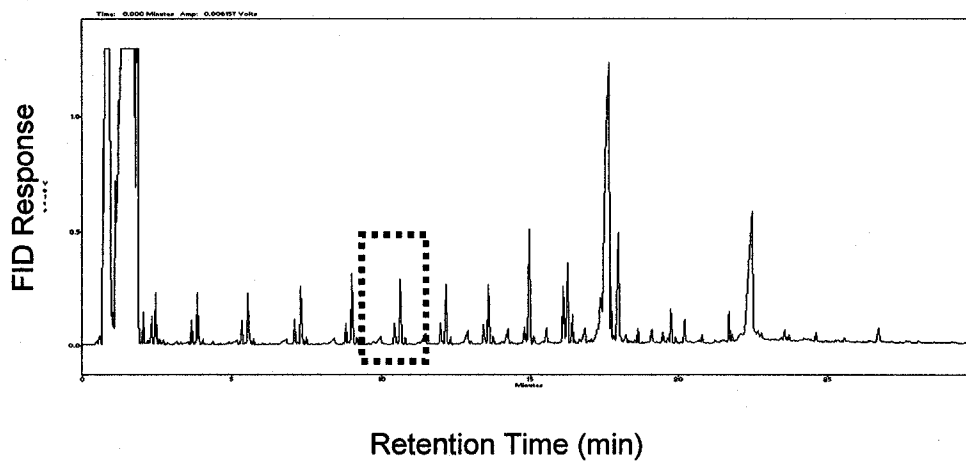


**Figure 4.5** Identification of the typical ladder series formed during pyrolysis of stearic acid. Reaction was conducted in  $N_2$  atmosphere and was initially at atmospheric pressure.

carboxyl group: however, this was not confirmed by NMR (nuclear magnetic resonance). It is also likely that the second alkene series is an isomer with the double bond in a different position, but again this was not confirmed by NMR. The results of the NIST search for compounds formed at 550 °C indicated that many of the compounds were likely aromatic.

#### **4.1.2.2 Product verification using external standards on GC-FID**

Two external standards including (1) a mixture of C<sub>8</sub>-C<sub>20</sub> n-alkanes purchased from Fluka and (2) a mixture of carboxylic acids prepared in-house using carboxylic acids from Sigma, were run on GC-FID under the same conditions as the samples. The resulting chromatograms are shown in Figure 4.6. A series of n-alkanes from octane (C<sub>8</sub>) to heptadecane (C<sub>17</sub>) as well as a series of carboxylic acids between C7:0 (heptanoic acid) and C18:0 (stearic acid) were identified in the pyrolysis mixture by comparing the retention times of the standard and the samples. The information from the external standards coupled with the GC/MS data was used to identify many of the compounds on the chromatograms as shown in Figure 4.6. Figure 4.7 shows a complete series of n-alkanes and alkenes from C<sub>8</sub>-C<sub>20</sub> and carboxylic acids, both saturated and unsaturated, from C<sub>4</sub> – C<sub>18</sub>.

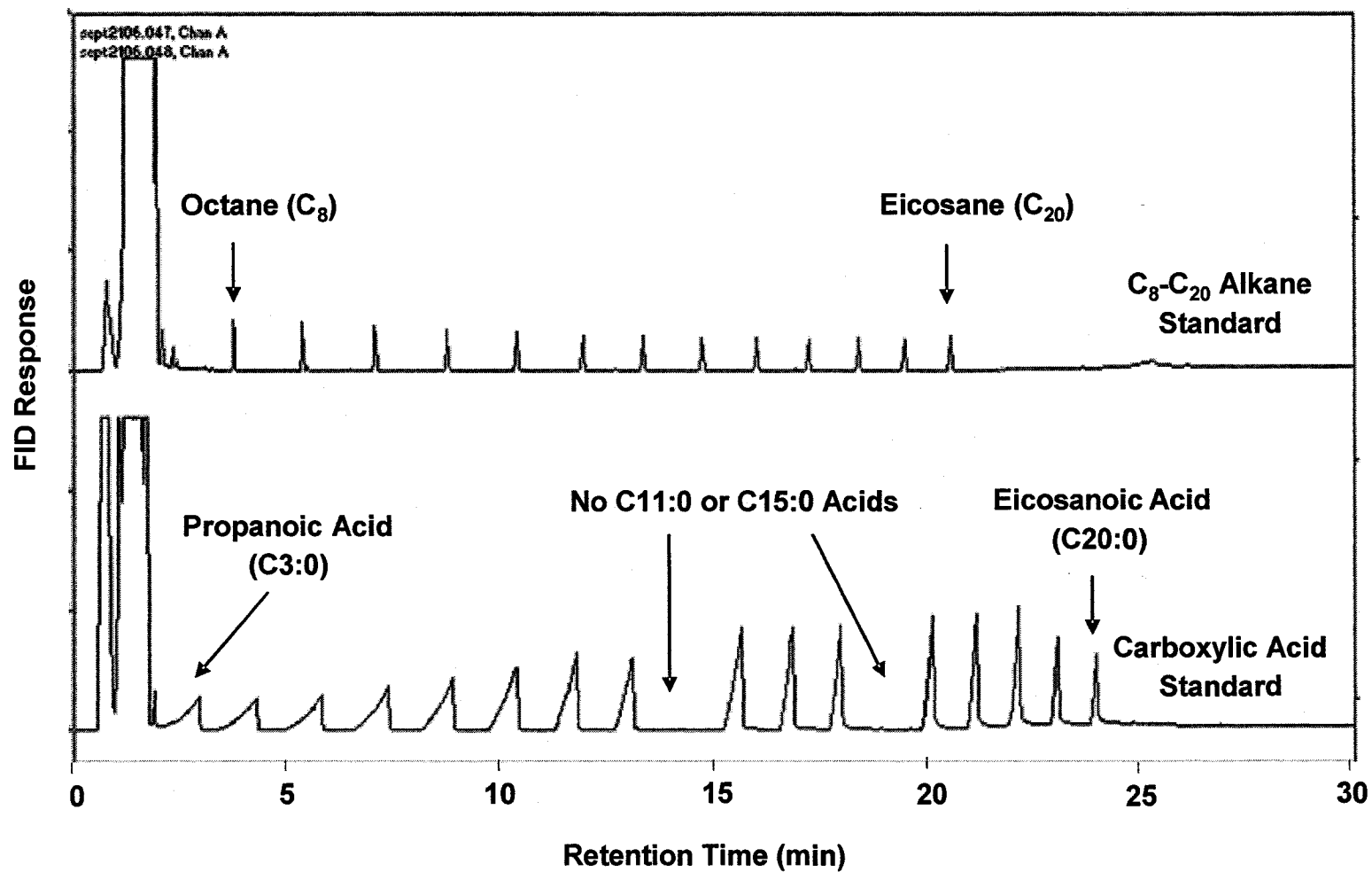


**Figure 4.6** GC-FID chromatogram showing the external standards run for verification of pyrolysis products. The standards were (1) a C<sub>8</sub>-C<sub>20</sub> n-alkane mixture purchased from Fluka (Table 3.1) and (2) a carboxylic acid standard prepared in-house using carboxylic acids.

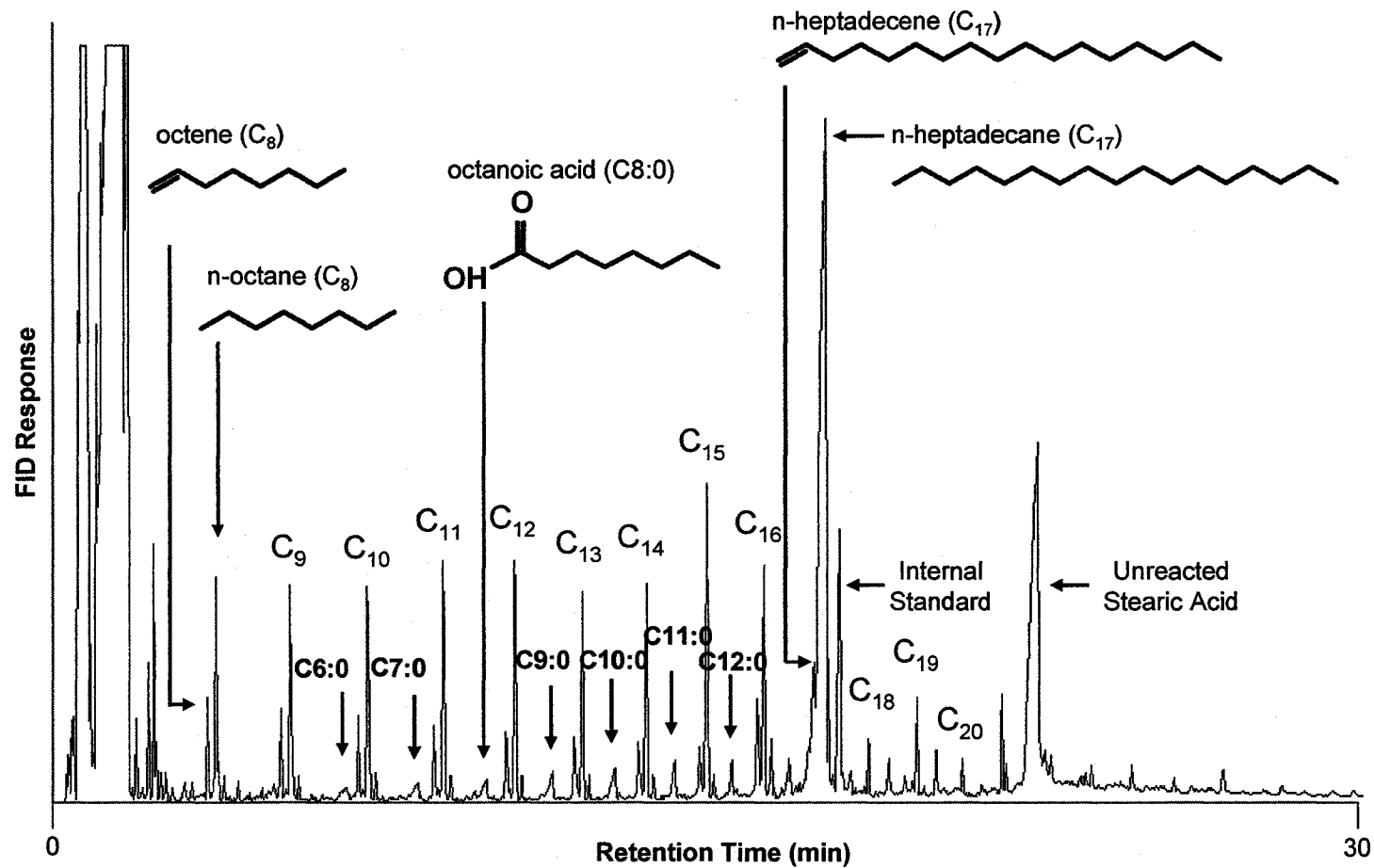


**Figure 4.7** Typical pentane soluble pyrolysis products of stearic acid after 5 min at 500 °C verified by running external standards. Reaction was conducted in N<sub>2</sub> atmosphere and was initially at atmospheric pressure.



### 4.1.3 STEARIC ACID PYROLYSIS AT VARIOUS TIMES AND TEMPERATURES

Reactions were conducted at various temperatures and times to determine stearic acid pyrolysis products at a broader range of conditions. One and 6 h runs were conducted at temperatures between 350-500 °C and 1 and 6 h. The resulting GC-FID chromatograms are presented in Figures 4.8-4.10 and the conditions are presented in Table 4.3. Reactions were conducted in N<sub>2</sub> atmosphere and were initially at atmospheric pressure. Figures 4.8 and 4.9 show GC-FID chromatograms for 1 h reactions at temperatures between 390 and 500 °C. At 390 °C, a series of C<sub>7</sub> to C<sub>20</sub> n-alkanes and alkenes are evident with n-heptadecane (C<sub>17</sub>) being the major reaction product followed by n-pentadecane (C<sub>15</sub>). At these conditions, there is starting feed still present in the reaction products. It is also interesting to note that there appears to be slightly more hexadecene formed than n-hexadecane, which differs from all other carbon numbers where the n-alkane is clearly formed preferentially over the alkene. At 400 °C more n-hexadecane is formed than hexadecene (alkene series #1, Figure 4.5); however, in comparison to other carbon numbers, the ratio between the n-alkane and alkene appears to be smaller (i.e. in the case of C<sub>16</sub>, more alkene is formed relative to the n-alkane). There also appears to be a cluster of peaks in the C<sub>16</sub> range. In contrast, the other carbon numbers have one distinct n-alkane and alkene. The second n-alkane series shown in Figure 4.5 is also present alongside the n-alkane and alkene pairs but in much smaller amounts. As discussed in previous sections, the peaks in this C<sub>16</sub> “cluster” are likely alkene isomers or branched products. As temperature increases the n-alkane and alkene

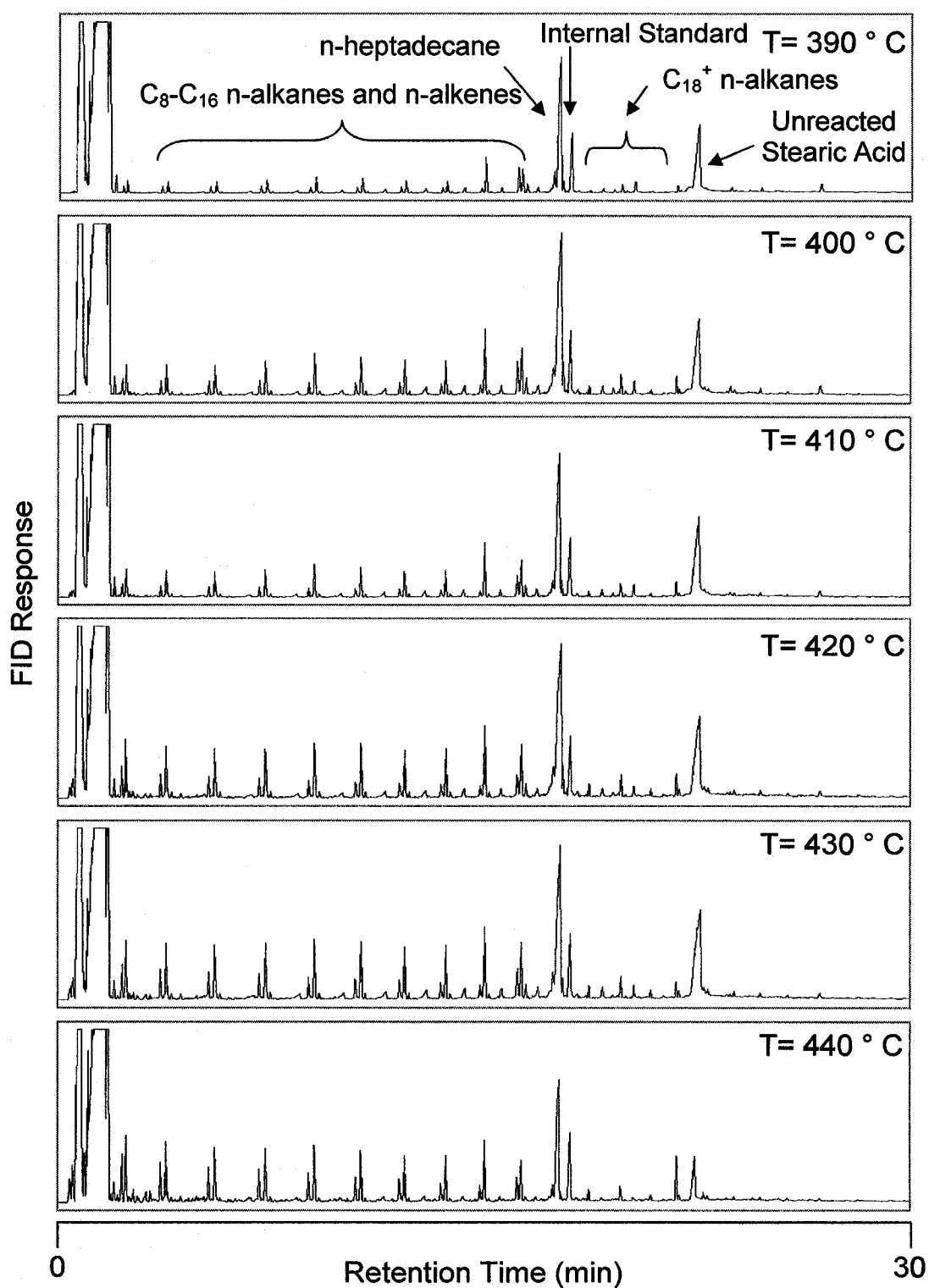


**Figure 4.8** GC-FID chromatograms showing stearic acid pyrolysis products for 1 h reactions at temperatures ranging from 390-440 °C. Reactions were conducted in N<sub>2</sub> atmosphere and were initially at atmospheric pressure.

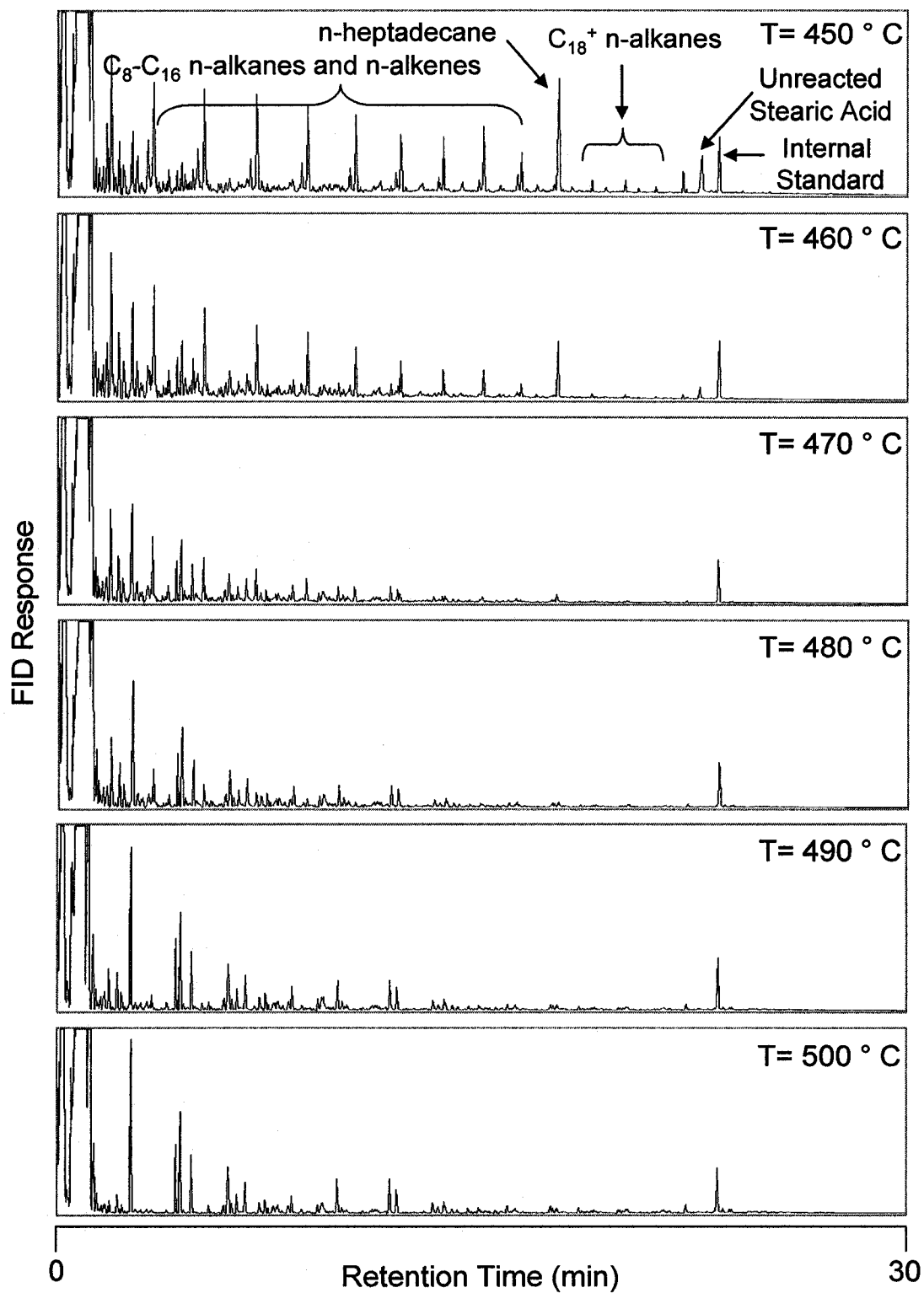


**Figure 4.9** GC-FID chromatograms showing stearic acid pyrolysis products for 1 h reactions with temperatures ranging from 450-500 °C. Reactions were conducted in  $N_2$  atmosphere and were initially at atmospheric pressure.

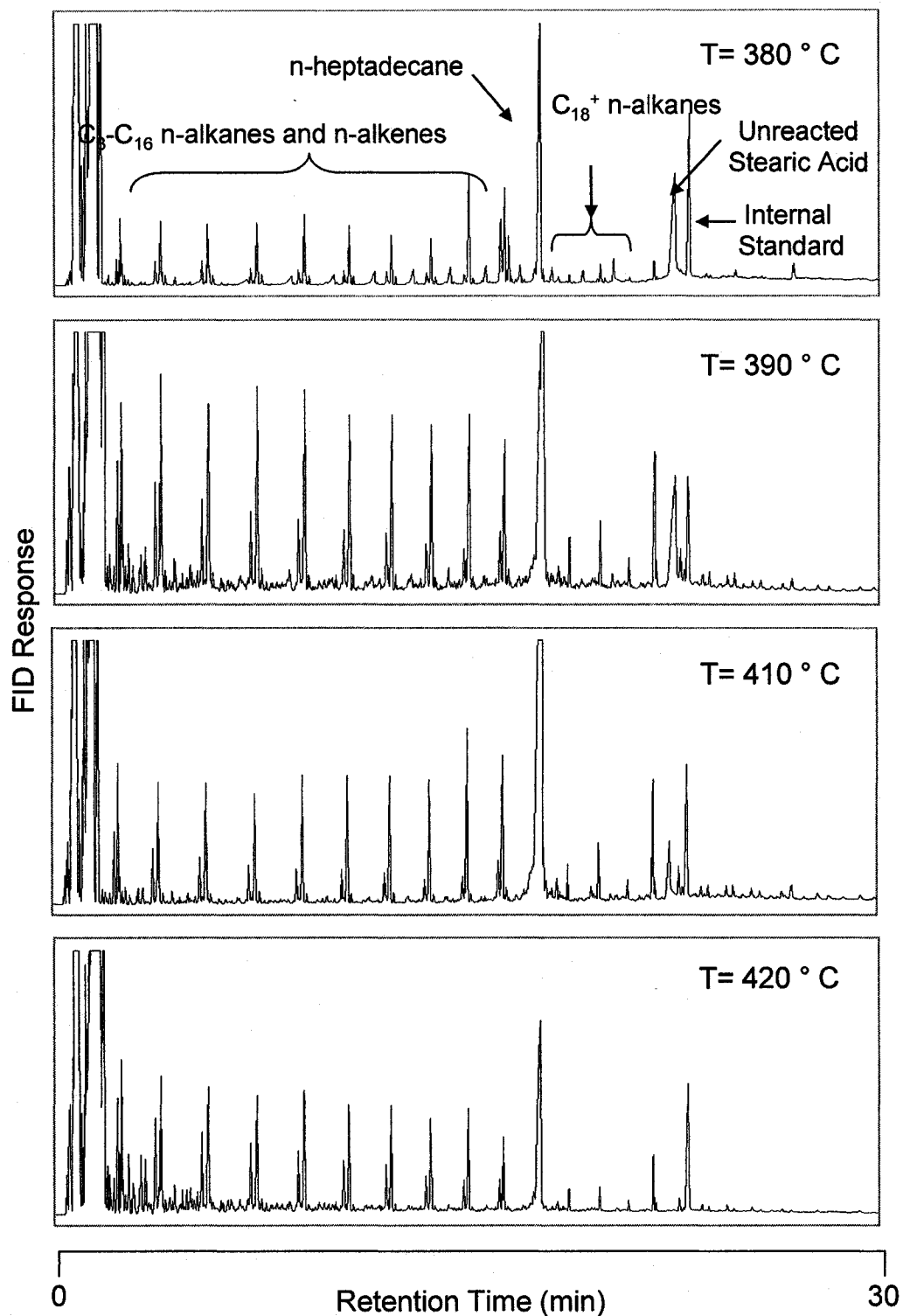


**Figure 4.10** GC-FID chromatograms showing stearic acid pyrolysis products for 6 h reactions with temperatures ranging from 380-420 °C. Reactions were conducted in N<sub>2</sub> atmosphere and were initially at atmospheric pressure.

**Table 4.3** Experimental conditions for stearic acid pyrolysis at various times and temperatures (each X represents a single reaction run).

Time (hr)	Temperature (°C)												
	380	390	400	410	420	430	440	450	460	470	480	490	500
1	X	X	X	X	X	X	X	XX	XX	XX	XX	XX	XX
6	XX	XX	XX	XX	XX	-	-	-	-	-	-	-	-

series increase in intensity as expected based on previous results but are still present in a relatively even distribution. At 420 °C, additional peaks not representative of the series begin to form at low retention times showing the first evidence that the series are beginning to deteriorate or decompose. The chromatograms at 430 and 440 °C are similar to that of 420 °C except at 440 °C the amount of stearic acid starts to decrease. It is likely that the stearic acid peaks at 390-430 °C represent the maximum amount of acid that was dissolved in the extraction solvent as they all appear to be roughly the same size. It would be expected that they would decrease as the temperature is increased and more feed is converted. At 440 °C, the decrease in size of the stearic acid peak likely indicates that all the unreacted stearic acid is now being fully dissolved in the solvent. At 450 °C (Figure 4.9), the product distribution begins to shift to the production of lower n-alkanes and alkenes (i.e. C<sub>7</sub>-C<sub>11</sub>) and other low retention compounds begin to form. The amount of unreacted feed decreases even further and is almost entirely gone at 470 °C. At temperatures above 460 °C, the hydrocarbon series have almost completely disappeared.

Up until this point the reaction times chosen were relatively short. It was of interest to conduct longer reactions to obtain information at a wider range of conditions. The

conditions for this experiment are outlined in Table 4.3. Figure 4.10 shows the GC-FID chromatograms for these 6 h reactions. Comparing 6 and 1 h reactions at the same temperatures, it is evident that the product distribution remains relatively unchanged over 6 h, however the intensity of the peaks increases resulting in more reaction product formation. At 420 °C, there is some formation of lower retention time peaks as well as a slight shift towards formation of the shorter chain hydrocarbons. Results from these experiments helped select the conditions used for a larger time/temperature experiment as described in the next section.

#### **4.1.4 QUANTITATION OF IN STEARIC ACID PYROLYSIS PRODUCTS**

Based on results from the preliminary experiments, it was of interest to study the pyrolysis products of stearic acid over an even wider range of temperatures and times to gain a better understanding of how to manipulate the final product composition. In this experiment, reactions were conducted at temperatures between 350-500°C and times ranging from 0.5-8 h. The times and temperatures chosen for this study were based on preliminary results and are outlined in Table 4.4. The conditions range from mild, where very little conversion took place, to severe, where there is a substantial product breakdown and where the hydrocarbon series discussed in previous sections have degenerated. It is within this range of conditions that the products of interest are formed. The reactions were conducted as described in section 3.3.1.1. For these reactions, nonadecanoic acid methyl ester was added as an internal standard at known concentrations to allow for quantification of the reaction products. At the GC conditions

used in this experiment, the nonadecanoic acid methyl ester elutes from the column at approximately 22.6 min (Figure A.2, Appendix A).

#### 4.1.4.1 Appearance of reactions products

The appearance of the reaction products varied greatly with time and temperature. At the

**Table 4.4** Experimental conditions for the pyrolysis of stearic acid (each X represents a single reaction run).

Time (h)	Temperature (C°)						
	350	370	390	410	430	450	500
0.5	-	-	XX	XX	XX	XX	XX
1	-	XX	XX	XX	XX	XX	XX
4	XX	XX	XX	XX	XX	XX	XX
8	XX	XX	XX	XX	XX	XX	-

more mild conditions, the products were solid powders, either white or slightly brown.

As the temperatures increased, the color of the products shifted from white to darker brown and the appearance shifted from a solid powder to a solid lumped mass at the bottom of the reactor. When the temperature was high enough the products were in the liquid state and resembled a dark oil. It was difficult to differentiate any differences between the dark, liquid oils in the reactor so observations were made based on their appearance dissolved in pentane. These observations are presented in Table 4.5. The letters on the table represent similar appearance between the products of reactions at

different conditions. For example, the products of an 8 h reaction at 370 °C, denoted letter C, resembled the products of a 1 h reaction at 390 °C and a 30 min reaction at 410 °C. The appearance and color of the reaction products followed observable trends with both reaction temperature and time being a factor as clearly illustrated in Table 4.5. Initial products were white to light brown and were very cloudy dissolved in the pentane. Over time, many solid particles settled to the bottom of the storage vial. As the reaction conditions became more severe, a dark brown oil with few solid particles resulted. These products, denoted letter D, were observed at 410 °C after 4 and 1 h reactions and at 430 °C after 30 min of reaction. At slightly more severe conditions (letter E) the products were almost the same as D, but were very slightly cloudy and a slightly lighter in color. At 430 °C after a 4 h reaction, the appearance of the products changed dramatically. The mixture became orange in color and was clear. There was some black solid particles that formed and settled to the bottom and could not be dissolved in toluene . This was likely coke although the true tests for coke (i.e. solubility in tetrahydrofuran (THF)) were not conducted. These particles also adhered to the reactor walls and were difficult to remove. As temperature increased even further, the products remained clear but turned from orange to yellow to green. At the most severe conditions, a 4 h reaction at 500 °C, the products had a greenish tinge and there was substantial formation of the solid, black particles.



**Table 4.5** Appearance of reaction products after pentane extraction at various times and temperatures

Time (hr)	Temperature (°C)						
	350	370	390	410	430	450	500
0.5	X	X	B light-medium brown cloudy settled solids	C medium brown cloudy settled solids	D dark brown slightly cloudy few, if any, visible solids	E medium-dark brown slightly cloudy few visible solids	H orange/yellow clear some dark black solids
1	X	A whiteish-light brown cloudy settled solids	C medium brown cloudy settled solids	D dark brown slightly cloudy few, if any, visible solids	E medium-dark brown slightly cloudy few visible solids	G orange clear some dark black solids	I yellow clear some dark black solids
4	A whiteish-light brown cloudy settled solids	B light-medium brown cloudy settled solids	D dark brown slightly cloudy few, if any, visible solids	D dark brown slightly cloudy few, if any, visible solids	F brown/orange clear no visible solids except for some coke	H orange/yellow clear some dark black solids	J yellow/green clear dark black solids
8	A whiteish-light brown cloudy settled solids	C medium brown cloudy settled solids	D dark brown slightly cloudy few, if any, visible solids	E medium-dark brown slightly cloudy few visible solids	G orange clear some dark black solids	I yellow clear some dark black solids	X

#### 4.1.4.2 Product distributions

Figures 4.11 to 4.17 show the chromatograms from the reactions conducted at the conditions outlined in Table 4.4. These chromatograms demonstrate the product distribution at various conditions. It is important to note that due to the nature of the extraction solvent and the extraction method, it is possible that not all of the stearic acid, which is not very soluble in pentane, and heptadecane ( $C_{17}$  n-alkane) which is solid at room temperature, was dissolved in the pentane. It is likely that these peaks are underestimated. In terms of the types of products formed at the various conditions, duplicate chromatograms (not shown) were virtually identical. The results of this experiment confirm previous results. Both time and temperature are shown to have a substantial effect on the product distribution. At 350 °C (Figure 4.11), the main product was heptadecane ( $C_{17}$  n-alkane). The n-alkane ladders were just starting to form at 4 h and were slightly more developed at 8 h. There was also some starting feed material remaining, shown by the stearic acid peak: however, the actual quantity cannot be estimated from the size of the peak area as previously explained. Analysis of the amount of unreacted feed at different conditions is discussed in later sections. As temperature and time increased, the development of different series was evident. At 390 °C and 8 h (Figure 4.13), 410 °C and 1, 4, and 8 h (Figure 4.14), and 430 °C at 0.5 and 1 h (Figure 4.15), these ladders appeared to be the most developed. At 430 °C, there was evidence of low retention compounds, possibly aromatics, beginning to develop. At 450 °C after 4 h (Figure 4.16) and at 500 °C (Figure 4.17), the series have degenerated.

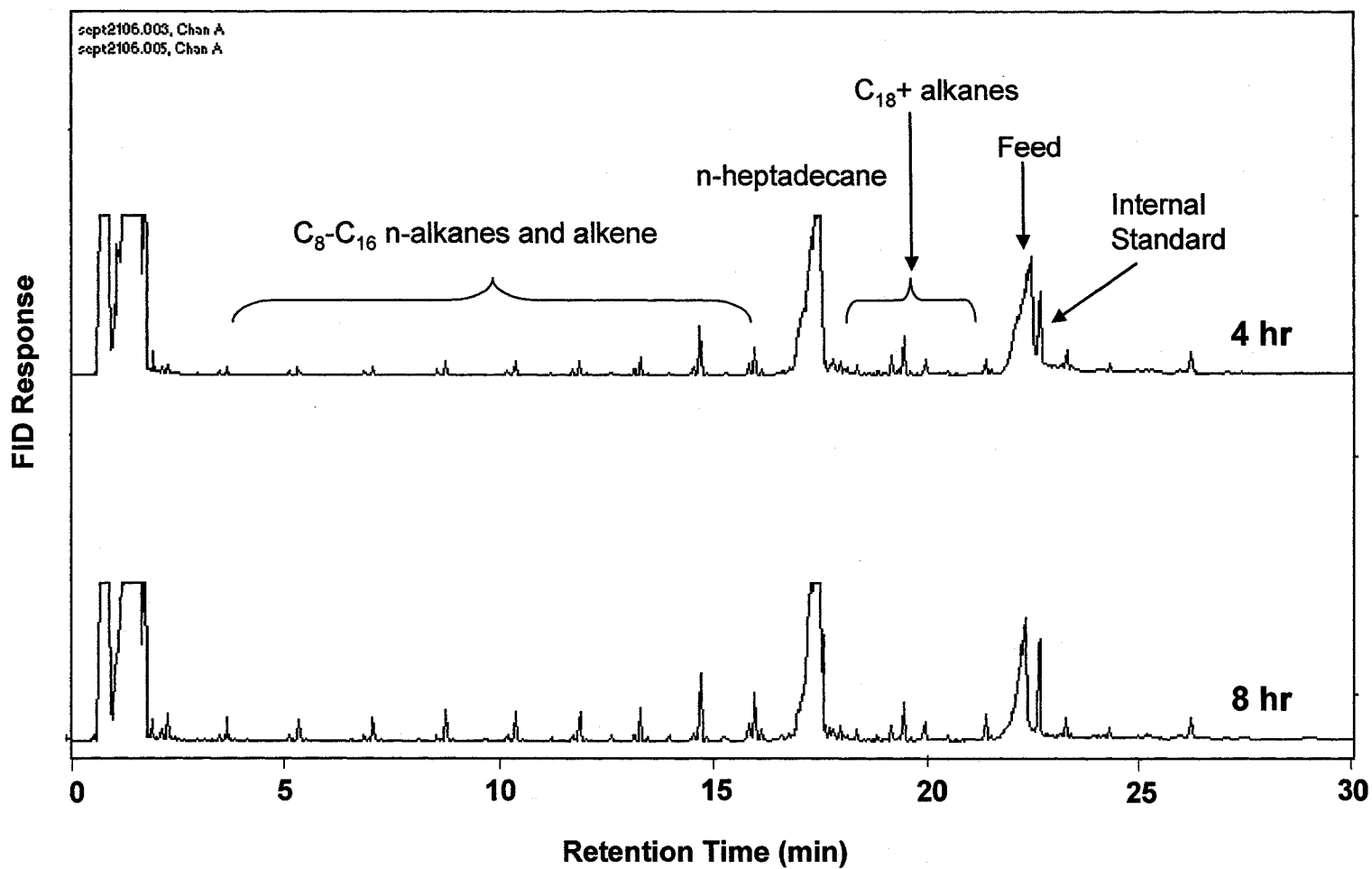


**Figure 4.11** GC-FID chromatograms showing pentane soluble stearic acid pyrolysis products from batch reactions at  $T = 350$  °C and  $t = 4$  and  $8$  hrs. Reactions were conducted in  $N_2$  atmosphere and were initially at atmospheric pressure.

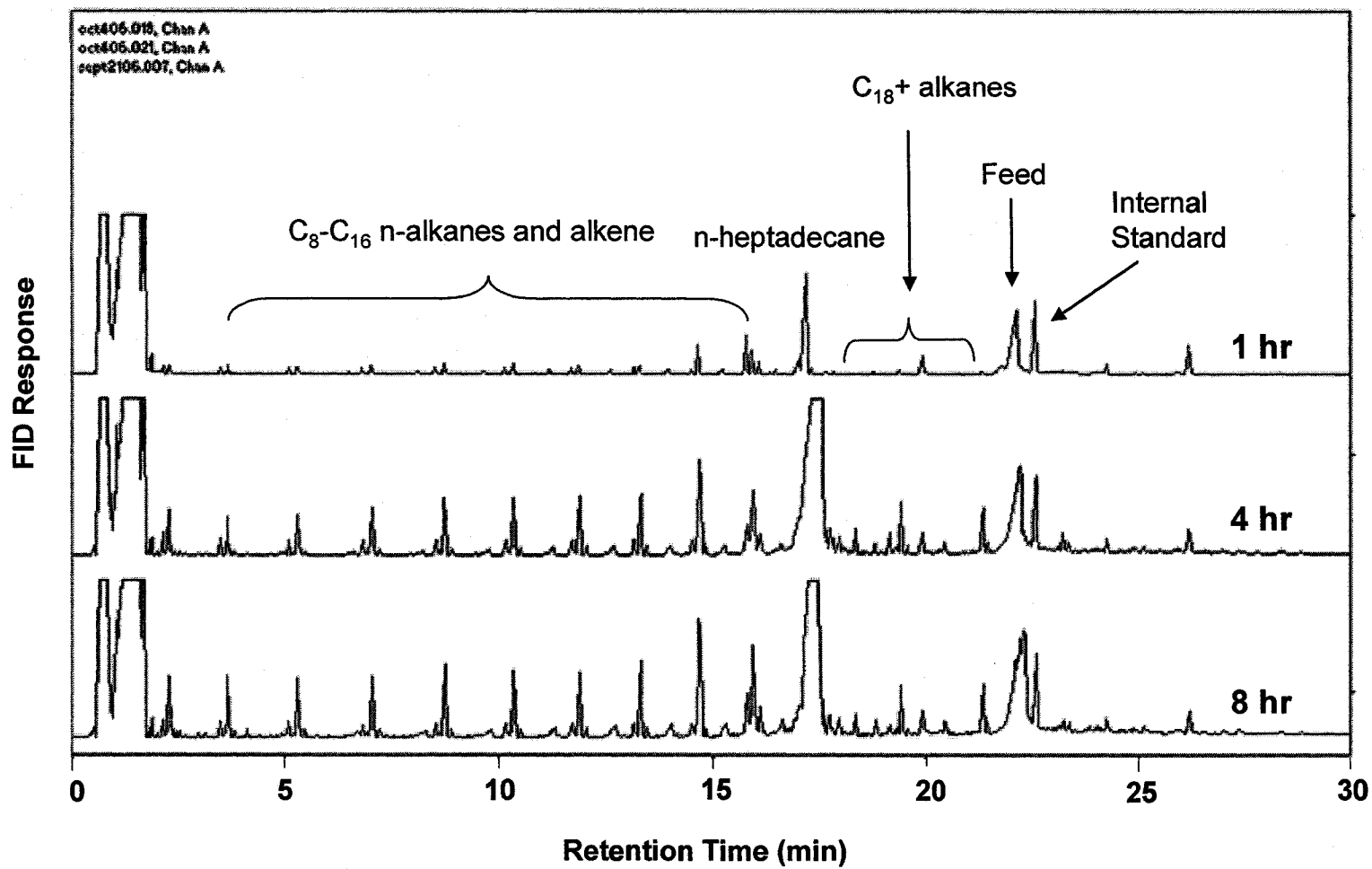


**Figure 4.12** GC-FID chromatograms showing pentane soluble stearic acid pyrolysis products from batch reactions at  $T = 370$  °C and  $t = 1-8$  hrs. Reactions were conducted in  $N_2$  atmosphere and were initially at atmospheric pressure.

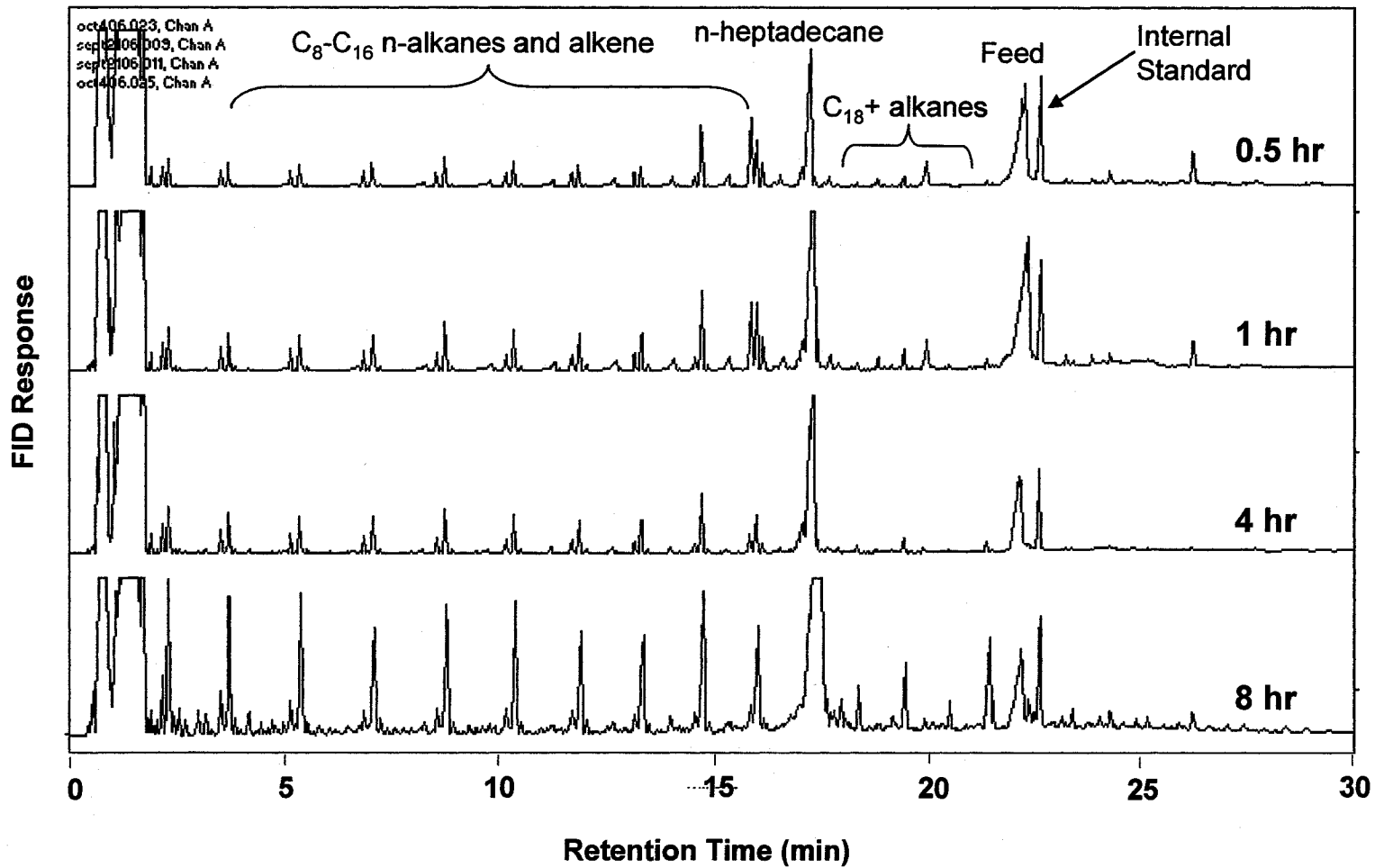


**Figure 4.13** GC-FID chromatograms showing pentane soluble stearic acid pyrolysis products from batch reactions at  $T = 390$  °C and  $t = 0.5$ -8 hrs. Reactions were conducted in  $N_2$  atmosphere and were initially at atmospheric pressure.

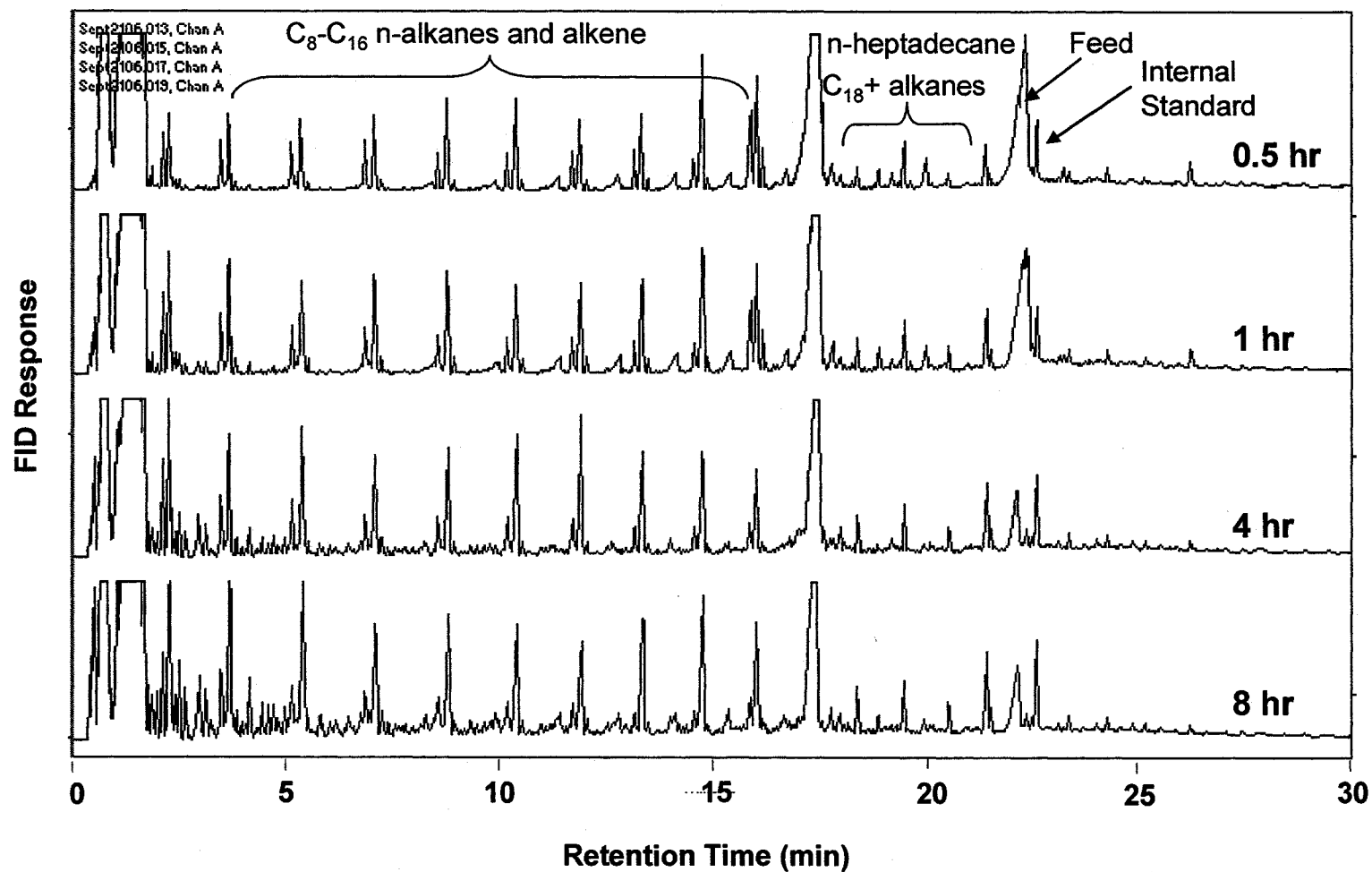


**Figure 4.14** GC-FID chromatograms showing pentane soluble stearic acid pyrolysis products from batch reactions at  $T = 410$  °C and  $t = 0.5-8$  hrs. Reactions were conducted in  $N_2$  atmosphere and were initially at atmospheric pressure.

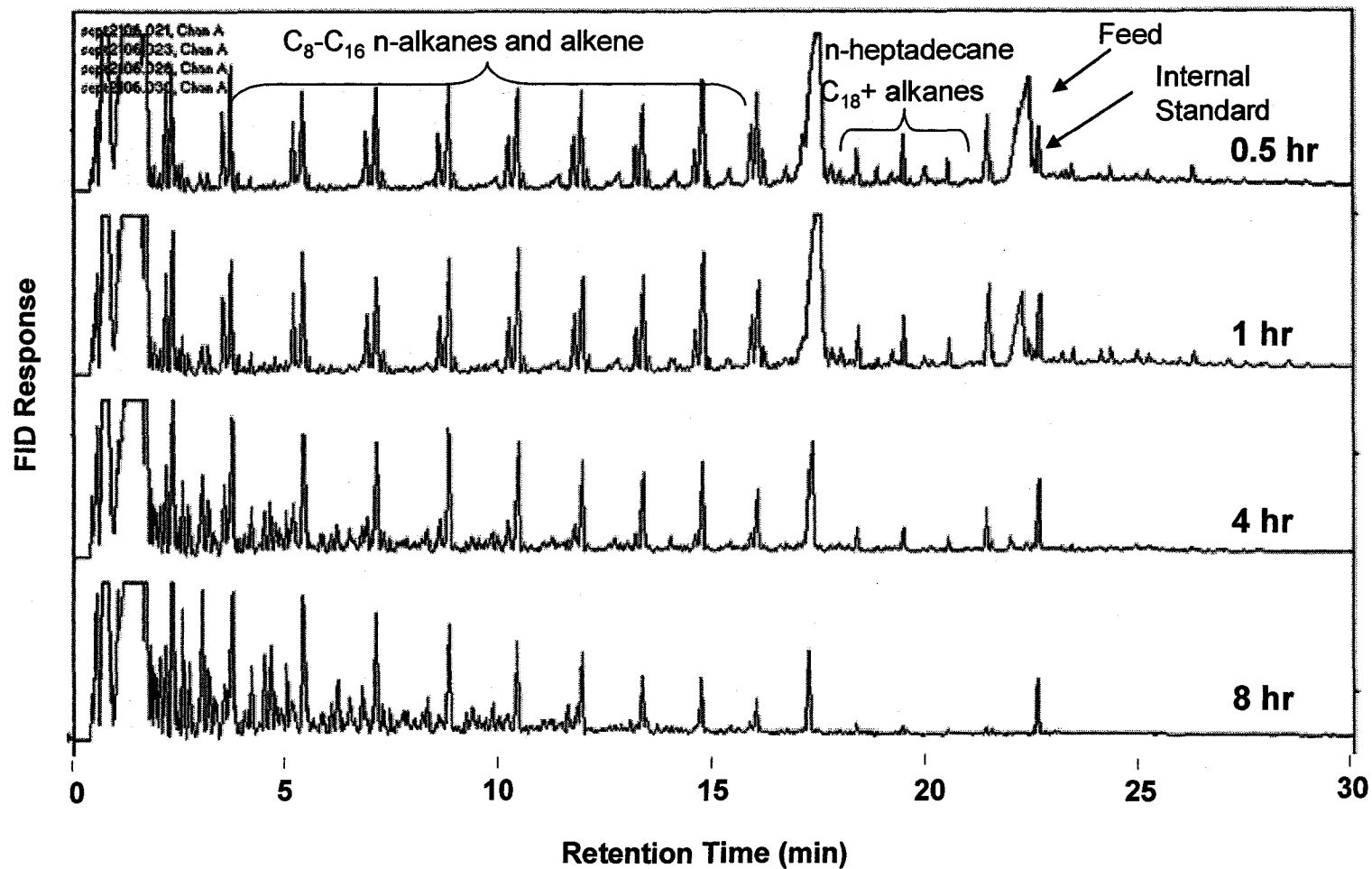


**Figure 4.15** GC-FID chromatograms showing pentane soluble stearic acid pyrolysis products from batch reactions at  $T = 430$  °C and  $t = 0.5-8$  hrs. Reactions were conducted in  $N_2$  atmosphere and were initially at atmospheric pressure.

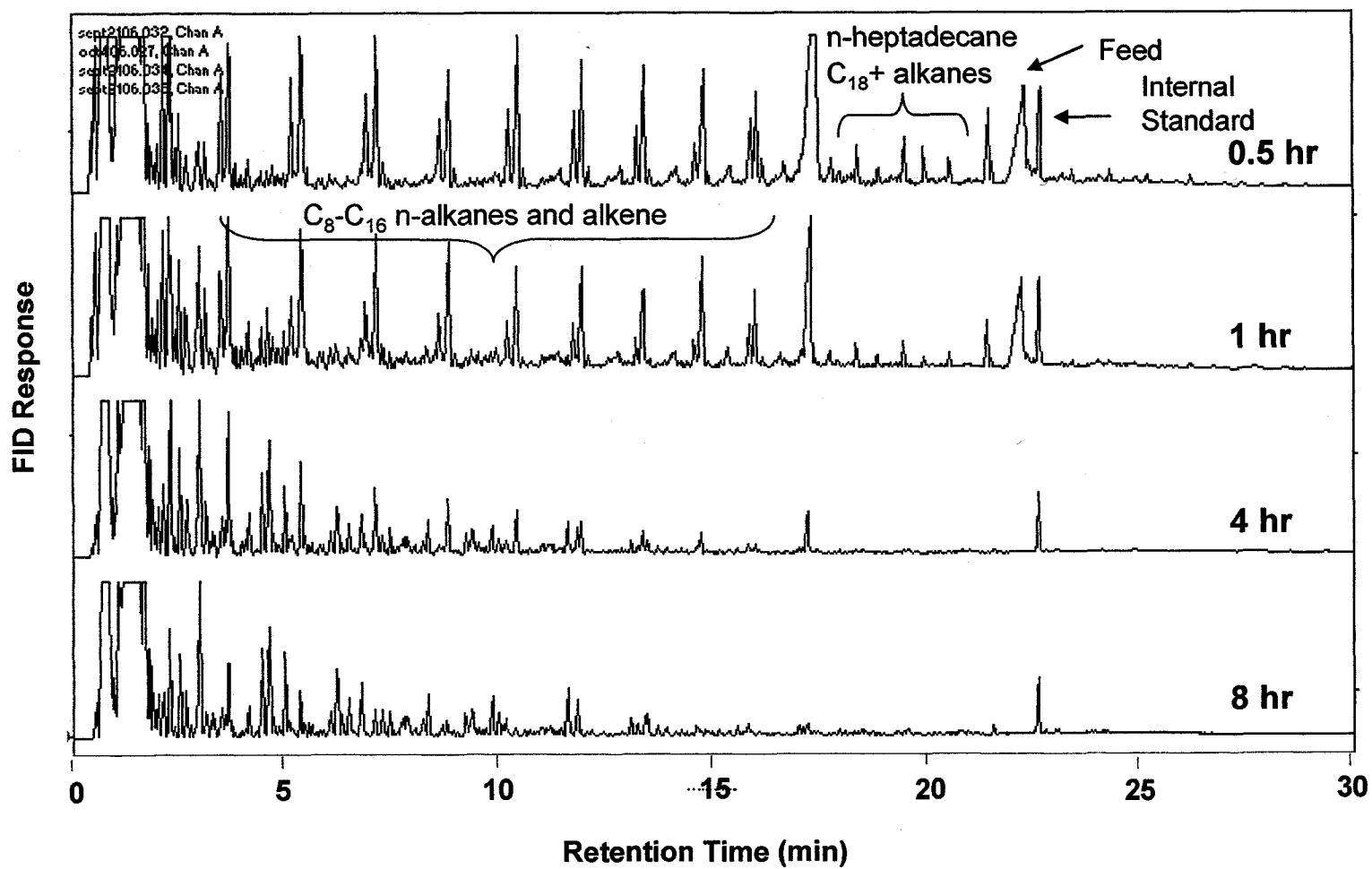


**Figure 4.16** GC-FID chromatograms showing pentane soluble stearic acid pyrolysis products from batch reactions at  $T = 450$  °C and  $t = 0.5$ -8 hrs. Reactions were conducted in  $N_2$  atmosphere and were initially at atmospheric pressure.



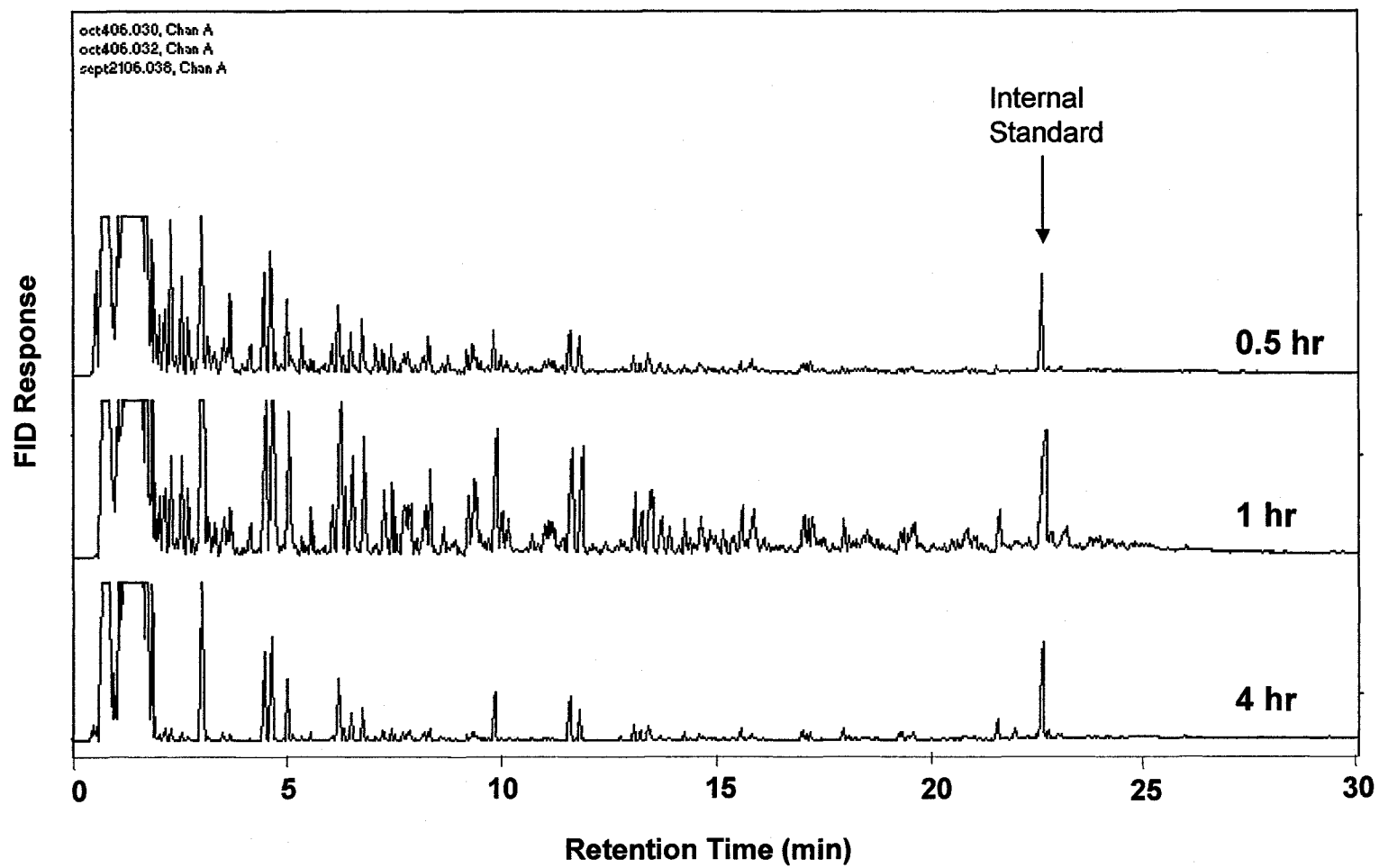


**Figure 4.17** GC-FID chromatograms showing pentane soluble stearic acid pyrolysis products from batch reactions at  $T = 500$  °C and  $t = 0.5-4$  hrs. Reactions were conducted in  $N_2$  atmosphere and were initially at atmospheric pressure.

#### 4.1.4.3 Estimation of C<sub>8</sub>-C<sub>20</sub> n-alkanes and alkenes

The main products of interest are the n-alkanes and alkenes (alkene series #1, Figure 4.5). These compounds form the two most prominent series in the pyrolysis products. n-Alkanes and alkenes from C<sub>8</sub>-C<sub>20</sub> were identified on the chromatograms using the GC/MS data and external standards. Peak areas were used to semi-quantitatively determine the amount of each compound in the product mixture relative to the internal standard of known concentration (Appendix B). It is possible that at the milder reaction conditions heptadecane (C<sub>17</sub>) and C<sub>17</sub><sup>+</sup> compounds are underestimated as described in the previous section. Although it might not be completely accurate, the data should still provide, at worst, a conservative estimate of yield. It should also be noted that integration parameters on the GC were such that peak areas less than a certain value were not included in the results. The minimum areas corresponds to concentrations between 0.36-0.56 mg/g of feed meaning that any products comprising less than 0.06 wt % of the feed will result in a value of BLD (below detectable limits). Figures 4.18 and 4.19 show the percentage of C<sub>8</sub>-C<sub>20</sub> n-alkanes and alkenes, respectively, formed at different reaction temperatures and times. It is important to note that the alkenes that are considered in this analysis were the alkenes that directly preceded the n-alkane peak in the chromatograms (alkene series #1 in Figure 4.5, likely the 1-alkene). It is likely that there is at least one other alkene series with the double bond in a different position (Figure 4.5); however, these peaks were diluted out at the concentrations used for this analysis. The samples were diluted prior to analysis because the C<sub>17</sub> peak overloaded the detector when a more

concentrated sample was analyzed. Figures 4.11-4.17 represent the GC-FID analysis from the more concentrated samples (i.e. all reaction product dissolved in 10 mL of pentane); however, peak integrations were conducted using the diluted samples (chromatograms not shown). Because the method used to quantitate the compounds is relative to the internal standard, which was added during extraction of the products from the reactor, it should not affect these results. As such, the small alkene peak that appears after the n-alkane in the chromatogram is not considered in this analysis but will be discussed later. The data represents the averages of duplicate runs and the error bars represent the standard error between the two runs (Appendix B). Based on Figures 4.18 and 4.19, it is clear that more n-alkanes are formed compared to alkenes. As well, the error bars at the more severe reaction conditions are smaller than those at the milder conditions. At 350, 370, 390, and 410 °C, the amount of n-alkanes and alkenes formed increases with time. At 430 °C and above, the amount of n-alkanes and alkenes in the C<sub>8</sub>-C<sub>20</sub> range start to decrease as the reaction time is increased. For example, at 430 °C a 4 h reaction results in a combined total of 25.2 wt % C<sub>8</sub>-C<sub>20</sub> n-alkanes and alkenes while after 8 h of reaction, this value decreases to 10.7 wt %. At 450 °C and reactions longer than 4 h, and at 500 °C, relatively small amounts of product in the C<sub>8</sub>-C<sub>20</sub> range are formed. The maximum amounts of C<sub>8</sub>-C<sub>20</sub> n-alkane and alkenes are formed at 410°C after 4 h (32.7 wt %) and 8 h (32.1 wt %) reactions and at 390 °C after 8 h (32.9 wt %). These values were calculated based on the initial feed weight. Due to limitations in the analysis method, the stearic acid peak was not quantified for this set of experiments and it is not possible to analyze the data based on the converted feed. Analysis of the amount of

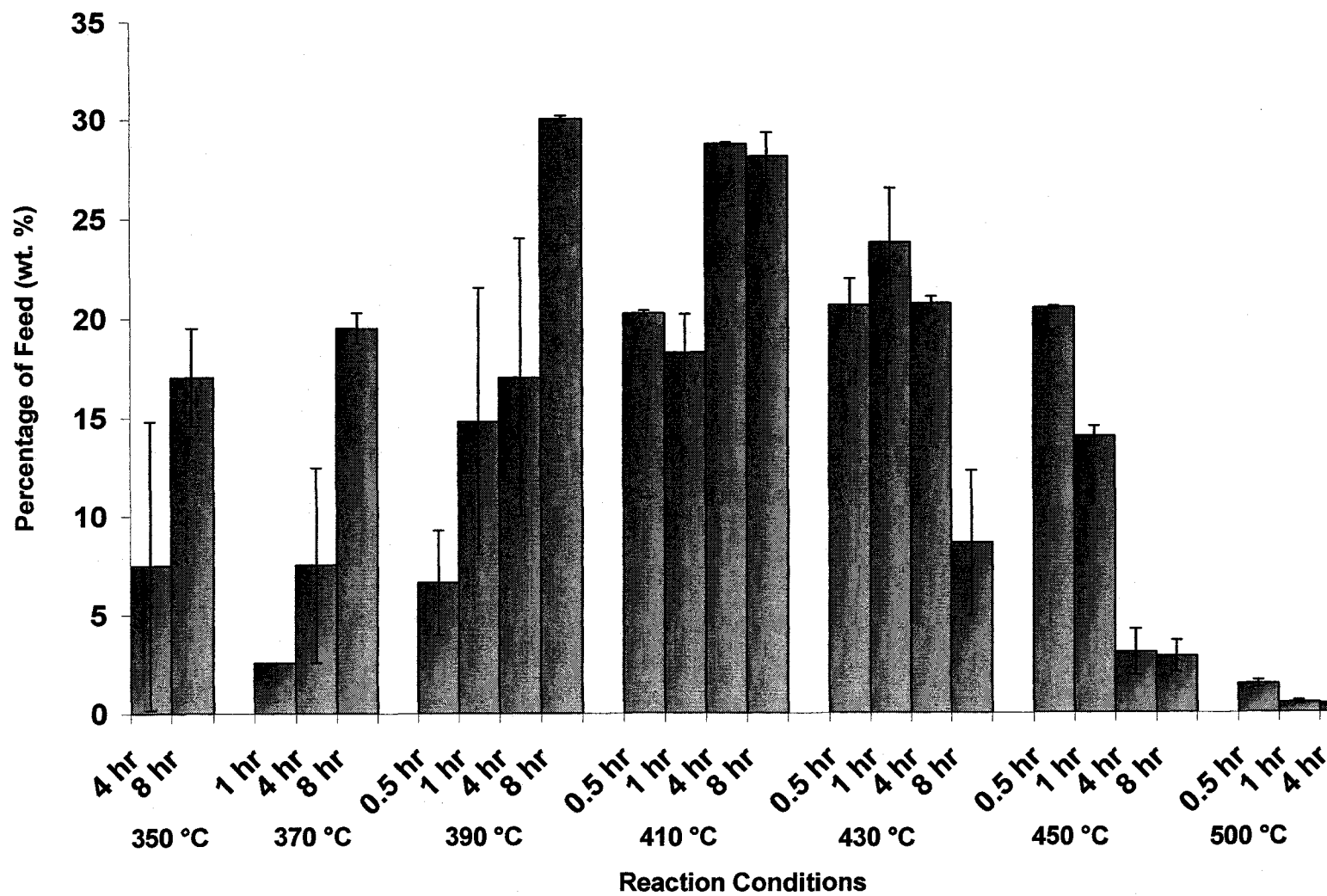


Figure 4.18 Percentage (wt) of C<sub>8</sub>-C<sub>20</sub> n-alkanes formed based on initial feed weight as a function of temperature and time

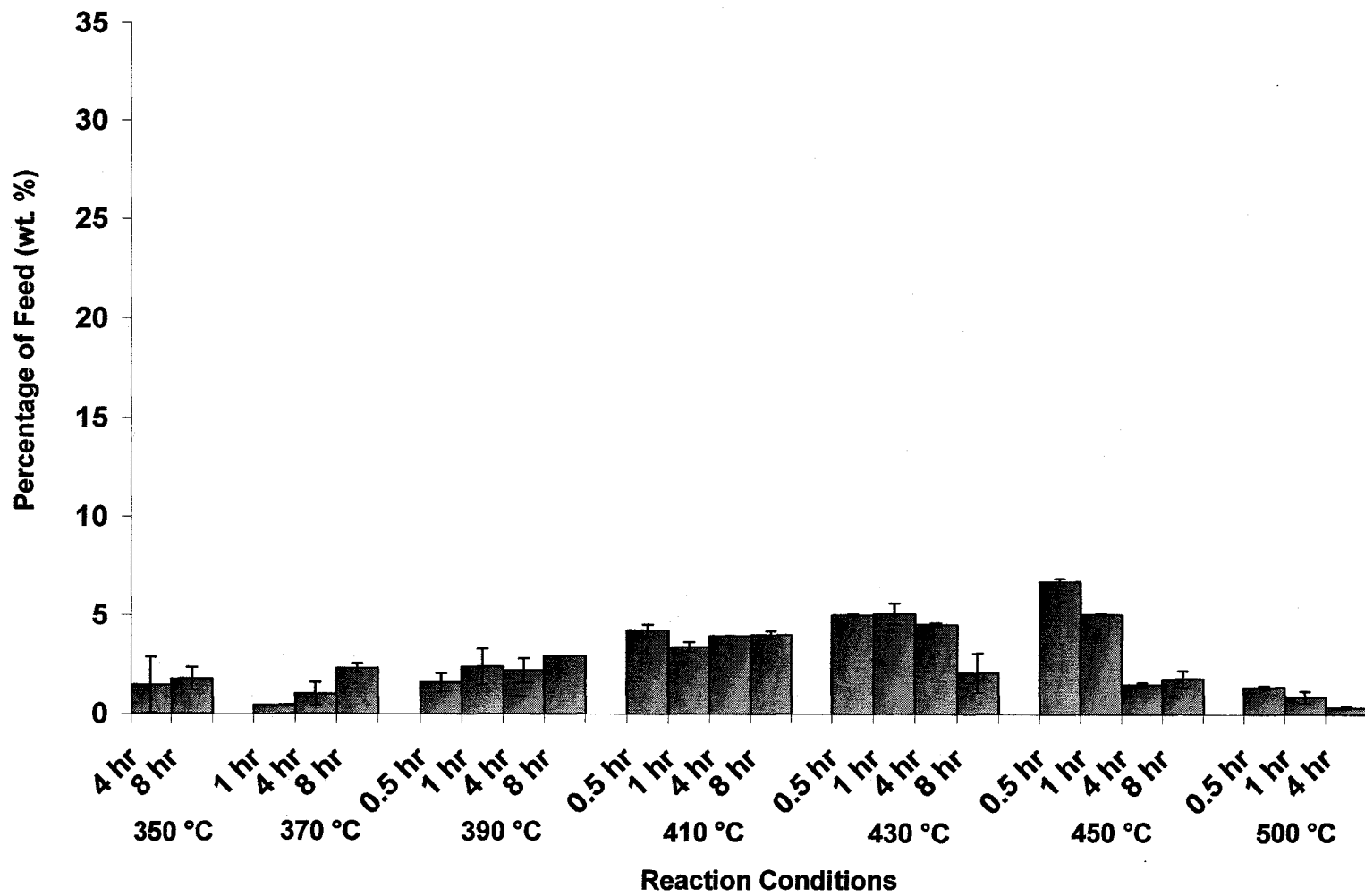


Figure 4.19 Percentage (wt) of C<sub>8</sub>-C<sub>20</sub> alkenes formed based on initial feed weight as a function of temperature and time

feed converted at the same conditions was conducted in a different experiment and these values were used to determine n-alkane/alkene yield at 390 °C, 410 °C, and 450 °C for 1 h reactions. This data is presented in Figure A.3 (Appendix A). The results indicate a different trend when yield is based on converted feed. At lower temperatures, such as 390 °C, there was less C<sub>8</sub>-C<sub>20</sub> n-alkanes and alkenes compared to 410 °C and 450 °C however; there was also less conversion at 390 °C. As a result, the amount of C<sub>8</sub>-C<sub>20</sub> n-alkanes and alkenes formed based on the amount of converted feed is actually greater at 390 °C than at 410 °C and 450 °C.

It is important to emphasize that although these yields may seem small, the compounds that were chosen for analysis represent only a fraction of the products. Due to the analytical procedures used for the liquid products, compounds lower than C<sub>8</sub> could not be clearly measured. Although the heptane and heptene (C<sub>7</sub>) peaks were visible in some of the chromatograms, C<sub>7</sub> was not included in the analysis because at mild conditions the peak was not visible and at harsh conditions, where many compounds are beginning to appear at lower retention times, it was difficult to identify which peaks represented heptane and heptene. Thus, the focus was on C<sub>8</sub>+ hydrocarbons but it is expected that the lower hydrocarbons follow the same trends.

#### **4.1.4.4 Cracking behavior of C<sub>8</sub>-C<sub>20</sub> hydrocarbons**

The data from the chromatograms (Figures 4.11-4.17) provides decent estimation of yields but it can also be used to study cracking behavior. Both molar yields and n-alkane

to alkene ratios can provide insight to the cracking behavior as a function of temperature and time. These two parameters will be discussed in the next sections. In both cases, peak integration data were converted into molar yields and molar ratios (Appendix B) and the standard error (error bars) was calculated between the duplicate runs. It is important to note that because this data represents the average of duplicate runs significance tests are generally not considered valid and thus were not conducted; however, it is the general trends that are of interest and these will be noted based on the graphs. Due to the integration parameters, any values with a molar yield less than 0.0014 mol<sub>i</sub>/mol<sub>feed</sub> will appear as BDL. In the case of the molar ratio, an alkene value (which are small compared to the n-alkanes value) less than this threshold would result in division by zero and thus, no corresponding ratio was reported for these circumstances.

#### *4.1.4.4.1 Molar Yields of C<sub>8</sub>-C<sub>17</sub> n-Alkanes*

Molar yields of n-alkanes are shown in Figures 4.20-4.23. For clarity, the lower temperatures (350-390 °C) are illustrated with open data point markers and dashed lines while the higher temperatures (430-500 °C) are illustrated with solid data point markers and solid lines. The middle temperature, 410 °C is illustrated with x's and a longer dashed line (see legend).

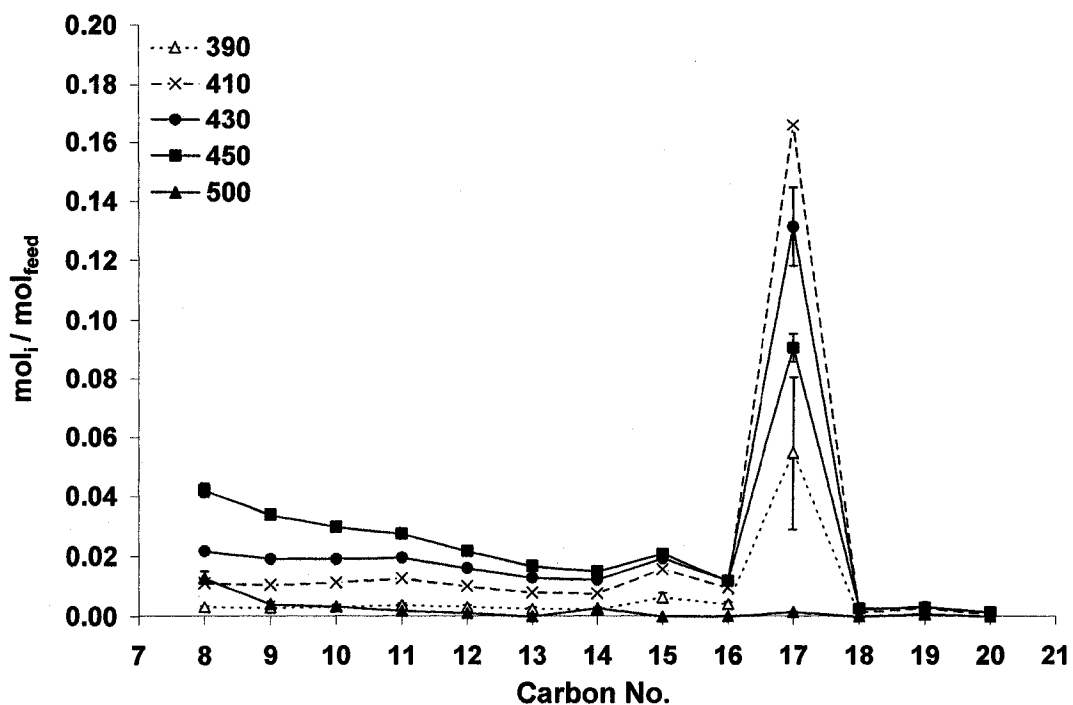


Figure 4.20 Molar yields of C<sub>8</sub>-C<sub>20</sub> n-alkanes as a function of temperature for 0.5 hr reactions

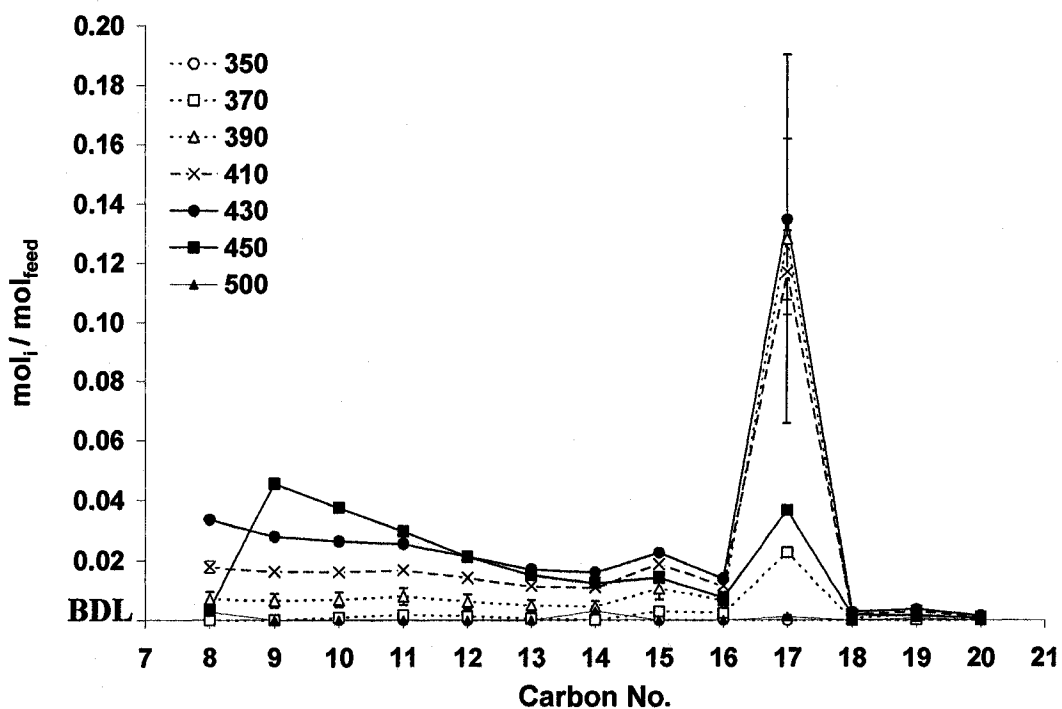


Figure 4.21 Molar yields of C<sub>8</sub>-C<sub>20</sub> n-alkanes as a function of temperature for 1 hr reactions



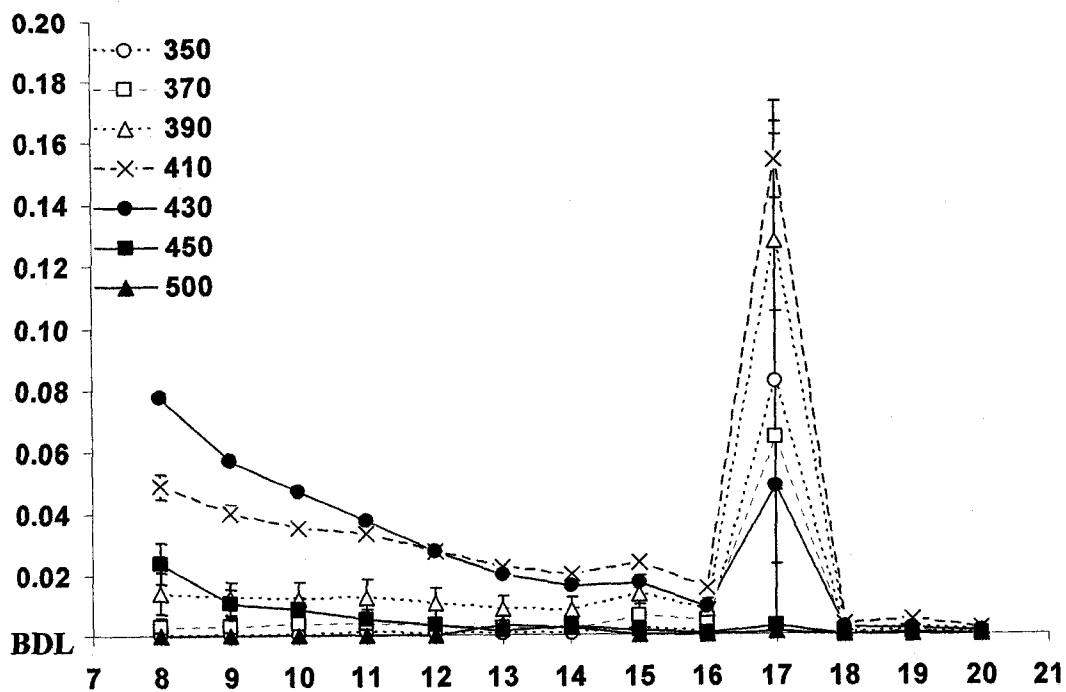


Figure 4.22 Molar yields of C<sub>8</sub>-C<sub>20</sub> n-alkanes as a function of temperature for 4 hr reactions

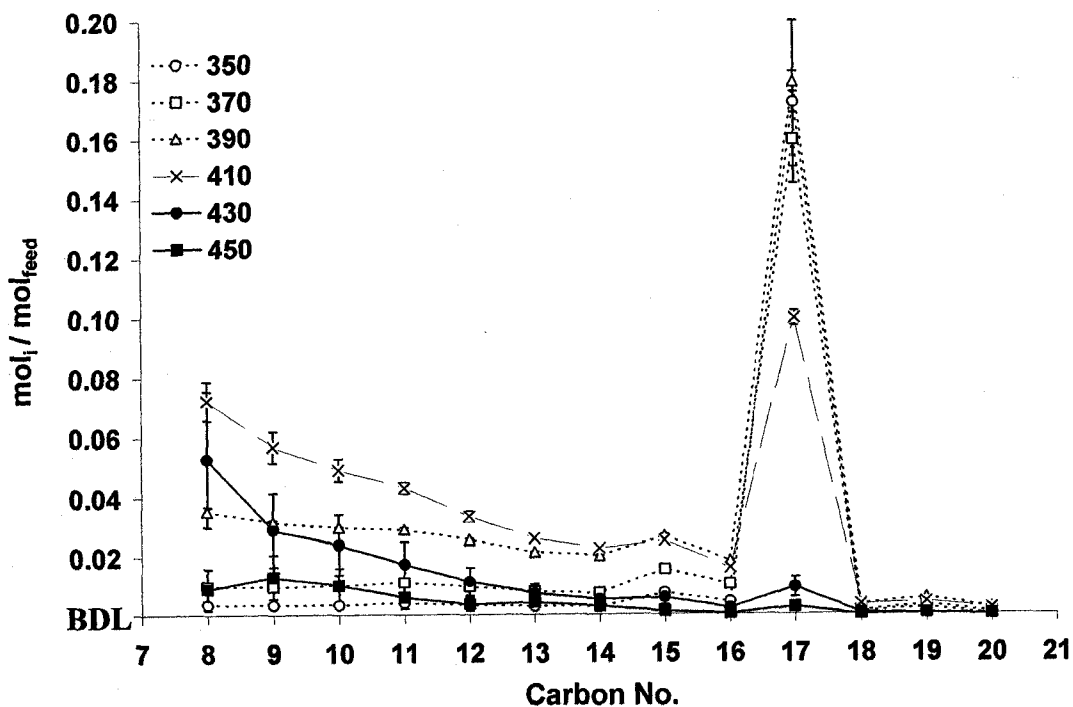


Figure 4.23 Molar yields of C<sub>8</sub>-C<sub>20</sub> n-alkanes as a function of temperature for 8 hr reactions

From Figures 4.20-4.23, it is evident that similar trends occur at each reaction time of 0.5, 1, 4, and 8 h; however, they occur at different temperatures. At most conditions, aside from the most mild and severe, C<sub>17</sub> is clearly present at the highest concentrations. In most cases, C<sub>18</sub>-C<sub>20</sub> product is present in relatively small concentrations; however, the formation of these products is definitely favored at certain conditions and will be addressed later.

#### *Temperature and time effects*

At the most mild conditions (low temperature, low time), small amounts of product was formed. Figure 4.20 (0.5 h reaction at 390 °C), shows that n-alkanes were just starting to be produced. At 410 °C, the largest amount of C<sub>17</sub> was present and the C<sub>8</sub>-C<sub>16</sub> n-alkanes were just starting to form. As the temperature was increased to 430 and 450 °C, the amount of C<sub>17</sub> decreased while the amount of C<sub>8</sub>-C<sub>16</sub> n-alkanes increased. At longer reaction times, higher temperatures resulted in a decrease of C<sub>8</sub>-C<sub>16</sub> n-alkanes. Similar temperature trends were evident at 1, 4, and 8 h; however, as reaction time was increased, the temperatures at which these trends occurred decreased. For example, at 0.5, 1, and 4 h, a reaction temperature of 410 °C resulted in the maximum amount of C<sub>17</sub> however; at 8 h, the maximum amount of C<sub>17</sub> occurred at a lower temperature of 390 °C. Similarly, the amount of C<sub>8</sub>-C<sub>16</sub> n-alkanes was present in the highest concentrations at 450 °C for 0.5 and 1 h reactions but for 4 and 8 h reactions, C<sub>8</sub>-C<sub>16</sub> n-alkanes are present in the highest concentrations at 430 and 410 °C, respectively. Reaction time also influenced the molar yields of n-alkanes with the same general trends as temperature. At the lowest reaction

times, C<sub>17</sub> began to form first, with relatively little C<sub>8</sub>-C<sub>16</sub> n-alkane production. This is shown in Figure 4.20 at 390 °C. As reaction time was increased, the amount of C<sub>8</sub>-C<sub>16</sub> n-alkanes also began to increase as the higher n-alkanes, C<sub>17</sub> in particular, began to decrease. The time at which these trends began to occur depended heavily on the reaction temperature. For example, at 390 °C after 8 h of reaction (Figure 4.24), C<sub>17</sub> was still present in relatively large concentrations but at 410 °C, C<sub>17</sub> concentration began to decrease and the C<sub>8</sub>-C<sub>16</sub> n-alkanes began to increase. It is clear from these figures that both temperature and time affect the yields of n-alkanes.

#### *Effect of carbon number*

It was already noted that C<sub>17</sub> was present in the highest concentrations for the majority of the conditions. The other interesting feature is that C<sub>15</sub> was present in greater concentration than both C<sub>14</sub> and C<sub>16</sub>. This is evident at the majority of conditions tested.

#### *4.1.4.4.2 Molar Yields of C<sub>18</sub>+ n-alkanes*

The formation of small amounts of addition products was observed at most of the reaction conditions. Generally, these compounds were formed in relatively small amounts compared to the other reaction products (Figures 4.20-4.23); however, they appear to follow similar time and temperature trends. For example, the conditions at which the n-alkane/alkene series are present in high concentrations also result in

increased in the C<sub>18</sub><sup>+</sup> products. Generally, C<sub>19</sub> is produced in greater concentrations than C<sub>18</sub>, C<sub>20</sub>, and C<sub>21</sub>.

#### *4.1.4.4.3 2-Nonadecanone*

At a retention time of approximately 20.490 min (peak preceding the stearic acid peak) there is a peak which is not part of one of the series discussed to this point. GC/MS results indicate that this peak is 2-nonadecanone. This product is favored at higher temperatures and lower reaction times such as 430 °C at 0.5 and 1 h reactions and 450 °C at 0.5 h reactions as well as lower temperatures at longer reaction times such as 370 and 390 °C at 4 and 8 h reactions.

#### *4.1.4.4.4 n-Alkane:Alkene Ratio*

Figures 4.24-4.27 show the molar ratios of n-alkanes to alkenes as a function of carbon number and time at different reaction temperatures. Chains with 17 carbons (heptadecane/heptadecene ratio) were excluded from these figures because the ratio was so large that it made it difficult to see the changes in C<sub>8</sub>-C<sub>16</sub> ratios. This ratio is discussed separately in the next section. Errors were generally smaller for this data (as shown by the error bars) than for the estimations of yield. It is likely that a large percentage of the error between the two samples is due to the extraction method and the amount of compound that is extracted. This would likely affect the amount of compound in the

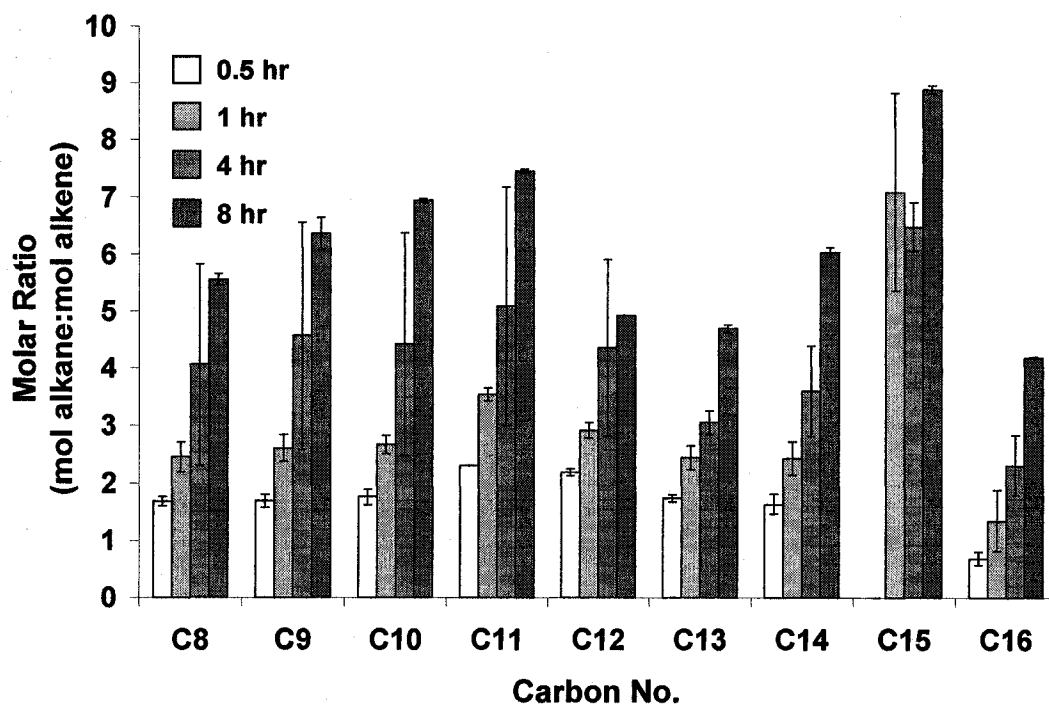


Figure 4.24 Molar ratio of n-alkanes to alkenes as a function of carbon number and reaction time at T=390°C

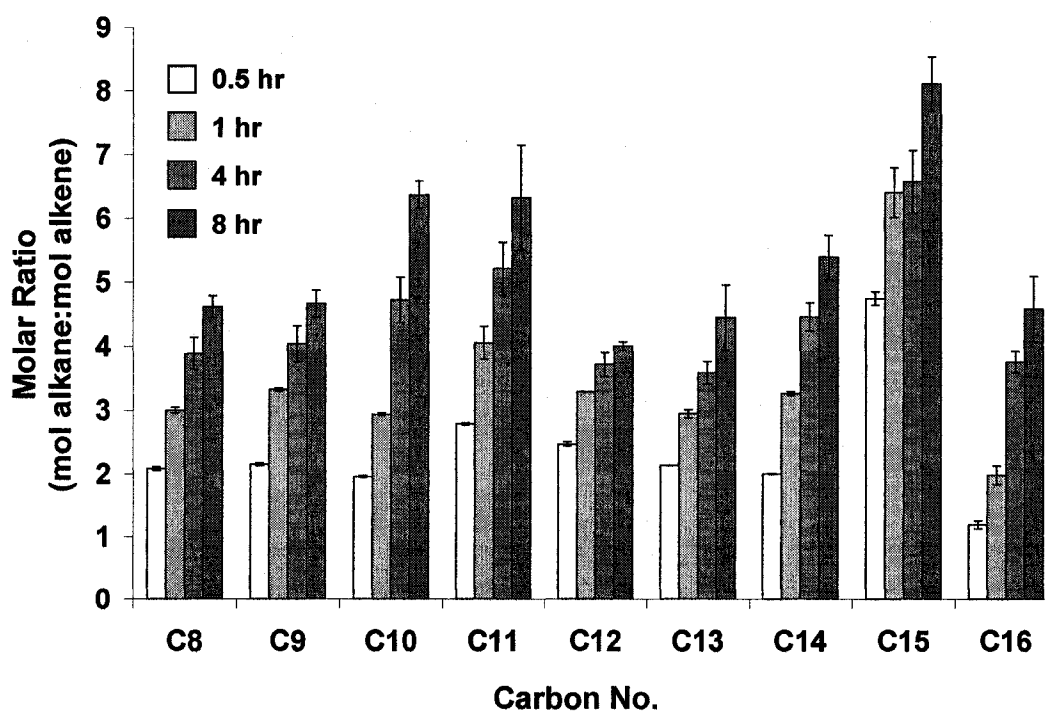


Figure 4.25 Molar ratio of n-alkanes to alkenes as a function of carbon number and reaction time at T=410°C

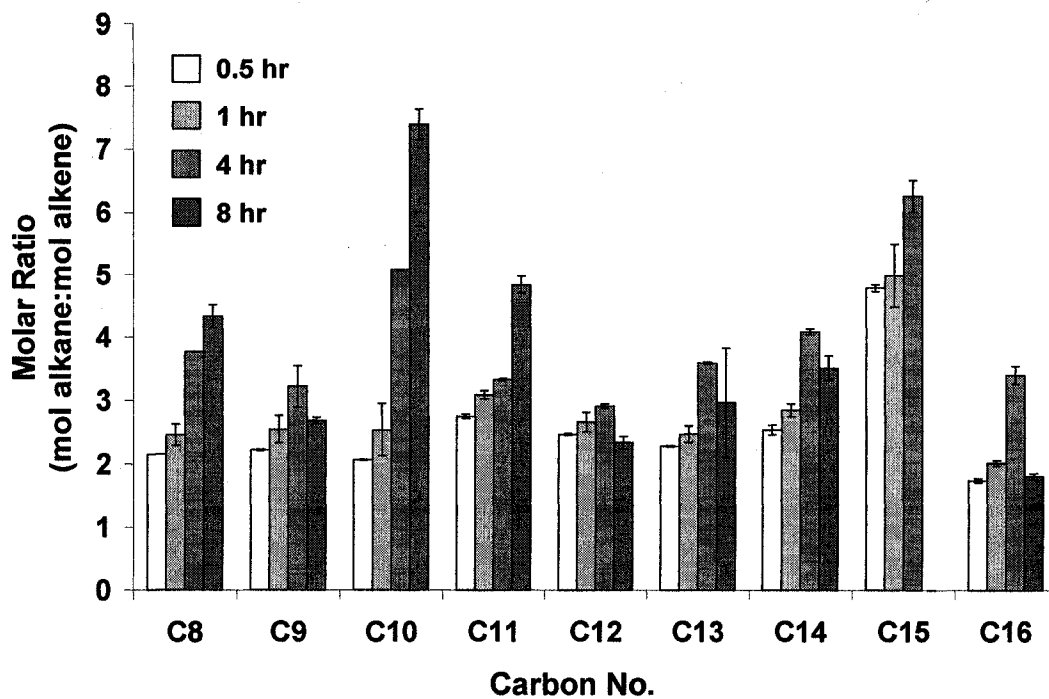


Figure 4.26 Molar ratio of n-alkanes to alkenes as a function of carbon number and reaction time at T=430°C

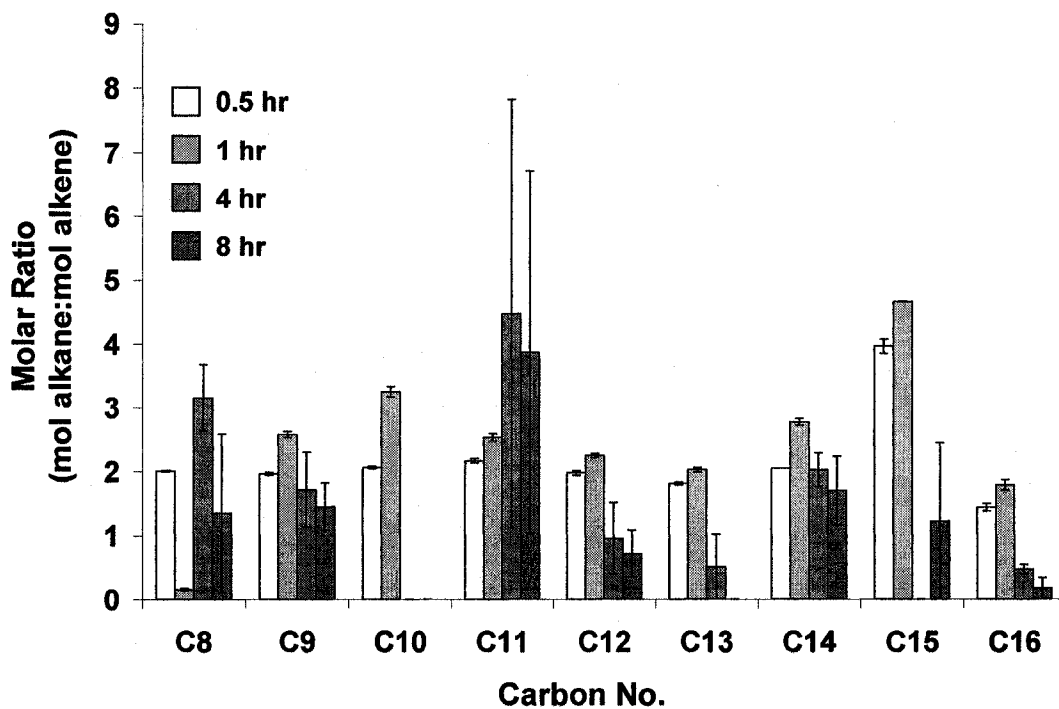


Figure 4.27 Molar ratio of n-alkanes to alkenes as a function of carbon number and reaction time at T=450°C

extracts, but is unlikely to affect the ratio of n-alkanes to alkenes, which should be independent of concentration.

For this set of experiments, the molar ratios are almost always greater than 1, meaning that more n-alkanes are produced than alkenes. Looking back at the results of the initial studies (Figure 4.2), it is clear that during the 5 min reactions at 500 °C, the alkenes were produced in greater quantities than the n-alkanes. This is also evident for the 0.5 h reactions at 450 °C, but to a lesser extent. The results of the current experiment show that the molar ratio is less than one at only a few conditions, most noticeably at 450°C for the 4 and 8 h reactions and only for certain carbon numbers, namely C<sub>12</sub>-C<sub>14</sub> and C<sub>16</sub>.

#### *Temperature and time effects*

Figures 4.24-4.27 demonstrate that at 390 °C (Figure 4.24) and 410 °C (Figure 4.25), the molar ratio increases with time. A higher molar ratio indicates that more n-alkanes are produced relative to alkenes, or n-alkanes are produced preferentially to alkenes. For example, at 390 °C the molar ratio of C<sub>8</sub> increases from  $1.69 \pm 0.07$  after 0.5 h to  $5.55 \pm 0.09$  after 8 h. Likewise, the molar ratio of C<sub>16</sub> increases from  $0.69 \pm 0.11$  after 0.5 h to  $4.17 \pm 0.22$  after 8 h. Similar trends are observed for the carbon numbers in between. At 430 °C, some compounds (C<sub>8</sub>, C<sub>10</sub>, C<sub>11</sub>, and C<sub>15</sub>) show increasing molar ratio with time; however, others (C<sub>9</sub>, C<sub>12</sub>, C<sub>14</sub>, C<sub>16</sub>) show a decrease in molar ratio between the 4 and 8 hr reactions. At 450 °C, it seems as if the molar ratio begins to decrease even earlier, between the 1 and 4 hr reaction. In summary, the molar ratio increases with time from

0.5-8 hrs until a certain temperature where the longer reaction times result in a decrease in molar ratio.

It appears that temperature does not have as much of an influence on the molar ratio as time does at temperatures between 390 °C and 430°C but follows the same general trend as the time effects. In other words, as the reaction time is increased the temperature at which the maximum ratio occurs decreases. For example, for 0.5 min reactions, the maximum ratios appear to be at 410 °C or 430 °C while for 8 hr reactions, the maximum ratios occur at much lower temperatures around 370 °C or 390 °C. Good data was only obtained for the 8 h reaction at 370 °C and is not shown in these figures; however, the data are included in Appendix A (Table A.1).

It is clear that both temperature and time affect the molar ratio. The mildest conditions (low temperatures and times) results in relatively low molar ratios but so do the most severe (longest times and highest temperatures). The largest ratio lies somewhere in between these two extremes. At the conditions tested, the largest ratio occurred at 370°C for 8 hr reactions. The 8 hr reaction at 350 °C (Appendix A, Table A.1) did result in a slightly lower ratio; however, since reactions were not conducted at times longer than 8 hrs, it is possible that reactions longer than this at 350 or 370 °C could result in higher molar ratios.



### *Carbon number*

The other important variable to consider is the number of carbons that the n-alkane and alkene chains have. The distributions of molar ratios for each compound relative to one another appears to be fairly consistent over the range of times and temperatures studied. At most of the reaction temperatures, C<sub>8</sub>-C<sub>11</sub> and C<sub>15</sub> have larger molar ratios than C<sub>12</sub>-C<sub>14</sub>, and C<sub>16</sub>. It is also clear that C<sub>15</sub> has the highest molar ratio (except for an 8 hr reaction at 430 °C where C<sub>10</sub> has a higher ratio), while C<sub>16</sub> has the lowest. For example, at 410 °C a 1 hr reaction results in a molar ratio of  $4.75 \pm 0.06$  for C<sub>15</sub> but only  $1.20 \pm 1.16$  for C<sub>16</sub>. At 390 °C an 8 hr reaction results in a molar ratio of  $8.86 \pm 0.07$  for C<sub>15</sub> and  $4.17 \pm 0.02$  for C<sub>16</sub>.

#### *4.1.4.4.5 Molar ratios of C<sub>17</sub>*

Figure 4.28 shows the molar ratio for C<sub>17</sub>, or heptadecane to heptadecene. It has been established that heptadecane is the major reaction product and that there is very little heptadecene. Although the mechanism of decarboxylation, which yields the heptadecane differs from the free radical mechanisms of the subsequent thermal cracking, the ratio still provided good information regarding cracking behavior. The molar ratios, which are substantially higher for C<sub>17</sub> than for C<sub>8</sub>-C<sub>16</sub>, reflect this. In the C<sub>8</sub>-C<sub>16</sub> range, C<sub>15</sub> had the highest molar ratios. At 390 °C the molar ratio for C<sub>15</sub> after an 8 h reaction was  $8.86 \pm 0.07$ . In contrast, at the same condition the molar ratio for C<sub>17</sub> was  $39.0 \pm 0.71$ . Again, because reactions longer than 8 h were not conducted, it is possible that the maximum

molar ratio lies outside the conditions tested. The largest molar ratio for C<sub>17</sub>, 43.53 ± 3.59, occurred at 410 °C for an 8 hr reaction. It appears as if C<sub>17</sub> follows the same trends as the C<sub>8</sub>-C<sub>16</sub> hydrocarbons. For example at 390-430 °C, the molar ratio increases with time, but at higher temperatures such as 450 °C, longer times (4 and 8 h) result in decreased ratios. At 500 °C, the ratios are low for all of the times tested.

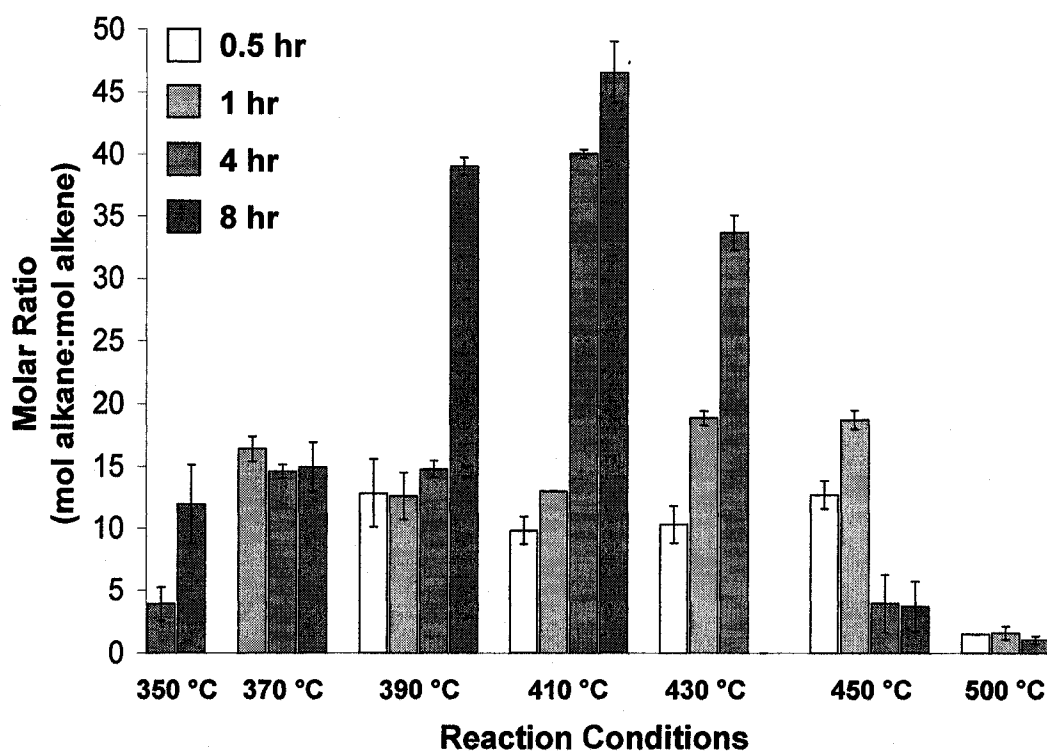


**Figure 4.28** Molar ratio of n-alkanes to alkenes for C<sub>17</sub> as a function of temperature and time

## 4.1.5 ANALYSIS OF LIGHT ENDS (GAS FRACTION)

### 4.1.5.1 Composition

Typical chromatograms showing the composition of the gas fraction as analyzed on GC-TCD are presented in Figure 4.29. Methane ( $\text{CH}_4$ ), carbon dioxide ( $\text{CO}_2$ ), and room air standards were also analyzed and are shown in Figure 4.30. Due to the chromatography protocols used,  $\text{N}_2$  and  $\text{O}_2$  are detected as a single peak ( $\text{N}_2/\text{O}_2$  peak). Comparing peak retention times from the sample (Figure 4.28) with the peak retention times from the standards (Figure 4.29) it is evident the gaseous fractions contain both " $\text{N}_2/\text{O}_2$ ",  $\text{CH}_4$ , and  $\text{CO}_2$ . The

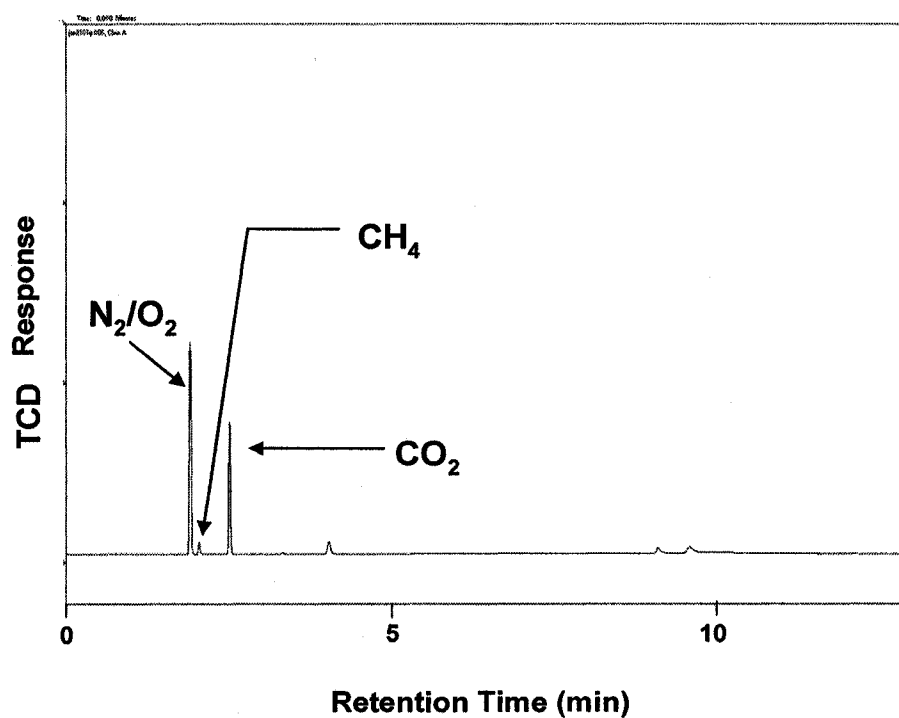


**Figure 4.29** Typical gas composition from stearic acid pyrolysis from a 1 hr reaction at 410 °C as analyzed on GC-TCD

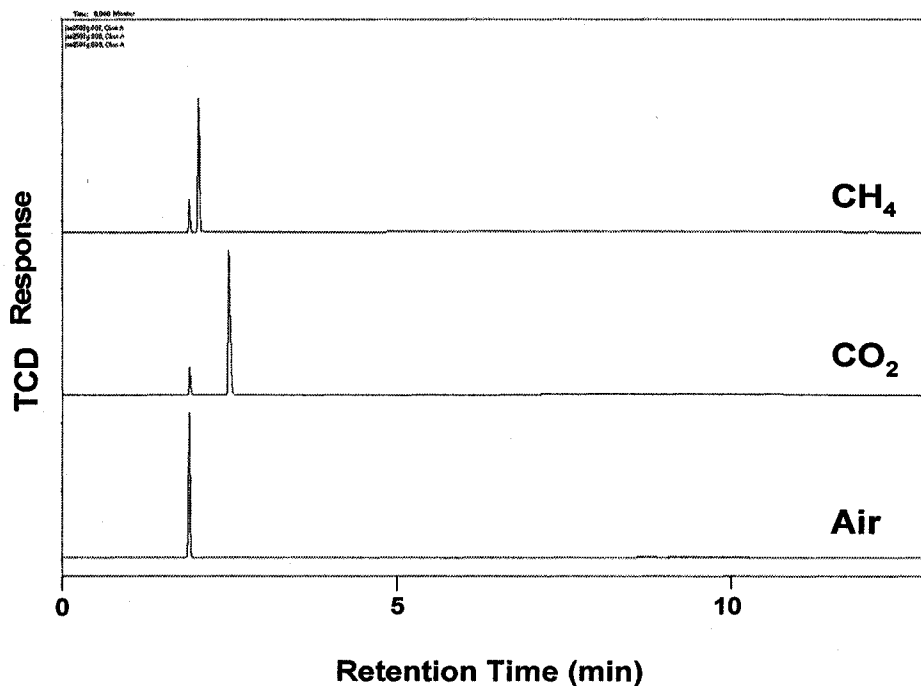


**Figure 4.30** Methane (CH<sub>4</sub>), carbon dioxide (CO<sub>2</sub>), and air standards as analyzed on GC-TCD

majority of the N<sub>2</sub>/O<sub>2</sub> peak can likely be attributed to the N<sub>2</sub> atmosphere inside the reactor and small amounts of air from the sample vial or the injection syringe. Small amounts of N<sub>2</sub>/O<sub>2</sub> are also present in the CO<sub>2</sub> and CH<sub>4</sub> standards (Figure 4.29), indicating that small amounts of air are entering the GC, likely through the syringe. There are also two sets of smaller peaks at later retention times, which appear to be in doublets. These peaks are likely light hydrocarbon gases such as ethane and propane, however this was not confirmed analytically. Composition of the gaseous fraction was analyzed numerous times the fractions after 1 h reactions at 390 °C and 410 °C as well as a 30 min reaction at 500 °C all yielded similar results (Figure A.4 and A.5, Appendix A).

#### 4.1.5.2 Percent gas formed

Figure 4.31 shows the amount of gas formed as a percentage of feed at various temperatures during 1 hr reactions. For this experiment, reactions were conducted using approximately 5.000 g of stearic acid feed instead of the usual 1.000 g. More starting feed was used so that the difference in the weight of the gas, measured by weighing the reactor before and after venting, was detectable on the scales available in the lab. The data represents the averages of four runs with the error bars representing the standard error between the runs (Appendix B). Outliers were removed from the data as shown in Appendix B. Figure 4.31 shows that as the temperature increases so does the amount of gas products formed. At 370 °C, only  $0.50 \pm 0.06$  wt % of gas is formed but at 430 °C, an average of  $7.89 \pm 0.90$  wt% of gas product is formed. Reactions were also conducted at 450 °C; however, with that much feed the pressure build up was so high that two of the reactors leaked and two of the reactors spewed oil during venting despite the fact that the samples were allowed to cool overnight and the vent valve was turned slowly. Because this resulted in a loss of oil, it was not possible to obtain accurate data. The shape of this graph indicated that in the temperature range tested, the formation of gas is not linear with respect to temperature.

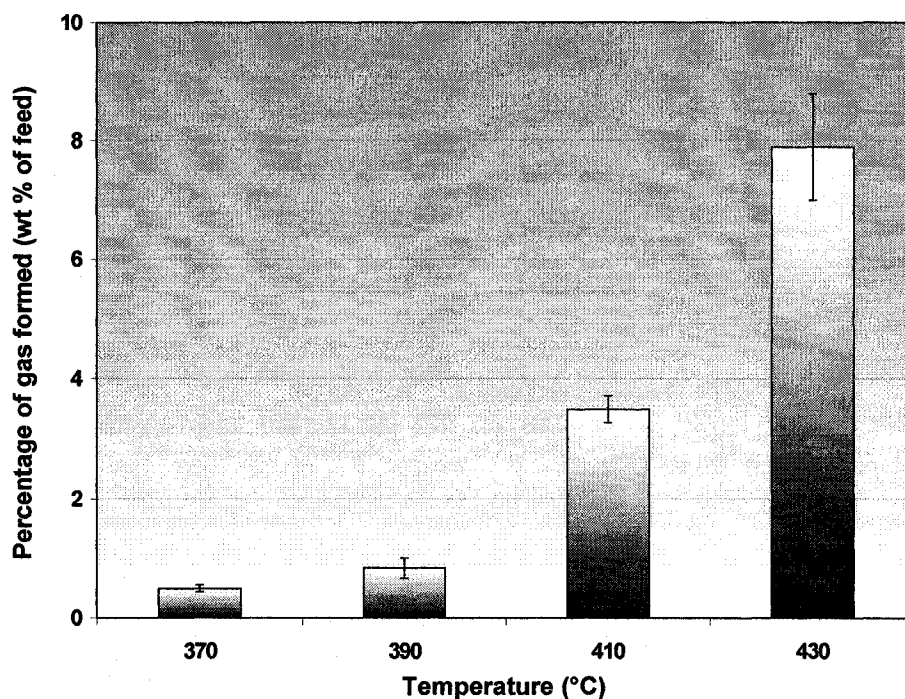


**Figure 4.31** Percent of gas products formed during 1 hr stearic acid pyrolysis reactions as a function of temperature. Initial pressure was atmospheric and the reactions were conducted in N<sub>2</sub>.

#### 4.1.6 ESTIMATE OF LIQUID YIELD

To get a crude estimate of liquid yield, the liquid product was extracted with a pasteur pipet from the reactor (no solvent was added) and weighed. Results are presented in Figure 4.32. The data represents the averages of multiple runs (3-6 depending on the time) with the error bars representing the standard error between the runs (Appendix B). Outliers were removed from the data as shown in Appendix B. At 390 °C, there was no liquid product in the reactor. The product consisted of whiteish-brown powder. At 410 °C, after 1 h reactions, three runs out of six runs (data not shown) also resulted in a

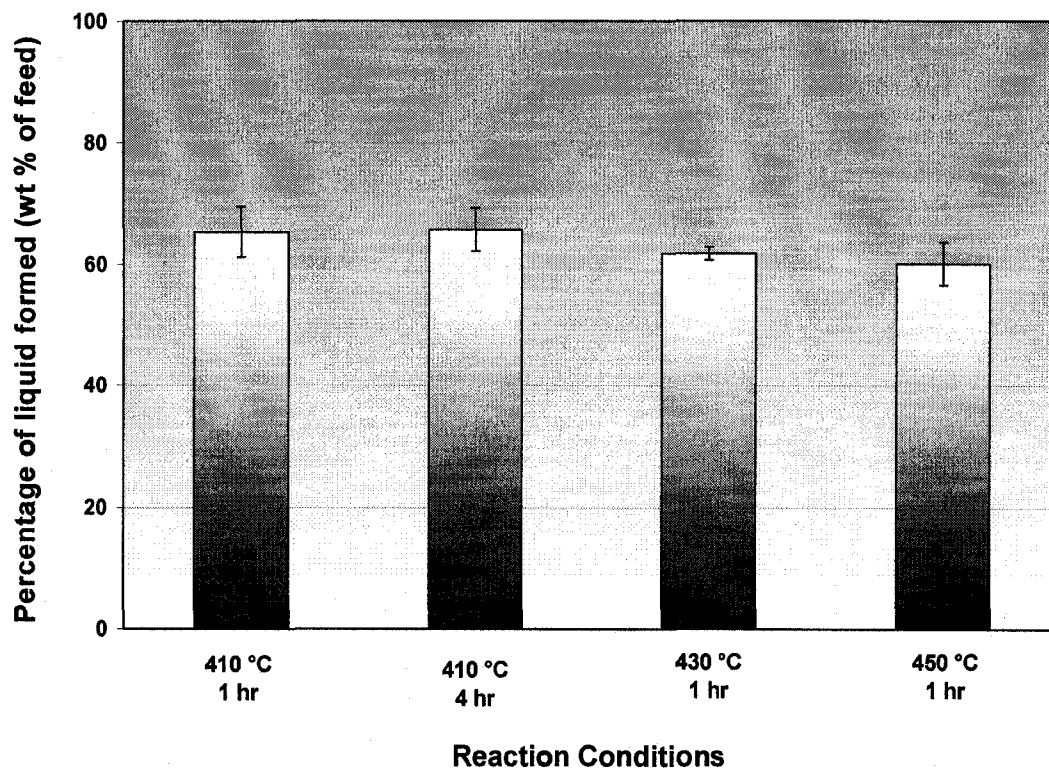


**Figure 4.32** Percent liquid products formed during stearic acid pyrolysis as a function of temperature and time. Initial pressure was atmospheric and the reactions were conducted in  $N_2$ .

whiteish-brown powder; however, the other 3 runs resulted in oil-like, liquid products between 58-71 wt %. This indicates that there was a certain point during the reactions when enough liquid product had formed that it began to behave as a solvent, dissolving the remaining solid products and that at 410 °C, this point occurred approximately 1 h into the reaction. Although these reactions were conducted at similar conditions, it is possible that they were immersed in areas of the bath with slightly different temperatures

(the sand bath temperature was not completely uniform), which could account for these observed differences. The 1 h reactions at 430 °C and 450 °C resulted in  $61.9 \pm 1.1$  wt % and  $60.1 \pm 3.6$  wt % yield of liquid product, respectively while the 4 h reaction at 410 °C resulted in  $65.8 \pm 3.5$  wt % yield of liquid product.

#### 4.1.7 EXTENT OF REACTION

Generally, fatty acids do not create nice sharp peaks on the GC. They have a tendency to spread on the column resulting in wide, “shark fin” peaks that are difficult to quantify. For this reason, fatty acids are first derivatized into methyl esters before GC analysis. Fatty acid methyl esters are more volatile than fatty acids and more appropriate to analyze by GC. To avoid changing the structure of the other sample products, none of the samples were derivatized prior to analysis. Therefore, quantitation of unreacted feed based on the underivatized samples is not likely to be accurate as the stearic acid peak is not likely to be totally representative of the actual amount of unreacted material. Furthermore, pentane was used as the primary extraction solvent, which is not the best choice for dissolving fatty acids but chosen for other reasons as discussed later. To get amore accurate determination of the amount of unreacted stearic acid feed, the extraction procedures were modified as outlined in section 3.3.1.4. Figure 4.33 shows the percentage of stearic acid feed converted into product during the reactions (i.e. 100-percent of unreacted stearic acid). The data represents the average of four runs and the error bars represent the standard error (Appendix B). Outliers were removed from the data if needed as per methods outlined in Appendix B. As expected, as the temperature



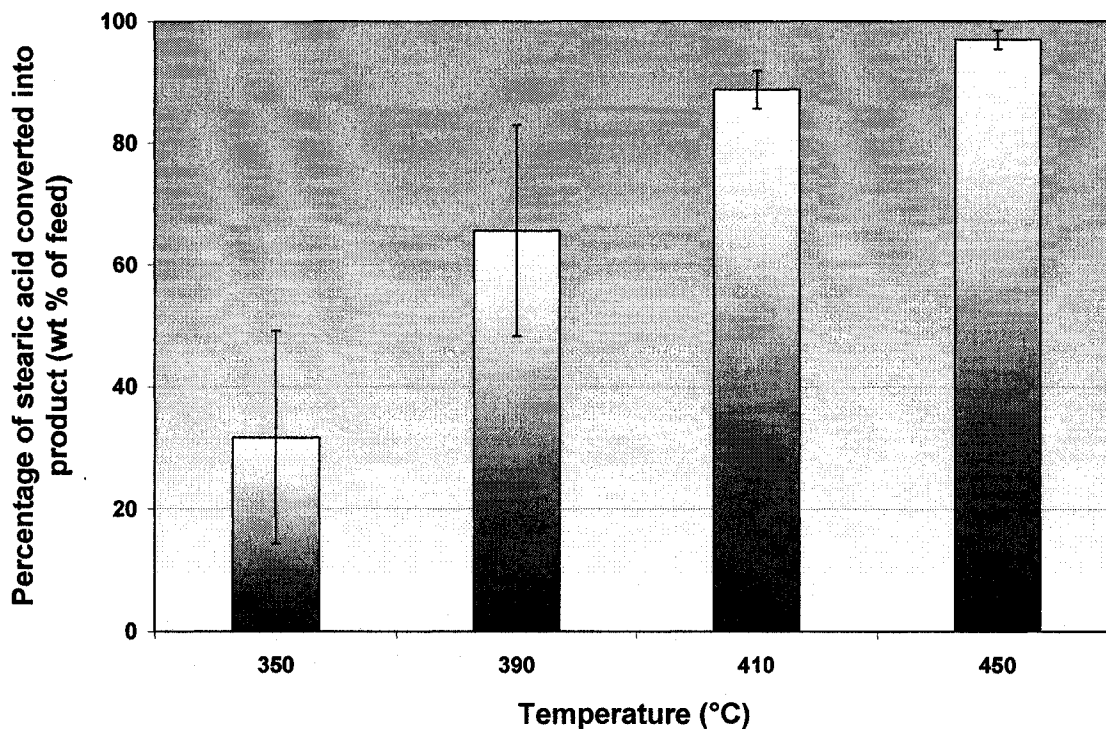


**Figure 4.33** Percentage of initial stearic acid feed that was converted during 1 hr pyrolysis reactions as a function of temperature. Initial pressure was atmospheric and the reactions were conducted in N<sub>2</sub>.

increased, more feed was converted into product. At the lowest temperature, 350 °C, only 31.7 ± 8.7 % of the stearic acid is converted but at 450 °C, 96.9 ± 0.78 % of the product was converted.

#### 4.1.8 MINIMUM CRACKING TEMPERATURE

To determine the minimum temperature at which decarboxylation occurs, 4 h reactions were conducted starting at 350°C and working downwards. Duplicate runs at 255°C still

showed a C<sub>17</sub> peak (Figure 4.34). Analysis of the gas sample taken from this reaction showed an extremely small, but evident CO<sub>2</sub> peak as shown in Figure 4.35. Injection of room air did not result in any CO<sub>2</sub> detection (Figure 4.30) therefore the CO<sub>2</sub> peaks in this experiment come from the gaseous reaction products. Subsequent experiments showed that a 1 h reaction at 200 °C still showed a small amount of n-heptadecane being produced.

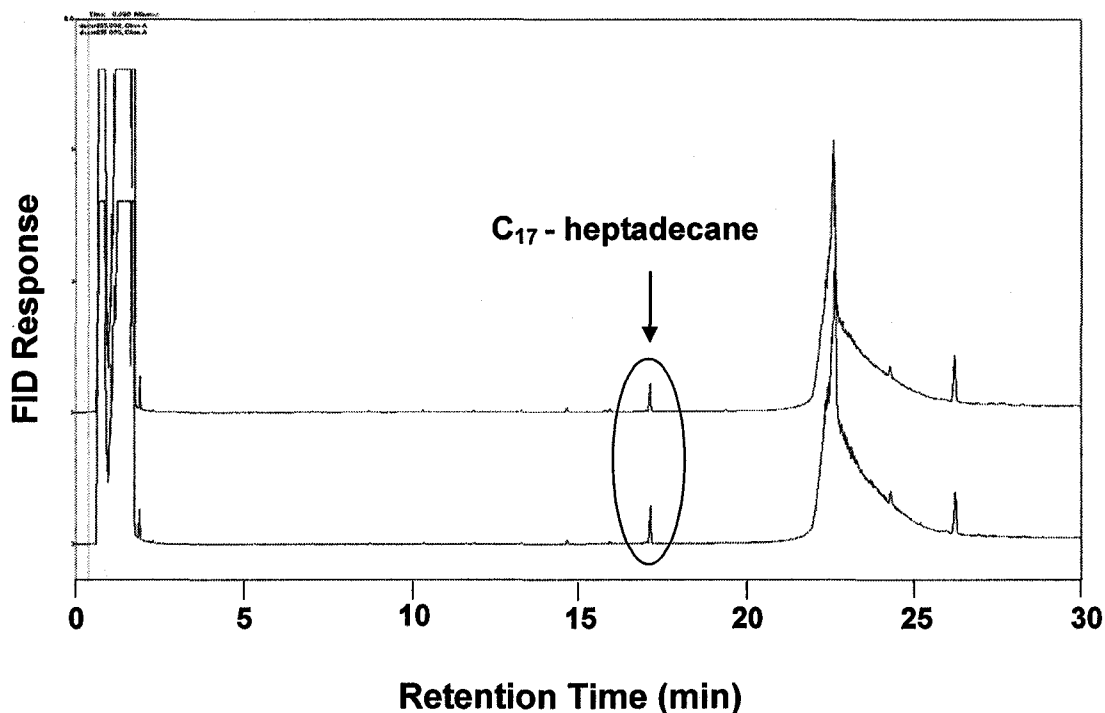


**Figure 4.34** Chromatogram (GC-FID) showing stearic acid pyrolysis products after a 4 hr reaction at 255°C. Initial pressure was atmospheric and the reactions were conducted in N<sub>2</sub>.

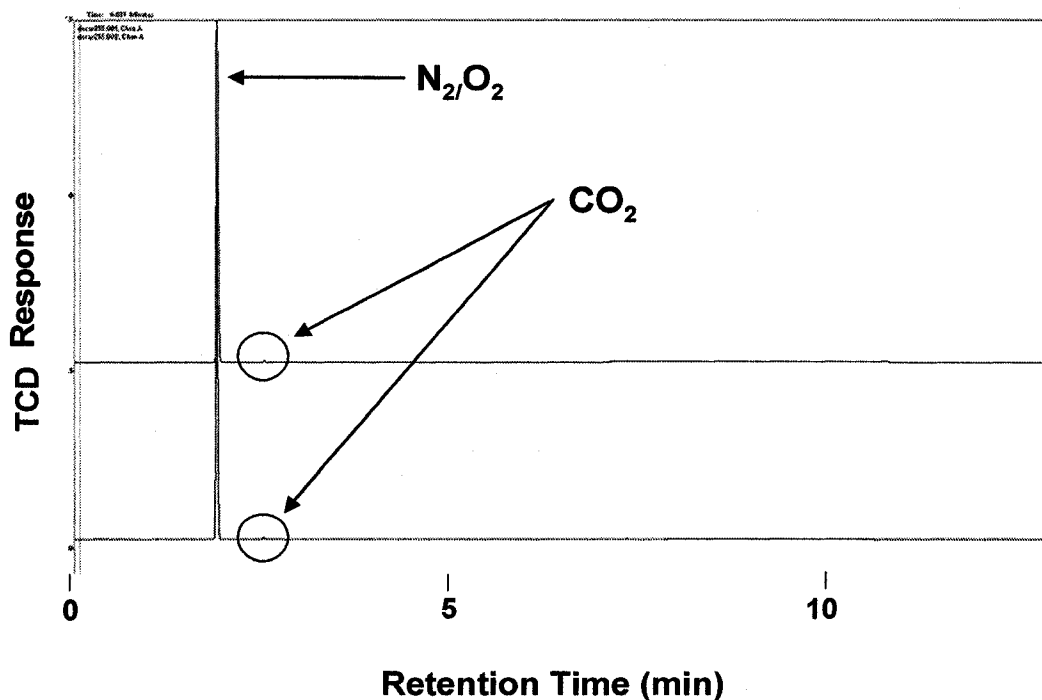


**Figure 4.35** Chromatogram (GC-TCD) showing gaseous reaction products after a 4 hr reaction at 255°C. Initial pressure was atmospheric and the reactions were conducted in  $N_2$ .

#### 4.1.9 PYROLYSIS OF OLEIC ACID

All model work to this point was conducted using stearic acid as reactor feed. Although beef tallow is more saturated than vegetable oils, it still contains large percentages of unsaturated fatty acids. It is of interest to see if the cracking behavior of an unsaturated fatty acid differs from that of a saturated fatty acid. Oleic acid, a free fatty acid with *cis* double bond in the 9 position, was pyrolyzed for 1 h at 410 °C using standard reaction and extraction procedures. The main products were identified using the GC-FID chromatograms and comparing them to the external n-alkane and fatty acid mixtures as well as GC/MS (Figure 4.36). The amounts of various compounds were determined semi-quantitatively (Appendix B) and are presented in Figure 4.37. This graph shows the

averages of the four runs and the error bars represent standard error (Appendix B). Outliers were removed if needed (Appendix B). The figures show that the largest amount of product formed was 8-heptadecene. Figure 4.37 shows two bars show 8-heptadecene, possibly due to a difference in conformation. This indicates that decarboxylation is likely an initial step in oleic acid cracking. One of the most notable features of oleic acid pyrolysis is the absence of the prominent n-alkane/alkene ladder series at higher carbon numbers (Figure 4.36). This ladder is evident at lower carbon numbers (C<sub>9</sub> and lower) and Figure 4.37 shows that n-heptane/heptene, n-octane/octene, and n-nonane/nonene were among the primary reaction products formed. This would be consistent with cracking at the double bond of the decarboxylated chain. It is also interesting to note the presence of nonanoic and decanoic acid, at concentrations of  $11.31 \pm 0.52$  and  $18.41 \pm 1.01$  mg/g feed, respectively.

The sum of the products identified in Figure 4.37 only represents 18.4 wt % of the total products formed. It is evident from the chromatogram (Figure 4.36) that there are a lot of minor peaks. Analysis of these peaks by GC/MS indicate that a lot of them are likely cyclic components such as cyclopentanes and cyclohexanes with different methyl and ethyl groups attached.

Gas samples were also collected from the pyrolysis of oleic acid and analysed on GC-TCD. The chromatograms are shown in Figure 4.38. Results are similar to the gas products formed during pyrolysis of stearic acid. The results show a large N<sub>2</sub>/O<sub>2</sub> peak, a small CH<sub>4</sub> (methane) peak, and a CO<sub>2</sub> (carbon dioxide) peak.

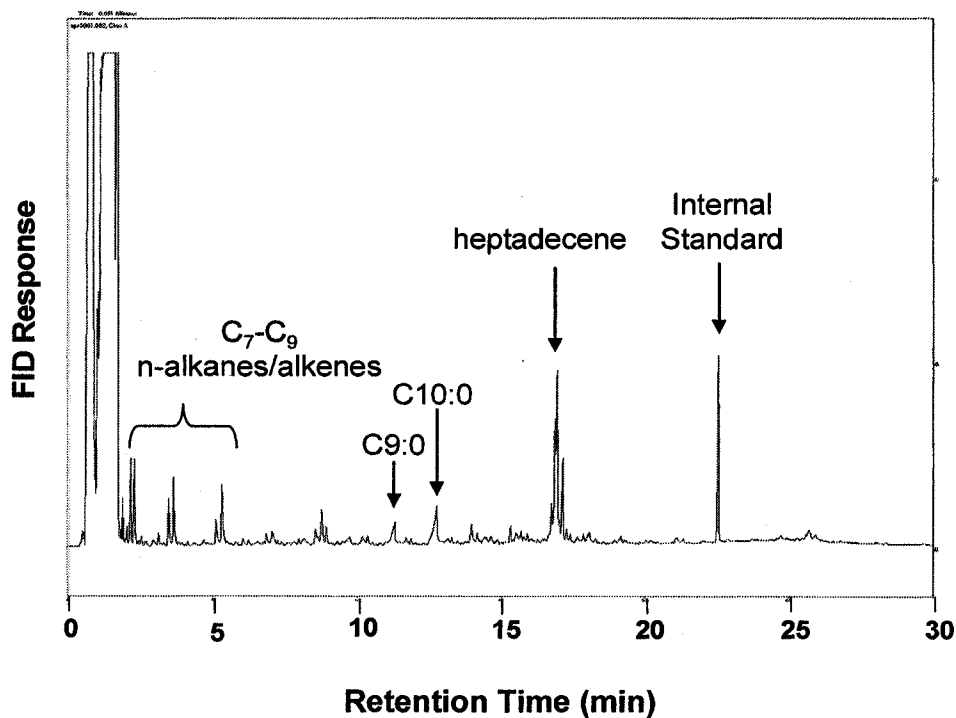


**Figure 4.36** Chromatogram (GC-FID) showing oleic acid pyrolysis products after a 1 hr reaction at 410°C. Initial pressure was atmospheric and the reactions were conducted in N<sub>2</sub>.

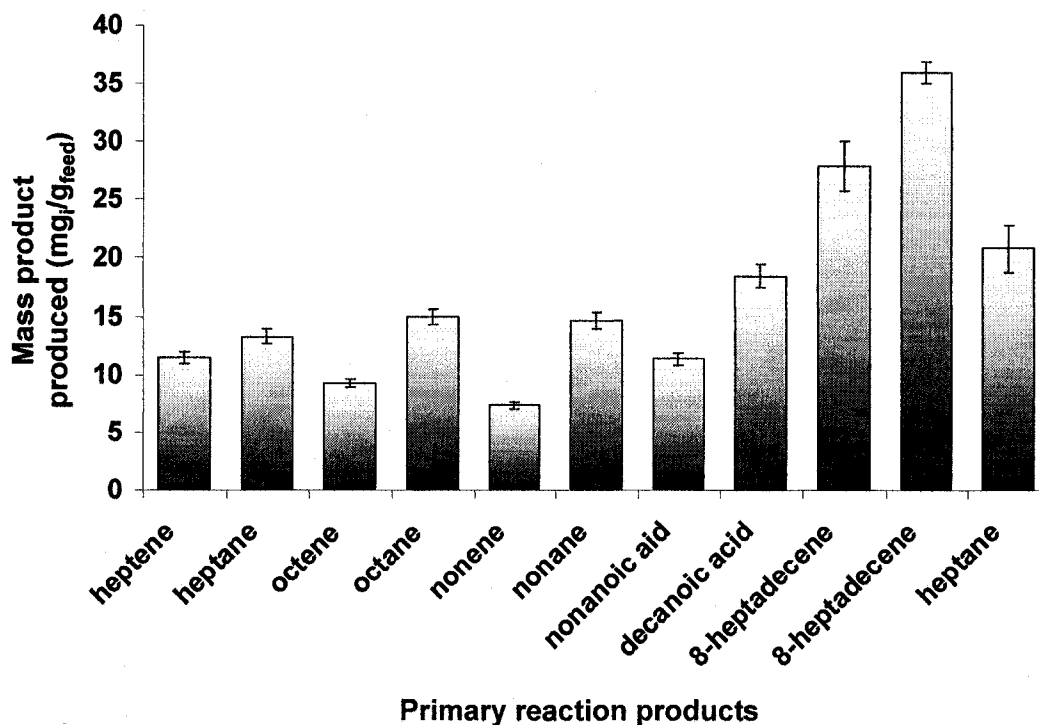


**Figure 4.37** Main products of oleic acid pyrolysis after 1 hr at 410 °C.

#### 4.1.10 PYROLYSIS AT HIGH PRESSURE

To determine the effects, if any, of pressure on the reaction products, duplicate runs were conducted at 400 and 410 °C at 6.89 MPa (1000 psi). The GC-FID chromatograms from these runs were compared to those of reactions conducted at the same conditions but with the reactor initially at atmospheric pressure. The resulting GC-FID chromatograms are presented in Figures 4.39 and 4.40. In terms of product distribution, the chromatograms appear to be virtually identical. The internal standards shown in Figure 4.40 were of a slightly different concentration so it is difficult to assess differences in yield and molar ratio visually. The molar yields of C<sub>8</sub>-C<sub>16</sub> n-alkanes and alkenes and the n-alkane/alkene

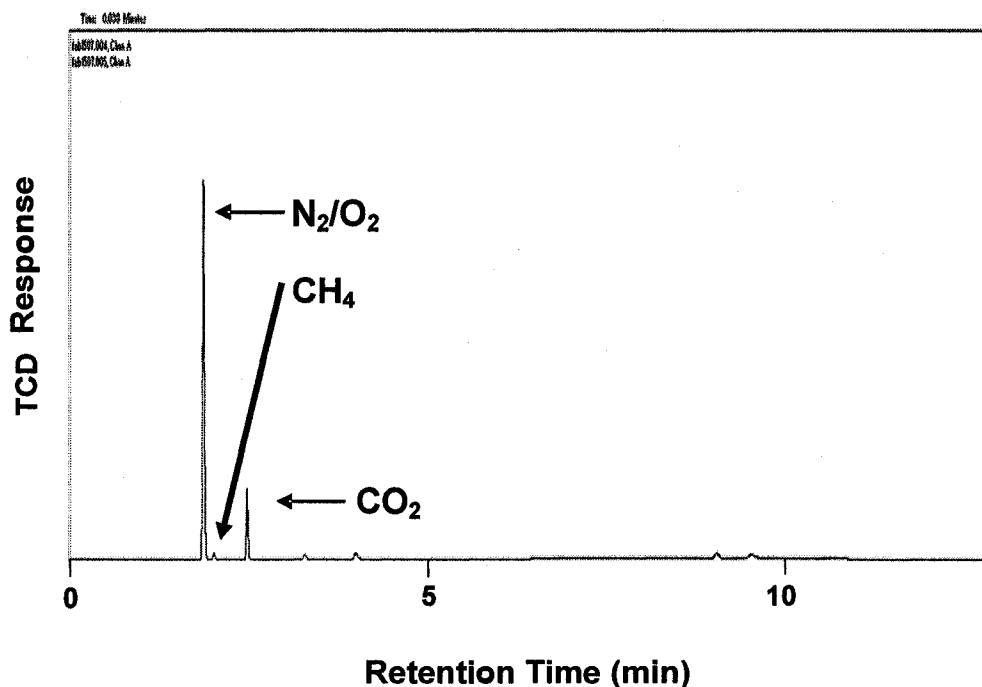


**Figure 4.38** GC-TCD chromatogram showing the gas products from oleic acid pyrolysis after 1 hr at 410 °C. Initial pressure was atmospheric and the reactions were conducted in N<sub>2</sub>.

molar ratio were computed using data from the samples at 410 °C (Figure C.A and C.A, Appendix A). The results show that reactions under pressure had lower yields of C<sub>8</sub>-C<sub>16</sub> n-alkanes and alkenes and lower n-alkane/alkene ratios compared to the runs at atmospheric pressure. According to Figure 4.39 (note that in this case the internal standards are the same concentration), it is very clear that reactions under pressure result in lower yields of the C<sub>8</sub>-C<sub>16</sub> n-alkanes and alkenes. These experiments represent preliminary findings and a more detailed study would have to be conducted to obtain more conclusive data over a greater range of conditions.

#### **4.1.11 PYROLYSIS WITH ALUMINA CATALYST**

To determine if the addition of an alumina catalyst affects the reaction products duplicate reactions were conducted at 410 °C for 1 hr with and without the addition of alumina. Approximately 0.100 g of alumina beads were crushed and added to the reactor with approximately 1.000 g of stearic acid for a catalyst ratio of about 10 wt % of the feed. Controls were run where the crushed alumina was thermally treated without the stearic acid. The results are presented in Figure 4.41. It should be noted that the amount of internal standard in the chromatogram with no added alumina (“stearic acid”) was approximately half of that added to the reaction with catalyst. Taking this point into consideration, it still appears that the addition of alumina causes a decrease in the yields of C<sub>8</sub>-C<sub>16</sub>. As well, the addition of alumina appears to result in a decrease in n-alkane/alkene ratio for most carbon numbers indicating a preference to alkene formation.

This is especially evident for at C<sub>16</sub>. To gain more conclusive results a more comprehensive study would have to be conducted, looking at different times, temperatures, and catalyst contents.

#### **4.1.13 AROMATIC CONTENT**

GC/MS analysis of reaction products obtained at 500 °C and 5 min showed that it is likely some aromatic compounds are beginning to form. Since aromatics are undesired components it is of interest to identify at what reaction conditions they begin to form. Looking at the chromatograms from earlier experiments there is a point at which the clean hydrocarbon series start to decompose producing compounds that start to form or cluster at the lower retention times. This phenomenon is fairly evident by visual inspection of the chromatograms; however, whether or not these compounds are aromatic requires more detailed analysis.

##### **4.1.13.1 Nuclear Magnetic Resonance (NMR)**

Two samples were taken to the NMR laboratories in University of Alberta Chemistry Department for proton and carbon 13 analysis. Both samples were from 1 hr reactions conducted at 410 °C under normal conditions. Results show that neither of these reactions resulted in the production of any detectable aromatics. The NMR scans are presented in Figures C.8 and C.9 (Appendix A).



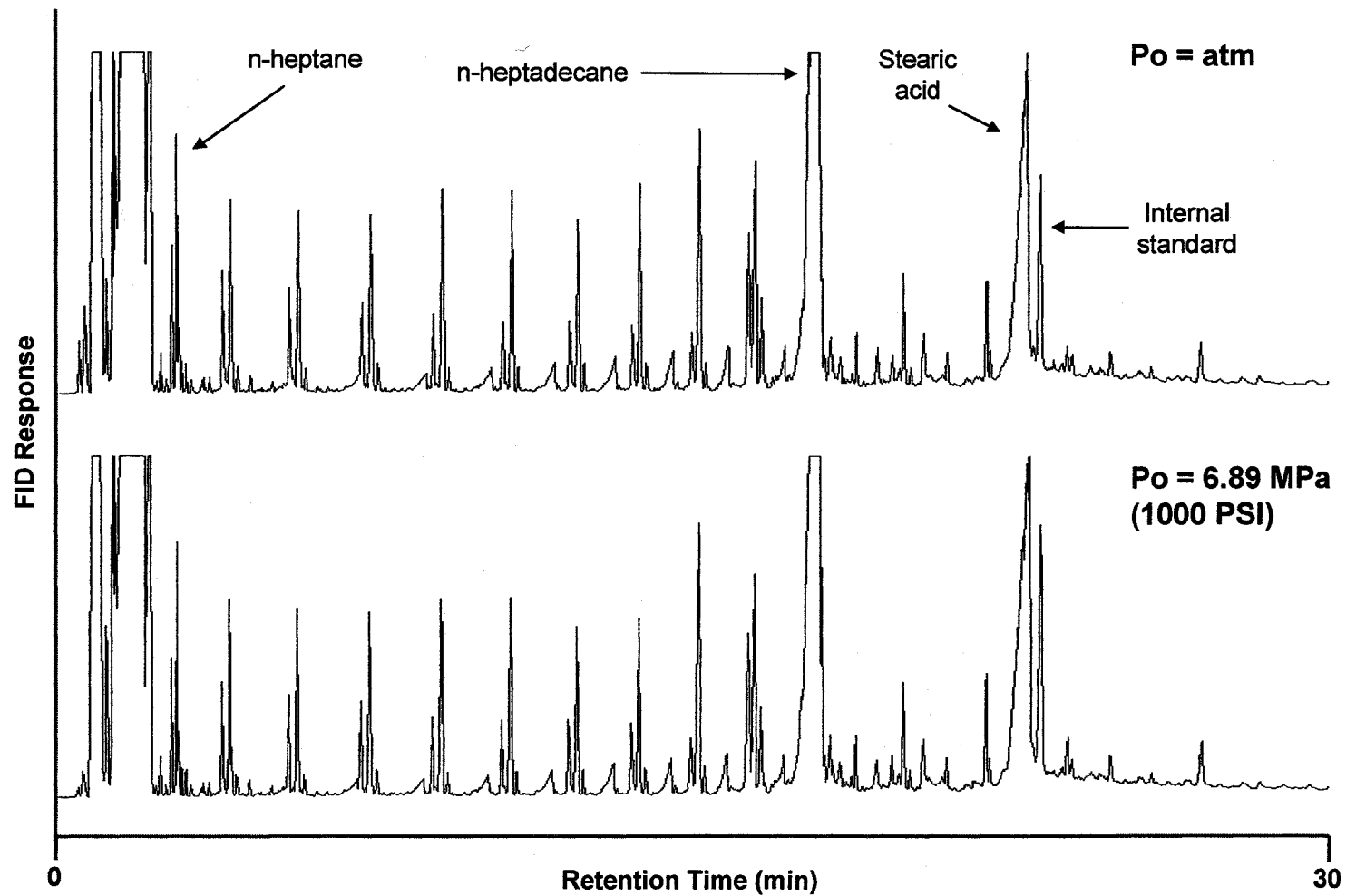


**Figure 4.39** GC-FID chromatograms showing the pentane soluble pyrolysis products of stearic acid after 1 hr reactions at 400 °C with an initial reactor pressure at atmospheric and 6.89 MPa. Reactions were conducted in N<sub>2</sub> atmosphere.

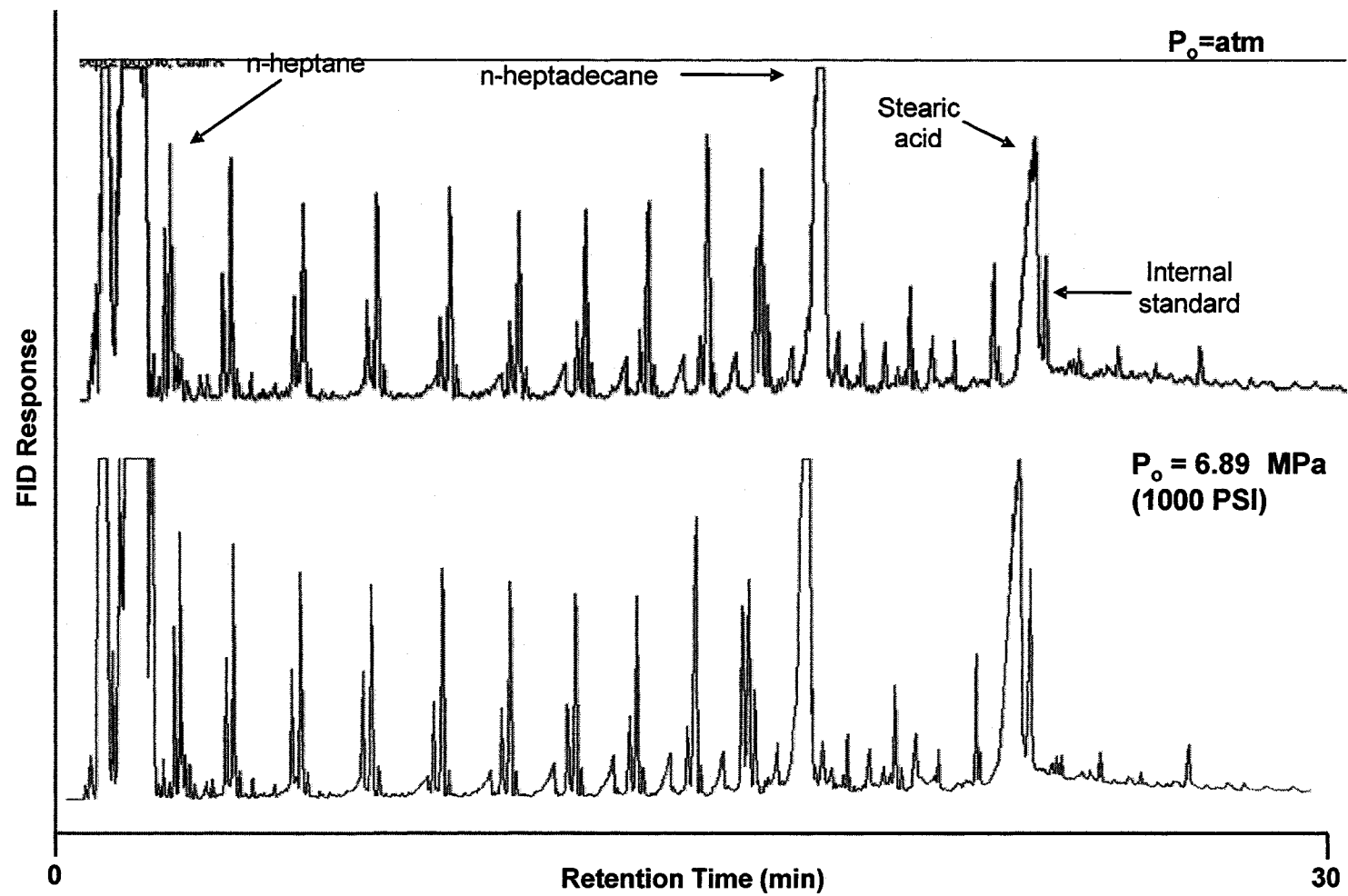
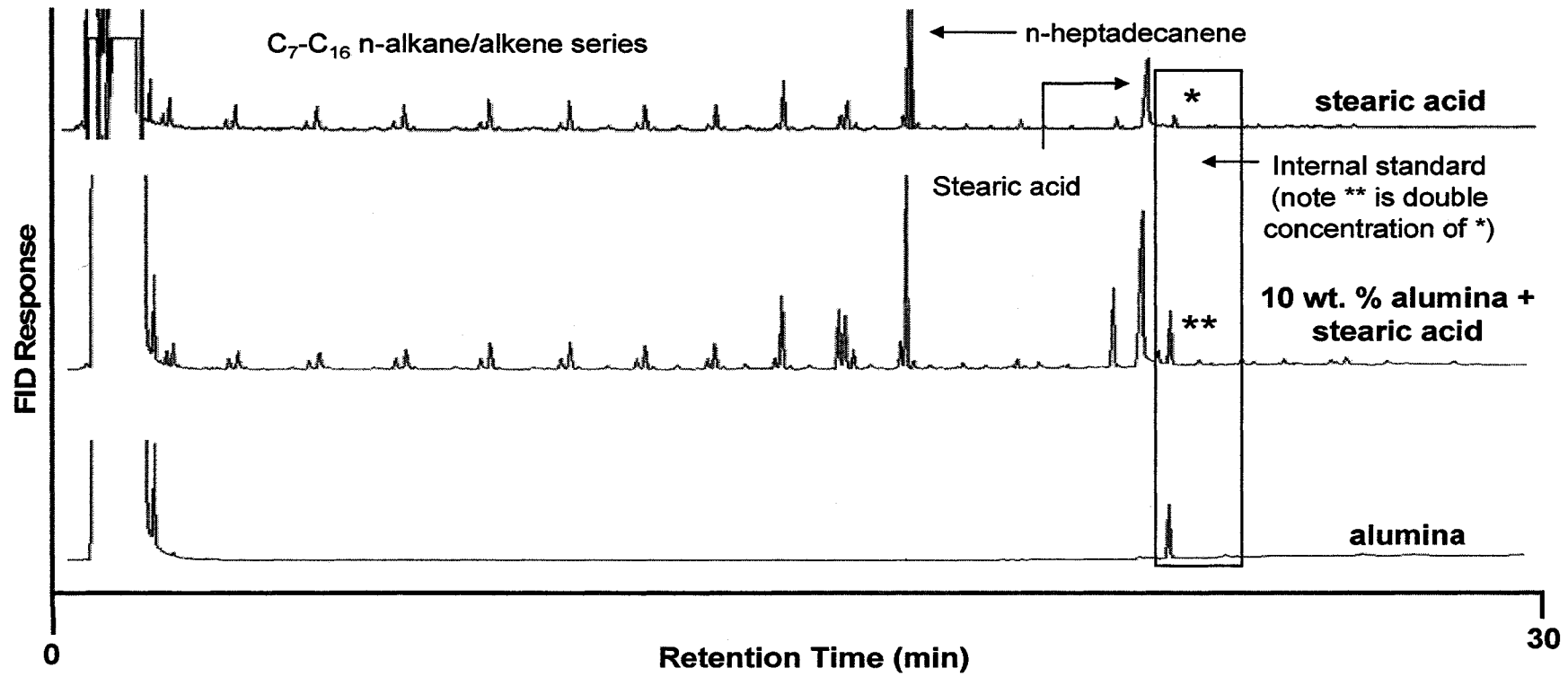


Figure 4.40 GC-FID chromatograms showing the pentane soluble pyrolysis products of stearic acid after 1 hr reactions at 410 °C with an initial reactor pressure at atmospheric and 6.89 MPa. Reactions were conducted in  $N_2$  atmosphere.



**Figure 4.41** GC-FID chromatograms showing the pentane soluble pyrolysis products of stearic acid after 1 hr reactions at 410 °C with and without catalyst and alumina control. Reactions were conducted in N<sub>2</sub> atmosphere.

#### 4.1.13.2 GC/MS analysis

The availability of another GC/MS unit has allowed analysis of samples toward the end of this work. Figure 4.42 shows chromatograms of reaction products obtained at 430 °C, 450 °C, and 500 °C. The aromatic compounds identified by using the NIST library search of GC/MS analysis are labeled. At 430 °C, there are very few aromatic compounds in the reaction products. Small amounts of toluene, ethylbenzene, and xylene were identified. At 450 °C, slightly more aromatic compounds begin to form. The n-alkane/alkene series are still prominent; however, small amounts of benzene compounds and naphthalene compounds begin to form in addition to the toluene, ethylbenzene, and xylenes, which increase in intensity. At 500 °C, almost all of the compounds are aromatic, with toluene being the most abundant. Analysis of products at 400 °C showed no toluene in the sample.

#### 4.1.14 DETAILED CHARACTERIZATION OF PRODUCTS

Most of the analysis has focused on the n-alkane/alkene series, the alkenes being the first alkene series identified in Figure 4.5. Amongst the reaction products there were also series of carboxylic acids and alkenes with the double bond in different positions. Samples used for this analysis were also used for NMR analysis therefore there was a slight change in procedure. Four samples were reacted at 390 °C using approximately 250 mg of starting feed. Smaller amounts of feed were used so the samples could be prepared for NMR analysis using chloroform-d (deuterated chloroform) as a solvent. As

such, the mass was too small to measure gas formation, if any. Previous experiments showed that at 390 °C, less than 1 wt % of gas product is formed. At 390 °C, the reaction products were solid; however, this temperature was selected because chromatograms showed little or no aromatics forming at this temperature. Sufficient chloroform-d spiked with internal standard was used to dissolve all of the reaction products (based on a solubility of 1 g stearic acid/2 mL chloroform, MERCK index, 2006). Samples were then derivatized with diazomethane in ether without the drying steps (to eliminate loss of volatiles) and analyzed on GC/MS. To ensure that elimination of the drying step prior to derivatization did not affect the products, samples were run without derivatization and compared to the derivatized sample. Chromatograms showing underivatized versus samples for a different set of experiments are shown in a later section. For these samples (chromatograms not shown) one new peak was identified in the derivatized samples and it was identified as one of the diazomethane reactants. This peak did not overlap any of the other peaks and because of the semi-quantitative nature of the analysis relative to the internal standard, this additional peak should not influence the results. Using the GC/MS results an alkene series as well as saturated carboxylic acid series were identified in addition to the n-alkane and alkene series already discussed in earlier sections. The unsaturated carboxylic acid series could not clearly be identified using the NIST library search and was not included in this analysis. Peak areas were used to semi-quantitatively determine the yields of each compound (wt % of feed). The averages of the four runs were computed and are shown graphically in Figure 4.43. Outliers, if any, were eliminated (Appendix B) and the standard error for each grouping ranged from 0.08-4.68 wt %.

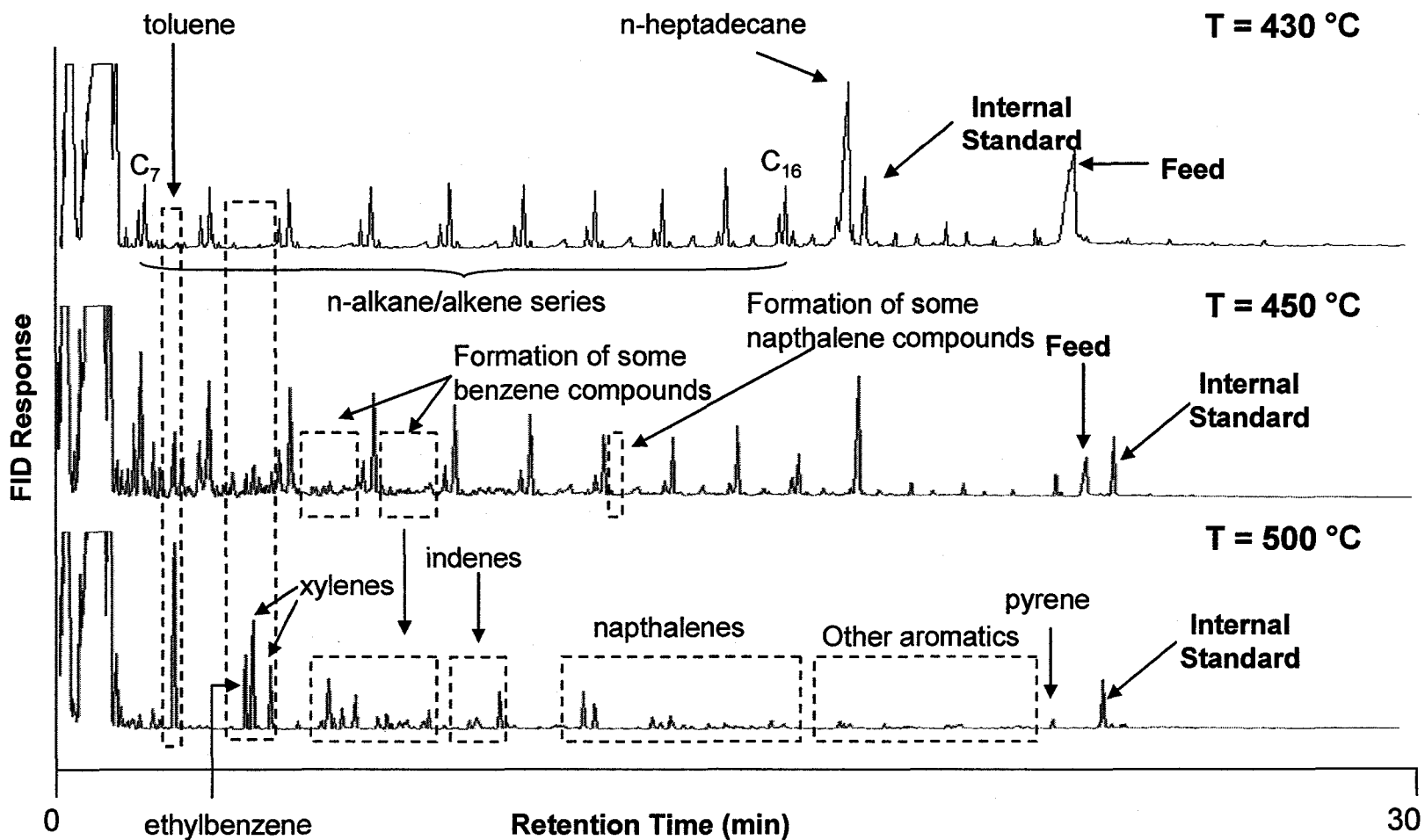


**Figure 4.42** GC-FID chromatograms showing aromatic compounds formed at 430 °C, 450 °C, and 500 °C after 1 hr reactions. Initial pressure was atmospheric and the reactions were conducted in N<sub>2</sub>.

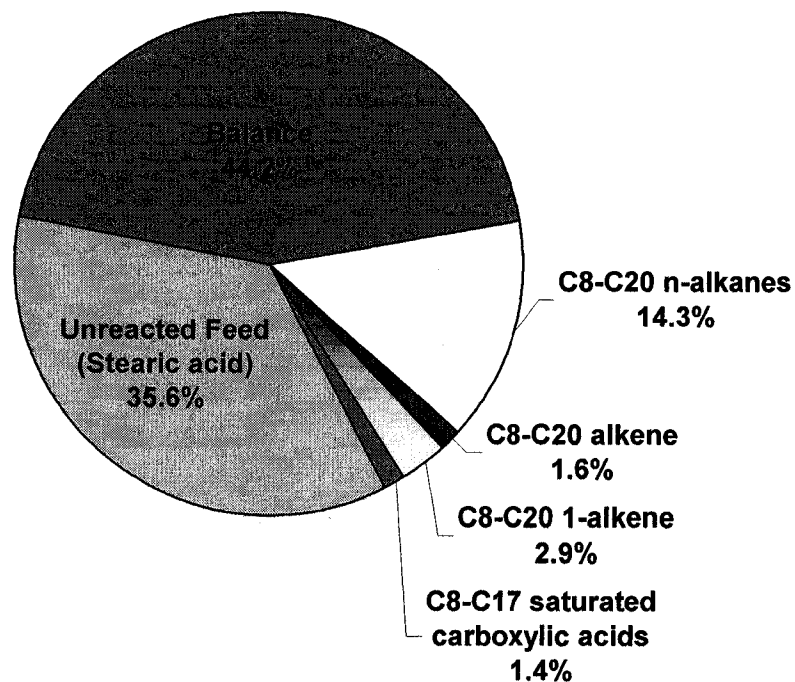


**Figure 4.43** Reaction products formed after a 1 hr reaction at 390 °C. Initial pressure was atmospheric and the reactions were conducted in N<sub>2</sub>.

## 4.2 HYDROLYSIS AND PYROLYSIS OF NEAT OILS AND FATS

### 4.2.1 HYDROLYSATE ANALYSIS

#### 4.2.1.1 TLC-FID analysis

As mentioned before, when oils and fats are used as starting feed, they must first be hydrolyzed into free fatty acids. After hydrolysis, the lipid layer was collected and analyzed by TLC-FID and GC-FID. Figures 4.44-4.47 show select chromatograms from

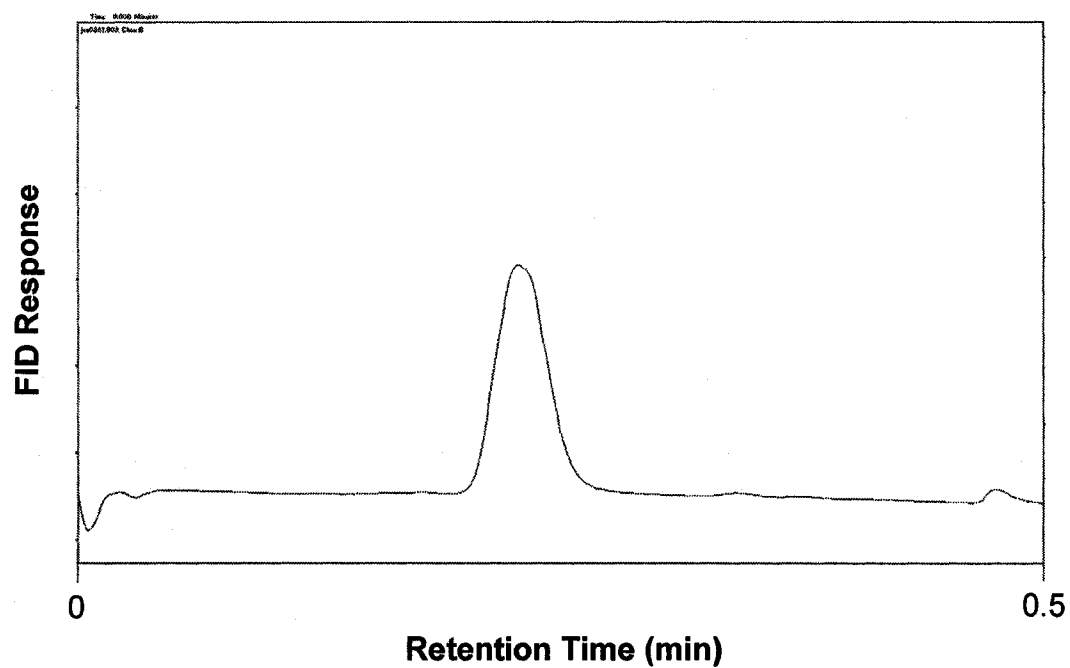


**Figure 4.44** TLC-FID chromatogram showing canola oil hydrolysates

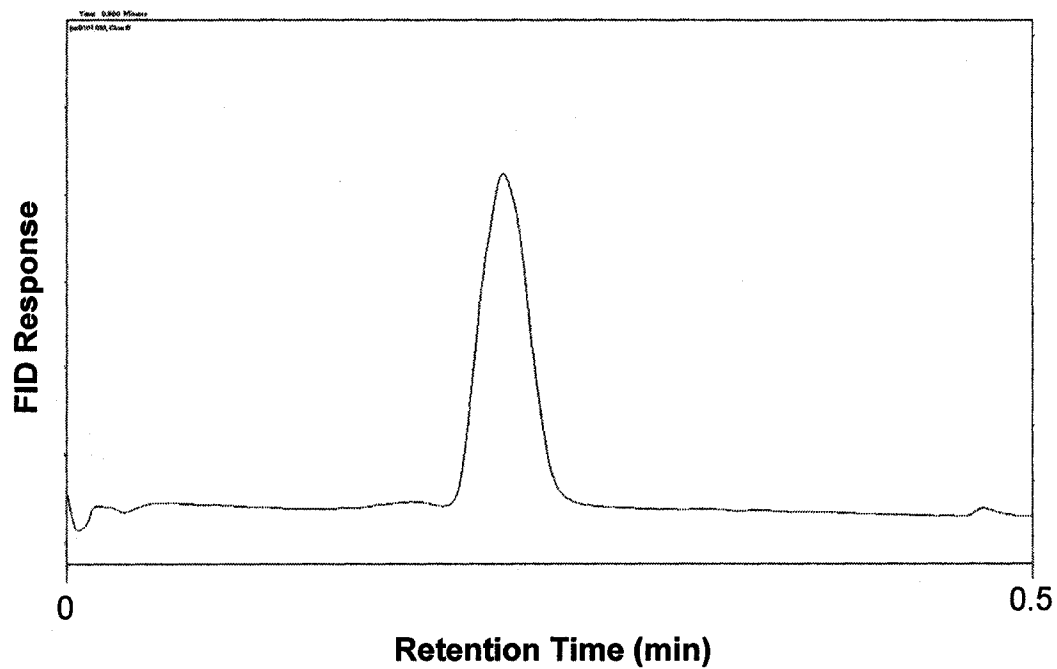


**Figure 4.45** TLC-FID chromatogram showing the bleached fancy tallow hydrolysates



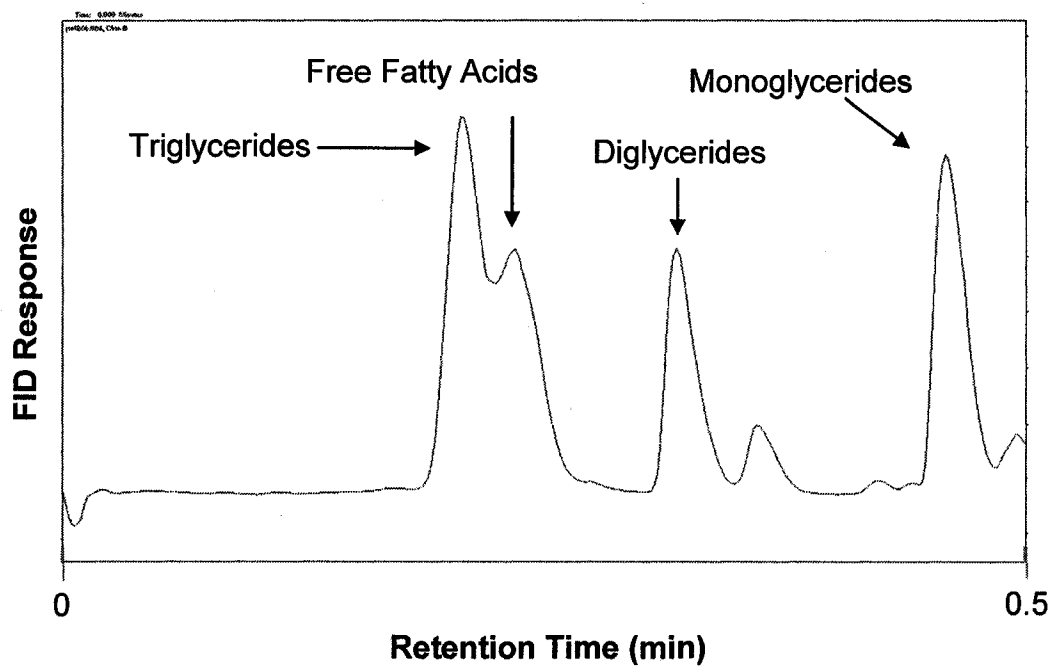


**Figure 4.46** TLC-FID chromatogram showing the oleic acid standard mixture

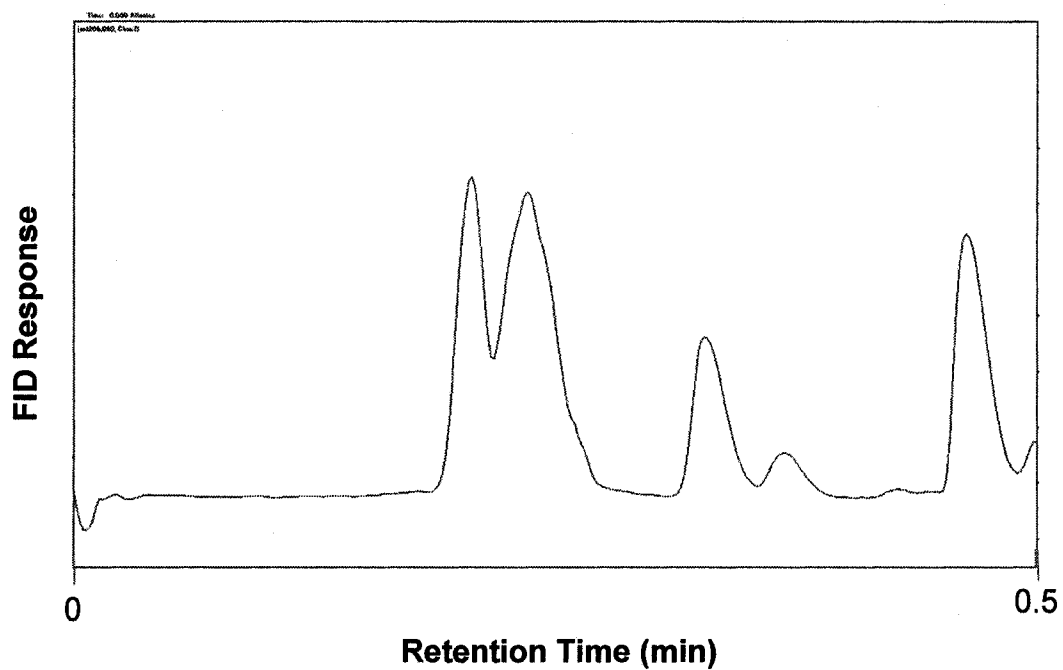


**Figure 4.47** TLC-FID chromatogram showing the oleic acid standard mixture spiked with bleached fancy tallow hydrolysates (2:1 by volume standard:sample).

the TLC-FID analysis of the hydrolysate fractions. Figure 4.44 shows the chromatogram for canola oil hydrolysates and Figure 4.45 shows the chromatogram for bleached fancy tallow hydrolysates. It is clear that a single peak results likely indicating that only one type or class of lipid is present. Duplicate chromatograms (not shown) showed similar results. The hydrolysis conditions, 250 °C at 3.5 MPa, were chosen based on literature (Brockmann et al., 2005). At these conditions, almost all TAG's are converted to FFA's (free fatty acids). Because the conditions were severe and a single peak is evident, it is very likely that all of the TAG's (triglycerides) are converted to FFA's. To confirm this, the retention times of different types of lipids were determined by analyzing a standard mixture of oleic acid TAG, DAG (Diglyceride), MAG (monoglyceride), and FFA's using the same method. These results are presented in Figure 4.46. The chromatogram analysis is such that the FID detector will scan down the rod. This means that the first peak to appear on the chromatogram (lowest scan time) will be the one that travels furthest up the rod during the TLC. In this case, the TAG fraction should appear first followed by the FFA's, DAG's and then MAG's. This is labeled on the standard curve and has been verified several times in other studies (Moquin et al., 2006). The DAG and MAG peaks are clearly separated, however, there is not clear separation between the TAG and FFA peaks. It is evident that there are two separate peaks and that the TAG peak is larger than the FFA peak. The same trend has been shown in duplicate samples. Comparing the single peak from the hydrolysate samples and the standard, it is clear that the single peak aligns with the TAG and FFA peaks, however because of the poor separation, it can not be stated conclusively that the samples contain nearly 100% FFA. Because the results indicate that there are no

intermediate DAG or MAG, the only other possibility is that the peak represents unreacted triglycerides. To confirm that the single peak does indeed represent FFA, samples were plotted on the chromarods and then spiked with the standard. Figure 4.47 shows that when the sample is spiked with standard, the height of the FFA peak increases relative to the height of the triglyceride peak. In this case, there is better separation between the TAG and FFA peaks and the peaks appear to be nearly equal in size. Comparing this to the standard chromatogram, where the TAG peak is clearly larger than the FFA peak, it is evident that the single peak of the hydrolysate added on to the second FFA peak from the standard. This indicates that the hydrolysed canola oil and bleached fancy tallow hydrolysates are composed almost completely of FFA. It is assumed that the hydrolysates of the poultry tallow and the yellow grease tallow are also composed predominantly of FFA. Although no lipid analysis was performed on these hydrolysates, analysis of the pyrolysis fractions of all four oils and fats appeared similar.

#### **4.2.1.1 GC-FID analysis**

The above results indicate that the lipids in the hydrolysate feed were comprised mainly of FFA. To further confirm this, samples of bleached fancy tallow and yellow grease tallow hydrolysates were derivatized using different agents as described in section 3.3.2.3. Figures 4.48 and 4.49 show samples derivatized with both methanolic HCL and diazomethane, respectively. Duplicate samples yielded similar results. The peaks were identified by running a standard mixture of various fatty acids (Figure A.10, Appendix A). Between 8-16 wt. % of compounds were unidentified. The amounts of the individual

fatty acids were determined semi-quantitatively by comparison to an internal standard (Appendix B). Heptadecanoic acid (C17:0) was chosen as the internal standard because this fatty acid is relatively uncommon in natural fats and oils and if present, is only so in trace amounts. Enough internal standard was used so that any trace C17:0 naturally occurring in the oils and fats was negligible in comparison to the amount of C17:0 from the internal standard solution. Figures 4.49 and 4.50 show similar composition between the two samples indicating the different types of derivatization agents did not affect the outcome. Hydrolysis products conducted under similar conditions were analyzed. The figures show that slightly more lipid content in the samples derivatized by methanolic HCl. This is expected as the methanolic HCl derivatizes all types of lipids where the diazomethane only derivatizes FFA. This means that the difference in peak areas between the samples derivatized with diazomethane and methanolic HCl likely represents a very small amount of mono-, di- or tri- glycerides that were not captured in the TLC-FID.

## **4.2.2 PYROLYSIS REACTIONS**

### **4.3.2.1 Analysis of product on GC-FID**

Initially, hydrolysates from poultry tallow were pyrolyzed for 4 h at 410 °C as per normal procedures and extracts were analyzed on GC-FID. The chromatogram is presented in Figure 4.50. Canola oil, and two grades of beef tallow (Bleached Fancy tallow (BF) and Yellow Grease tallow (YG) ), were pyrolyzed at 410 °C for 1 h. Bleached fancy tallow hydrolysates were also pyrolyzed at 390 °C for 1 h. The chromatograms are presented in

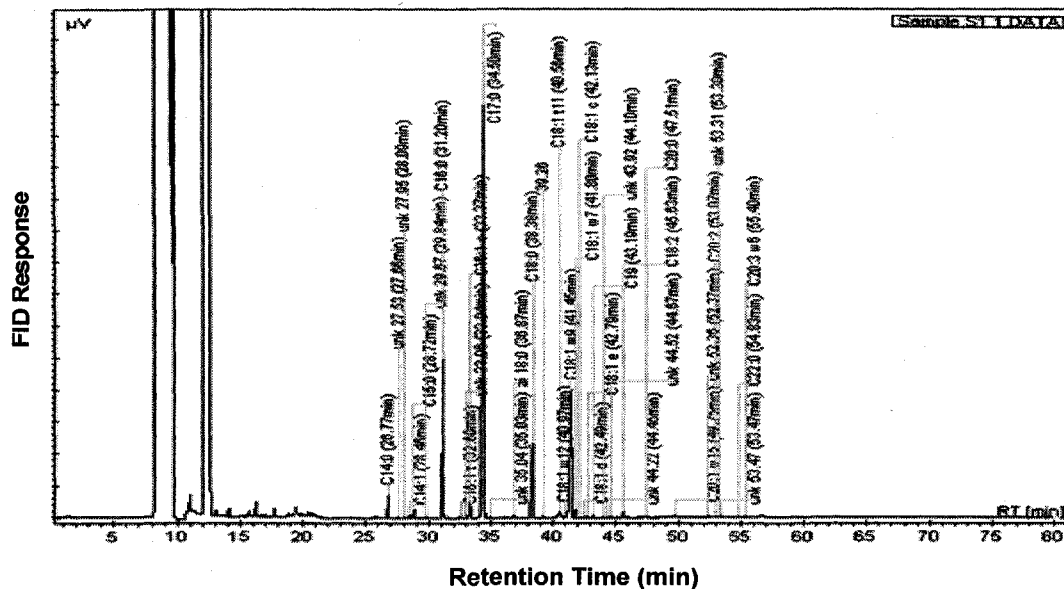


Figure 4.48 GC-FID chromatogram showing the fatty acid profile of bleached fancy tallow hydrolysates after derivatization with diazomethane

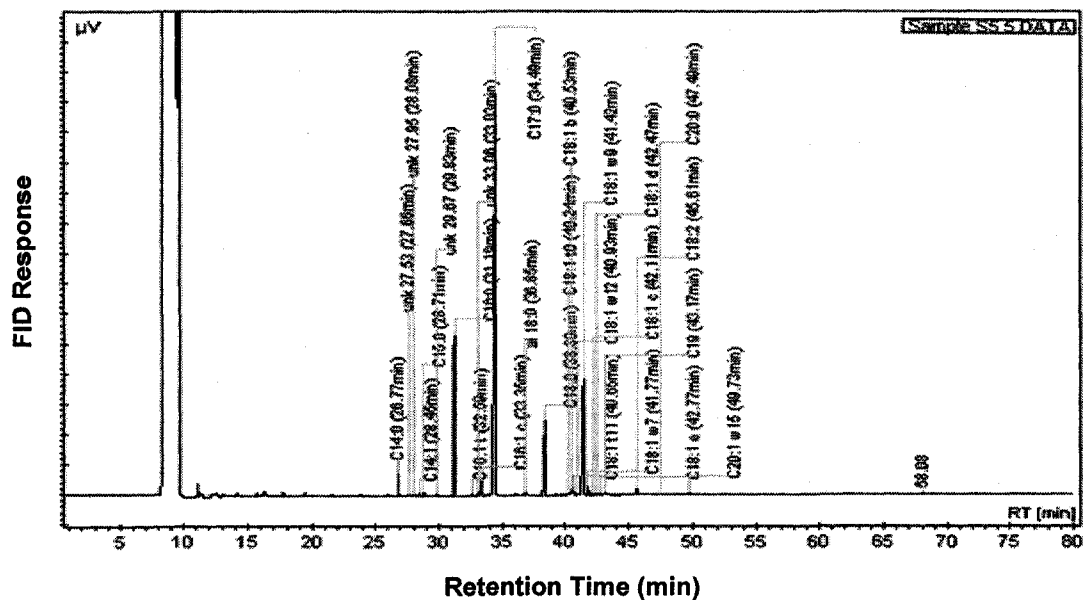
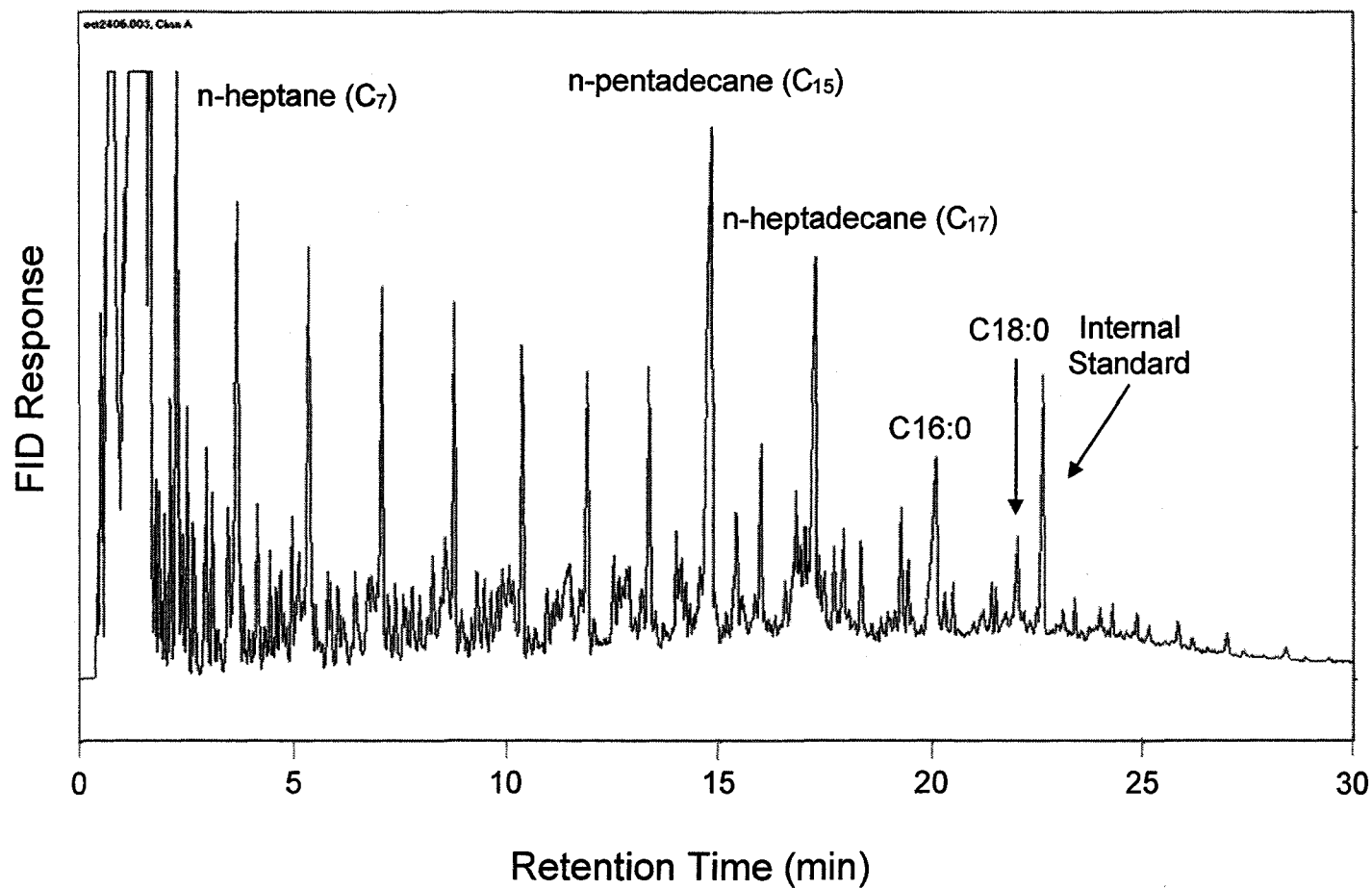


Figure 4.49 GC-FID chromatogram showing the fatty acid profile of bleached fancy tallow hydrolysates after derivatization with methanolic HCL

Figures 4.51-4.54. In Figure 4.53, the bleached fancy tallow pyrolysis products are compared to the pyrolysis products from stearic acid at similar conditions. Note that the samples were prepared at different concentrations.

Looking at Figures 4.50-4.54, the n-alkane/alkane ladder is evident. The chromatograms show that there are numerous compounds in between these ladders. The chromatograms of the neat oils and fats are not as clean as the chromatograms from the stearic acid pyrolysis. Numerous analyses of hydrolysates indicate the feed contains mainly free fatty acids and there was no evidence of any contamination that may account for these peaks. To verify this, hydrolysates were dissolved in pentane and run on GC-FID (Figure A.11, Appendix A), which gave a large peak at a retention time of approximately 20-25 min. Due to the spreading along the baseline, it is likely that this peak is composed of a mixture of fatty acids. No additional peaks were evident. To see if any of the compounds in the pyrolysis products were water soluble contaminants, a simple water extraction was conducted on the pyrolytic oil. After washing with water, the organic sample was separated and re-analyzed on GC-FID (Figure A.12, Appendix A). The chromatograms showing the pyrolysis products before and after water extraction are very similar, indicating that the water extraction had little effect on the extraction products. These simple experiments show that the peaks are organic in nature and are likely the result of the pyrolysis reaction. It is possible that the peaks are lower carbon number free fatty acids. Since these have a tendency to spread on the baseline they are difficult to separate and result in a poor baseline. Also, the results of the oleic acid analysis show



**Figure 4.50** GC-FID chromatogram showing poultry tallow pyrolysis products from a 4 hr reaction at 410 °C. Reactions were conducted in N<sub>2</sub> atmosphere and were initially at atmospheric pressure.

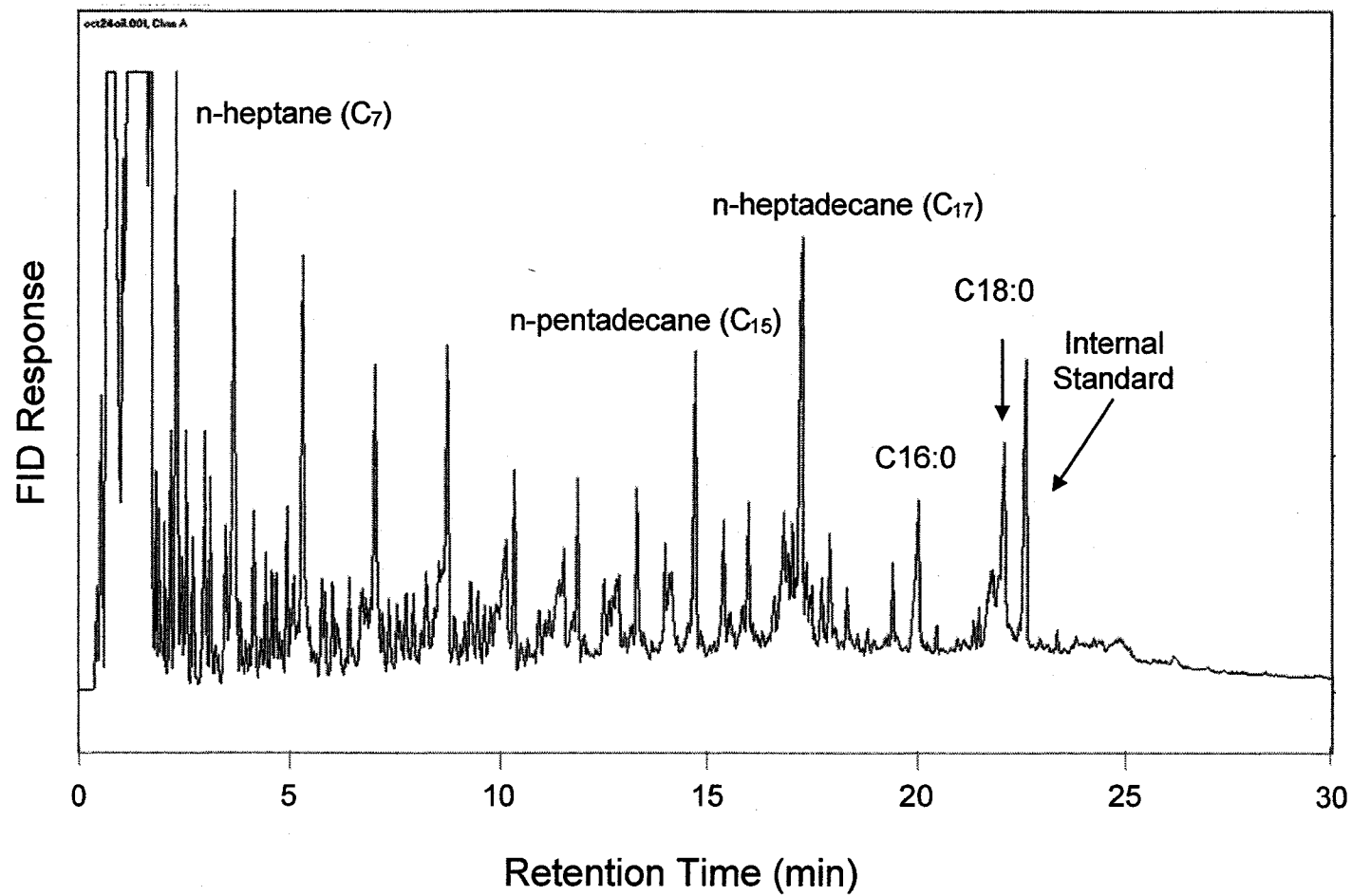


**Figure 4.51** GC-FID chromatogram showing canola oil pyrolysis products from a 1 hr reaction at 410 °C. Reaction was conducted in N<sub>2</sub> atmosphere and was initially at atmospheric pressure.



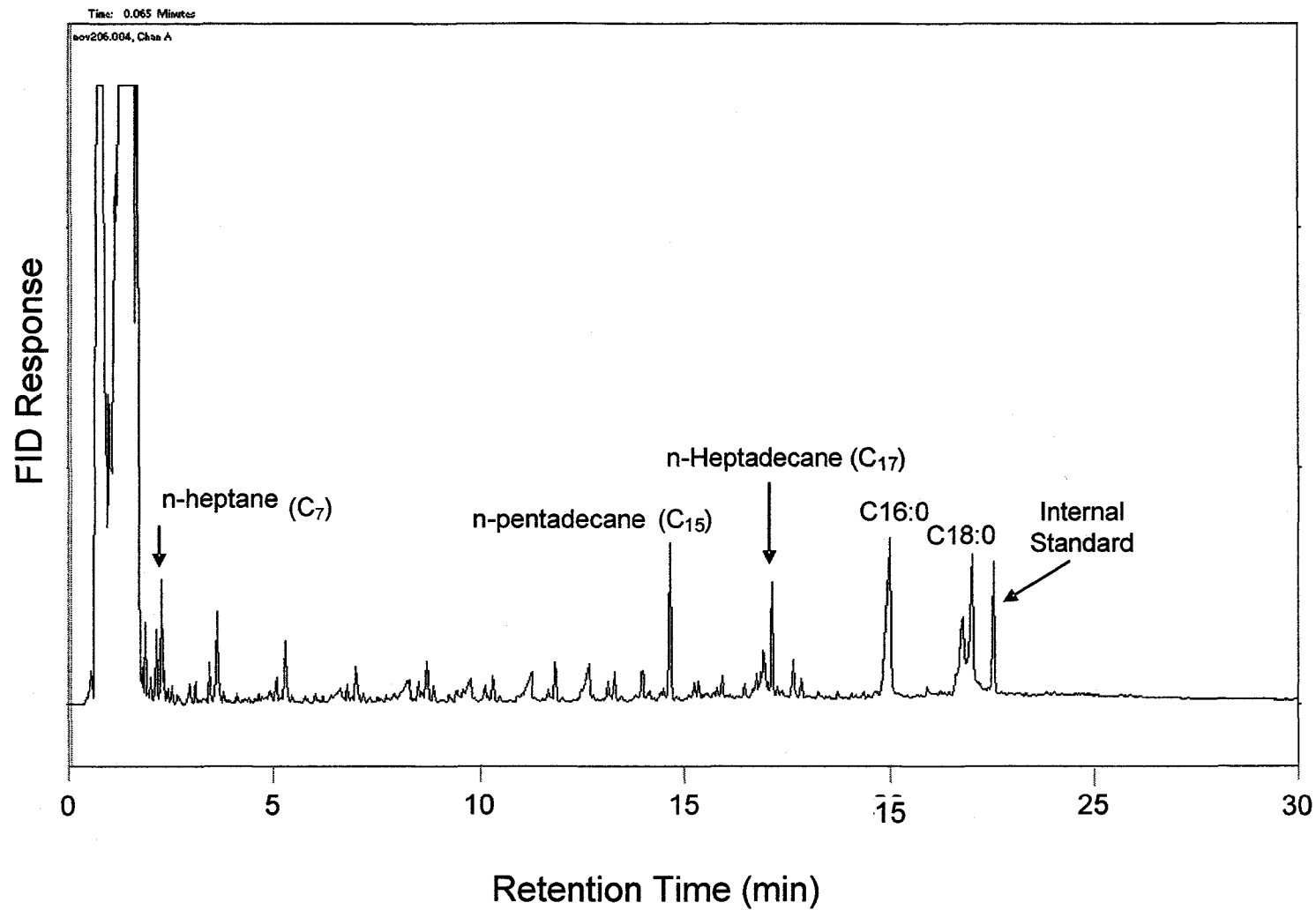


**Figure 4.52** GC-FID chromatogram showing yellow grease tallow pyrolysis products from a 1 hr reaction at 410 °C. Reactions were conducted in N<sub>2</sub> atmosphere and were initially at atmospheric pressure.

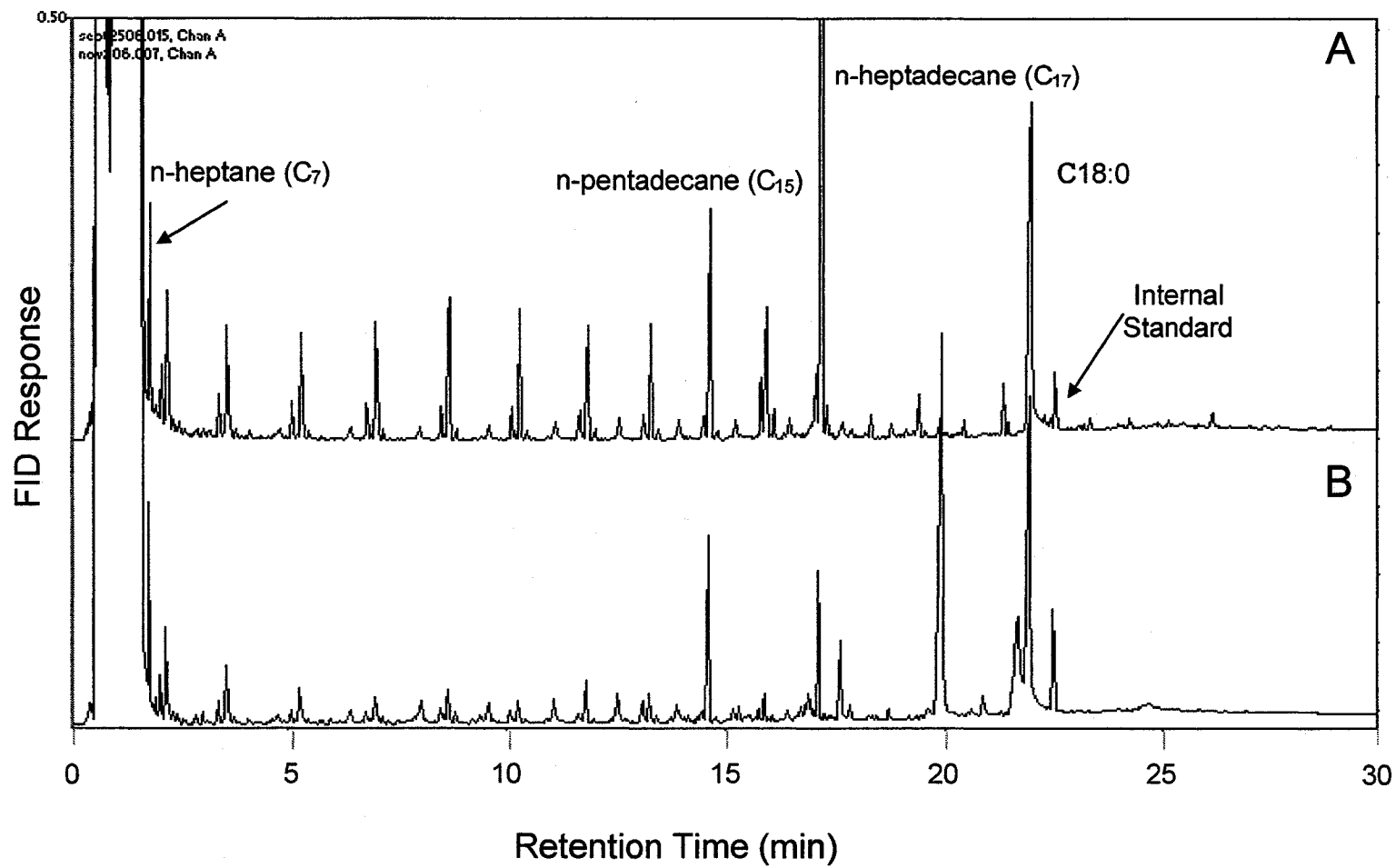


**Figure 4.53** GC-FID chromatogram showing bleached fancy tallow pyrolysis products from a 1 hr reaction at 410 °C compared to stearic acid pyrolysis products at the same conditions. Reactions were conducted in N<sub>2</sub> atmosphere and were initially at atmospheric pressure.

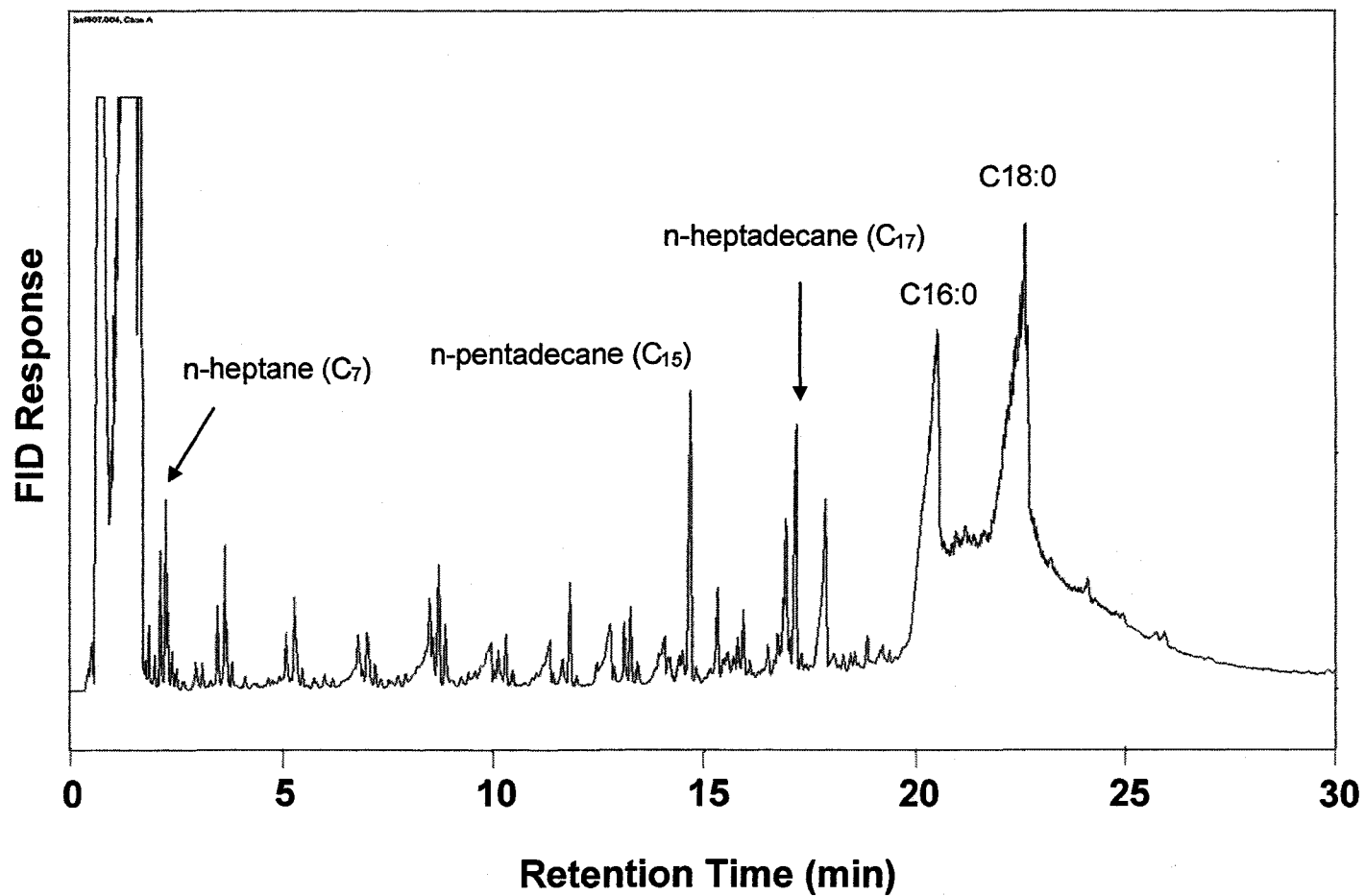


**Figure 4.54** GC-FID chromatogram showing bleached fancy tallow pyrolysis products from a 1 hr reaction at 390 °C. Reaction was conducted in N<sub>2</sub> atmosphere and was initially at atmospheric pressure.

that pyrolysis of unsaturated free fatty acids is likely to form numerous cyclic or branched hydrocarbon compounds.

Although the cracking pattern appears similar for the different lipid sources, but it appeared that product yield of the canola oil hydrolysates (Figure 4.51) is much higher than the tallow yields. This is discussed in greater detail in the discussion.

#### **4.2.2.2 GC/MS analysis after derivatization with diazomethane**

One of the main challenges with GC analysis was the diversity of the reaction products. As previously mentioned, underivatized fatty acids do not result in clean sharp peaks on the GC column and conditions that were utilized in this work for the analysis of the hydrocarbon product and because they spread on the column, they may overlap with other compounds. Products were not routinely derivatized because of the potential risk of changing the product distribution during the derivatization process and also because the stearic acid feed resulted in relatively clean chromatograms where the fatty acids and hydrocarbons were clearly separated. To estimate the unreacted feed this approach was taken as described previously: however, in these experiments the hydrocarbons were considered for analysis (thus the need to eliminate drying from the process so as not to volatilize the lighter ends). Because the pyrolysis products from neat fats and oils contained many unidentified compounds, it was of interest to analyze them using GC/MS. In an attempt to clean up the chromatogram by eliminating any fatty acid spreading along the baseline, bleached fancy tallow pyrolytic oil was first derivatized

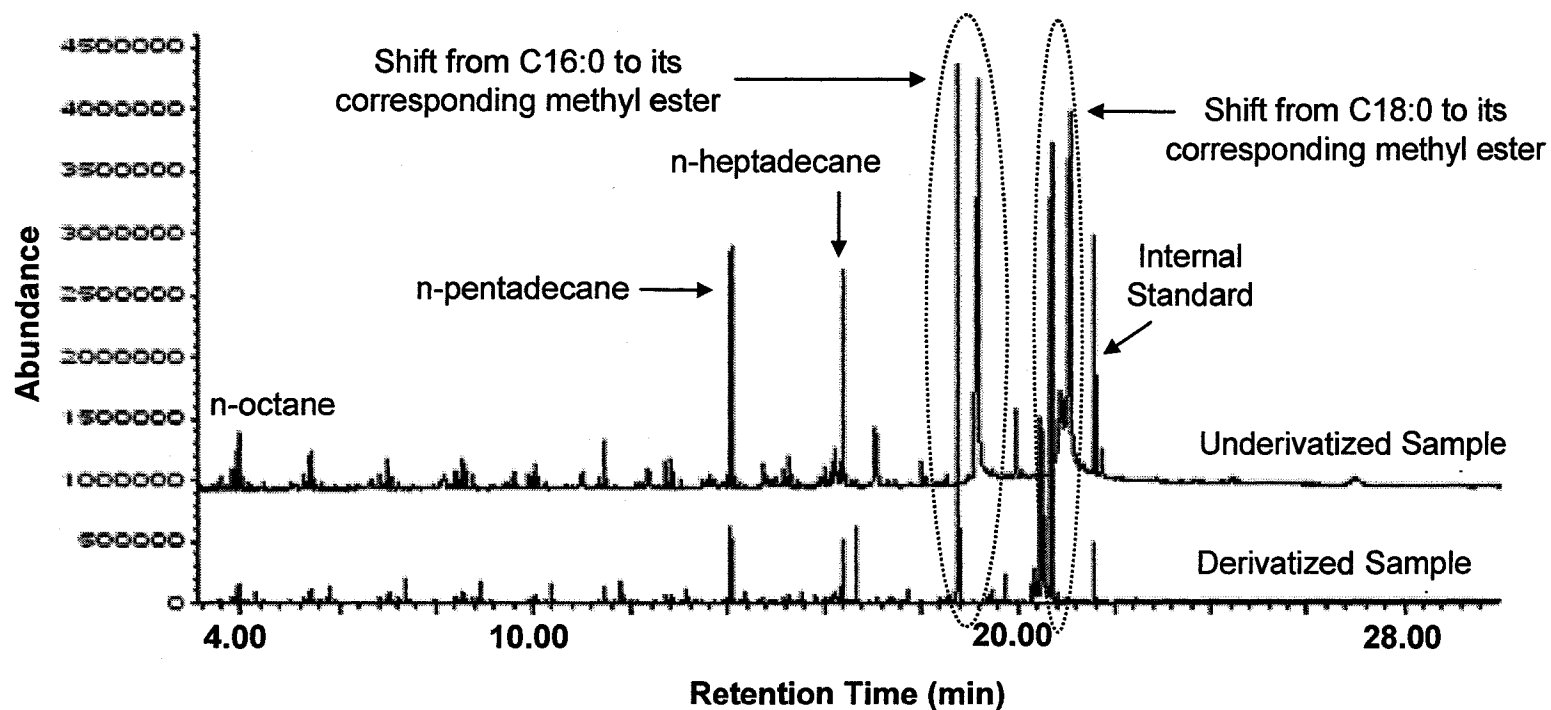


**Figure 4.55** GC/MS chromatogram showing derivatized and underivatized samples of bleached fancy tallow pyrolysis products after 1h reaction at 410 °C. Reactions were conducted in N<sub>2</sub> atmosphere and were initially at atmospheric pressure.

with diazomethane (without drying) and analyzed by GC/MS. An underivatized sample was also analyzed to determine any effects of running the derivatized samples without the drying steps. These chromatograms are shown in Figure 4.55. Although very dilute, the figure shows two things. Firstly, the fact that the solvent was not dried prior to derivatization did not appear to affect the reaction products or introduce contaminants. Secondly, it is clear that the fatty acid peaks, which are now in the form of methyl esters, sharpen eliminating the potential overlapping of compounds, specifically the internal standard by unreacted stearic acid. Although the methyl esters shifted along the baseline, they were easily identified by GC/MS. Figure 4.56 shows a labeled chromatogram from GC/MS analysis of derivatized bleach fancy hydrolysates reacted at 410 °C for 1 h. The chromatogram shows identical clusters of peaks along the baseline. A close-up of one of these clusters was labeled and is presented in Figure 4.57.

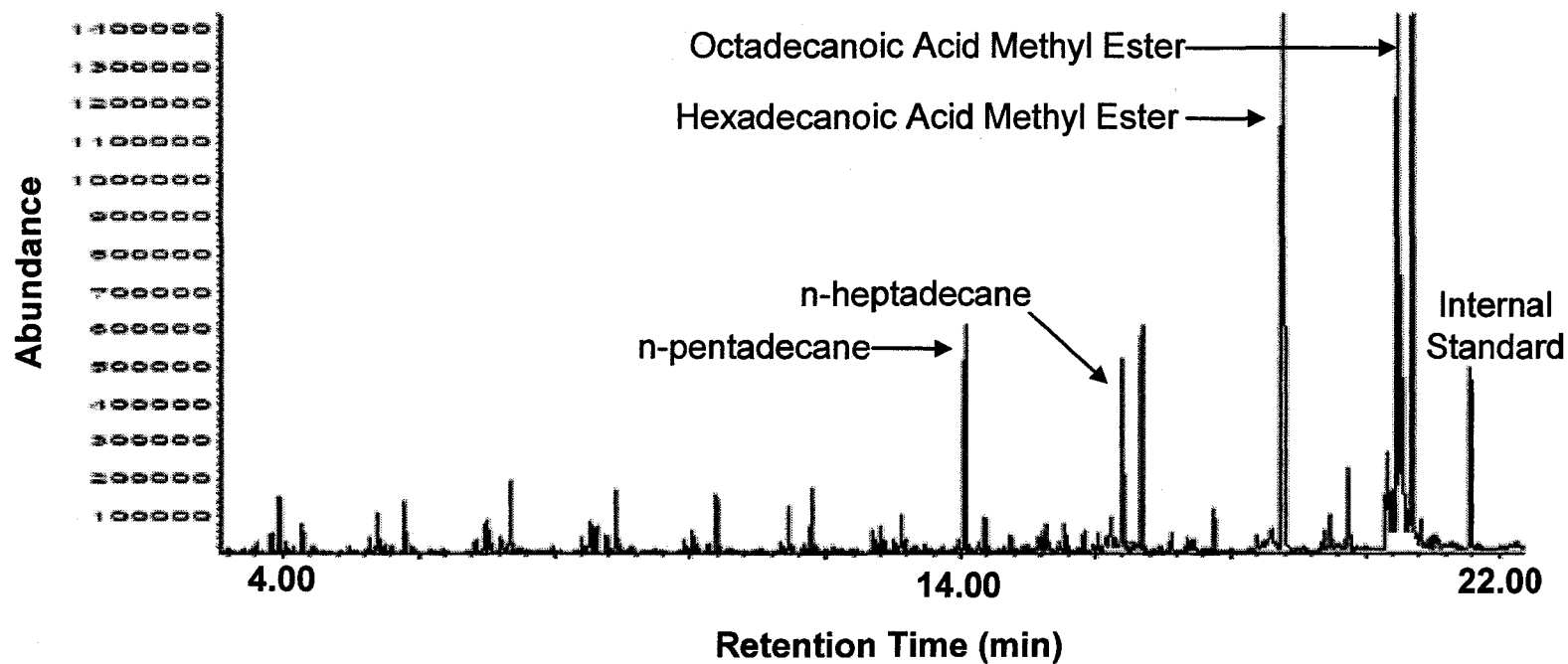


**Figure 4.56** GC/MS chromatogram showing derivatized bleached fancy tallow pyrolysis products after 1 h reaction at 410 °C. Reactions were conducted in N<sub>2</sub> atmosphere and were initially at atmospheric pressure.

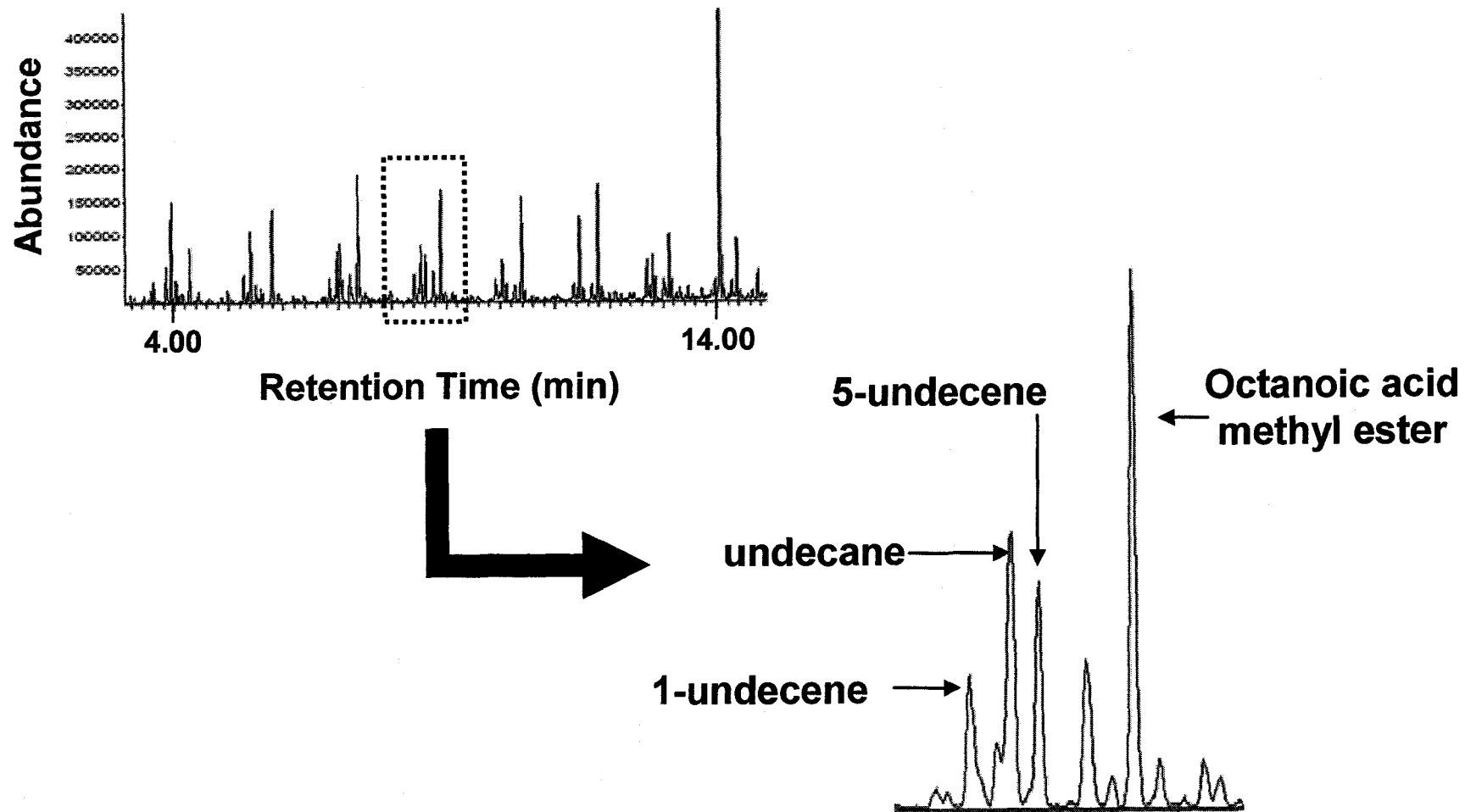


**Figure 4.57** Close-up of GC/MS chromatogram showing derivatized bleached fancy tallow pyrolysis products after 1 h reaction at 410 °C. Reactions were conducted in N<sub>2</sub> atmosphere and were initially at atmospheric pressure.



## **CHAPTER 5: DISCUSSION**

The intent of this work was to investigate the pyrolysis of lipid feeds for the production of deoxygenated liquid hydrocarbons for applications as chemicals and fuels. Figure 1.3 outlines the proposed flow diagram, which was used as the basis for this work. An initial hydrolysis step was used to convert triglycerides into free fatty acids followed by a pyrolysis step to further break down the free fatty acid chain. The major hypothesis is that the free fatty acid chain will first undergo decarboxylation to yield a linear, deoxygenated hydrocarbon that would then undergo further thermal treatment to form shorter chain hydrocarbons.

The primary objective of this research was to collect fundamental information at key process points identified in Figure 1.3, with a focus on the pyrolysis of stearic acid as a model compound. The first objective was to identify the major reaction products resulting from the pyrolysis of stearic acid and to determine the effect of reaction time and temperature on the reaction products. Data regarding yield of liquid and gas products and the extent of the reactions was also collected. This work was followed by studying the combination of hydrolysis and pyrolysis using oils and fats.

### **5.2 MODEL COMPOUND WORK**

#### **5.2.1 MAJOR REACTION PRODUCTS**

The first objective of this thesis research was to determine the types or classes of compounds formed during lipid pyrolysis. The project originated from a need to utilize beef tallow so stearic acid, one of the main saturated fatty acids present in beef tallow, was chosen as a model compound. The goal of this work was to produce a product with composition similar to conventional petroleum products so it is of interest to be consistent with terminologies used by petroleum industry. In crude oil upgrading, oil is fractionated based on solubility in various solvents such as n-pentane and toluene. Products that are soluble in n-pentane are called maltenes (Gray, 2002). Pentane was chosen as the primary extraction solvent because the products of interest were in this fraction. The majority of experiments were conducted using pentane as the extraction solvent and therefore in terms of solubility, the products described in this work would be equivalent to the maltene fractions in the heavy oil industry.

#### **5.2.1.1 n-Alkanes and alkene series**

Pyrolysis of stearic acid resulted in distinct series of n-alkanes and alkenes with n-heptadecane being the most prominent reaction product at the majority of conditions tested. The n-alkane/alkene series were evident from C<sub>7</sub>-C<sub>20</sub>, which is expected based on hydrocarbon cracking theory (Fabuss et al, 1962, 1964; Khorasheh and Gray, 1993). Analysis of gas fractions showed the presence CH<sub>4</sub>, which is also consistent with hydrocarbon cracking theory (Fabuss et al, 1962, 1964; Khorasheh and Gray, 1993). Initial results also showed that time and temperature substantially affected the product profiles and that relatively milder reaction conditions result in low conversion while the

most severe conditions resulted in almost complete breakdown of the free fatty acid chain into aromatics and small chain hydrocarbons, as well as an appreciable amount of gas. A second alkene series, possibly a 2-alkene, was also observed in minor concentrations. This has also been reported in literature (Khorasheh and Gray, 1993).

### **5.2.1.2 Carboxylic acid series**

In addition to the n-alkane and alkene series there were also series of shorter chain fatty acids present in the reaction products. A series of saturated carboxylic acids was evident in most of the reaction conditions. Initial results showed a corresponding series of unsaturated fatty acids (Figure 4.2 and 4.3): however, these were not clearly evident on all chromatograms. The chromatograms in Figure 4.11-4.17 represent reactions that were conducted with more initial feed (1.000 g compared to 0.5000 g used during the preliminary studies) and less extraction solvent. It is possible that these compounds were not dissolved in the pentane or that they are overlapped by the saturated fatty acid peak, which appears to have spread along the baseline (Figure 4.11-4.17). These figures also show more compounds between the n-alkane/alkene pairs, likely because it is more concentrated (for GC purposes) and it is possible that one of these peaks represents the unsaturated fatty acid. Furthermore, the preliminary 5 and 30 min reactions (Figure 4.2 and 4.3) appear to favor alkene production (especially for the 5 min reactions) and in turn may also favor the production of unsaturated fatty acids. The preference for alkene formation indicates that the reaction conditions result in increased B-scission reactions a concept that is discussed in greater detail in Section 5.3.2. As well, these reactions were

not only conducted at short times, but always with less initial feed stock, which also may influence the reaction products.

### **5.2.1.3 Other products**

There were minor compounds present in between the main series mentioned above. It is possible that these were branched alkanes and alkenes formed by isomerization, which has been reported in n-hexadecane cracking (Khorasheh and Gray, 1993; Wu et al., 1996). It has been shown that series of branched alkanes form through additions of lower radicals and  $\alpha$ -olefins. The other interesting product was the presence of 2-nonadecanone, a methyl ketone indicating that some side reaction is also occurring. In the literature, the formation of ketones has been reported when metal catalysts are used in a process known as ketonic decarboxylation (Renz, 2005), however these ketones are usually present in a series. There was no evidence of a ketone series in this work. It is possible that the metal reactor walls had some sort of activity; however, it has been found that the reactor walls in similar 15 mL batch reactors did not result in any sort of catalytic activity (Kanada, 2003). Furthermore, the use of metal catalysts favor the production of symmetrical ketones, not methyl ketones. If a symmetrical ketone was first formed and then thermally cracked into a methyl ketone it would be expected that a series of ketones at various chain length would result. Ketone products have also been reported with the addition of alumina catalyst as reported by Billaud et al. (2002); however, no alumina catalyst was used for the majority of the reactions in this work.

### **5.2.2 INITIAL DECARBOXYLATION**

The fact that n-heptadecane was the primary reaction product at most of the reaction conditions coupled with the presence of CO<sub>2</sub> in the gas fractions indicate that decarboxylation of the fatty acid chain is occurring. At more mild reaction conditions, it showed that appreciable amounts of n-heptadecane were produced before other reaction products began to form indicating that decarboxylation is likely the first step in thermal cracking of stearic acid. Similar work has since been published verifying this in temperature ranges between 300-360 °C (Maki-Arvela et al., 2007). Subsequent experiments were conducted to determine the lowest temperature at which decarboxylation occurs. GC/MS analysis of products from a 1 h reaction at 200°C showed trace amounts of n-heptadecane being produced.

### **5.2.3 CRACKING BEHAVIOR AND PRODUCT DISTRIBUTIONS AT DIFFERENT REACTION TIMES AND TEMPERATURES**

The data from the stearic acid pyrolysis at different times and temperatures gave valuable insight into cracking behavior of saturated fatty acids. The literature is lacking on the thermal cracking of free fatty acids; however, if the process involves decarboxylation to yield an n-alkane, it is possible that the cracking behavior is similar to that of longer chain n-alkanes, which has been studied. It is well known that organics undergo complex free radical reactions and that these mechanisms depend on numerous variables including the reaction conditions and the concentration of the free radicals. In this work, the most

prominent reaction products were series of n-alkanes and alkenes, which is in agreement with free radical mechanisms. Cracking of n-hexadecane predicts series of C<sub>1</sub>-C<sub>14</sub> n-alkanes and C<sub>2</sub>-C<sub>15</sub> α-olefins (Khorasheh and Gray, 1993), therefore the cracking of n-heptadecane should result in C<sub>1</sub>-C<sub>15</sub> n-alkanes and C<sub>2</sub>-C<sub>16</sub> alkenes. Due to analytical methods employed, n-heptane and heptene (C<sub>7</sub>) were the lightest compounds that were clearly evident on the chromatograms and not overlapped by the solvent peak. GC-FID analysis of the gas fraction showed numerous light ends, which are likely to be C<sub>1</sub>-C<sub>3</sub> n-alkanes and alkenes (Appendix C). Complete series of both the n-alkanes and alkenes were observed. Although some C<sub>16</sub> n-alkane (hexadecane) was formed, the molar ratios of C<sub>16</sub> were lower than other carbon numbers indicating relatively more alkene formation than other carbon numbers. The molar ratio for C<sub>16</sub> might not be completely representative of the true amount of alkenes formed because unlike other carbon numbers, there appeared to be several hexadecene peaks formed in addition to the first alkene that was used in the molar ratio calculation. If all the hexadecene peaks were taken into account, it is possible that more hexadecene is formed than hexadecane at many of the conditions for C<sub>16</sub>.

It is also important to mention the formation of addition products of C<sub>18</sub>+. Addition products including C<sub>18</sub>-C<sub>31</sub> n-alkanes have been reported for high pressure thermal cracking of n-hexadecane (Fabuss et al., 1962, 1964; Khorasheh and Gray, 1993). These higher n-alkanes were formed through addition of the parent hexadecyl radicals to lower α-olefins. C<sub>17</sub> on the other hand was formed in minor concentrations through addition of lower primary alkyl radicals to α-olefins. This is in agreement with the results of

this work which showed the formation of n-octadecane (C<sub>18</sub>) in minor concentrations but the formation of n-nonadecane (C<sub>19</sub>) in comparatively greater concentrations.

At the majority of the conditions studied, more n-alkanes were formed in comparison to alkenes as shown by molar ratios greater than 1 (Figures 4.24-4.27). This indicates that bimolecular hydrogen abstraction reactions were preferred over B-scission. These products would be consistent with the one step F-S-S mechanism described by Fabuss et al (1962, 1964); however, these products were predicted for gas phase cracking at high temperatures (550-600) and moderate pressures (1-7 MPa). In this work, experiments were conducted at atmospheric pressures and moderate temperature. Wu et al. (1996) showed that at low temperature (330-375 °C) gas phase cracking always resulted in more alkenes and n-alkanes and vice versa for liquid phase cracking. According to the results from this study, it is possible that reactions occurring in this thesis work were occurring in the liquid phase. As well, Wu et al. (1996) reports that addition products were not formed during gas phase cracking. This would also point to liquid phase cracking in this work as addition products were formed at the majority of conditions tested.

Theoretically, n-alkanes and alkenes should be present in equimolar concentrations, or in a 1:1 ratio. The results of this research has shown that the n-alkane:alkene ratio is greater than 1 and that how much greater than 1 it is, depends on the reaction conditions. If the ratio is expected to be 1:1, yet substantially more alkanes are formed relative to alkenes, then reactions must be occurring to subtract or remove the alkenes from the system. The two possibilities could be cracking at the unsaturated (highly reactive) site to yield two

shorter chain n-alkanes, or hydrogen addition to the reactive site to form an n-alkane. Because the ratios did not seem drastically different over the range of carbon numbers analyzed, the latter option is more likely.

The cracking behavior in these experiments was investigated for carbon numbers between C<sub>8</sub>-C<sub>20</sub> due to analytical constraints. It must be emphasized that cracking patterns of hydrocarbons with carbon numbers less than C<sub>8</sub> would be expected to follow similar behavior. This has been confirmed by other studies that have investigated alkane cracking and have reported complete series on n-alkanes and alkenes (Koresheh and Gray, 1993).

## **5.2.4 EFFECT OF OTHER VARIABLES ON REACTION PRODUCTS**

### **5.2.4.1 Initial feed weight**

The concentration of the reactants represents another important variable in free radical reactions. Although this was not studied formally, different feed weights were used with different procedures throughout the course of this work. During the preliminary studies, it was shown that more alkenes were formed than n-alkanes, which is different for most of the studies. These reactions were conducted at slightly elevated temperatures and a very short times of 5 min (no other reactions were conducted at 5 min) which, may account for alkene production. In addition, only 0.5000 mg of stearic acid feed was used instead of the typical 1.0000 g of the reactants used for the majority of reactions in this work. Over the course of this work, different feed weights were used and there was some



evidence that lesser feed weights resulted in products with physically different appearances compared to the products of reactions with higher starting feed weights conducted at identical conditions. For example, at the same reactions conditions, using lesser feed weight resulted in a solid powder product while reactions with a greater initial feed weight resulted in a liquid product. It would be expected that more feed would result in greater free radical concentrations, which can influence products.

#### **5.2.4.2 Alumina catalyst**

Studies have been conducted showing that triglycerides in the presence of activated alumina reacted at 450 °C result in up to 79 % conversion to an oxygen free mixture of n-alkanes and alkenes (Boocock et al., 1992a, 1992b). Model fatty acids were also tested in this work to verify the theories. The mechanism by which the catalyst work is via ketonization of two acid molecules condensing on a molecule followed by conversion into methyl ketones,  $\alpha$ -olefins, and paraffins via a  $\gamma$ -hydrogen transfer (Billaud et al., 2002). Billaud et al., (2002) found that pyrolysis of octanoic acid at 450 °C resulted in the production of C<sub>6</sub>, C<sub>9</sub>, C<sub>15</sub> olephins, 8-pentadecanone, and 2-nonanone as primary reaction products. In this work, the addition of alumina resulted in the same n-alkane/alkene series as observed in stearic acid pyrolysis without the addition of alumina, which differs from the observations by Billaud et al. (2002). In addition the alumina appeared to decrease the yield of C<sub>8</sub>-C<sub>20</sub> n-alkanes and alkenes as well as the molar ratio indicating preference toward alkene formation compared to the stearic acid pyrolysis products without alumina.

### 5.2.4.3 Pressure

According to hydrocarbon cracking theory an increase in pressure should result in higher alkanes as major reaction products due to the bimolecular reactions that are favored under these conditions (Fabuss et al., 1962, 1964). In this work, the experiments show that a difference in initial pressure from zero to 6.89 MPa had little to no effect on the product distributions for 1 h reactions at 400 and 410 °C (Figures 4.39 and 4.40) but did cause a decrease in C<sub>8</sub>-C<sub>20</sub> n-alkane yield and molar ratio. Similar to the addition of alumina, the increase in pressure appeared to result in preferential alkene formation in comparison to the reactions initially at atmospheric pressure. Generally, pressures greater than 10 MPa are considered, high meaning the pressures used in this experiment would be considered intermediate. These pressures still fall within the conditions described by Fabuss et al. (1962, 1964) and are not likely high enough to significantly change the product distribution. It is possible that higher pressures may influence the product distribution.

### 5.2.6 OLEIC ACID PYROLYSIS PRODUCTS

Beef tallow contains 44-55 wt % of monounsaturated fatty acids and 7-19 wt % polyunsaturated fatty acids (Table 3.3). The major unsaturated fatty acid present in beef tallow is oleic acid, which is present in 37-47 wt % (Table 3.2). The results from the stearic acid pyrolysis give good insight to the behavior of saturated fatty acids but because tallow is such a heterogeneous mixture of saturated and unsaturated fatty acids, it is important to determine how unsaturated fatty acids behave under similar conditions.

The results of the oleic pyrolysis show very different product profiles indicating that the cracking behavior differs from that of the stearic acid (Figure 4.36 and 4.37). The main product is n-heptadecene, which suggests that decarboxylation of the unsaturated fatty acids is occurring first resulting in an alkene. Results from the analysis of the gas fractions from these experiments confirm the presence of CO<sub>2</sub>. The most noticeable difference is the absence of the prominent n-alkane/alkene ladders above C<sub>9</sub>. The presence of nonane/nonene (C<sub>9</sub>) and the C<sub>8</sub> and C<sub>7</sub> n-alkane/alkene pairs suggest that the linear chain is breaking at the C-C double bond in n-heptadecene. The presence of both nonanoic acid (C<sub>9</sub>:0) and decanoic acid (C<sub>10</sub>:0) suggest that at more severe conditions when thermal cracking increases, breaking of the same C-C double bond and decarboxylation of oleic acid are occurring simultaneously.

### 5.2.7 PRODUCT YIELDS

Understanding the cracking behavior is one important aspect of process development, another is yield. Good yields are vital for process feasibility. Analysis of the unreacted acids showed that after a 1 h reaction at 450 °C less than 5 wt % of the initial stearic acid feed remained. This means that over 95 % of the initial stearic acid was converted into some kind of product. As expected, a decrease in process temperature resulted in a decrease in percent conversion.

Looking at the data in Figures 4.18 and 4.19, the maximum percentage of C<sub>8</sub>-C<sub>20</sub> n-alkanes and alkenes was approximately 32 wt % and was formed at 4 and 8 h reactions at

410 °C. Although these may seem low it must be stressed that these only represent a fraction of the reaction products. Even though there was a decrease in the wt % of C<sub>8</sub>-C<sub>20</sub> at temperatures greater than 410 °C, it is possible that if lower carbon numbers were included, this number would be greater. Lower n-alkanes and alkenes (C<sub>7</sub> and below) are also desirable compounds but were not quantified due to analytical methods employed. As well, it was discussed that the C<sub>17+</sub> values may be underestimated due to the nature of the solvent extraction. It was described why pentane was chosen however, fatty acids are not very soluble in pentane. This is why chloroform was used to determine the amount of unreacted feed present and to attempt to do get better mass balance.

#### 5.2.7.1 Mass Balance

Figure 4.43 shows the breakdown of products for a 1 h reaction at 390 °C. From other experiments, it is known that at these conditions less than 1 wt % of gas is formed (Figure 4.31). The other compounds that were identified included the n-alkane series, two alkene series, and a saturated carboxylic acid series. The presence of unsaturated carboxylic acid series was not clearly identified. There most interesting thing to note is that the amount of saturated carboxylic acids (< C<sub>18:0</sub>) is very small (<1 wt %). This is result is promising and shows that decarboxylation is occurring at much higher rates than the reactions which result in shorter chain saturated carboxylic acids. This reaction could potentially include cracking of the carboxylic acid at one of the C-C bonds to yield the acid and an n-alkane or by the addition of CO<sub>2</sub> to a lower alkane or alkene. Figure 4.43 indicates a “balance” of 44 % meaning that 44 % of the compound could not be

identified. In these experiments, the product was a solid powder and all of it was dissolved by washing the reactor with excess amounts of chloroform. As well, there appeared to be no coke formation (based on observations). Therefore, the balance of compounds can not be attributed to coke, unreacted starting material or any residue left in the reactor. Therefore, the balance must be composed of other compounds. One possibility is that these compounds, or a portion of these compounds, are light components that eluted from the GC quickly (with or before the solvent) and were not detected by the GC-FID protocols employed. These could be C<sub>4</sub>-C<sub>7</sub> hydrocarbons of varying saturations and configurations. Alternatively, these compounds could represent heavier components that did not elute from the column. This would indicate that other side reactions are occurring causing addition or polymerization reactions. Polymerization reactions can occur in hydrocarbon free radical reactions (Poutsma, 2000). It is also possible that the CO<sub>2</sub> liberated during decarboxylation could react with free radicals formed during pyrolysis. More accurate and detailed work would need to be conducted to get a more accurate mass balance and gain better understanding of all the compounds in the mixture. This is very challenging and time consuming task due to the complexity of the reactions and the numerous products.

### **5.2.8 SELECTION OF OPTIMAL CONDITIONS**

There are many things to consider when selecting the best conditions including:

1. Maximizing liquid yield,

2. Minimizing gas formation,
3. Minimizing coke formation, and
4. Minimizing aromatic formation.

It is obvious that the main goal is to optimize the products of interest. In this work, the products of interest are not clearly defined. The objective was to look at the entire spectrum of products. While this may have caused challenges in extraction and analysis, it will also allow for more flexibility during potential scale-up. Whether the desired product is a specific compound such as hexane, a certain boiling fraction of the product, or a range of hydrocarbons, the data from this work will provide information to select good starting conditions during scale-up. It is important that the products are in liquid form for ease of handling, processing storage, and transport. In these experiments, n-heptadecane, a solid at room temperature, was the most prominent product and as a result, many of the reaction product mixtures, especially less than 410 °C, were solid. There is a specific time/temperature combination that will result in the liquid versus a solid product. At 410 °C and 1 h reactions three out of six reactions resulted in completely solid, whiteish-brown product while the other three reactions resulted in approximately 60 wt % brown, liquid, oil like product. It appears that at these conditions some sort of critical miscibility has been reached and the liquid products begin to behave as a solvent, dissolving the solids still in the reactor. Although the reaction conditions were similar, the difference may have occurred because of something simple, like one reactor being slightly lower in the bath. Therefore, to obtain a liquid product, the minimum conditions would have to be reactions conducted at 390 °C for longer than 4 h,

410 °C for longer than 1 h, or 430 °C for longer than 1 h. It is also important to consider gas formation. The less gas that is formed, the more potential there is for liquid products to be formed; however, if the conditions are too mild, then the product will not be liquid. Therefore, at low temperatures such as 370 °C and 390 °C where there is almost negligible gas formation, the product is solid and yields of the products of interest are not as good. At 410 °C and 1 h reactions, there is less than 4 wt % gas being formed but at 430 °C, 8 wt % gas is being formed (Figure 4.31). Coke formation is also an important parameter to consider. Not only does coke formation lower yield, it also causes cleaning and plugging issues of process equipment (Gray, 2002). Although coke was not tested as per definition (insoluble in THF), there was formation of solid, black particles that were insoluble in toluene and adhered to the reactor walls. At the majority of the conditions tested, the formation of this solid material was not significant but at higher temperatures and longer reactions (430 °C and 8 h and 450 °C and 500 °C at 4 h) the formation of these solids increased. The final important aspect to consider when determining the optimal conditions is the formation of aromatics. For this process, aromatics are not desired. Figure 4.42 shows that some aromatization begins to occur after a 1 h reaction at 430 °C, but in very small amounts. Based on the listed criteria, the optimal conditions for production of the products of interest would be between 410 °C-430 °C at times longer than 1 h at 410 °C and no longer than 4 h at 430 °C.

### 5.2.8.1 Supercritical Nitrogen

It is worth mentioning that at the conditions in this study, it is possible that the nitrogen is in supercritical phase. Supercritical fluids are fluids that are above their critical pressure ( $P_c$ ) and temperature ( $T_c$ ) (Elliot and Lira, 1999). Supercritical fluids are neither gases nor a liquids but have properties representative of both (McHugh and Krukonis, 1994). They have been described as being a single phase. Supercritical fluids exhibit high densities like liquids but low viscosities such as gases and have diffusion coefficients that lie somewhere in between a gas and liquid (McHardy and Sawan, 1998). The unique properties of supercritical fluids make them good solvents and they have been applied in cleaning and extraction industries. In this thesis work, the reaction atmosphere was nitrogen. The supercritical pressure of nitrogen is 3.394 MPa and temperature is - 147 °C (Elliot and Lira, 1999) The reaction temperature was well above  $T_c$  for nitrogen therefore, pressure was the determining factor as to what state the nitrogen was in. Pressure was not measured during every reaction but was measured for select runs during the verification of the sandbath as outlined in Appendix C. In only one run, the maximum pressure during the reaction exceeded the critical pressure limit for nitrogen and this result was inconsistent with the rest of the pressures (it was substantially higher and the value was attributed to error (Appendix C)). The most severe reaction at which pressure was measured was a 1 h reaction at 450 °C. There were more severe conditions applied in other experiments in this work (where pressure was not measured) so it is possible that the nitrogen was in a supercritical phase during these reactions. In future work is will be important to understand if the nitrogen is in supercritical phase as this



may cause processing issues, especially if the supercritical nitrogen must be separated from the reaction products.

### **5.3 HYDROLYSIS AND PYROLYSIS OF NEAT OILS AND FATS**

The model compound work gave good information regarding cracking behavior and yields for some of the components of beef tallow; however, tallow is a complex mixture and is not likely to behave in the exact same way as the model compounds. Different types of oils and fats were first hydrolyzed and then pyrolyzed. Both the hydrolysates and pyrolysates were analyzed.

Severe hydrolysis conditions were selected to ensure that the majority of the triglycerides were converted to free fatty acids. Both TLC-FID and GC-FID analysis of the hydrolysates showed that the hydrolysate mixtures consisted almost completely of free fatty acids. A simple water extraction experiment eliminated the possibility of any water soluble contaminants that may have still been present in the hydrolysates fraction and that may have influenced the pyrolysis. For these experiments the hydrolysate products were sufficient for pyrolysis and no further work was done in terms of experimenting with different hydrolysis conditions. It is likely that this process could be optimized; however, that was not within the scope of this project and is discussed further in the recommendations.

Pyrolysis of the neat oil and fats hydrolysates resulted in similar chromatograms as the model compounds. Results of all four oils and fats tested show that decarboxylation is the first step during thermal treatments. All four chromatograms (Figures 4.47-4.51) show substantial n-heptadecane ( $C_{17}$ ) peaks as would be expected from the decarboxylation of stearic acid. The oils and fats also contain substantial amounts of n-pentadecane ( $C_{15}$ ), indicating the decarboxylation of the palmitic acid present in the beef tallow is also occurring. The n-pentadecane peak is actually larger than the n-heptadecane peak in the tallow samples because there is more  $C_{16:0}$  (palmitic acid) present in the original oil (Table 3.2) compared to stearic acid and because this peak would also represent n-pentadecane from thermal cracking of the n-heptadecane. As expected, canola oil, which contains lesser amounts of  $C_{16:0}$  also has substantially less n-pentadecane in the reaction products.

The n-alkane series from  $C_{17}$  upwards in the pyrolysis products from the oil and fat hydrolysates are clearly evident. The alkene series is not as clear as there are numerous peaks in between the n-alkanes, but GC/MS analysis has confirmed their presence as well as the presence of a secondary alkene peak preceding the n-alkane peak (Figure 4.56). Because the feed is a mixture of unsaturated and saturated fatty acids, it would be expected that the cracking behavior be a combination of the cracking patterns observed in the model studied. It has already been shown that a prominent n-alkane series is formed, which is mainly due to the cracking of  $C_{17}$  and  $C_{15}$  n-alkanes resulting from the decarboxylation of the stearic and palmitic acids. As well there appears to be large amounts of  $C_7$ - $C_9$  n-alkanes, more than that observed during the model cracking of stearic

acid at similar conditions. The cracking of model oleic acid showed that the n-alkane/alkene series was most prominent at C<sub>7</sub>-C<sub>9</sub> likely due to cracking at the unsaturation in the chain. The higher amounts of C<sub>7</sub>-C<sub>9</sub> n-alkanes in the oil and fat pyrolysis products would make sense, as these peaks would represent the addition of the C<sub>7</sub>-C<sub>9</sub> n-alkanes from both the saturated and unsaturated fatty acids. The numerous peaks in between the n-alkane/alkene series were also observed in the cracking of the oleic acid and are likely due to the cracking of the unsaturated fatty acids. GC/MS analysis indicated that these are isomers or branched hydrocarbons. As well, the fact that many of these compounds can be in *-cis* or *-trans* formation also increases the number of possible products. As described previously, the presence of branched products has also been observed in hydrocarbon cracking (Khorasheh and Gray, 1993; Wu et al., 1996).

Although the oil and fat pyrolysates showed similar or predictable cracking patterns, the product yields from the canola oil pyrolysis appeared to be much higher than the tallow pyrolysates. This is clear when Figures 4.52 and 4.54 and are compared to Figure 4.51. It would be expected that the canola oil would exhibit different cracking behavior than the tallows due to increase amount of unsaturation, but the substantial increase in canola oil pyrolysates yield was unexpected. The main differences between the tallow and oil feeds were the quality and the viscosity. The canola oil was a high quality, refined, food grade oil, that had been subjected to numerous processing steps to remove impurities. The tallows were lower quality materials. It is possible that they contained some contaminants that were not discovered during the initial compositional analysis or the analysis of the hydrolysates and that may have affected the pyrolysis. As well, tallow is

solid at room temperature and after the hydrolysis reactions, when the glycerol and water layer was allowed to separate from the lipid layer, the lipid layer quickly solidified. It is possible that water or glycerol that had not yet separated from the fat, became trapped within the solidified fat molecules. No additional extraction steps (i.e. hexane extraction) were conducted on the lipid hydrolysate layer. The analytical methods used to determine the composition of the hydrolysates (GC-FID and TLC-FID) would not have detected either glycerol or water. The tallow hydrolysates did not appear to be significantly different in terms of product distribution, so if there were additional contaminants, glycerol or water present in the reactor during pyrolysis, they did not change the types of products but only affected the rates of the reaction. In other words, they inhibited the reaction. In the crude oil industry, there is research devoted to removing naphthenic acids from crude oils because they can cause corrosion and are highly viscous, which cause difficulties in pipeline transfer (Blum et al., 1998). One method used to breakdown the naphthenic acids is thermal (Blum et al., 1998) or catalytic (Zhang et al., 2006) decomposition. It is clear that water, especially in the presence of CO<sub>2</sub>, inhibits the decomposition of naphthenic acid and must be continually removed during the process as described by Blum et al., however; the mechanism behind this inhibition is not explained.

The focus of this process was on the lipid fraction and not the glycerol. It was noted in Chapter 2 how an increased supply of glycerol from biodiesel production has caused a decrease in value. This is a concern for this thesis work as glycerol is also a bi-product that would likely have to be sold for a profit for feasibility of project economics.

Although economics were not discussed in this thesis, they will become very important

as the project progresses. One advantage of the glycerol from this process is that it does not contain traces of methanol as does the glycerin from biodiesel production. This could offer a market advantage where high quality glycerine is required.

## CHAPTER 6: CONCLUSIONS AND RECOMMENDATIONS

The main objective of this work was to collect fundamental information regarding hydrolysis and pyrolysis of lipid feeds. The major conclusions of this work are listed below:

- Decarboxylation was the initial reaction during thermal treatment of free fatty acids resulting in the formation of n-heptadecane as the primary reaction product. Subsequent thermal cracking resulted in a hydrocarbon mixture with prominent n-alkane and alkene series, which closely followed hydrocarbon cracking theory published in literature.
- Stearic acid pyrolysis products were substantially affected by time and temperature. Mild conditions (low temperature, short time) resulted in little to no formation of the n-alkane and alkene series but substantial formation of n-heptadecane. As the severity of conditions increased, conversion increased, the hydrocarbon series increased in intensity and shifted toward production of lower carbon number compounds, aromatic compounds began to form, and some formation of toluene insoluble black particulates was evident. At the most severe conditions, the series were completely degenerated and there was substantial gas and formation of black particulates.
- Pyrolysis of an unsaturated model compound (oleic acid) showed that decarboxylation was the initial reaction step resulting in the formation of n-heptadecene. The product profile differed from that of stearic acid. The product

profile indicated that cracking at the double bond in n-heptadecene was a major reaction and more minor compounds, likely cyclic or branched compounds, were formed.

- The optimal conditions to maximize the products of interest appear to be 410° C (1-8 h) and 430 °C (<1 h).
- Hydrolysis of canola oil, bleached fancy tallow, yellow grease tallow, and poultry tallow into free fatty acids and subsequent pyrolysis resulted in a product mixture that contained a series of n-alkanes and alkenes. The products were consistent with pyrolysis products from both the unsaturated (oleic acid) and saturated (stearic acid) model compounds.
- The results of this work show that production of liquid hydrocarbons through pyrolysis of free fatty acids hydrolyzed from lipid feeds is technically feasible.

Although the science behind the proposed novel process has been proven, there are still experiments that could be conducted to compliment the results of this work and explore some of the findings in more detail. As well, the next step would likely involve scale up. Below is a list of suggested experiments that could be conducted as well as considerations for future design and scale-up of the process.

### **1. Optimization of the hydrolysis reaction and determination of hydrolysis selectivity**

Optimization of the hydrolysis reaction was beyond the scope of this work. The conditions chosen were based on literature and analysis of the hydrolysates indicated nearly complete conversion into the free fatty acids needed for these experiments. Long term feasibility of the process would likely require optimization of this energy intensive process. It is possible that lower pressure, shorter reaction times, and the addition of an acid catalyst could aid in reducing process costs. During process scale-up the batch reactors will likely be replaced with a continuous reactor with a recycle stream, which would further improve process efficiency. An important consideration with the addition of the recycle stream would be to ensure that the composition of this stream is the same as the composition of the feed to ensure process consistency. This would mean that there would have to be little or no selectivity during the hydrolysis step. Because complete conversion from triglycerides into fatty acids was achieved in this work, it was difficult to assess whether or not there was any selectivity for certain fatty acids during the hydrolysis step. To determine this, it would be necessary to study the composition of the hydrolysates at various time points during the hydrolysis reaction (i.e. at different conversions) and calculate the rates of conversion of the different fatty acids.

## **2. Scale-up to a continuous flow reaction system**

In this work, small scale batch reactors were used. These reactors were chosen because they were inexpensive, easy to use, and provided accurate information,



especially regarding reaction products, in relatively quick periods of time. The next step in development of this process would be scale-up. This would likely involve switching to a continuous flow reactor, which are generally more feasible in large scale processes as they allow for continuous removal of the desired products. Future work will include designing a more efficient reactor possibly by the addition of the recycle streams and heat exchangers. Based on the results of this work, the ideal temperature range for obtaining a liquid product with high hydrocarbon yields would be between 410-430 °C at times greater than 1 hr. If shorter residence times are desired, higher temperatures must be employed. This may be possible; however, the formation of both coke and aromatics would have to be considered at higher temperatures.

**3. In-depth time/temperature study of oleic acid (unsaturated model compound) and model mixtures of unsaturated and saturated model compound.**

The results of the oleic acid (unsaturated) pyrolysis showed a very different cracking pattern compared to that of stearic acid (saturated). It would be interesting to conduct a more comprehensive study evaluating at the influence of time and temperature on oleic acid pyrolysis products as well as experimenting with model mixtures of oleic and stearic acid. This would allow for more accurate prediction of products from neat oils and fats, which contain complex mixtures of both saturated and unsaturated fatty acids.

#### **4. In-depth study on increased pressure**

Although pressure was not studied in depth and the pressure used was not substantially high, literature suggests that pressure can influence the reaction products, namely the n-alkane to alkene ratio. If n-alkane products are desired, then pressure might be a variable worth exploring.

#### **5. Quantification of the CO<sub>2</sub> produced**

With the new regulations on CO<sub>2</sub> emissions and potential carbon credits, it would be vital to determine the amount of CO<sub>2</sub> produced by this process. Although in a full life cycle analysis of this process CO<sub>2</sub> production would be off-set by the CO<sub>2</sub> used during the growth of the plant or animal, it is still an important environmental concern that must be addressed.

#### **6. Development of downstream separation**

In future stages of this work, it will be necessary to separate the products. Options may include column distillation or fractionation. Separation of hydrocarbons is well known in petroleum processing but the first step would be identifying the products or fractions of interest.

## CHAPTER 7: REFERENCES

- Adebanjo, A.O., Dalai, A.K., Bakhishi, N.N., 2005. Production of Diesel Like Fuel and Other Value-Added Chemicals from the Pyrolysis of Animal Fat. *Energy Fuels* 19, 1735-1741.
- Anozie, A.N., Dzobo, J.M. 2006. Kinetics of the hydrolysis of palm oil and kernel oil. *Ind. Eng. Chem. Res.* 45, 1604-1612.
- Agra, I. B., Warnijati, S. and Pratama, M. S., 1992. Catalytic Pyrolysis of Nyamplung Seeds Oil to Mineral Oil Like Fuel. *Renewable Energy: Technology and the Environment: Proceedings of the 2nd World Energy Congress*, Reading, UK.
- Alencar, J. W., Alves, P. B. and Craveiro, A. A., 1983. Pyrolysis of Tropical Vegetable-Oils. *J. Agric. Food Chem.* 31 (6), 1268-1270.
- Ali, Y. and Hanna, M. A., 1994. Alternative Diesel Fuels from Vegetable-Oils. *Bioresour. Technol.* 50 (2), 153-163.
- ASTM, 2006. Standard Specification for Diesel Fuel Oils. Designation: D 975-04c. Annual Book of ASTM Standards, 05.01:363-381. ASTM, Philadelphia, PA.
- ASTM, 2005. Standard Specification for Automotive Spark-Ignition Engine Fuel. Designation: D 4814-04a. Annual Book of ASTM Standards, 05.02:833-855. ASTM, Philadelphia, PA.
- ASTM, 2005. Standard Specification for Biodiesel Fuel Blend Stock (B100) for Middle Distillate Fuels. Designation: D 6751-03a. Annual Book of ASTM Standards, 05.04:609-614. ASTM, Philadelphia, PA.
- Bahadur, N. P., 1994. Liquid hydrocarbons from catalytic pyrolysis of sewage sludge lipid and canola oil: Evaluation of fuel properties. M.A.Sc. Thesis, Department of Chemical Engineering, University of Toronto, Toronto, Canada.
- Bahadur, N. P., Boocock, D. G. B., Konar, S. K., 1995. Liquid Hydrocarbons from Catalytic Pyrolysis of Sewage-Sludge Lipid and Canola Oil - Evaluation of Fuel Properties. *Energy Fuels* 9 (2), 248-256.
- Billaud, F., Guitard, Y., Minh, A. K. T., Zahraa, O., Lozano, P., Pioch, D., 2003. Kinetic studies of catalytic cracking of octanoic acid. *J. Mol. Catal. A-Chem.* 192 (1-2), 281-288.
- Billaud, F., Minh, A. K. T., Lozano, P., Pioch, D., 2001. Catalytic cracking of octanoic acid. *J. Anal. Appl. Pyrolysis* 58, 605-616.
- Blouri, B., Hamdam, F., Herault, D. 1985. Mild hydrocracking of high molecular weight hydrocarbons. *Ind. Eng. Chem. Process Des. Dev.* 24, 30-37.
- Blum, S.C.; Olmstead, W.N.; Bearden, R. 1998. Thermal Decomposition of Naphthenic Acids. US Patent 5820750.
- Boerrigter, H., den Uil, H. and Calis, H. P., 2002. Green diesel from Biomass via Fischer-Tropsch synthesis: New Insights in Gas Cleaning and Process Design. *Pyrolysis and Gasification of Biomass and Waste, Expert Meeting, Strasborg France*. [Online]. Available: [http://www.senternovem.nl/mmfiles/28277\\_tcm24-124223.pdf](http://www.senternovem.nl/mmfiles/28277_tcm24-124223.pdf) [Visited Jan 7, 2006].
- Boocock, D. G. B., Konar, S. K., Leung, A., Ly, L. D., 1992a. Fuels and Chemicals from Sewage Sludge 1.

- The Solvent Extraction and Composition of a Lipid from a Raw Sewage Sludge. *Fuel* 71 (11), 1283-1289.
- Boocock, D. G. B., Konar, S. K., Mackay, A., Cheung, P. T. C., Liu, J., 1992b. Fuels and Chemicals from Sewage Sludge 2. The Production of Alkanes and Alkenes by the Pyrolysis of Triglycerides over Activated Alumina. *Fuel* 71 (11), 1291-1297.
- Bressler, D.C., Gray, M.R., 2003. Hydrotreating chemistry of model products from bioprocessing of carbazoles. *Energy Fuels*, 16, 1076-1086.
- Bridgwater, A. V., 2003. Renewable fuels and chemicals by thermal processing of biomass. *Chem. Eng. J.* 91 (2-3), 87-102.
- Bridgwater, A. V., Peacocke, G. V. C., 2000. Fast pyrolysis processes for biomass. *Renew. Sust. Energ. Rev.* 4 (1), 1-73.
- Brockman, R., Demmering, G. Kreutzer, U., Lindemann, M., Plachenka, J., Steinberner, U. 2005. Fatty Acids. Ullman's Encyclopedia of Chemical Technology 6<sup>th</sup> edition. (Online Edition). Published by Wiley-VCH Verlag GmbH & Co. KGaA.
- Brown, R. C., 2003. Biorenewable Resources Engineering New Products From Agriculture, first ed. Iowa State Press, Ames.
- Campbell, I. M., 1983. Biomass, Catalysts and Liquid Fuels. Holt, Rinehart and Winston, London.
- CANMET Energy Technology Center, National Resources Canada, 2004. Super Cetane Technology. [Online]. Available: [http://www.nrcan.gc.ca/es/etb/cetc/cetc01/html/docs/factsheet\\_supercetane\\_e.html](http://www.nrcan.gc.ca/es/etb/cetc/cetc01/html/docs/factsheet_supercetane_e.html) [visited May 10, 2004].
- Chang, C. C., Wan, S. W., 1947. Chinas Motor Fuels from Tung Oil. *Ind. Eng. Chem.* 39 (12), 1543-1548.
- Chantal, P., Kaliaguine, S., Grandmaison, J. L., Mahay, A., 1984. Production of Hydrocarbons from Aspen Poplar Pyrolytic Oils over H-ZSM5. *Appl. Catal. A* 10 (3), 317-332.
- Cheng, Z. Y., Xing, J., Li, S. Y., Li, L., 2004. Thermodynamics calculation of the pyrolysis of vegetable oils. *Energy Sources* 26 (9), 849-856.
- Chow, P. W., 1993. Production of Synthetic Crude Petroleum. United States Patent 5,233,109.
- Craig, W., 1991. Production of hydrocarbons with a relatively high cetane rating. United States Patent 4,992,605.
- Craig, W., Coxworth, E., 1987. Conversion of vegetable oils to conventional liquid fuel extenders In: Granger, C. (Ed.), Proc. Sixth Can. Bioenergy R&D Seminar, Richmond, Canada, pp. 407-411.
- Craig, W., Soveran, D., 1993. Production of hydrocarbons with a relatively high cetane rating. Canadian Patent 1,313,200.
- Crossley, A., Heyes, T. D., Hudson, B. J. F., 1962. Effect of Heat on Pure Triglycerides. *JAOCS* 39 (1), 9-14.
- Czernik, S., Bridgwater, A. V., 2004. Overview of applications of biomass fast pyrolysis oil. *Energy Fuels* 18 (2), 590-598.
- da Rocha Filho, G. N., Bentes, M. H. S., Brodzki, D., Djega-Mariadassou, G., 1992. Catalytic Conversion

- of *Hevea brasiliensis* and *Virola sebifera* Oils to Hydrocarbons Oils. *JAOCS* 69 (3), 266-271.
- da Rocha Filho, G. N., Brodzki, D., Djega-Mariadassou, G., 1993. Formation of alkanes, alkylcycloalkanes and alkylbenzenes during the catalytic hydrocracking of vegetable oils. *Fuel* 72 (4), 543-549.
- Dandik, L., Aksoy, H. A., 1998a. Converting Used Oil to Fuel and Chemical Feedstock Through a Fractionating Pyrolysis Reactor. In: Kaseoglu, S.S, Rhee, K.C., Wilson, R.F. (Eds.), Proceedings of the World Conference on Oilseed and Edible Oil Processing, Istanbul, Turkey.
- Dandik, L., Aksoy, H. A., 1998b. Pyrolysis of used sunflower oil in the presence of sodium carbonate by using fractionating pyrolysis reactor. *Fuel Process. Technol.* 57 (2), 81-92.
- Dandik, L., Aksoy, H. A., Erdem-Senatar, A., 1998. Catalytic conversion of used oil to hydrocarbon fuels in a fractionating pyrolysis reactor. *Energy Fuels* 12 (6), 1148-1152.
- Dandik, L., Aksoy, H. A., 1999. Effect of catalyst on the pyrolysis of used oil carried out in a fractionating pyrolysis reactor. *Renew. Energy*, 16 (1-4), 1007-1010.
- Demirbas, A., 2002. Diesel fuel from vegetable oil via transesterification and soap pyrolysis. *Energy Sources* 24 (9), 835-841.
- Demirbas, A., 2003a. Biodiesel fuels from vegetable oils via catalytic and non-catalytic supercritical alcohol transesterifications and other methods: a survey. *Energy Conv. Manag.* 44 (13), 2093-2109.
- Demirbas, A., 2003b. Current advances in alternative motor fuels. *Energy Explor. Exploit.* 21 (5-6), 475-487.
- Dos Anjos, J. R. S., Gonzalez, W. D., Lam, Y. L., Frety, R., 1983. Catalytic Decomposition of Vegetable Oil. *Appl. Catal. A* 5 (3), 299-308.
- Egloff, G., Morrell, J. C., 1932. The cracking of cottonseed oil. *Ind. Eng. Chem.* 24, 1426-1427.
- Egloff, G., Nelson, E. F., 1933. Cracking Alaskan fur-seal oil. *Ind. Eng. Chem.* 25, 386-387.
- Elliot, D. C., 2004. Biomass, Chemicals from. Elsevier Inc., San Diego, CA.
- Elliot, J.R.; Lira, C.T., 1999. Introductory Chemical Engineering Thermodynamics. Prentice Hall PTR, Upper Saddle River, NY.
- Evans, R. J., Milne, T., 1988. Molecular-Beam, Mass-Spectrometric Studies of Wood Vapor and Model Compounds over an H<sub>2</sub>Sm-5 Catalyst. In: Soltes, E.J., Milne, T.A. (Eds.), ACS Symposium Series 376, 311-327.
- Fabuss, B.M., Smith, J.O., Lait, R.I., Borsanyi, A.S., Satterfield, C.N. 1962. Rapid thermal cracking of n-hexadecane at elevated pressures. *Ind. Eng. Chem. Process Des. Dev.* 1, 293-299.
- Fabuss, B.M., Smith, Satterfield, C.N. 1964. Thermal cracking of pure saturated hydrocarbons. *Adv. Pet. Chem. Ref.* 9, 157-201.
- Feng, Y., Wong, A., Monnier, J., 1993. Chemical composition of tall oil based cetane enhancer for diesel fuels. In: Kyritsis, S. (Ed.), Proceedings: first biomass conference of America, Sevilla, Spain, pp. 863-875.
- Ford, T.J. 1986. Liquid phase thermal decomposition of hexadecane: reaction mechanisms. *Ind. Eng. Chem. Fundam.* 25, 240-243.

- Fortes, I. C. P., Baugh, P. J., 1994. Study of Calcium Soap Pyrolysates Derived from Macauba Fruit (*Acrocomia Sclerocarpa M.*) - Derivatization and Analysis by GC/MS and CI-Ms. *J. Anal. Appl. Pyrolysis* 29 (2), 153-167.
- Fortes, I. C. P., Baugh, P. J., 1999. Study of analytical on-line pyrolysis of oils from Macauba fruit (*Acrocomia sclerocarpa M.*) via GC/MS. *J. Braz. Chem. Soc.* 10 (6), 469-477.
- Fortes, I. C. P., Baugh, P. J., 2004. Pyrolysis-GC/MS studies of vegetable oils from Macauba fruit. *J. Anal. Appl. Pyrolysis* 72 (1), 103-111.
- Graboski, M. S., McCormick, R. L., 1998. Combustion of fat and vegetable oil derived fuels in diesel engines. *Prog. Energy Combust. Sci.* 24 (2), 125-164.
- Gray, M R. 2002. Hydrocarbon properties and processing (ChE 522 course notes), University of Alberta, Edmonton AB. Pg. 4-6.
- Greensfelder, B. S., Voge, H. H., Good, G. M., 1949. Catalytic and Thermal Cracking of Pure Hydrocarbons - Mechanisms of Reaction. *Ind. Eng. Chem.* 41 (11), 2573-2584.
- Gusmao, J., Brodzki, D., Djega-Mariadassou, G., Frety, R., 1989. Utilization of vegetable oils as an alternative source for diesel-type fuel: hydrocracking on reduced Ni/SiO<sub>2</sub> and sulphided Ni-Mo/□-Al<sub>2</sub>O<sub>3</sub>. *Catal. Today* 5, 533-544.
- Hartman, L. 1953. Effect of temperature on the Twitchell fat splitting process and its catalysts. I 30 (9), 349-350.
- Higman, E. B., Schmeltz, I., Higman, H. C., Chortyk, O. T., 1973. Studies on Thermal Degradation of Naturally Occurring Materials 2. Products from Pyrolysis of Triglycerides at 400 Degrees. *J. Agric. Food Chem.* 21 (2), 202-204.
- Hochhauser, A. M., 2004. Gasoline and Other Motor Fuels. Kirk-Othmer Encyclopedia of Chemical Technology [Online Addition]. John Wiley & Sons, New York. [Online] Available: <http://www.mrw.interscience.wiley.com/login.ezproxy.library.ualberta.ca/kirk/articles/gasohoch.a01/frame.html> [visited October 20, 2005].
- Horne, P. A., Williams, P. T., 1994. Premium Quality Fuels and Chemicals from the Fluidized-Bed Pyrolysis of Biomass with Zeolite Catalyst Upgrading. *Renew. Energy* 5 (5-8), 810-812.
- Hsu, H. L., Osburn, J. O., Grove, C. S., 1950. Pyrolysis of the Calcium Salts of Fatty Acids. *Ind. Eng. Chem.* 42 (10), 2141-2145.
- Huber, G. W., Chheda, J. N., Barrett, C. J., Dumesic, J. A., 2005. Production of liquid alkanes by aqueous-phase processing of biomass-derived carbohydrates. *Science* 308 (5727), 1446-1450.
- Idem, R. O., Katikaneni, S. P. R., Bakhshi, N. N., 1996. Thermal cracking of Canola oil: Reaction products in the presence and absence of steam. *Energy Fuels* 10 (6), 1150-1162.
- Jaw, K. S., Hsu, C. K., Lee, J. S., 2001. The thermal decomposition behaviors of stearic acid, paraffin wax and polyvinyl butyral. *Thermochim. Acta* 367 165-168.
- Kanda, W.S., 2003. Quinoline conversion in the presence of Athabasca derived heavy oil fractions. University of Alberta M.Sc. Dissertation.
- Kann, J., Rang, H., Kriis, J., 2002. Advances in Biodiesel Research. *Proc. Estonian Acad. Sci. Chem.* 51 (2), 75-117.

- Karaosmanoglu, F., 1999. Vegetable oil fuels: A review. *Energy Sources* 21 (3), 221-231.
- Karaosmanoglu, F., Tetik, E., Gollu, E., 1999. Biofuel production using slow pyrolysis of the straw and stalk of the rapeseed plant. *Fuel Process. Technol.* 59 (1), 1-12.
- Katikaneni, S. P. R., Adjaye, J. D., Bakhshi, N. N., 1995a. Studies on the Catalytic Conversion of Canola Oil to Hydrocarbons - Influence of Hybrid Catalysts and Steam. *Energy Fuels* 9 (4), 599-609.
- Katikaneni, S. P. R., Adjaye, J. D., Bakhshi, N. N., 1995b. Catalytic Conversion of Canola Oil to Fuels and Chemicals over Various Cracking Catalysts. *Can. J. Chem. Eng.* 73 (4), 484-497.
- Katikaneni, S. P. R., Adjaye, J. D., Bakhshi, N. N., 1995c. Performance of Aluminophosphate Molecular-Sieve Catalysts for the Production of Hydrocarbons from Wood-Derived and Vegetable-Oils. *Energy Fuels* 9 (6), 1065-1078.
- Katikaneni, S. P. R., Adjaye, J. D., Idem, R. O., Bakhshi, N. N., 1996. Catalytic conversion of Canola oil over potassium-impregnated HZSM-5 catalysts: C-2-C-4 olefin production and model reaction studies. *Ind. Eng. Chem. Res.* 35 (10), 3332-3346.
- Kitamura, K., 1971. Studies of Pyrolysis of Triglycerides. *Bull. Chem. Soc. Jpn.* 44 (6), 1606-1609.
- Klass, D. L., 2004. Biomass for Renewable Energy and Fuels. In: Cleveland, C.J. (Eds.), *Encyclopedia of Energy*, Volume 1. Elsevier, San Diego, pp.193-212. [Online]. Available: <http://www.bera1.org/cyclopediaofEnergy.pdf> [Visited July 15, 2005].
- Knothe, G., Dunn, R., O., Bagby, M. O., 1997. Biodiesel: The Use of Vegetable Oils and Their Derivatives as Alternative Diesel Fuels, In: Saha B.C. (Eds.), *Fuels and Chemicals from Biomass*. American Chemical Society, Washinton D.C., pp.172-208.
- Knothe, G., Steidley, K.R. 2005. Lubricity of Components of Biodiesel and Petrodiesel. The Origin of Biodiesel Lubricity. *Energy Fuels* 19, 1192-1200.
- Knothe, G., Van Gerpen, J., Krahl, J. 2005. *The Biodiesel Handbook*. AOCS Press, Champaigne, Ill.
- Konar, S. K., Boocock, D. G. B., Mao, V., Liu, J. N., 1994. Fuels and Chemicals from Sewage-Sludge 3. Hydrocarbon Liquids from the Catalytic Pyrolysis of Sewage-Sludge Lipids over Activated Alumina. *Fuel* 73 (5), 642-646.
- Konwer, D., Taylor, S. E., Gordon, B. E., Otvos, J. W., Calvin, M., 1989. Liquid Fuels from Mesua-Ferrea L Seed Oil. *JAACS* 66 (2), 223-226.
- Korasheh, F., Gray, M.R. 1993. High-pressure thermal cracking of n-hexadecane. *Ind. Eng. Chem. Res.* 32, 1853-1863.
- Kossiakoff, A., Rice, F.O. 1943. Thermal decomposition of hydrocarbons, resonance stabilization and isomerization of free radicals. *J. Am. Chem. Soc.* 65, 590-595.
- Kubickova, I., Snare, M., Eranen, K., Maki-Arvela, P Murzin D.Y., 2005. Hydrocarbons for diesel fuel via decarboxylation of vegetable oils. *Catal. Today* 106, 197-200.
- Kulkarni, M.G., Dalai, A.K. 2006. Waste Cooking Oil – An Economical Source For Biodiesel: A Review. *Ind. Eng. Chem. Res.* 45, 2901-2913.
- Lascaray, L. 1949. Mechanism of fat splitting. *Ind. Eng. Chem.* 41 (4), 786-790.

- Leung, A., Boocock, D. G. B., Konar, S. K., 1995. Pathway for the Catalytic Conversion of Carboxylic-Acids to Hydrocarbons over Activated Alumina. *Energy Fuels* 9 (5), 913-920.
- Lima, D. G., Soares, V. C. D., Ribeiro, E. B., Carvalho, D. A., Cardoso, E. C. V., Rassi, F. C., Mundim, K. C., Rubim, J. C., Suarez, P. A. Z., 2004. Diesel-like fuel obtained by pyrolysis of vegetable oils. *J. Anal. Appl. Pyrolysis* 71 (2), 987-996.
- Lipinsky, E. S., Anson, D., Longanbach, J. R., Murphy, M., 1985. Thermochemical Applications for Fats and Oils. *JAOCS* 62 (5), 940-942.
- Liu, D. D. S., Monnier, J., Tourigny, G., Kriz, J., Hogan, E., Wong, A., 1998. Production of high quality cetane enhancer from depitched tall oil. *Pet. Sci. Technol.* 16 (5-6), 597-609.
- Ma, F. R., Hanna, M. A., 1999. Biodiesel production: a review. *Bioresour. Technol.* 70 (1), 1-15.
- Maki-Arvela, P., Kubickova, I., Snare, M., Eranen, K., Murzin D.Y., 2007. Catalytic deoxygenation of fatty acids and their derivatives. *Energy Fuels* 21, 30-41.
- McHardy, J.; Sawan, S.P. 1998. *Supercritical Fluid Cleaning - Fundamentals, Technology, and Applications*. William Andrew Publishing Norwich, NY. [Online]  
<http://www.knovel.com/login.ezproxy.library.ualberta.ca/knovel2/Toc.jsp?BookID=446&VerticalID=0>  
 [Visited September 25, 2007].
- McHugh, Mark A.; Krukonis, Val J. 1994. *Supercritical Fluid Extraction (2nd Edition)*. Elsevier Inc. San Diego, CA. [Online]  
<http://www.knovel.com/login.ezproxy.library.ualberta.ca/knovel2/Toc.jsp?BookID=447&VerticalID=0>  
 [Visited September 25, 2007].
- Merck Index: an encyclopedia of chemicals, drugs, and biologicals. 2006 (1y<sup>th</sup> ed.). Ed: O'Neil, Maryadele. Whitehouse Station, NJ.
- Megahed, O. A., Abdelmonem, N. M., Nabil, D. M., 2004. Thermal cracking of rapeseed oil as alternative fuel. *Energy Sources* 26 (11), 1033-1042.
- Milne, T. A., Evans, R. J., Nagle, N., 1990. Catalytic Conversion of Microalgae and Vegetable-Oils to Premium Gasoline, with Shape-Selective Zeolites. *Biomass* 21 (3), 219-232.
- Monnier, J., Tourigny, G., Soveran, D., 1994. Conversion of depitched tall oil to diesel fuel additive. Canadian Patent 2,149,685.
- Monnier, J., Tourigny, G., Soveran, D., Wong, A., Hogan, E. and Stumborg, M., 1998. Conversion of biomass feedstock to diesel fuel additive. United States Patent 5,705,722.
- Moquin, P.H.L, Temelli, F., Sovova, H., Saldana, M.D.A, 2006. Kinetic modeling of glycerolysis-hydrolysis of canola oil in supercritical carbon dioxide media using equilibrium data. *J. Supercrit. Fluids*, 37 (3), 417-424.
- National Biodiesel Board, 2005. Biodiesel Backgrounder Factsheet. [Online]. Available:  
[www.biodiesel.org/pdf\\_files/fuelfactsheets/backgrounder.pdf](http://www.biodiesel.org/pdf_files/fuelfactsheets/backgrounder.pdf) [Visited October 30, 2005].
- Nawar, W. W., 1969. Thermal Decomposition of Lipids – a Review. *J. Agr. Food Chem.* 17 (1), 18-21.
- Nichols, P. C., Holman, R. T., 1972. Pyrolysis of Saturated Triglycerides. *Lipids* 7 (12), 773-779.
- Niehaus, R. A., Goering, C. E., Savage, L. D., Sorenson, S. C., 1986. Cracked Soybean Oil as a Fuel for a Diesel-Engine. *Trans. ASAE* 29 (3), 683-689.



- Onay, O., Kockar, O. M., 2004. Fixed-bed pyrolysis of rapeseed (*Brassica napus L.*). *Biomass Bioenerg.* 26 (3), 289-299.
- Pahl, G. 2005. Biodiesel: Growing a New Energy Economy. Chelsea Green Publishing Company, White River, VT.
- Paster, M., Pellegrino, J. L., Carole, T. M., 2003. Industrial Bio-Products: Today and Tomorrow. [Online]. Available: <http://www.bioproducts-bioenergy.gov/pdfs/BioProductsOpportunitiesReportFinal.pdf> [Visited July 15, 2005]
- Pinto A.C, Guarieiro, L.L.N., Rezende, M.J.C., 2005. Biodiesel: An Overview. *J. Braz. Chem. Soc.* 16 (6B), 1313-1330.
- Poutsma, M.L. 2000. Fundamental reactions of free radicals relevant to pyrolysis reactions. *J. Anal. Appl. Pyrolysis* 54, 5-35.
- Prasad, Y. S., Bakhshi, N. N., Mathews, J. F., Eager, R. L., 1986a. Catalytic Conversion of Canola Oil to Fuels and Chemical Feedstocks 1. Effect of Process Conditions on the Performance of HZSM-5 Catalyst. *Can. J. Chem. Eng.* 64 (2), 278-284.
- Prasad, Y. S., Bakhshi, N. N., Mathews, J. F., Eager, R. L., 1986b. Catalytic Conversion of Canola Oil to Fuels and Chemical Feedstocks 2. Effect of Co-Feeding Steam on the Performance of HZSM-5 Catalyst. *Can. J. Chem. Eng.* 64 (2), 285-292.
- Rao, K. V. C., 1978. Production of hydrocarbons by the thermolysis of vegetable oils. United States Patent 4,102,938.
- Renz, M. 2005. Ketonization of carboxylic acids by decarboxylation: Mechanism and scope. *Eur. J. Org. Chem.* 6, 979-988.
- Rice, F.O., Herzfeld, K.F. 1934. The thermal decomposition of organic compounds from the standpoint of free radicals. IV. The mechanism of some chain reactions. *J. Am. Chem. Soc.* 55, 3035-3040.
- Richardson, S.M., Gray M.R., 1997. Enhancement of residue hydroprocessing catalysts by doping with alkali metals. *Energy Fuels*, 11, 1119-1126.
- Royal Dutch Shell Group, 1983. The Petroleum Handbook. Elsevier Science Publishing. New York.
- Sang, O. Y., Twaiq, F., Zakaria, R., Mohamed, A. R., Bhatia, S., 2003. Biofuel production from catalytic cracking of palm oil. *Energy Sources* 25 (9), 859-869.
- Sang, O. Y., Zakaria, R., Mohamed, A. R., Bhatia, S., 2004. Catalytic conversion of palm oil-based fatty acid mixture to liquid fuel. *Biomass Bioenerg.* 27 (5), 477-484.
- Savage, P.E. 2000. Mechanism and kinetic models for hydrocarbon pyrolysis. *J. Anal. Appl. Pyrolysis* 54, 109-126.
- Schuchardt, U., Sercheli, R. and Vargas, R. M., 1998. Transesterification of vegetable oils: a review. *J. Braz. Chem. Soc.* 9 (3), 199-210.
- Schwab, A. W., Dykstra, G. J., Selke, E., Sorenson, S. C. and Pryde, E. H., 1988. Diesel Fuel from Thermal-Decomposition of Soybean Oil. *JAACS* 65 (11), 1781-1786.
- Sedelies, R., Johannsbauer, W., Wozny, G., Jeromin, L., Dieckelm, G., Lindemann, M., Matrong, G. 1992.

- Process for the acid catalyzed cleavage of fatty acid glycerides and apparatus. US patent 5, 128, 070.
- Shay, E. G., 1993. Diesel Fuel from Vegetable-Oils - Status and Opportunities. *Biomass Bioenerg.* 4 (4), 227-242.
- Sheehan, J., Camobreco, V., Duffield, J., Graboski, M., Shapouri, H. 1998. Life Cycle Inventory of Biodiesel and Petroleum Diesel for use in an Urban Bus. Prepared for the U.S. Department of Energy's Office of Fuels Development and U.S. Department of Agriculture's Office of Energy by the National Renewable Energy Laboratory, Golden, CO. [Online]. Available: <http://www.nrel.gov/docs/legosti/fy98/24089.pdf> [Visited July 1, 2006]
- Sonntag, N. O. V., 1979. Structure and Composition of Fats and Oils. John Wiley & Sons Inc., New York.
- Srivastava, A., Prasad, R., 2000. Triglycerides-based diesel fuels. *Renew. Sust. Energ. Rev.* 4 (2), 111-133.
- Stumborg, M., Wong, A., Hogan, E., 1996. Hydroprocessed vegetable oils for diesel fuel improvement. *Bioresour. Technol.* 56, 13-18.
- Tanabe, K., Gray, M.R., , 1997. Role of fine solids in the coking of vacuum residues. *Energy Fuels*, 11, 1040-1043.
- Tat, M. E., Van Gerpen, J. H., 2000. The specific gravity of biodiesel and its blends with diesel fuel. *JAOCS* 77 (2), 115-119.
- Twaiq, F. A., Mohamed, A. R., Bhatia, S., 2003a. Liquid hydrocarbon fuels from palm oil by catalytic cracking over aluminosilicate mesoporous catalysts with various Si/Al ratios. *Microporous Mesoporous Mat.* 64 (1-3), 95-107.
- Twaiq, F. A., Zabidi, N. A. M., Bhatia, S., 1999. Catalytic conversion of palm oil to hydrocarbons: Performance of various zeolite catalysts. *Ind. Eng. Chem. Res.* 38 (9), 3230-3237.
- Twaiq, F. A., Zabidi, N. A. M., Mohamed, A. R., Bhatia, S., 2003b. Catalytic conversion of palm oil over mesoporous aluminosilicate MCM-41 for the production of liquid hydrocarbon fuels. *Fuel Process. Technol.* 84 (1-3), 105-120.
- Twaiq, F. A. A., Mohamad, A. R., Bhatia, S., 2004. Performance of composite catalysts in palm oil cracking for the production of liquid fuels and chemicals. *Fuel Process. Technol.* 85 (11), 1283-1300.
- Voge, H.H., Good, G.M. 1949. Thermal cracking of higher paraffins. *J. Am. Chem. Soc.* 71, 593-597.
- Vonghia, E., Boocock, D. G. B., Konar, S. K., Leung, A., 1995. Pathways for the Deoxygenation of Triglycerides to Aliphatic-Hydrocarbons over Activated Alumina. *Energy Fuels* 9 (6), 1090-1096.
- Watanabe, M., Tsukagoshi, M., Hirakoso, H., Adschiri, T., Arai, K. 2000. Kinetics and product distribution of n-hexadecane pyrolysis. *AIChE Journal* 46 (4), 843-856.
- Weisz, P. B., Haag, W. O., Rodewald, P. G., 1979. Catalytic Production of High-Grade Fuel (Gasoline) from Biomass Compounds by Shape-Selective Catalysis. *Science* 206 (4414), 57-58.
- Wu, G., Katsumura, Y., Matsuura, C., Ishigure, K. 1996. Comparison of liquid phase and gas phase pure thermal cracking of n-hexadecane. *Ind. Eng. Chem. Res.* 35, 4747-4754.

Zhang, A.; Ma, Q.; Wang, K.; Liu, A.; Shuler, P.; Tang, Y. 2006. Naphthenic acid removal from crude oil through catalytic decarboxylation on magnesium oxide. *Appl. Cat. A* 303(1), pp.103-109.

Yaman, S., 2004. Pyrolysis of biomass to produce fuels and chemical feedstocks. *Energy Conv. Manag.* 45 (5), 651-671.

Zaher, F. A. and Taman, A. R., 1993. Thermally Decomposed Cottonseed Oil as a Diesel-Engine Fuel. *Energy Sources* 15 (3), 499-504.

## APPENDIX A: ADDITIONAL TABLES AND FIGURES

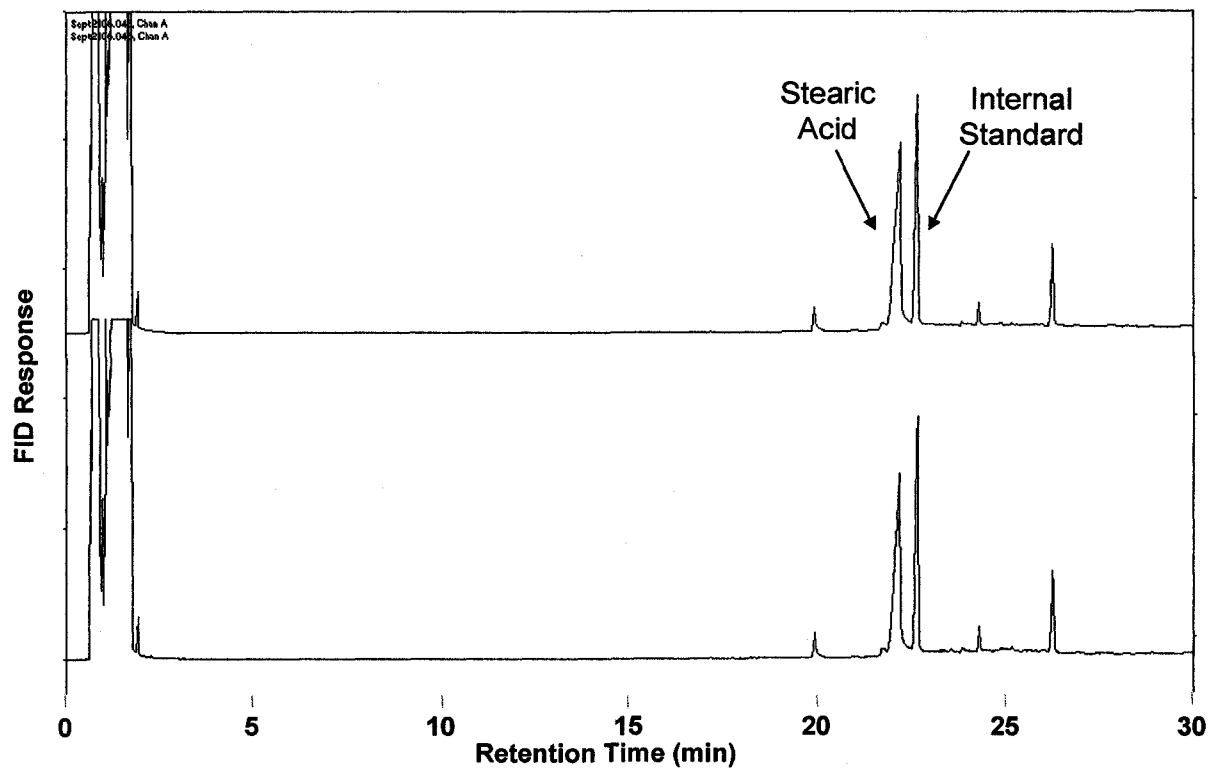


**Figure A.1** GC-FID chromatogram showing stearic acid with no thermal treatment

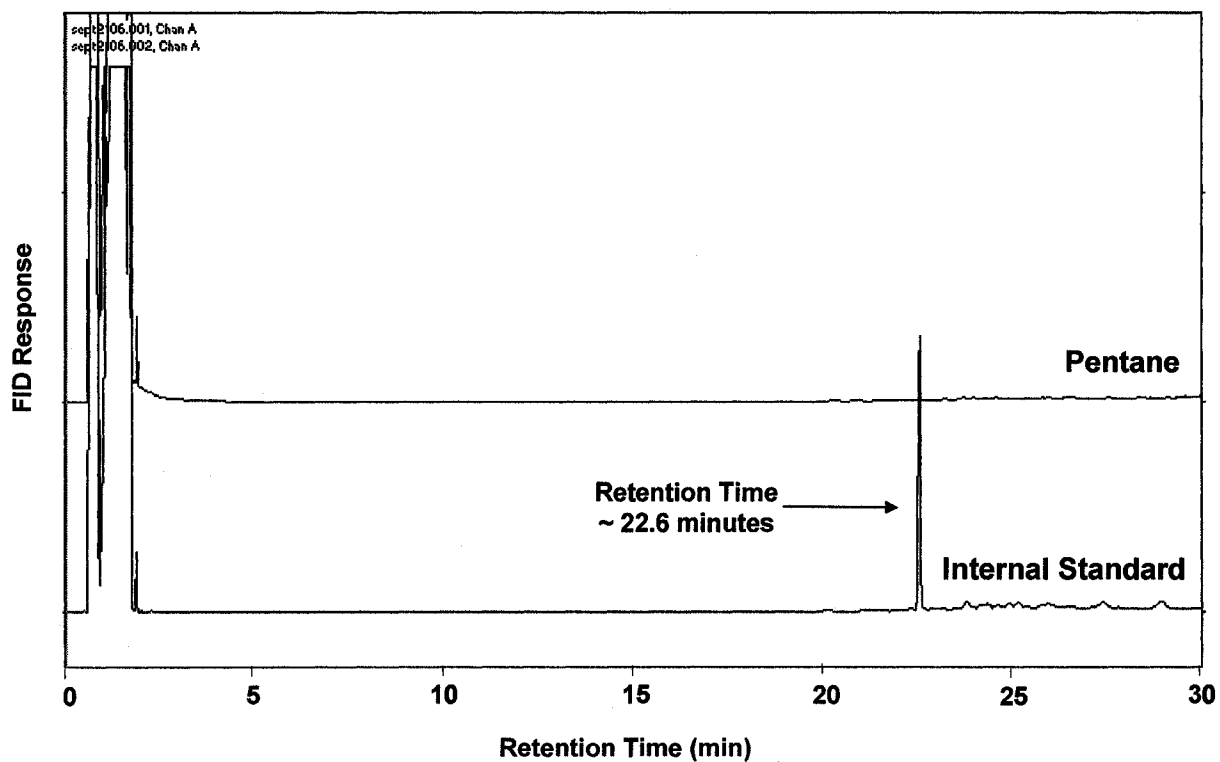


**Figure A.2** GC-FID Chromatogram showing the retention time of the primary internal standard used in this work, nonadecanoic acid methyl ester

Table A.1 n-Alkane/alkene molar ratio as a function of temperature and time for complete set of conditions

Reaction Conditions		Average Molar Ratio (mol <sub>n-alkane</sub> /mol <sub>alkene</sub> )																		
		Carbon No.																		
t (hr)	T (°C)	8	9	10	11	12	13	14	15	16	17	18	19	20	17	18	19	20		
4	350	-	-	-	-	-	-	-	5.4	2.5	4.9	-	-	-	-	-	-	-		
8	350	-	-	-	-	10.3	3.9	4.2	8.5	2.3	10.1	-	-	-	-	-	-	-		
1	370	-	-	-	-	-	-	-	-	0.6	15.5	-	-	-	-	-	-	-		
4	370	4.3	5.1	6.5	7.8	5.6	3.8	3.8	14.3	1.1	13.5	-	-	0.0	-	-	-	-		
8	370	5.7	6.3	5.8	7.4	6.2	4.1	4.4	9.1	1.9	13.9	5.3	5.2	0.9	-	-	-	-		
0.5	390	1.7	1.7	1.8	2.3	2.2	1.8	1.7	9.0	0.7	10.6	-	0.0	-	-	-	-	-		
1	390	2.6	2.7	2.8	3.6	3.0	2.5	2.5	6.2	1.3	11.3	-	-	0.9	-	-	-	-		
4	390	4.2	4.7	4.6	5.3	4.7	3.3	3.9	6.7	2.4	14.3	-	7.8	2.0	-	-	-	-		
8	390	5.7	6.4	7.0	7.5	5.0	4.7	6.1	8.9	4.0	37.1	-	7.9	2.0	-	-	-	-		
0.5	410	2.1	2.2	2.0	2.8	2.5	2.2	2.0	4.8	1.1	9.2	4.5	0.0	1.0	-	-	-	-		
1	410	3.1	3.4	3.0	4.1	3.3	3.0	3.3	6.4	1.9	12.4	2.2	5.1	1.6	-	-	-	-		
4	410	4.0	4.1	4.8	5.3	3.8	3.6	4.5	6.6	3.6	38.1	5.4	7.4	2.4	-	-	-	-		
8	410	4.7	4.7	6.4	6.3	4.0	4.5	5.4	8.2	4.3	44.2	3.5	6.2	6.4	-	-	-	-		
0.5	430	2.2	2.3	2.1	2.8	2.5	2.3	2.6	4.8	1.7	9.7	2.1	0.0	1.3	-	-	-	-		
1	430	2.5	2.6	2.5	3.1	2.7	2.5	2.9	5.0	1.9	18.0	4.4	5.6	2.2	-	-	-	-		
4	430	3.8	3.2	5.1	3.4	2.9	3.6	4.1	6.3	3.2	32.0	3.1	-	4.4	-	-	-	-		
8	430	4.3	2.7	7.4	4.8	2.3	2.4	3.4	-	1.7	21.2	-	-	4.4	-	-	-	-		
0.5	450	2.0	2.0	2.1	2.2	2.0	1.8	2.1	4.0	1.4	11.9	3.4	0.0	1.4	-	-	-	-		
1	450	0.2	2.6	3.3	2.6	2.3	2.1	2.8	4.7	1.7	17.8	-	-	-	-	-	-	-		
4	450	3.3	1.8	9.3	3.6	1.0	0.4	2.1	1.4	0.4	3.2	-	-	-	-	-	-	-		
8	450	0.9	1.6	-	3.4	0.8	1.8	1.7	0.8	0.2	2.9	-	-	-	-	-	-	-		
0.5	500	2.3	1.0	-	1.2	0.4	0.0	2.0	0.0	0.0	1.4	-	0.0	-	-	-	-	-		
1	500	1.4	-	-	0.0	0.0	0.0	2.3	0.0	0.0	1.6	-	-	-	-	-	-	-		
4	500	-	-	-	0.0	-	-	1.8	0.0	0.0	1.0	-	0.0	-	-	-	-	-		

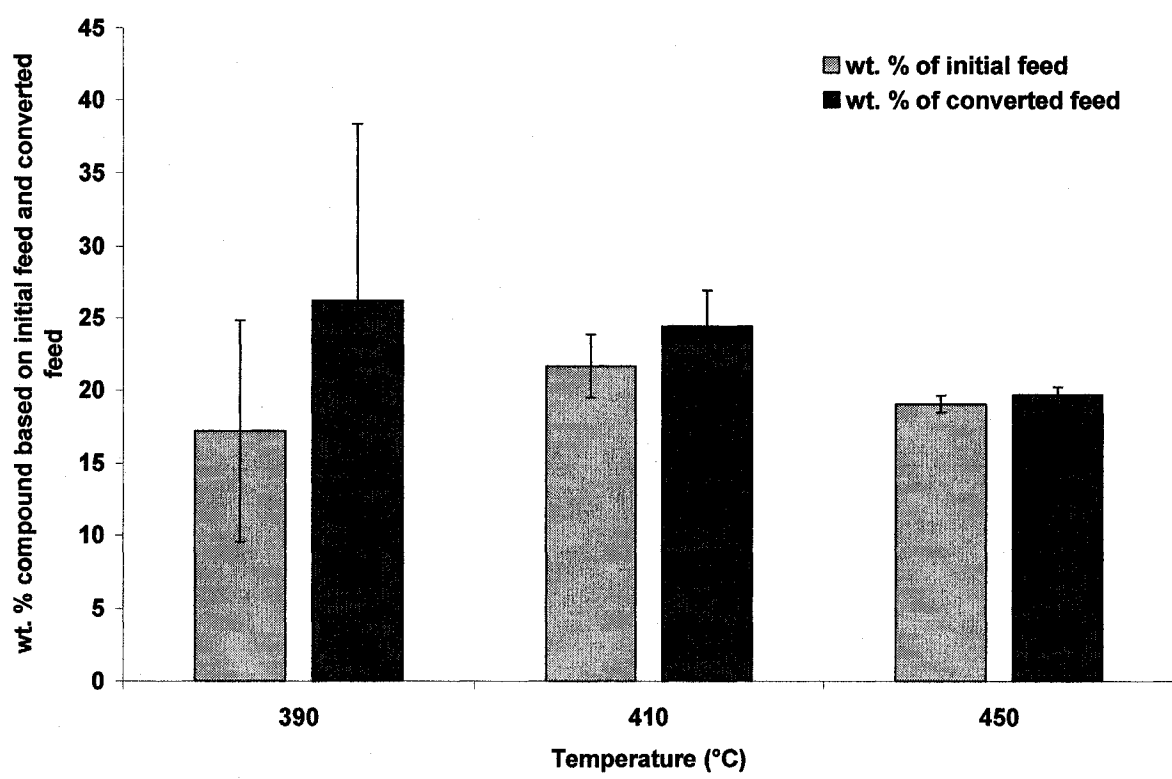


Figure A.3 Mass yield of C<sub>8</sub>-C<sub>20</sub> n-alkanes and alkenes based on converted feed

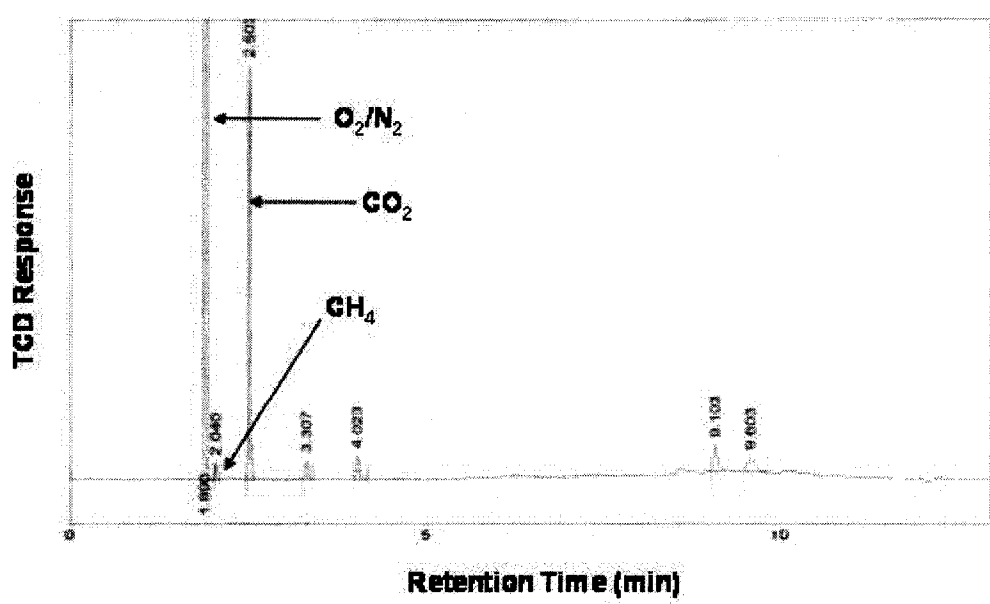


Figure A.4 GC-FID chromatograms showing the gas products from stearic acid pyrolysis at 390 °C after 1 hr

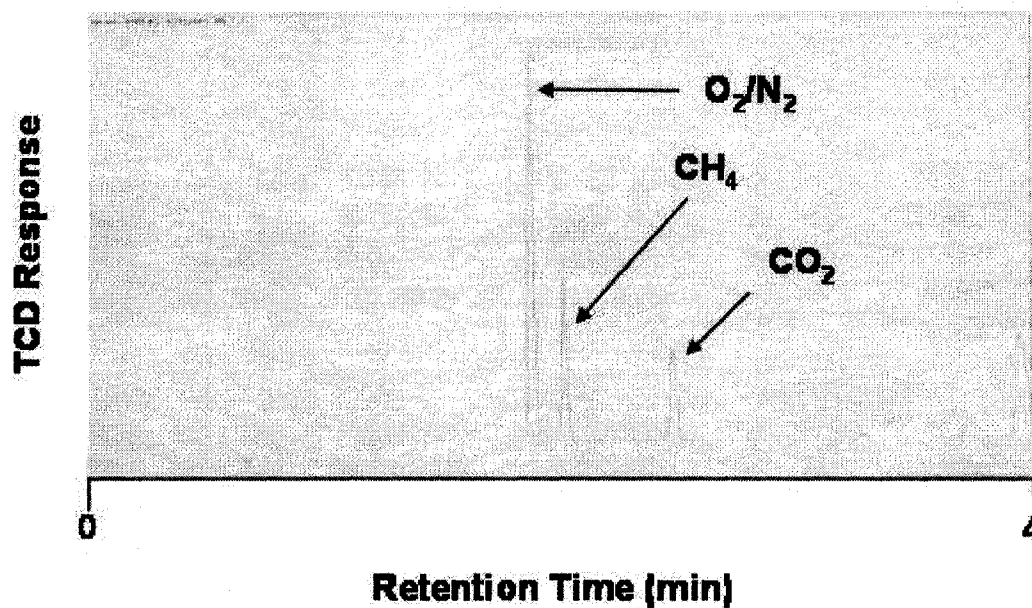
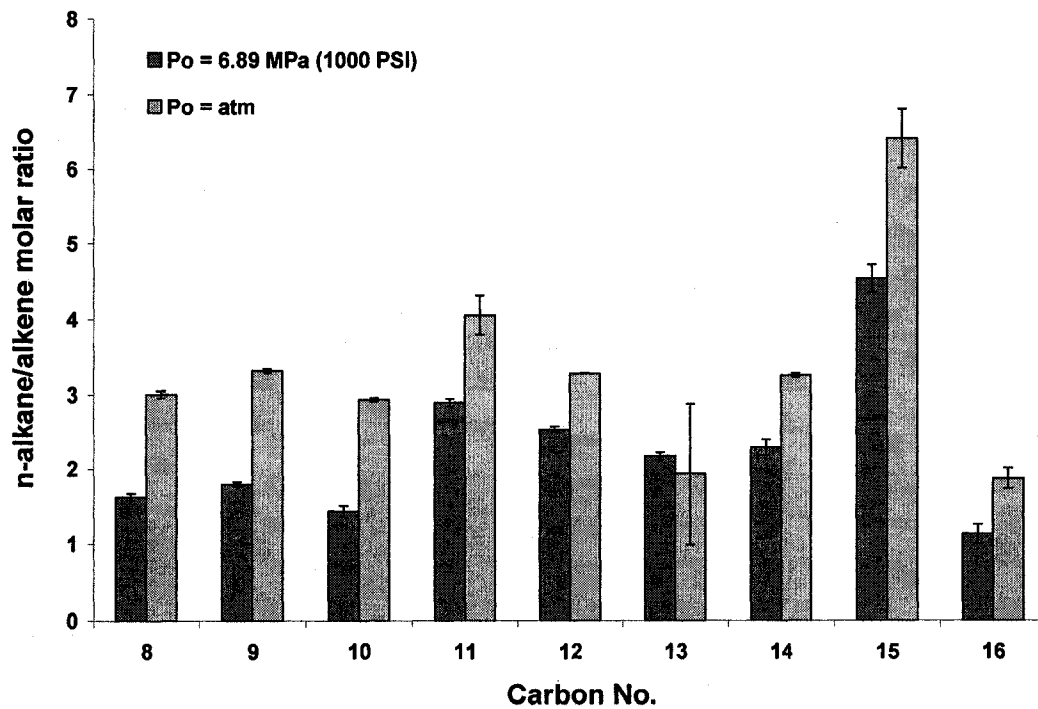
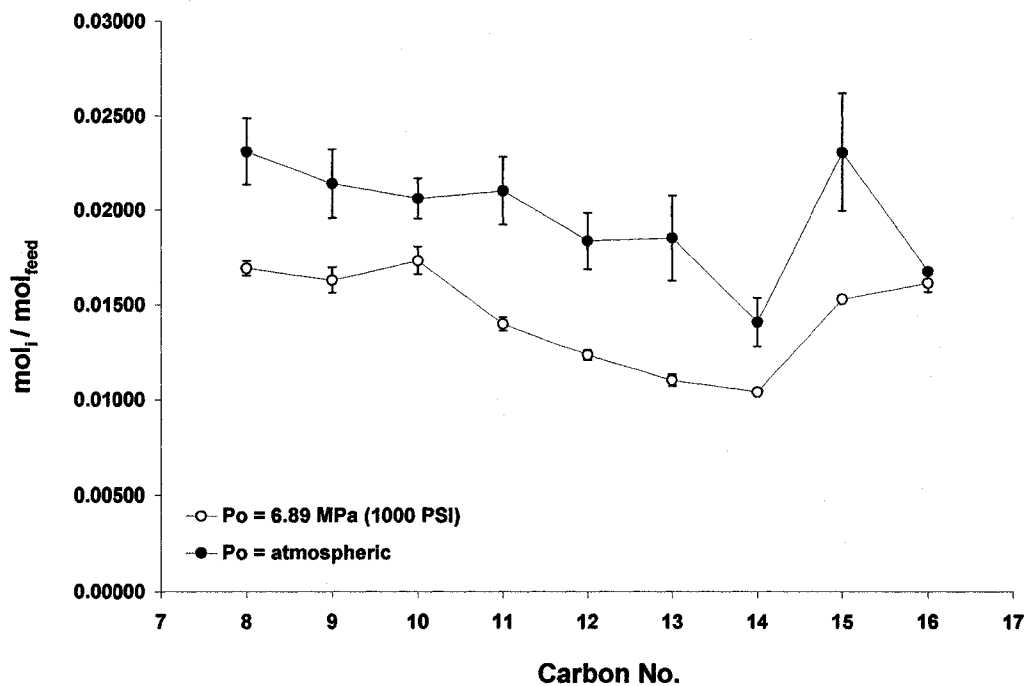


Figure A.5 GC-FID chromatogram showing the gas products from stearic acid pyrolysis at 500 °C after 30 min





**Figure A.6** n-Alkane/alkene molar ratios for 1 hr reactions conducted at 410 °C as a function of initial pressure



**Figure A.7** Alkane yeild for 1 hr reactions conducted at 410 °C as a function of initial pressure

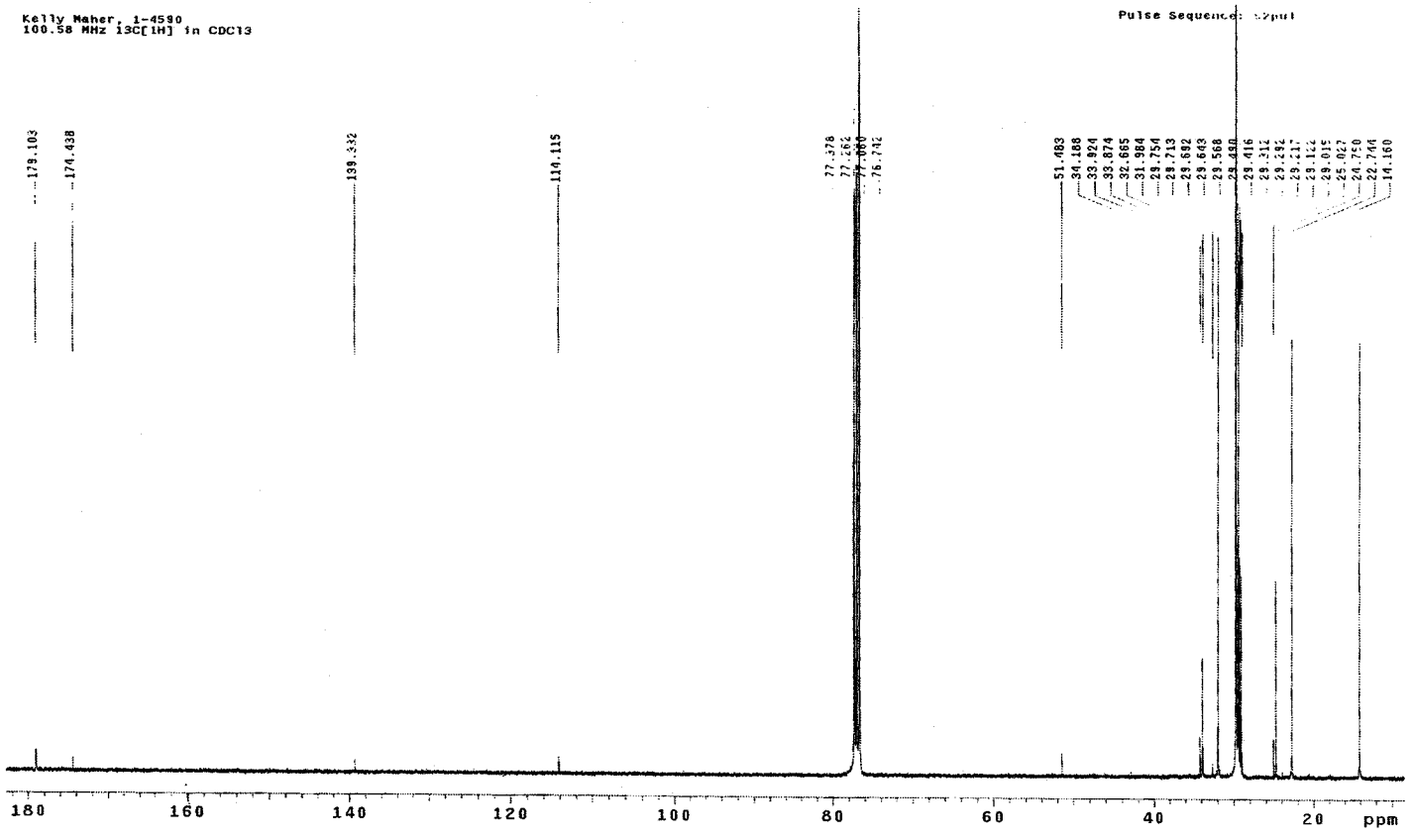


Figure A.8 C13 NMR scan of stearic acid pyrolysis products at 390 °C after 1 hr

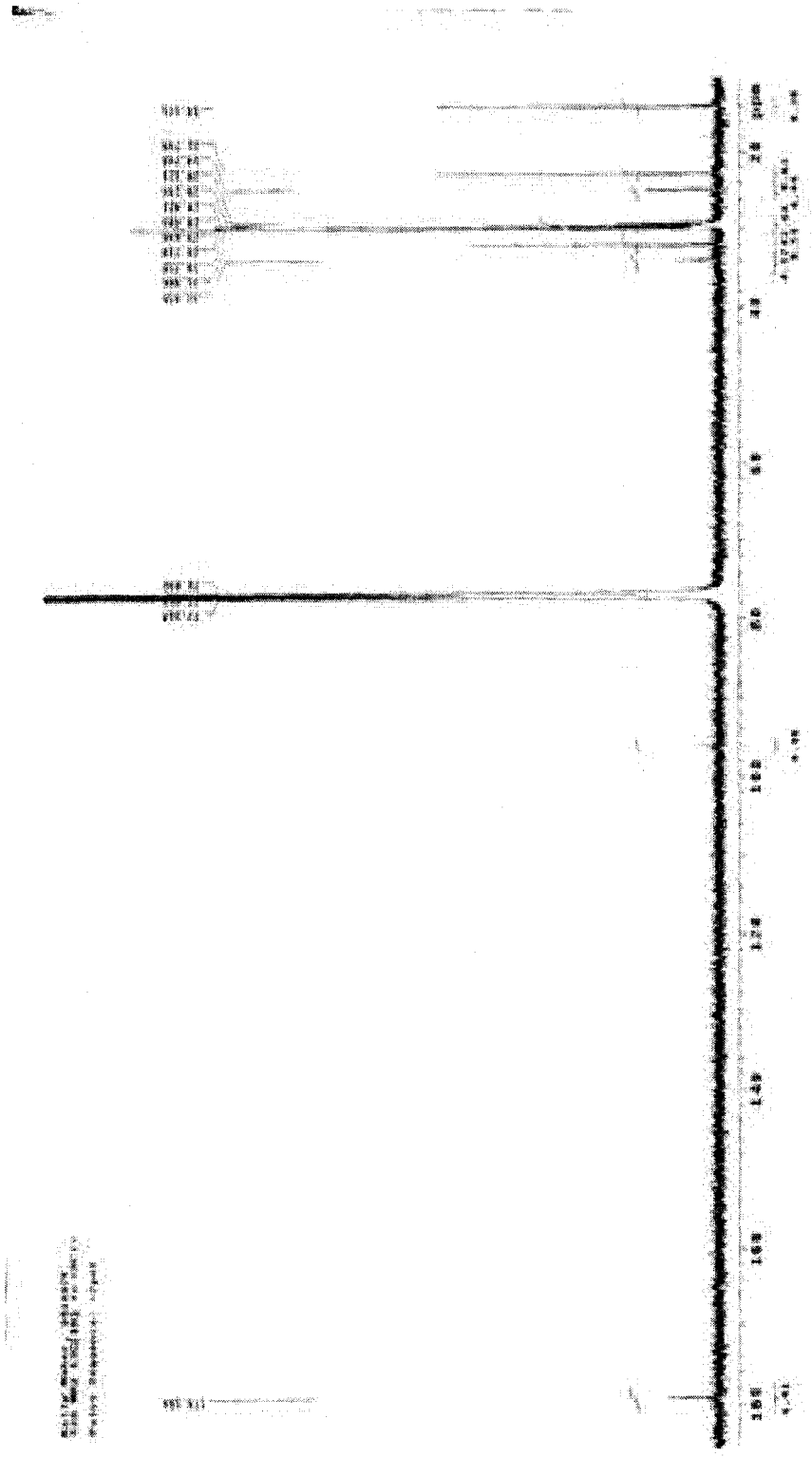


Figure A.9 C-13 NMR Scan of stearic acid pyrolysis products at 410 °C after 1 hr

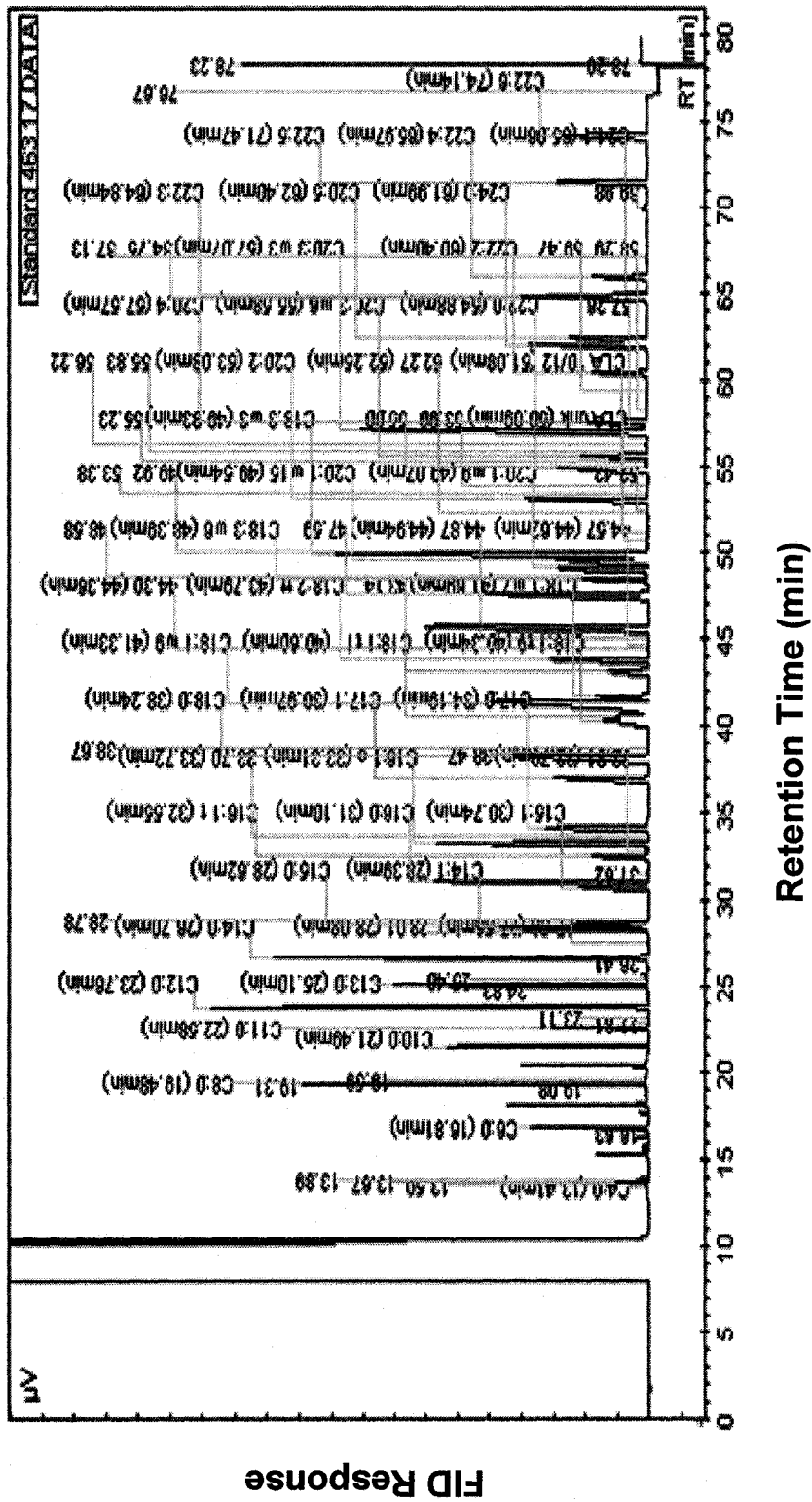
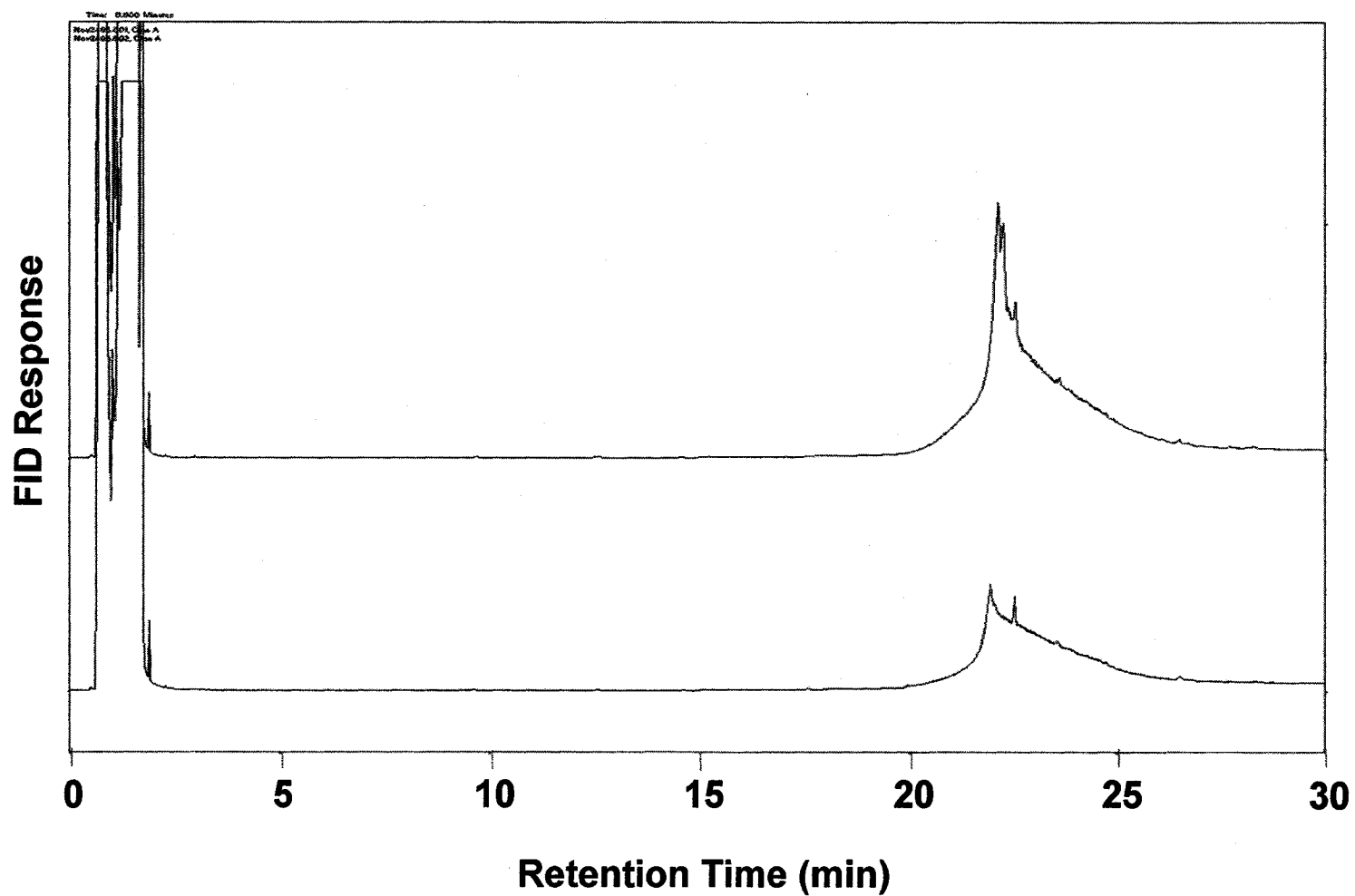
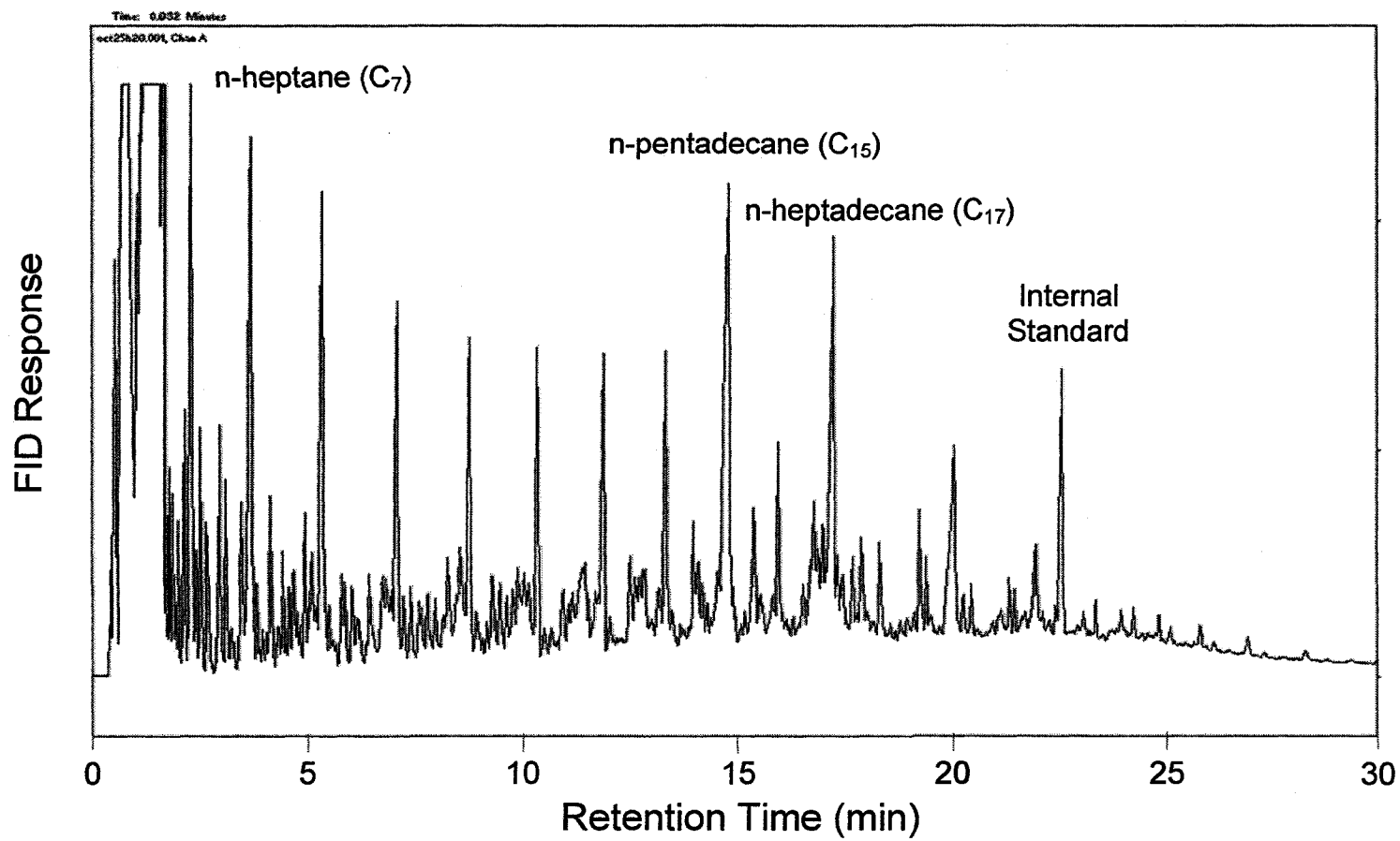


Figure A.10 GC-FID chromatogram showing the standard fatty acid curve. GC conditions were the same as sample conditions outlined in section 3.3.2.3.



**Figure A.11** GC-FID chromatogram showing bleached fancy tallow hydrolysates from a 1 hr reaction at 410 °C dissolved in pentane. Reactions were conducted in N<sub>2</sub> atmosphere and were initially at atmospheric pressure.



**Figure A.12** GC-FID chromatogram showing poultry tallow pyrolysis products from a 4 hr reaction at 410 °C after a water extraction step. Reaction was conducted in N<sub>2</sub> atmosphere and was initially at atmospheric pressure.

## APPENDIX B: SAMPLE CALCULATIONS

### B.1 Semi-quantitative calculation of mass and moles of specific compounds in the product extract

From the GC integration, peak areas were obtained for the product compounds and the internal standard of known concentration. A semi-quantitative approach was used to determine the mass of the product compound. Assuming a relative response factor of 1 for all compounds analyzed and a constant injection volume of 1  $\mu\text{l}$ , the following equation can be used:

$$m_i = \frac{A_i}{A_s} \times m_s \text{ ..... Equation B.1}$$

where  $m$  and  $A$  represent mass and peak area, respectively. The subscript  $i$  denotes the compound of interest and  $s$ , the internal standard. The mass of internal standard in the reactor,  $m_s$ , can be calculated as follows:

$$m_s = C_s \times V_{ext} \text{ ..... Equation B.2}$$

Where  $C_s$  is the concentration of the internal standard solution in mg/ml and  $V_{ext}$  is the volume of this solution used for extraction in ml. To determine the actual mass of

compound  $i$  per mg of feed (or the wt% of feed converted to compound  $i$ ) the following equation can be used:

$$\frac{m_i}{m_{feed}} = \frac{C_S \times V_{ext} \times A_i}{m_{feed} \times A_S} \dots\dots\dots \text{Equation B.3}$$

Equation B.3 can be converted from mass to moles using the following equation:

$$\frac{n_i}{n_{feed}} = \frac{C_S \times V_{ext} \times A_i \times M_i}{m_{feed} \times A_S \times M_{feed}} \dots\dots\dots \text{Equation B.4}$$

where  $M$  is the molar mass in g/mol for compound of interest,  $i$ .

### B.2 Calculation of n-alkane:alkene Ratio

The molar ratio of alkanes to alkenes were calculated for each carbon number as follows:

$$\text{alkane : alkene ratio} = \frac{n_{i \text{ alkane}}}{n_{i \text{ alkene}}} \dots\dots\dots \text{Equation B.5}$$

### B.3 Sample calculations

The data from two 1 hr reactions at 410 °C was used to calculate the mass and molar yields (Eqn.3 and 4) and molar ratios (Eqn. 5) for C<sub>8</sub>-C<sub>20</sub> alkanes and alkenes. Reaction data and sample calculations are outlined in Tables B.1-B.4.



**Table 0.1** Reaction data for duplicate 1 hr reactions at 410 °C

Reaction Conditions	Sample 060806A	Sample 060806B
Reaction Time	1 hr	1 hr
Reaction Temperature	410 °C	410 °C
Reaction Date	8-Jun-06	8-Jun-06
Concentration of internal standard solution, $C_s$	0.518 mg/ml	0.518 mg/ml
Extraction Volume, $V_{ext}$	10 ml	10 ml
Feed weight, $m_{feed}$	1.0031 g	1.0051 g

**Table 0.2** Peak integrations for duplicate 1 hr reactions at 410 °C

Carbon No.	Peak Areas from GC Integration ( $A_i$ )			
	Sample 060806 A		Sample 060806 B	
	Alkene	Alkane	Alkene	Alkane
C <sub>8</sub>	69890	210522	75883	235372
C <sub>9</sub>	65743	223208	69786	233633
C <sub>10</sub>	80864	239003	87026	261339
C <sub>11</sub>	71315	274312	68172	298062
C <sub>12</sub>	76562	276868	83166	276868
C <sub>13</sub>	72088	244339	83882	244339
C <sub>14</sub>	68619	251302	75598	251302
C <sub>15</sub>	62135	447176	73544	447176
C <sub>16</sub>	159174	294885	145538	294885
C <sub>17</sub>	230492	3309804	267232	3309804
C <sub>18</sub>	24083	56857	25070	56857
C <sub>19</sub>	17444	94591	18345	94591
C <sub>20</sub>	31750	34856	10415	34856
Internal Standard		169604		154060

**Table 0.3** Sample calculation of mass yield for C<sub>8</sub>-C<sub>20</sub> alkanes and alkenes based on initial feed (Eqn. B.3)

Carbon No.	mg/g <sub>feed</sub> (Appendix B, Eqn. 3)			
	Sample 060806 A		Sample 060806 B	
	Alkene	Alkane	Alkene	Alkane
C <sub>8</sub>	2.13	6.41	2.54	7.87
C <sub>9</sub>	2.00	6.80	2.33	7.82
C <sub>10</sub>	2.46	7.28	2.91	8.74
C <sub>11</sub>	2.17	8.35	2.28	9.97
C <sub>12</sub>	2.33	7.75	2.78	9.26
C <sub>13</sub>	6.69	6.69	2.81	8.17
C <sub>14</sub>	2.09	6.83	2.53	8.41
C <sub>15</sub>	1.89	13.00	2.46	14.96
C <sub>16</sub>	4.85	8.47	4.87	9.86
C <sub>17</sub>	7.02	86.55	8.94	110.72
C <sub>18</sub>	0.73	1.51	0.84	1.90
C <sub>19</sub>	0.53	2.63	0.61	3.16
C <sub>20</sub>	0.97	0.96	0.35	1.17

**Table 0.4** Sample calculation of molar yield for C<sub>8</sub>-C<sub>20</sub> alkanes and alkenes based on initial feed (Eqn. B.4)

Carbon No.	mol/mol <sub>feed</sub> (Appendix B, Eqn. 4)			
	Sample 060806 A		Sample 060806 B	
	Alkene	Alkane	Alkene	Alkane
C <sub>8</sub>	0.0054	0.0160	0.0064	0.0196
C <sub>9</sub>	0.0045	0.0151	0.0053	0.0173
C <sub>10</sub>	0.0050	0.0145	0.0059	0.0175
C <sub>11</sub>	0.0040	0.0152	0.0042	0.0181
C <sub>12</sub>	0.0039	0.0129	0.0047	0.0155
C <sub>13</sub>	0.0104	0.0103	0.0044	0.0126
C <sub>14</sub>	0.0030	0.0098	0.0037	0.0121
C <sub>15</sub>	0.0026	0.0174	0.0033	0.0200
C <sub>16</sub>	0.0061	0.0106	0.0062	0.0124
C <sub>17</sub>	0.0084	0.1024	0.0107	0.1310
C <sub>18</sub>	0.0008	0.0017	0.0009	0.0021
C <sub>19</sub>	0.0006	0.0028	0.0007	0.0034
C <sub>20</sub>	0.0010	0.0010	0.0004	0.0012

**Table 0.5** Calculation of n-alkane/alkene molar ratio (Eqn. B.5)

Carbon No.	mol <sub>n-alkane</sub> /mol <sub>alkene</sub> (Appendix B, Eqn. 5)	
	Sample 060806 A	Sample 060806 B
C <sub>8</sub>	2.96	3.05
C <sub>9</sub>	3.34	3.30
C <sub>10</sub>	2.91	2.96
C <sub>11</sub>	3.80	4.32
C <sub>12</sub>	3.29	3.29
C <sub>13</sub>	0.99	2.88
C <sub>14</sub>	3.23	3.29
C <sub>15</sub>	6.81	6.02
C <sub>16</sub>	1.73	2.01
C <sub>17</sub>	12.23	12.28
C <sub>18</sub>	2.04	2.25
C <sub>19</sub>	4.92	5.12
C <sub>20</sub>	0.98	3.32

#### B.4 Standard Error

The variation in the data was estimated by calculating the standard error as written below.

These values were used as error bars on the figures.

$$S_E = \frac{\sigma}{\sqrt{n}} \dots\dots\dots \text{Equation B.4}$$

where  $\sigma$  is the standard deviation between the runs and  $n$  is the sample size.

## **B.5 Removal out outliers when $n > 2$**

The majority of reactions were conducted in duplicate and the average and standard errors were taken between the two samples. If a known error occurred during one of the reactions (i.e. a major leak, spilled samples etc.) the reactions were repeated. In experiments where more than 2 runs were conducted, outliers were removed from the data based on  $1.5 \times \text{IQR}$  (Scheaffer and McClave, 1995). The third and first quartiles were calculated in Excel and the difference between these values (inter-quartile range, IQR) was multiplied by 1.5. This value ( $1.5 \times \text{IQR}$ ) was added and subtracted from the mean to obtain the lower and upper outlier limits. Data values outside this range were removed and the new mean, standard deviation, and standard error was calculated accordingly.

## **APPENDIX C: EXPERIMENTAL VALIDATION AND ADDITIONAL PROCEDURAL DEVELOPMENT**

### **C.1 Internal reactor temperature and pressure for the Techne SBS-4 sand bath**

The sand bath and controller set-up allows for the temperature of the sand to be measured and controlled, not the internal reactor temperature. Since the reactor walls are constructed with stainless steel and are relatively thin, and the amount of material inside the reactor is fairly small it is assumed that heat transfer should be quick and that the contents inside the reactor should reach the set-point temperature in a reasonable amount of time. Previous studies using similar reactors with a thermocouple mounted in the reactor have shown that when filled with oil, they reach 95 % of the steady-state temperature within 2 min and 40 s (Bressler and Gray, 2003). Because this is a new system, it was of interest to determine the heating rate for this particular sand bath under conditions similar to the ones used in this work. Since pressure may also have an influence on the reaction products, it was also of interest to determine the pressure inside the microreactor during the reaction. Although the initial pressure was typically atmospheric, increased temperature inside the reactor along with the formation of gaseous products should cause an increase in pressure.

Temperature profiles representing heating of the microreactors at 370, 410, and 450 °C are presented in Figure A.1. The data represents the average between duplicate runs and the error bars (not visible) represent the standard error between these runs (Appendix B). The average standard errors were 1.1 °C for the 370 °C runs, 1.5 °C for the 410 °C runs,

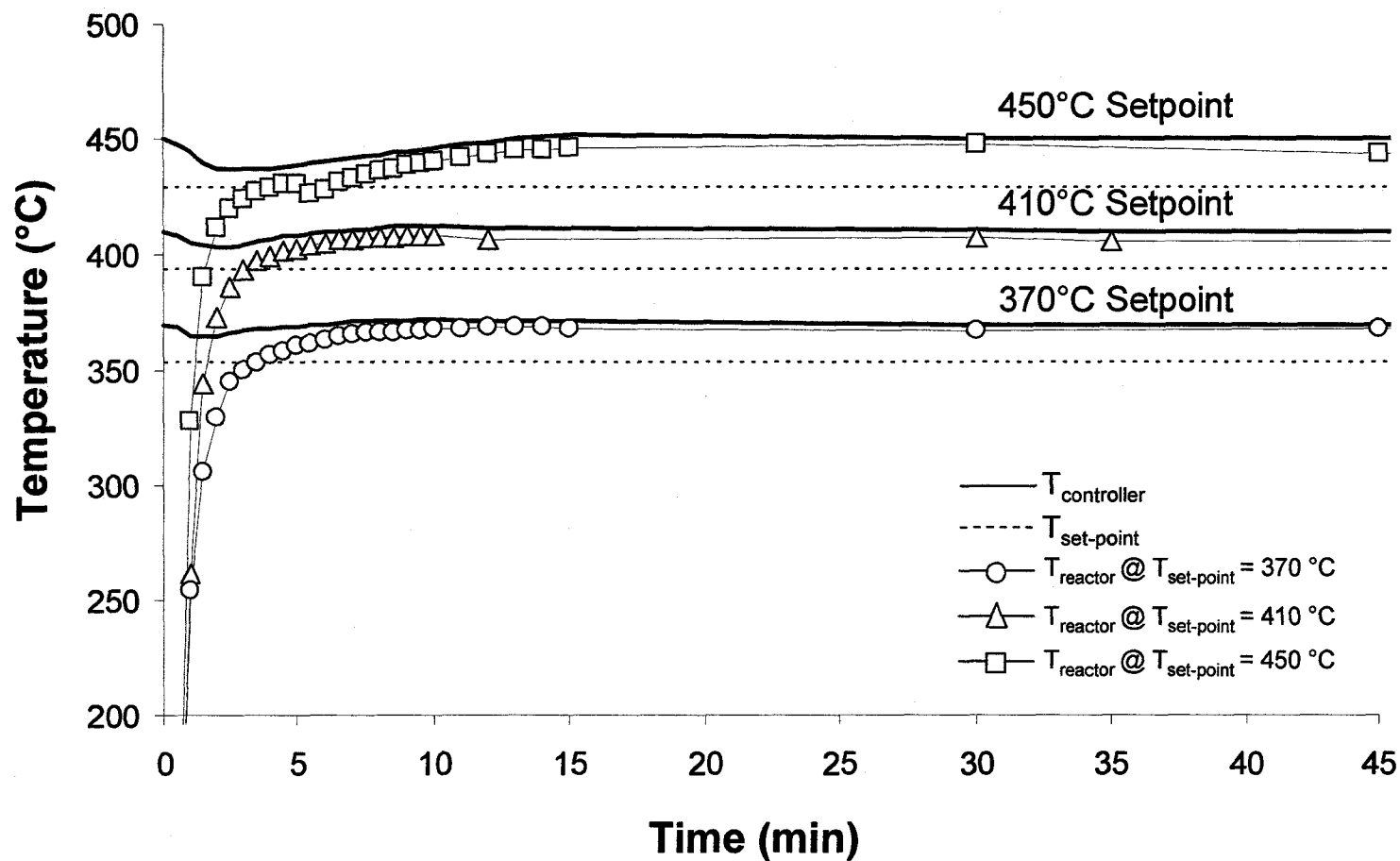


**Figure C.1** Internal reactor temperature during stearic acid pyrolysis as a function of time for controller set-point temperatures of 370 °C, 410 °C, and 450 °C. Reactions were conducted in N<sub>2</sub> atmosphere and were initially at atmospheric pressure.

and 2.8 °C for the 450 °C runs. The heating rate of the material inside the reactor appears to be fairly rapid as the reactor temperature,  $T_{\text{reactor}}$ , reaches 95% of the setpoint temperature (referenced from the starting temperature at time zero and shown on Figure 4.1 as the dashed line) within 3.5, 3, and 4 min for the three setpoint temperatures, respectively. As expected, there is a drop in the controller temperature (solid line), at all three temperatures, after the reactors are dropped in the bath. At a set-point temperature of 370 °C, it took approximately 6 min for the bath to heat back up to 370°C while at 410 °C it took 5.5 min. It took between 12-14 min for the bath to heat back up to temperature during the runs conducted at 450 °C.

The pressure gauge was checked throughout the reaction runs, however; the set-up made it difficult to read due to the agitation. As well, the scale on the gauge made it difficult to detect minor pressure fluctuations. Therefore, a full time/pressure profile was not obtained however, the maximum pressure during the run as well as the pressure after quenching was recorded. At 370 °C one of the reaction runs resulted in no pressurization during the reaction but the second run resulted in a maximum pressure of 1.0 MPa (150 psi). In both cases, the pressure gauge indicated zero pressure after quenching. This means that the pressure increase during the run was due to the high temperature of the reaction but not enough gas product was produced to result in increases reactor pressure at room temperature. At 450 °C, the maximum pressure reached during separate runs was 2.6 MPa (375 psi) and 3.1 MPa (450 psi). After quenching, the pressure inside the reactors was approximately 0.7 MPa (100 psi). At 410 °C, one of the runs exhibited an extremely large pressure increase at the end of the run to 4.5 MPa (650 psi). After

quenching, the pressure inside this reactor was 0.7 MPa (100 psi). This result is not consistent with the results from the other runs. The second run at 410 °C yielded results that would be expected based on the results of the other temperatures. A maximum pressure of 1.4 MPa (200 psi) was reached and after quenching, the gauge indicated zero pressure inside the reactor.

## **C.2 Effect of sample drying on the product profile**

For mass balance and quantification, the weight of the pentane soluble product is most easily determined by drying down the sample under nitrogen gas and then weighing. The problem with this method is that many of the reaction products are volatile and have the potential to be evaporated during the drying process. Before developing extraction methodologies, it was of interest to determine if drying under nitrogen affected the product profile. Duplicate reactions were conducted for one hour at 450 °C and 500 °C. The reactors were purged with nitrogen gas and were initially at atmospheric pressure. Ten ml of pentane was used to extract the reaction products (Section 3.5.1) and two 4 ml aliquots were transferred into sample vials. One of the samples was analyzed as is while the other sample was dried down with nitrogen and then re-suspended with 4 ml of pentane before analysis. Figure A.2 shows chromatograms before and after drying at 450 °C. It is clear that both the quantities and distribution of products changes substantially with drying, especially the lower retention compounds. At 500 °C, where the products are mostly light ends and possibly aromatics, the drying process evaporates the majority of those compounds (chromatogram not shown).



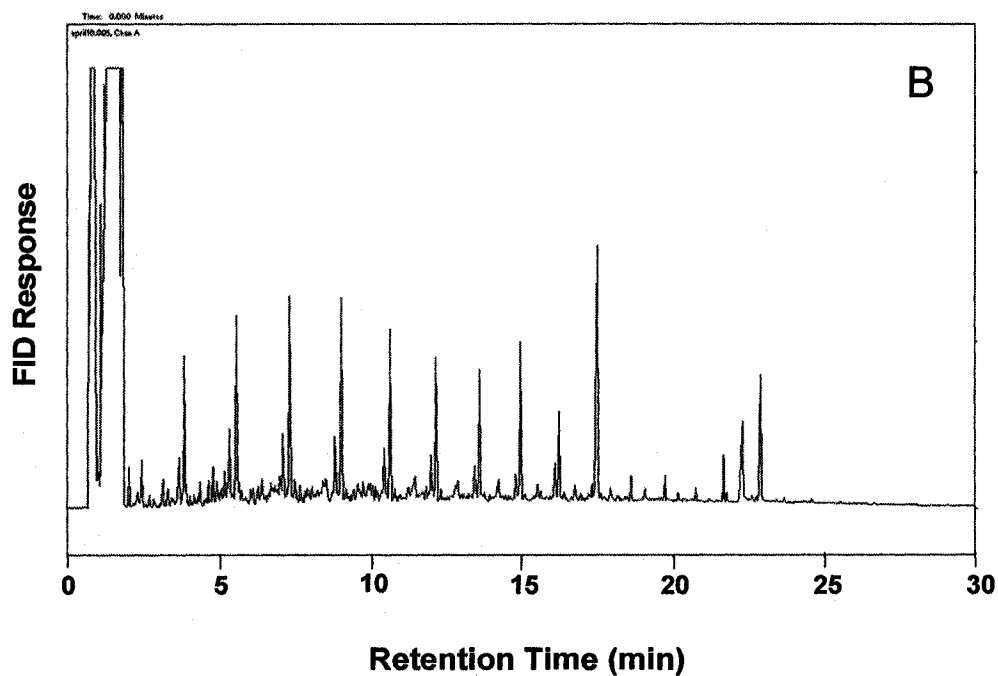
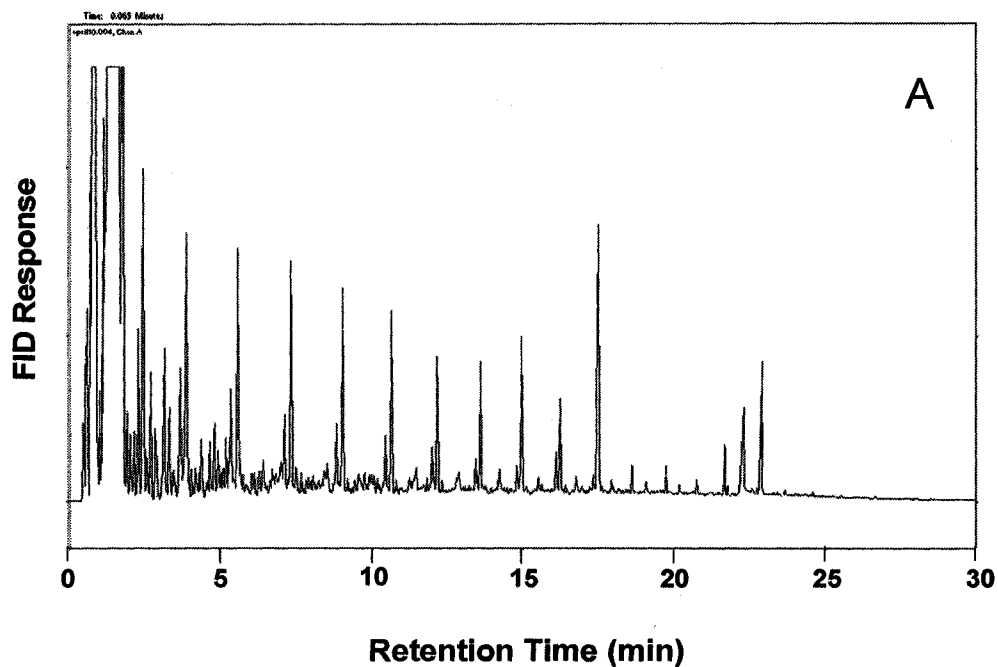


**Figure C.2** GC-FID chromatogram showing the difference in product distributions before (A) and after drying and re-suspension (B) of stearic acid pyrolysis products for 1 hr reactions conducted at 450 °C . Reactions were conducted in N<sub>2</sub> atmosphere and were initially at atmospheric pressure.